TECHNO-ECONOMIC ANALYSIS OF A GASIFICATION SYSTEM USING REFUSE-DERIVED FUEL FROM MUNICIPAL SOLID WASTE

by

ISMAIL BABATUNDE ADEFESO

BSc (Hons); MSc: Chemical Engineering

Thesis submitted in fulfilment of the requirements for the degree

Doctor of Engineering: Chemical Engineering

in the Faculty of Engineering

at the Cape Peninsula University of Technology

Supervisor: Prof Daniel Ikhu-Omoregbe

Co-supervisor: Dr Yusuf Isa

Cape Town

2017

DECLARATION

I, Ismail Babatunde Adefeso, declare that the contents of this thesis represent my own unaided work and that the thesis has not been previously submitted for academic examination towards any qualification. Furthermore, it represents my own opinions and not necessarily those of the Cape Peninsula University of Technology.

------------------------------------- ---

Signature Date

DEDICATION

This thesis is dedicated to people who have been deprived of their homeland and humanity – people of Palestine; my wife and children.

ABSTRACT

The search for alternatives to fossil fuel is necessary with a view to reducing the negative environmental impact of fossil fuel and most importantly, to exploit an affordable and secured fuel source. This study investigated the viability of municipal solid waste gasification for a fuel cell system.

Potential solid fuels obtained from the study in the form of refuse-derived fuel (RDF) had high heating value (HHV) between 18.17 MJ/Kg - 28.91 MJ/Kg with energy density increased from 4142.07 MJ/m^3 to 10735.80 MJ/m^3. The molecular formulas of RDF derived from Ladies Smith drop-off site, Woodstock drop-off site and an average molecular formula of all thirteen municipal solid waste (MSW) disposal facilities were $CH_{1.43}O_{1.02}$, $CH_{1.49}O_{1.19}$, and $CH_{1.50}O_{0.86}$ respectively. The comparative ratios of C/H were in the range of 7.11 to 8.90. The Thermo Gravimetric Analysis showed that the dehydration, thermal decompositions, char combustions were involved in the production of gaseous products but flaming pyrolysis stage was when most tar was converted to syngas mixture.

The simulation of RDF gasification allowed a prediction of the RDF gasification behaviour under various operating parameters in an air-blown downdraft gasifier. Optimum SFR (steam flowrate) values for RDF1, RDF2 and RDF3 were determined to be within these values 2.80, 2.50 and 3.50 and Optimum ER values for RDF1, RDF2 and RDF3 were also determined to be within these values 0.15, 0.04 and 0.08. These conditions produced the desired high molar ratio of H_2/CO yield in the syngas mixture in the product stream. The molar ratios of H_2/CO yield in the syngas mixture in the product stream for all the RDFs were between 18.81 and 20.16. The values of H_2/CO satisfy the requirement for fuel cell application.

The highest concentration of heavy metal was observed for Al, Fe, Zn and Cr, namely 16627.77 mg/Kg at Coastal Park (CP), 17232.37 mg/Kg at Killarney (KL), 235.01 mg/Kg at Tygerdal (TG), and 564.87 mg/Kg at Kraaifontein (KF) respectively.

The results of quantitative economic evaluation measurements were a net return (NR) of \$0.20 million, a rate of return on investment (ROI) of 27.88 %, payback time (PBP) of 2.30 years, a net present value (NPV) of \$1.11 million and a discounted cash flow rate of return (DCFROR) of 24.80 % and 28.20 % respectively. The results of the economic evaluations revealed that some findings of the economic benefits of this system would be viable if costs of handling MSW were further quantified into the costs analysis. The viability of the costs could depend on government responsibility to accept costs of handling MSW.

PUBLICATIONS

Ismail B. Adefeso, Ademola M. Rabiu, & Daniel I. Ikhu-Omoregbe (2015) Refuse-Derived Fuel Gasification for Hydrogen Production in High Temperature Proton Exchange Membrane Fuel Cell Base CHP System. *Waste and Biomass Valorizations 6(6): 967-974.* ISSN: 1877-2641.

Rabiu, A. **Adefeso, I.,** and Ikhu-Omoregbe, D. (2012). Municipal Solid Wastes Gasification/Polymer Electrolyte Membrane Fuel Cell Integrated CHP System. *The Online Journal of Science and Technology*, 2 (3): 28-34. ISSN 2146-7390

Daniel Ikhu-Omoregbe**, Ismail Babatunde Adefeso,** Isa Yusuf, and Ademola Rabiu Analysis of Heavy Metals Distribution in Municipal Solid Wastes in Cape Town. *International Conference on Chemical Engineering,* September 12-14, 2016, Phoenix, Arizona, USA. ISSN: 2157-7048

Adefeso, I.B., Ikhu-Omoregbe, D.I.O. and Rabiu, A.M. Cost and Environmental Analyses of an Integrated Municipal Solid Wastes Gasification and Fuel Cell Based CHP System. *5th International Conference on Engineering for Waste and Biomass Valorizations (WasteEng14),* 25-28 August 2014, Rio de Janeiro, Brazil. ISBN: 9791091526005

Adefeso, I.B., Rabiu, A.M., and Ikhu-Omoregbe, D.I.O. "Energy Diversification: Option in Waste to Energy/Fuel via Municipal Thermo-chemical Conversion. *ASSAF Third Annual South African Young Scientists*' Our Energy Future *(ASSAF 2012)* 16-18 October 2012, CSIR International Convention Centre, Brummeria, Pretoria, South Africa.

Adefeso, I.B., Ikhu-Omoregbe, D.I.O. and Rabiu, A.M. "Sustainable Co-generation Plant: Refuse-Derived Fuel Gasification Integrated with High Temperature PEM Fuel Cell System. *In: International Proceeding of Chemical, Biological and Environment, Engineering (IPCBEE 2012)* 33(1):125-129, 5-6 May 2012, Kuala Lumpur Malaysia. ISSN: 2010-4618

ACKNOWLEDGEMENTS

All thanks and glory are due to Almighty God for His special love and mercy, holy and total guidance, inspiration, provision and protection through the challenging period of this study.

I would like to thank my supervisor, Prof Daniel Ikhu-Omoregbe for the wonderful opportunity given to me and his profound understanding, and knowledge sharing during the study. I commend his approach throughout the painstaking tasks undergone during this research. I thank my co-supervisor, Dr Yusuf Isa, whom I have learned from his prowess of knowledge. Your support and guidance throughout the study are remarkable.

I thank my brother - Mr Ademola Rabiu whom I have gained a lot from his advice. You have done extremely well and wonderful. May Almighty God bless you beyond your imagination.

I acknowledge the financial supports of CPUT through Faculty of Engineering bursary and HYSA bursary. I also acknowledge the financial supports of Islamic Relief of South Africa.

I want to thank my colleagues and staffs of the department of chemical engineering for their supports during field work and laboratory work.

I thank my father, Mr. Adefeso and my mother Mrs Adefeso for your spiritual and psychological supports throughout the journey to accomplish this task. My father, you are my hero, and my mother, you are my inspiration wherever I go.

I thank my brothers and my sisters - Dr Hammed Adefeso, Basirat Adefeso, Mutiat Adefeso, Azeez Adefeso, and Tajudeen Adefeso for their encouragement and support.

The support of my brothers and sisters in faith in Nigeria and South Africa are appreciated. The supports of Prof Abubakr Sanusi and spiritual advice of Imam Abubakr Bello are appreciated.

My wife, Shakirah Folasade, I thank you from depth of my heart for your unrelenting understanding and support since I began the journey of my postgraduate research.

The journey is full of a mixture of happiness and joy, and obstacles and challenges as I went from one stage to another.

I commend your perseverance because it was key to my success. Thank you, my darling for keeping the flag flying. I want to thank my children - Ja’far, Muadh, Abdul Rahman, Abdul Raheem, and Ramlah for their patience and understanding.

TABLE OF CONTENTS

LIST OF FIGURES

LIST OF TABLES

LIST OF ABBREVIATIONS

Abbreviation	Definitions
ACF	Accumulated cash flow
AFC	Alkaline fuel cell
ARTS	Athlone transfer station
ASTM	American standard
BD	Bulk density
BEP	Breakeven price
BESP	Breakeven electricity selling price
BL	Belhar
CF	Compressibility factor
CHP	Combine heat and power
CP	Coastal park
CPCB	Central pollution control board
DC	Direct current
DCFROR	Discounted cash flow rate of return
DF	Delft
DO	Drop-off site
EJ	Exa joules
EMIP	Equivalent maximum investment period
ER	Equivalence ratio
EU	European Union
FC	Fixed carbon
GDP	Gross domestic product
GHG	Greenhouse gas
GMM	General MSW mixture

HDPE	High density polyethylene
HHV	High heating value
HTPEMFC	High temperature polymer electrolyte membrane fuel cell
ICE	Internal combustion engine
ICP-MS	Inductively coupled plasma mass spectrometry
IPCC	International panel on climate change
KF	Kraaifontein
KL	Killarney
LCC	Life-cycle cost
LDPE	Low density polyethylene
LHV	Lower heating value
LM	Ladies miles
LNG	Liquefied natural gas
LS	Landfill site
LTPEMFC	Lower temperature polymer electrolyte membrane fuel cell
M	Moisture
MARR	Minimum acceptable rate of return
MC	Moisture content
MCFC	Molten carbonate fuel cell
MEWR	Ministry of the environment and water resources
MSW	Municipal solid waste
MSWDF	Municipal solid waste disposal facility
MW	Mega watt
NEA	National environmental agency
NIST	National Institute of standards and technology
NPC	Net present cost

NPV	Net present value
NR	Net return
OECD	Organisation for economic cooperation and development
PAFC	Phosphoric acid fuel cell
PE	Polyethylene
PET	Polyethylene terephthalate
PFCs	Perfluorocarbons
PFD	Process flow diagram
PGM	Platinum group metals
PP	Polypropylene
PS	Polystyrene
PT	Payback time
PTFE	Polytetrafluoroethylene
PVC	Polyvinyl chloride
RDF	Refuse-derived fuel
ROI	Rate of return on investment
RT	Retreat
SOFC	Solid oxide fuel cell
SFR	Steam flow rate
TCC	Total capital cost
TG	Tygerdal
TGA	Thermo-gravimetric analysis
TS	Transfer station
UK	United Kingdom
US/USA	United States
USEPA/EPA	United state environmental protection agency

VM	Volatile matter
WG	Welgelegen
WGS	Water gas shift
WS	Woodstock
WTE	Waste-to-energy
WY	Wynberg
F-T	Fischer-tropics synthesis

GLOSSARY

Terms/Acronyms	Explanations
Acid Doped PBI (Polybenzimidazole)	is the thermally resistant acid-doped polymer electrolyte membrane with a glass transition temperature of 420 ^{0}C and allows for an operating temperature as high as 200 ^{0}C.
Aspen Plus Model	is a robust process-modelling tool for steady-state simulation, modelling chemical, power generation design, performance monitoring, optimisation and business planning for chemicals, petrochemicals and metallurgy industries.
Biomass Gasification	is a thermochemical conversion of biomass into a range of useful products with minimum supply of the oxidising agent via gasifying media like steam, air or oxygen.
Biomass	is a non-fossilised and biodegradable organic material originating or derived from plants, animals and micro-organisms. It includes forestry residues and non-fossilised and biodegradable organic fractions of industrial and municipal waste.
Cogeneration	is a term used to describe the combined generation of heat and electricity.
Combined Heat and Power System	is a power generation system that produces heat and electricity simultaneously?

CO-Poisoning	is associated with low temperature Polymer Electrolyte Membrane fuel cell where CO reduces the catalyst activity of the anode side of the fuel cell.
Electro-chemical Devices	are all forms of fuel cells that obtain electrical energy from chemical energy via membrane electrode assembly (MEA).
Environmental Degradation	is an environmental impact on land air and water resulting from fossil fuel utilisation.
Fossil Fuel	is a non-renewable energy source in the form of coal, crude oil, and natural gas.
Fuel Cell	is an electro-chemical device that produces electricity directly from chemical energy.
High Temperature Fuel Cells	are Solid Oxide Fuel Cell (SOFC) Molten Carbonate Fuel Cell (MCFC) Direct Methanol Fuel Cell (DMFC).
High Temperature Polymer Electrolyte Membrane Fuel Cell	is an electro-chemical fuel cell device converting chemical energy to electrical energy with acid doped-Polybenzimidazole polymer electrolyte membrane at an elevated temperature (120 ^{0}C - 200 ^{0}C).
Low Temperature Polymer Electrolyte Membrane Fuel Cell	is an electro-chemical fuel cell device converting chemical energy to electrical energy with Nafion-type polymer electrolyte membrane at low temperatures (80 ^{0}C)

Micro-CHP	is a low heat and electrical generation that is found in the range of 10 MW of energy.
Municipal Solid Waste	is a collection of solid waste with substantial biomass composition.
Nafion Polymer Electrolyte Membranes	are co-polymer structures of perfluorosulphonic acid polymers, which have a high hydrolytic and oxidative stability and excellent proton conductivity.
Proximate and Ultimate Analyses	are prescribed methods of determining moisture, volatile matter, fixed carbon, ash and elemental compositions (C-H-O-N-S-Cl) of organic compounds.
Refuse-Derived Fuel	these are pellets or briquettes produced by drying the combustible constituents of Municipal Solid Waste and compressed them into desired specifications.
Renewable Energy Sources	are alternative energy sources for fossil fuel and they are biomass, wind, solar, geothermal, ocean tides and hydro energy.
Techno-Economic Analysis	involves technical analysis and economic evaluation of systems.
Thermochemical Processes	are pyrolysis, gasification, and combustion processes.

CHAPTER ONE

1 INTRODUCTION

1.1 Background of the Study

Energy demand is increasing globally amid limited energy resources and environmental challenges from solid waste (Barbir, 2013). The energy security situation is reflected in the recent spate of power outages and the challenges of energy access by communities, for instance, below standard power supply and distribution to remote locations in South Africa and beyond (Scarlat et al., 2015).

High energy consumption and the generation of municipal solid waste (MSW) are indicators of population growth and prosperity. The steady economic growth and development have resulted in a rise in energy consumption and MSW production, necessitating alternative energy resources and a sustainable approach to municipal solid waste management (Imam et al., 2008, Song et al., 2013).

The choice of energy sources and rate of energy consumption will continue to increase with advancement in technology as the demand has been seen to be increasing historically. The world energy resources have undergone a revolution from simple wood log, waste wood and wood dung to coal, oil and gas, nuclear and emerging renewable energy resources as shown in Figure 1.1 and Figure 1.2. The over-reliance on fossil fuels as major energy sources worldwide is problematic because of their finite availability (Novatlantis, 2005) as shown in Figure 1.3 and associated environmental and global-warming effects (Friedrich and Trois, 2010). This has necessitated the search for other energy resources which pose less of an environmental threat. From the 20th century, the global energy production has been diversified, but the domination of fossil fuels persists and is responsible for 74 % of all CO_2 emissions (Barbir, 2013, Leggett and Ball, 2012).

In South Africa, fossil fuels remain significant fuel resources in the energy production sector (Africa, 2012). Coal energy resources still account for more than 70 % of energy resources in China, India and South Africa.

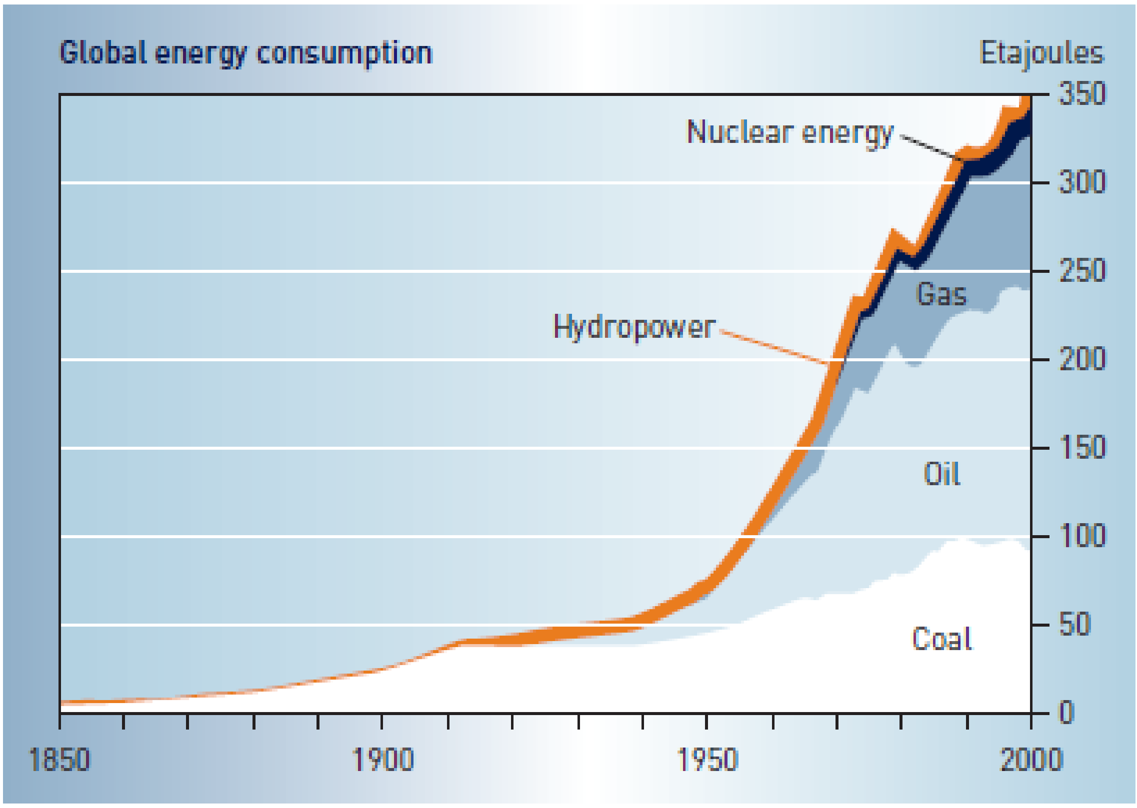

Figure 1.1: Drastic Change in Development of Energy Consumption (Novatlantis, 2005)

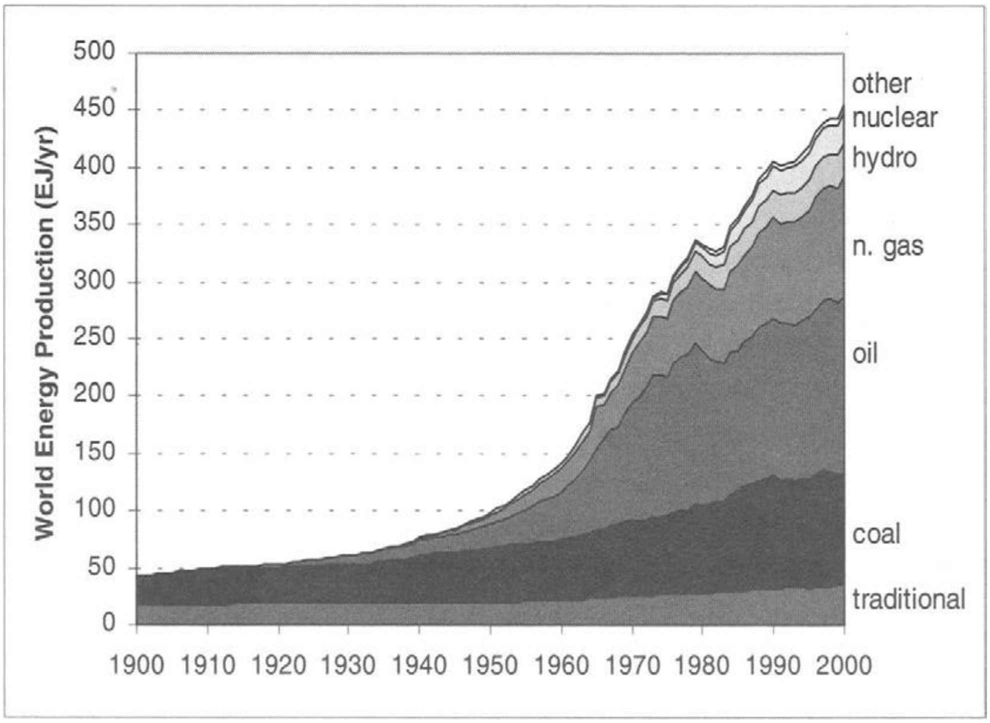

Figure 1.2: History of World Energy Production (Barbir, 2013)

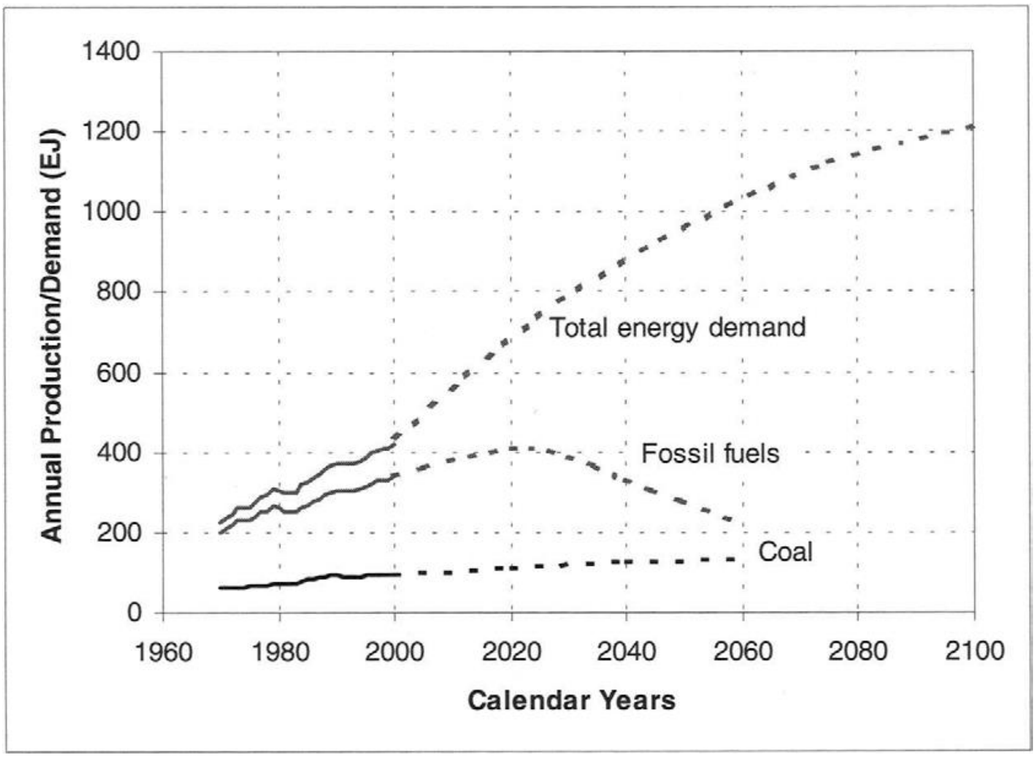

Figure 1.3: An Overview of World Energy Demand and Production Projection (Barbir, 2013)

Although efforts are ongoing on diversification, more is required to exploit abundant biomass energy resources. The immense production of municipal solid waste (MSW) is of global concern. These challenges have dominated and broadened the scope of research on MSW around the world (Kumar et al., 2011, Matsuo et al., 2013, Liu et al., 2013a). Despite many efforts, these forms of energy resources are still largely unexploited.

The MSW are mainly produced from domestic and commercial activities. Their management is hindered by continuous huge generations, limited technologies for disposal, treatment, recycling, conversions (conversion to fuel and energy) and cradle-to-grave management. The composition of MSW usually reflects living style, technological advancement, economic factors, climate, cultural habits and geographical location (Burnley et al., 2011). These are the factors responsible for physical and non-homogeneous characteristics of most MSW. The diverse characteristics of MSW make it very difficult to generalise the physicochemical properties of MSW. Before the advent of crude oil boom, gasification technologies were among prominent technologies for stationary applications, particularly wood gasification technology. The dynamics of energy resource diversification is now exploiting thermochemical conversion technology to address lingering challenges of the environmental impact and looks towards sustainable and renewable technology.

Thermochemical conversion technologies are very prominent for solid fuel conversion. Combustion, incineration, pyrolysis, torrefaction, and gasification are diverse thermochemical conversion technologies for solid fuel waste-to-energy conversion technology (Shi et al., 2016). They are not only useful for heat and energy production but also for the production of other energy-packed chemicals (syngas, methane, ethane, hydrogen and carbon monoxide) for further applications (Moghadam et al., 2014; Kocer et al., 2017).

Studies have been carried out on biomass gasification technology for production of energy and chemicals (Thakare and Nandi, 2016, Ramos et al., 2018, Sikarwar and Zhao, 2017, Fernandez-Lopez et al., 2017).

Gasification thermochemical conversion is one of the potential technologies to explore for the valorisation of solid fuel in the form of MSW. However, the trend of the carbon density of global energy resources is decreasing as its consumption migrates and diversifies from wood and coal to oil, gas and other renewable energy with fewer net carbon footprints (Barbir, 2013). Renewable energy research has produced opportunities for diversification; nonetheless, biomass-based MSW research still requires further studies.

Hence, there are needs to exploit the rich energy resources of solid waste conversion technology to reduce environmental problems, harness waste-to-energy via technology and the economic evaluation of municipal solid waste resources. The solid waste conversion technologies can contribute significantly to traditional heat and power system.

1.2 Combined Heat and Power System

A combined heat and power (CHP) System generates electrical and heat energy simultaneously from a single energy stream such as non-renewable energy resources (fossil fuels, oil, coal, natural or liquefied gas) and renewable energy sources (biomass, wind or solar energy). CHP, a form of cogeneration that produces two forms of energy, has been in use since the 20th century (Orlando, 1996, Dornburg and Faaij, 2001, Wood and Rowley, 2011). It has the potential to deliver relative energy savings, low cost, low emissions and better future energy prospects for the technology (Hinnells, 2008). However, the environmental impact of using fossil fuels is still under evaluation. The elements of a conventional CHP plant comprise one or more prime movers (a reciprocating engine, gas turbine or steam turbine) driving electrical generators and a long process of energy transformation – chemical-to-heat, heat-to-mechanical and mechanical-to-electrical energy. These energy transformations of the CHP plants affect the quality of efficiency of the traditional systems. In comparison with conventional systems, fuel cell-based CHP systems could provide efficiency greater than 80 %. These are key elements which are not mentioned in any power efficient economy (Wang et al., 2011, Suha Yazici, 2010, Yazici, 2011). The application of a fuel cell in a CHP system is another area of research waiting to be exploited fully because of a range of benefits (energy loss due to transformation, better efficiency and environmentally friendly) over the traditional CHP system. The CHP system generates heat and energy mainly from fossil fuel, but the challenges of energy resources still persist without system approach to improve energy mix.

1.3 Energy Resource Challenges

Global energy demand constitutes several challenges from time immemorial and still persists, arising from numerous needs. The global energy consumption dictates significant roles in the political landscape. Technology advancement, economic growth, safety and environmental concerns are determining factors navigating the choice of energy resources while energy demand and economic growth have an inherent relationship with economic growth as the driving force. Energy consumption projection is on the increase as a study predicted 1000 EJ by 2050 (Moriarty and Honnery, 2012). Renewable energy sources (hydro, solar, tidal, geothermal, wind and biomass) are primary sources of energy (Moriarty and Honnery, 2012, Melikoglu, 2013b, Melikoglu, 2013a). These sources are important in energy diversification, but some factors need to be taken into consideration for the sustainability of the energy mix.

The availability of renewable resources, the environmental implications of fossil fuel sources, safety and nuclear energy proliferation, technology and sustainability are vital factors for consideration in a sustainable energy diversification drive. Fossil fuels are the dominant energy resources in South Africa as shown in Figure 1.4 and Figure 1.5 The country is ranked the 14th largest emitter of greenhouse gases (GHG). This requires a comprehensive review of the present energy mix towards a sustainable, friendly environment with low carbon emissions. The annual report of the department of energy in South Africa, proposed an energy contribution of 23 % from nuclear energy by 2030 (see Figure 1.5) (Africa, 2012, Department of Energy South Africa, 2011) unlike previous nuclear energy contributions (see Figure 1.4) The nuclear energy proposal exceeds the global contribution trend of 5.8 % (Moriarty and Honnery, 2012). In this view, a renewable energy source option could be harnessed for cleaner and greener energy resources. Hydro, wind, solar, tidal, geothermal, and biomass are viable potentials for energy security and sustainability. Nonetheless, the biomass energy resource option from MSW holds a favourable opportunity for not only renewable energy sources but the production of a variety of chemical feedstocks for numerous applications. However, contributions of renewable energy resources are still minimal compared to its potential in South Africa (Figure 1.4). Understanding of the potential threats of primary resources and inherent impact is an important aspect of energy diversification and its sustainability.

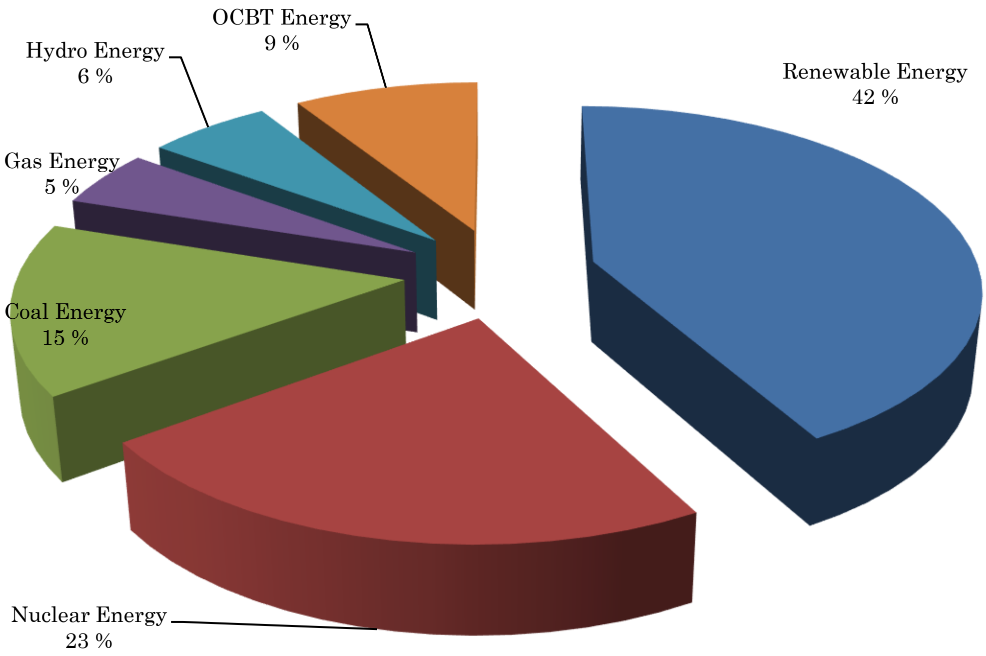

Figure 1.4: Proposed Energy Mix Capacity Plan for Next Twenty Years - 2030 (Department of Energy South Africa, 2011).

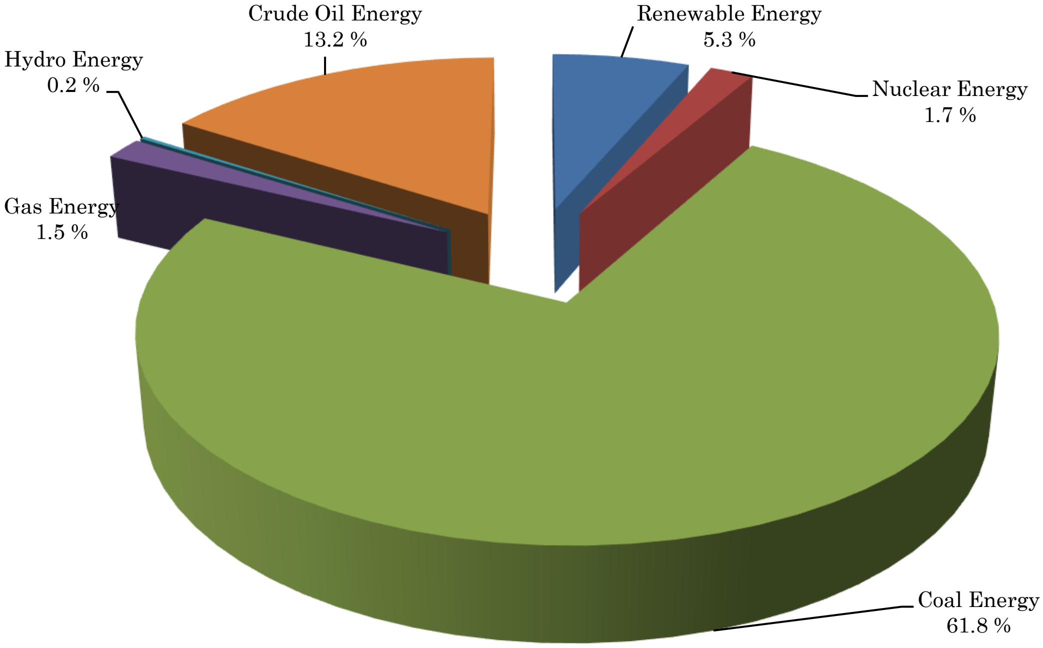

Figure 1.5: Supply of Primary Energy Sources in South Africa 2009 (Africa, 2012).

1.3.1 Energy Sources and their Inherent Impact

World energy production is struggling to reduce the capacity of carbon emission among other environmental and safety threats. Within a century (between 1900 and 2000), the production of world energy witnessed a significant diversification of its primary source with fossil fuel being dominant (Barbir, 2013). Another non-renewable source is nuclear energy which contributes to energy diversification. The impact of nuclear energy begins with the radioactivity of its fuel and the potential of nuclear proliferation. There have been a number of nuclear accidents. In 1957 and 1979 respectively, there were accidents at the atomic plant in Mayak, USSR, and at the nuclear power station at Three Mile Island USA. The accident at the Chernobyl Nuclear Power Plant occurred on 12 April 1986, which left a legacy of a red forest and a ghost town in the Ukraine with a large number of individuals being affected with high levels of radiation exposure with lasting effects to date and the recent event at the Fukushima Dai-chi nuclear power plant that happened on 11 March 2011 has led to the contamination of air mass over three continents (Ioannidou et al., 2012, Kortov and Ustyantsev, 2013). These were some experiences of nuclear disasters, either from nuclear energy technology or a nuclear warhead.

The consequences of the accidents have led to prolonged significant environmental impacts. The effects are downplayed by the politicians. Safety and technology are of great concern when considering nuclear energy. It also needs to be noted that coal, crude oil and liquefied natural gas (LNG) are fossil fuels without a carbon-neutral integrity and will soon be depleted (Leggett and Ball, 2012). An international treaty like Kyoto Protocol was initiated in 1997 to combat stabilisation of GHG in the atmosphere, a decade after the Montreal Protocol. The right response is necessary to tackle current global threats from our dominant fossil fuel resource utilisation.

The utilisation of renewable sources may minimise the impact of net GHG emission, but they are not completely immune from intrinsic and associated impacts, such as a solar source of energy, which may have an adverse effect on a fragile semi-arid land ecosystem, or competition for fresh water and the depletion of scarce resources, while wind as a source of energy may lead to possible habitat loss, vibration pollution and adverse effects of visual amenity. A hydro energy resource is highly determined by the topographical landscape of the environment while it may cause the loss of freshwater biodiversity, increased downstream erosion, declining soil fertility from the loss of deposits of sediment and GHG from the submerged biomass. A geothermal source of energy may lead to micro-seismicity and potential air and water pollution. Tidal sources of energy and other sources mentioned earlier are location dependent (Moriarty and Honnery, 2012, Melikoglu, 2013b, Melikoglu, 2013a).

Furthermore, some quantity of heavy metals are associated with combustible components of MSW particularly trace amount of heavy metals in organic salts and organic substance additives (Hasselriis and Licata, 1996, Jenkins et al., 1998, Smith 2009). Heavy metal found in MSW have fundamental implications to produce fly and bottom ash and their disposals (Haiying et al., 2010, Sekito et al., 2014, Liu et al., 2015). They might also be responsible for fouling effects, corrosion and pollutant emissions during gasification reactions (Jenkins et al., 1998, Quina et al., 2008, Nowak et al., 2013). The lack of detail research on heavy metals in MSW might be among the reasons for the lack of a sustainable approach to the understanding of the effective management of MSW and its final disposal (Li et al., 2013, Long et al., 2013, Tian et al., 2013, Hasselriis and Licata, 1996, Nowak et al., 2013).

Some renewable energy has some sort of limitations despite their prospects. Nonetheless, biomass sources (virgin biomass and MSW) have regeneration potentials, no depletion threat and are not location dependent as waste is continuously produced. Large fractions of MSW are organic substances (Zhou et al., 2014) that can be used for the preparation of solid fuel feedstock and for energy application if thermochemical conversion technologies are exploited (Chen et al., 2015).

1.3.2 Energy Diversification: Sustainable Alternative Approach

South Africa’s energy supply is around 42,000 MW and there are ongoing efforts to meet up with the challenge of increased energy demand. This is important for the sustainability of transportation and the energy needs for domestic energy use, as well as for manufacturing and tourism if economic growth (Scarlat et al., 2015) is to be sustained (Figure 1.5).

In 2007, South Africa experienced a power outage with serious economic implications. The same scenario occurred again in the early to mid-2015s when load-shedding schedules became the topic of conversation in households across the country. The consequences of the shortfall in power supply created a gap in economic prospects for some sectors of the country. The impact was more pronounced in some sectors of the economy particularly in manufacturing sectors (Africa, 2012) (Figure 1.6). South Africa has the potential for diverse renewable energy resources which can be exploited by considering natural energy resources, namely, wind (in the Western and Eastern Cape, it is 8.4 MW); solar (in the Northern Cape, it is 5 MW); hydro energy (in the Eastern Cape and KwaZulu-Natal it is 10 MW); and biomass and MSW energy resources (all municipal solid waste disposal facilities in South Africa) (Africa, 2012). Thus, MSW is available for thermochemical conversion for solid waste treatment and energy recovery while other renewable resources are not because they are neither intermittent energy resources nor location-dependent while the MSWs are generated continuously without fear of depletion. The thermochemical conversions of the combustible components of MSW eliminate the net effects of GHG from open incineration, landfill and other associated challenges of MSW management.

Cape Town has the generation capacity of approximately 1200 tonnes/day of combustible resources from MSW that can be exploited for relevant solid fuel and energy resource applications.

The availability of platinum group metal (PGM) in South Africa attracts research attention to fuel cell application for CHP system (Barrett, 2013b, Bessarabov et al., 2012). This is responsible for various researches towards hydrogen production for use in the fuel cell system. Hence, this study seeks for an alternative source of energy resources in line with the initiative of the programme (Pollet et al., 2014, Barrett, 2013a).

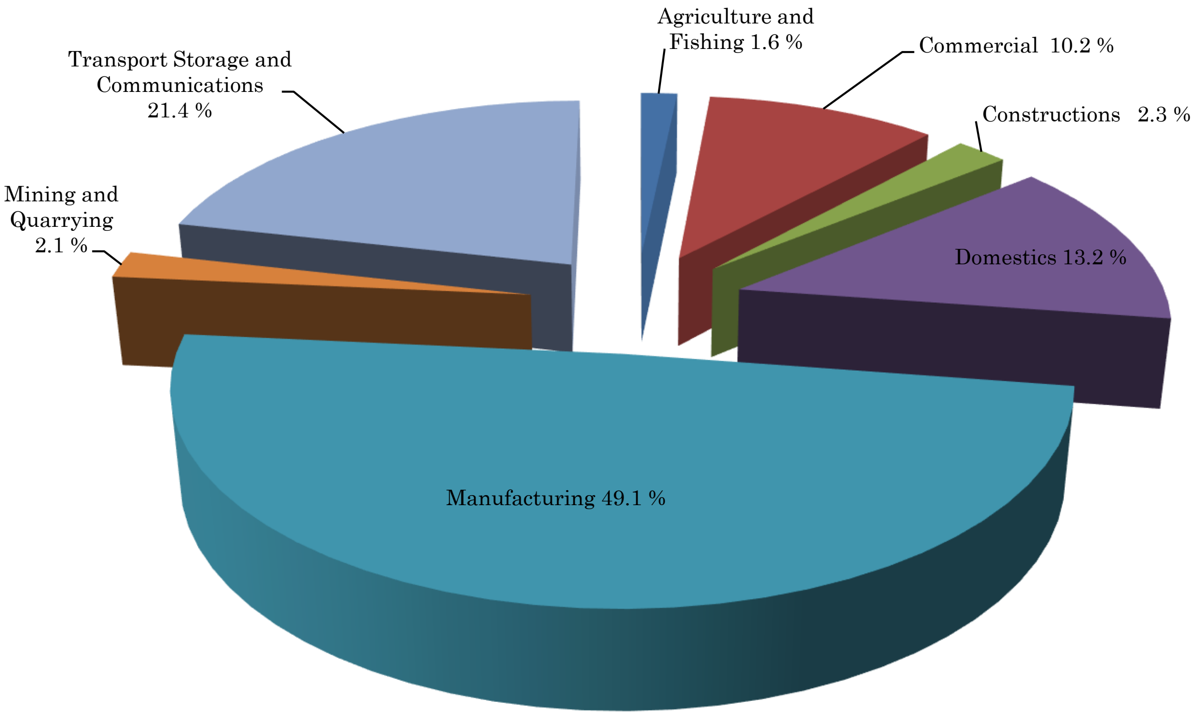

Figure 1.6: Main Consumers of Energy in South Africa 2009 (Africa, 2012).

Furthermore, the study of Demirbas (2009) reports a positive projection indicating a high demand for hydrogen fuel from renewable energy resources and this shows the future direction for demand for clean and green resources as shown in Figure 1.7. Biomass-derived solid fuel – RDF has a high net carbon-neutral integrity and its unique renewable energy source is a potential alternative to carbonaceous fossil fuel. Lignin-cellulosic base MSW constitutes a substantial fraction of the composition of MSW that is generated daily. The MSW is normally enhanced through pre-treatment and densification of the MSW. Thus, RDF thermochemical conversion technologies reduce corrosion and harmful GHG emissions while, on the other hand, it enhances material and energy recovery.

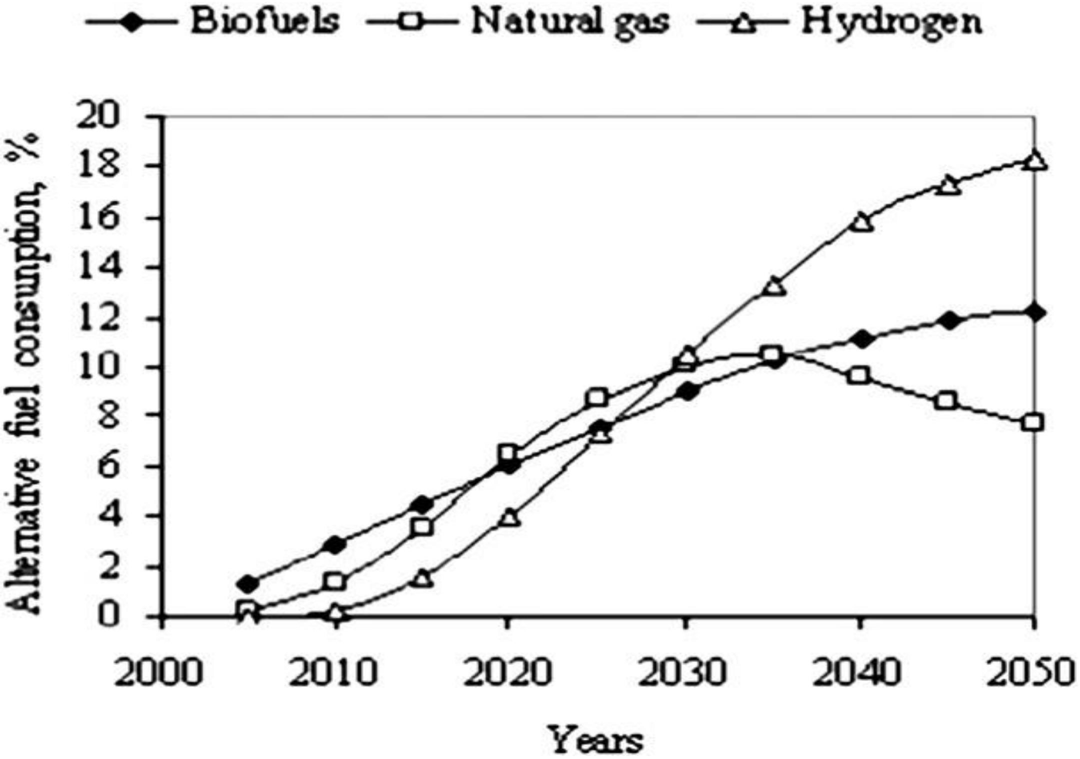

Figure 1.7: Alternative Fuel Source Consumption Projection (Demirbas, 2009).

The RDFs from pre-treated MSW will produce a more uniform feedstock (organic and combustible mixtures) for the thermochemical conversions. The hydrogen-rich gas from syngas produced from the thermochemical conversion of MSW would be used directly in fuel cells.

1.4 Statement of Research Problem

The environmental impact and the low efficiency of fossil fuel-based combined heat and power (CHP) systems are among the major drawbacks of such power systems. While the cogeneration of a heat and power from fossil-based fuel is a welcome idea, the demerits mentioned earlier call for a rethink on the need to search for possible alternatives to fossil fuel with a view to reducing the negative environmental impact, reduce over-dependence on fossil fuels and, most importantly, the harnessing or exploitation of affordable and secure fuel source

Biomass is a potential alternative to fossil fuels and could serve as cheap and secure fuel for a combined heat and power system. A fuel cell-based cogeneration system that produces heat and power from municipal solid waste (MSW), could be a sustainable alternative to fossil fuels while reducing the negative environmental impact of MSW disposal and net GHG emission due to fossil fuels. Development of a commercially viable MSW/fuel cell CHP system is gradually attracting desired interest despite its early stage of research. South Africa, with the world's largest reserve of platinum group metal (PGM), could surmount the major obstacle which is the cost of the platinum catalysts. Integration of MSW (rich in biomass) gasification and fuel cell at moderate temperatures could produce an efficient CHP system. However, this proposed system is at a developmental stage and not ready for the successful implementation of the idea. Dearth of engineering and economic data make it difficult to fully exploit the potential of integrating an MSW gasification with HT PEMFC system.

1.5 Aim and Objectives of the Research

The aim of the thesis is to evaluate the technical and economic viability of municipal solid waste gasification to produce H_2 for use in a high temperature polymer electrolyte membrane fuel cell-based CHP system. The objectives of the research are;

i. to investigate physicochemical characterisation of MSW and evaluate possible environmental impact of heavy metals in MSW;
ii. to design appropriate processes to produce a RDF gasification system, that maximises hydrogen production and simulate gasification of MSW to produce H_2-rich syngas for use in HTPEMFC system;
iii. to perform economic evaluation of the system, including cumulative cash flow and profitability measurements

1.6 Research Questions

In order to carry out this investigation, the study will have to provide answers to the following questions:

What is the current state of MSW management, and the challenges facing the sector?

What are the required processes, reaction media and conditions that will ensure a significant hydrogen production from MSW?

What is the impact of steam flow rate and equivalent ratios on quality of hydrogen from MSW for fuel cell-based system?

What is the unit cost and at what price does the system break-even?

What is the techno-economic performance of the system driven by hydrogen from MSW?

1.7 The Scope of the Research

The focus of the study is to carry out simulations to produce hydrogen from MSW through modelling of thermochemical conversion processes. Physicochemical characterization of Refuse-derived fuel (RDF) to evaluate the potential of hydrogen production will be done. RDF will be produced from MSW for hydrogen production from modelling thermochemical conversion processes. Heavy metals in the RDF will be determined. The cost evaluation will be obtained utilising simulation results.

1.8 Motivation for the Study

The study is very pertinent to energy demand and environmental challenges of processes from conventional CHP systems. The demand for energy from fossil fuel options needs a viable alternative to rescue fossil fuel depletion and environmental challenges through the use of alternative clean fuel and environmental-friendly energy technology. This research explores the use of available alternative clean syngas fuel produced from solid waste through simulation. The clean fuel (hydrogen) will be produced through gasification simulation used in fuel cell-based systems. The simulated gasification system has a low toxic emission, unlike conventional systems. The cost-effectiveness and low GHG emissions of the CHP pose an encouraging effect on energy demand and environmental challenges from the conventional systems.

1.9 Expected Contributions to Knowledge

The research contribution to knowledge focuses on environmentally friendly thermochemical conversion of municipal solid waste. The study will use thermochemical conversion gasification processes to produce rich hydrogen syngas from municipal solid waste and the selected gasification process will enhance reduction of environmental impacts of municipal solid waste management.

Simulation of gasification processes is used to produce the rich hydrogen syngas from pre-treated municipal solid waste and techno-economic evaluation of the gasification processes is also considered

Thus, this research will contribute to existing knowledge by addressing municipal solid waste management challenges and exploitation of municipal solid wastes as alternative energy resources.

1.10 Thesis Outline

Chapter one discusses the background of the study on MSW, CHP system, energy resource challenges from a historical perspective. The importance of energy diversification of energy mix to address the problem of MSW management and energy challenges were also introduced. The rudiment of research with the aim and objectives to the expected contribution to knowledge are presented.

Chapter two focuses on a detailed review of various descriptions of MSW and the specific composition of MSW. The generation capacities of MSW across the globe are also discussed. Physicochemical characteristics of MSW, Physicochemical characterisation procedures and gasification technologies and general economic evaluation are discussed. The preferred type of gasification technologies is discussed in the light of specific environmental merits.

Chapter three discusses the methodology of this study. It involves a brief description of locations and MSW from municipal solid waste disposal facilities in Cape Town, followed by pre-treatment and pelletisation of pre-treated MSW. The physicochemical characterisation of pre-treated MSW, gasification procedures, quantification of heavy metal concentration and costing procedures are also discussed.

Chapter four presents the results of analyses. Bulk and loose densities and pre-treated MSW densified to RDF are presented. The experimental results of HHV, proximate and ultimate analyses and thermo-gravimetric analysis are presented and discussed. The need for alternative energy resources is elaborated on including Refuse-Derived Fuel (RDF) hydrogen production enhancement and RDF gasification reaction schemes.

Chapter five briefly discusses thermochemical conversion technology and the results data from the chosen thermochemical conversion technology via simulation of the gasifcation of RDF are presented and discussed. The complementary impact of the quality of RDF, steam flow rate and equivalence ratio are also discussed. The impacts of specific gasification reaction are also discussed as they influence a higher hydrogen concentration in the syngas.

Chapter six presents the results of the quantification of heavy metal and discusses possible environmental challenges arising from the distribution of heavy metals in pre-treated MSW.

Chapter seven presents an overall economic evaluation of the system comprising a gasifier and water-gas shift system. A number of profitability parameters are used to evaluate the economic evaluation of the system.

Chapter eight presents findings of the research, conclusions and provides recommendations for future research. The study was presented by highlighting the state of energy demand globally, limited energy resources and environmental challenges as well as potential use of MSW. The research seeks to evaluate the technical and economic feasibility of municipal solid waste gasification through simulation to produce H_2 for use in a fuel cell system. The following chapter will address the literature review of key areas of this research.

CHAPTER TWO

2 LITERATURE REVIEW

The literature review addresses complex characteristics of municipal solid waste (MSW), MSW management and the renewable potential of MSW. Physicochemical characterisation procedures, gasification technologies and possible environmental impacts are also discussed. The choice of fuel cell application for combined heat power system is reviewed, as well as the cost implications of the system.

2.1 Municipal Solid Waste and the Environment

Recently, municipal solid waste (MSW) has become a topic of interest because waste composition studies have indicated that household waste contributes around 60 % of MSW (Metin et al., 2003, Abu Qdais, 2007, Sharholy et al., 2007, Sharholy et al., 2008, Athanassiou and Zabaniotou, 2008, Imam et al., 2008, Alavi Moghadam et al., 2009, Arafat and Jijakli, 2013, Ogwueleka, 2013, Edjabou et al., 2015, Hla and Roberts, 2015, Gupta et al., 2015). The daily contribution of household solid wastes to overall MSW composition is very significant because they are potential alternative energy resources.

Domestic MSW generation is associated with the daily activities of human consumption in homes, commercial institutions, including park and garden solid waste. Unlike sewage effluents from municipal households which are often managed with a centralised drainage system, the bulk of solid waste generated requires more than a collection and disposal system to manage the daily municipal solid waste effectively. MSWs are different from other solid waste (such as heavy industrial waste, nuclear waste, heavy sludge, hazardous waste, e-waste, construction debris, and other industrial waste) because it is routinely produced.

A number of solid waste management approaches have classified solid waste in the following categories: municipal solid waste, industrial solid waste and hazardous solid waste. MSW is of a high priority because of its substantial daily generation around municipalities in which its management is critical for the well-being of society. MSW is composed of a diverse mixture of paper, plastics, sawdust, wood waste, leather, glass, rubber, e-waste, ceramics or debris, metals, textiles, bones, ashes, putrescible, yard wastes, and inert solid wastes (Athanassiou and Zabaniotou, 2008, Parfitt and Bridgwater, 2008, Burnley et al., 2011). Other classifications are presented in Table 2.1.

Before considering all the different definitions of MSW, it needs to be pointed out that some factors make a significant contribution to the nature and characteristics of MSW. The MSW physical characteristics are quite heterogeneous. Their proportions in the total MSW composition generated vary, depending on several factors.

These variations in the solid waste composition are economic conditions, geographical location, energy resources, climate, standards and styles of living, socio-economic factors, tourism, government policies, modes of consumption, cultural habits and industrial structures. These factors vary widely among regions, and the characteristics of MSW generated from the different locations show a significant variability in this regard (Wang and Geng, 2015, Al-Khatib et al., 2007, Tian et al., 2013, Song et al., 2013). The various sources and factors affecting the characteristics of municipal solid waste are illustrated in Figures 2.1 and 2.2.

Table 2.1: Some Classification of Municipal Solid Waste

Municipal Solid Waste Classifications	Focus	References
MSW consists of daily consumable items including recyclable materials like paper, plastics, textiles, metals, glass, yard wastes; organic materials; inorganic materials such as dirt, a small amount of construction waste and other miscellaneous materials	Composting and recyclable materials	Tian et al. (2013)
MSW are classified into two main categories: organics (food waste, green wastes, paper, textiles, rubber, and plastic) and inorganics (ash, tiles, glass, metal, and other inert materials).	Organic and inorganic	Xu et al. (2017) and Zhou et al. (2014a)
MSW is as a low-quality solid fuel (worthy of exploring and research interest) containing a high amount of moisture	Energy quality	Liang et al. (2008)
MSW is a mixture of combustible and non-combustible components with miscellaneous pollution sources	Combustible potentials	Dalai et al. (2009) and Chen et al. (2013)
MSW includes food waste, newsprint, corrugated cardboard, mixed cardboard, and plastics; polyethylene (PE), polypropylene (PP), polystyrene (PS), polyvinyl chloride (PVC) and polyethylene terephthalate (PET)	Combustible potentials	Alvarez et al. (2014) and Wu and Williams (2010a)
MSW was classified into six categories: organic waste (food waste, yard waste and other degradable fractions); papers (fine paper, newspaper, corrugated cardboard and other cellulose fibre compounds); plastics [polyethylene (PE), polystyrene (PS), polypropylene (PP), polyvinyl chloride (PVC) high-density polyethylene (HDPE), low-density polyethylene (LDPE), polypropylene (PP), polystyrene (PS) and polyethylene terephthalate (PET)]; metals (beverage and food cans made of aluminium, tin, steel and other metals); glass (food and beverage glass containers); other waste (miscellaneous waste such as rubber, leather and building construction debris). E-waste, toxic domestic waste and hazardous solid waste are not mentioned nor classified because they contribute less fraction of waste to the composition of MSW	Broad	Diaz and Warith (2006)

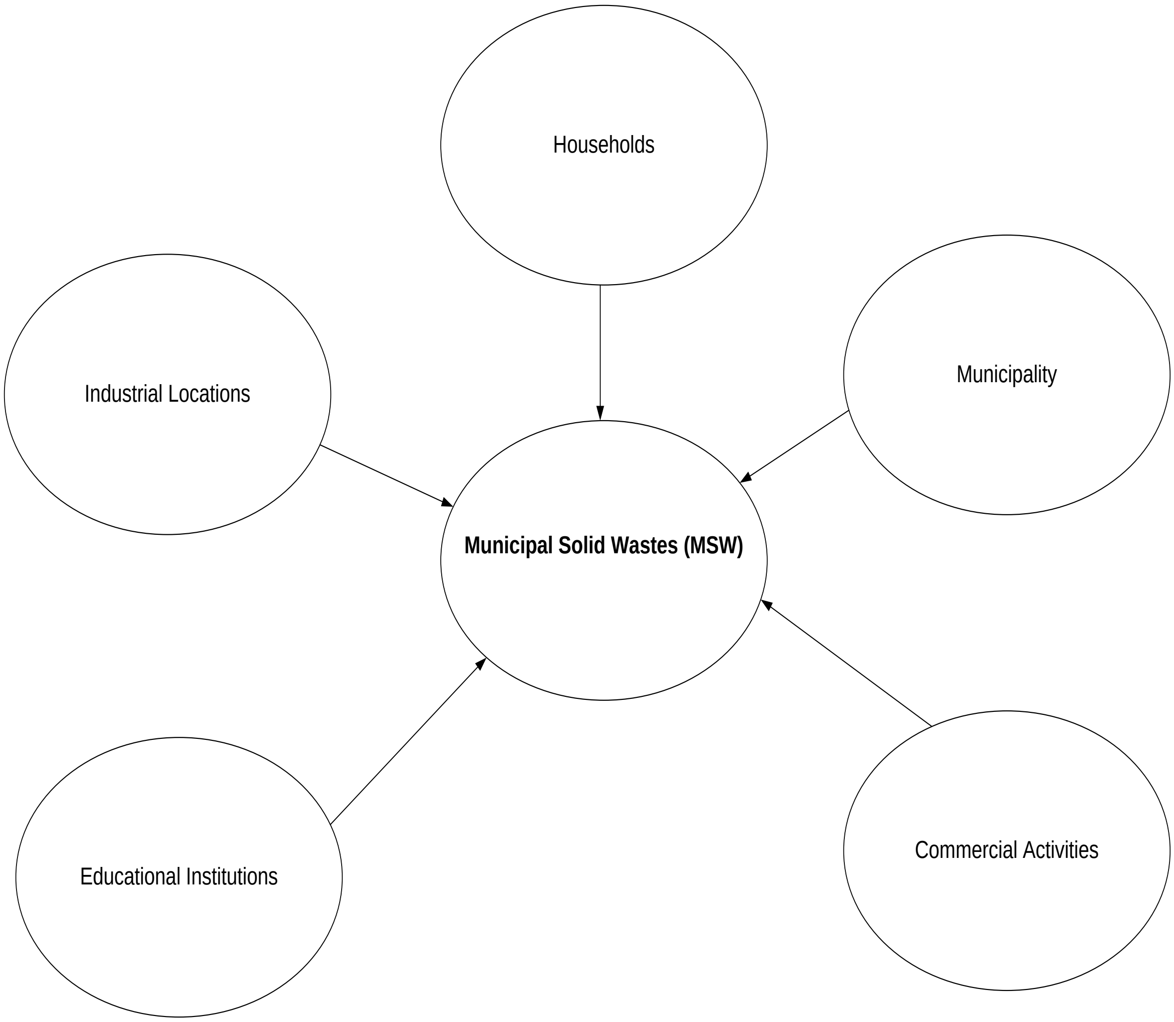

Figure 2.1: Re-defined Sources of Municipal Solid Waste (Song et al., 2004, Imam et al., 2008)

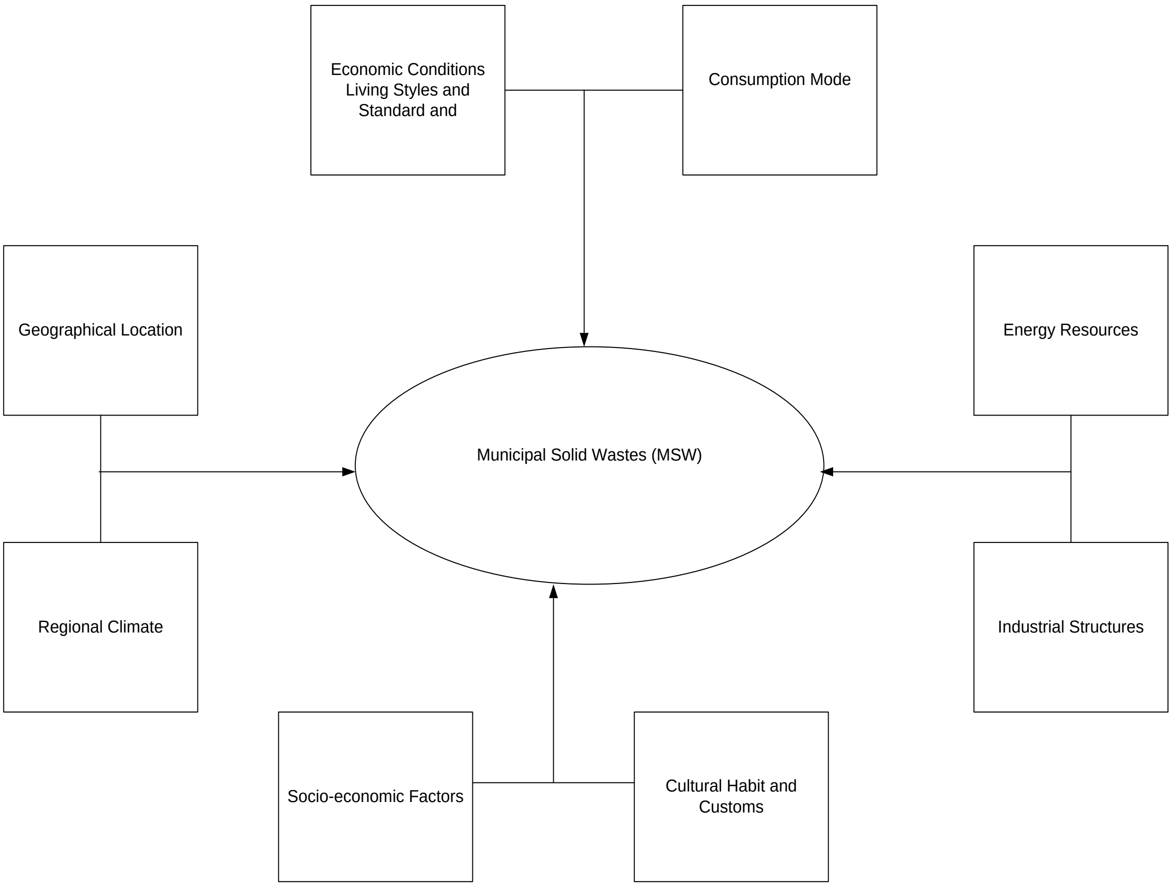

Figure 2.2: Factors Affecting the Characteristics of Municipal Solid Waste (Imam et al., 2008, Song et al., 2013)

From the different classifications discussed above, quite a few approaches have been used to describe MSW, including its physical characteristics, recycling and composting potentials, combustible and non-combustible substances, bio-resource capability, waste-sources approach and potential solid fuel. The extent of the diversity of the composition of the MSW, which is dependent on the sources of the solid waste, is evident in its physical appearance. The physical characteristics of MSW are diverse but a proportion of its chemical composition may be fairly uniform in all form of MSW. The solid fuel resource-based approach of MSW are useful because substantial part of MSW are re-use to harness its potential for solid fuel with a minimal adverse environmental footprint.

Thus, MSW in context of this study is referred to as solid waste emanating from households, municipalities, commercial activities, educational institutions and few industrials locations. The MSW will not include sludge (from wastewater treatment, pharmaceutical and dyeing processes), clinical solid waste, bulk e-waste, construction debris, etc. Some of the excluded solid waste may be found in the stream of MSW but the quantity will be insignificant. Now that the defined sources, compositions and the limitations, have been clarified, the focus can move to the formulation of a definition.

Therefore, MSW could be defined as solid waste with a high-energy resource base. The materials constituting MSW can be broadly divided into two categories, namely, combustible and non-combustible materials. The combustible components are organic materials, plastics, rubber, putrescible food waste, wood waste and textiles, while the non-combustible components are glass, metals, debris, and other inert substances. Combustible and non-combustible characteristics are reflections of the gasification potential of MSW as shown in Table 2.2. The combustible and non-combustible compositions of MSW are discussed in detail later in this chapter.

Table 2.2: Municipal Solid Waste Combustible Characteristics on Regional Basis

Regions	Combustible (wt. %)	Non-Combustible (wt. %)	Others (wt. %)
Asia			
Eastern Asia	67.30	5.80	26.90
South Central Asia	69.20	7.30	23.50
South Eastern Asia	77.10	7.30	15.60
West and Middle Asia	78.70	4.50	16.80
Africa			
Eastern Africa	76.90	7.30	15.80
Central Africa	73.70	8.00	18.30
Northern Africa	66.60	8.00	25.40
Southern Africa	77.20	20.30	2.50
Western Africa	88.00	3.10	8.90
Europe			
Eastern Europe	71.70	13.60	14.70
Northern Europe	79.40	15.00	-
Southern Europe	64.50	-	-
Western Europe	62.70	-	-
Oceania			
Australia and New Zealand	90.00	-	-
Rest of Oceania	76.00	-	-
America			
Northern America	76.10	12.00	11.90
Central America$^+$	83.10	13.50	4.40
Southern America	80.80	6.20	13.00
Caribbean	83.20	10.70	6.10

Source: IPCC Guideline for National Greenhouse Gas Inventories (International Panel on Climate Change and (IPCC), 2006)

2.2 Global Trends of Municipal Solid Waste Generations

Routine generation of municipal solid waste per individual is neither constant nor stable but varies because of a number of factors. One of these factors is that the world population is increasing. The average MSW generation in developing countries has been set at 0.70 - 0.80 Kg/capita/day while it is 0.40 - 2.27 Kg/capita/day in developed countries(Hui et al., 2006, Troschinetz and Mihelcic, 2009, Tian et al., 2013, Othman et al., 2013). The United States, China and India are global economic giants and the same trend has been experienced in the huge generation of MSW. The municipal solid waste generation has been lingering challenges across the world. Technological advancement, population growth, and economic prosperities are not unconnected with the huge generation of MSW(Fu et al., 2015, Song et al., 2017, Hwang et al., 2017).

The United States annual generation of MSW reached about 251 million tonnes with an approximate population of 315 million which is 4.43 % of the world population in 2012 (USEPA, 2015) while the corresponding MSW generation rates per capita in the United States had been reported to be higher than that of the previous average to around 1.20 - 2.00 Kg/capita/day between 1960 and 2013 (USEPA, 2015). 237 million tonnes of MSW are generated in the European Union (EU) annually with approximately a 20 % increase between 1995 and 2003 (European Commission, 2010). Thus, technological advancement, continuous urbanizations and population growth are contributing to this MSW generations. These are critical indices towards the challenges. Figure 2.3 illustrates the trend MSW generation and per capita MSW generation in the US while Figure 2.4 shows heterogenous properties and physical characterization of the US MSW.

Denmark and Australia have the highest contribution of MSW in Europe per capita while the United States and China contribute an amount which is more than the total MSW produced by Europe (Zhang et al., 2010). According to Dumble (2010), two members states from the Organisation for Economic Cooperation and Development (OECD), namely Denmark and Japan, had MSW generation rates of 2.27 and 1.04 Kg/capita/day respectively. These MSW generation rates from United State and other countries mentioned above are significant.

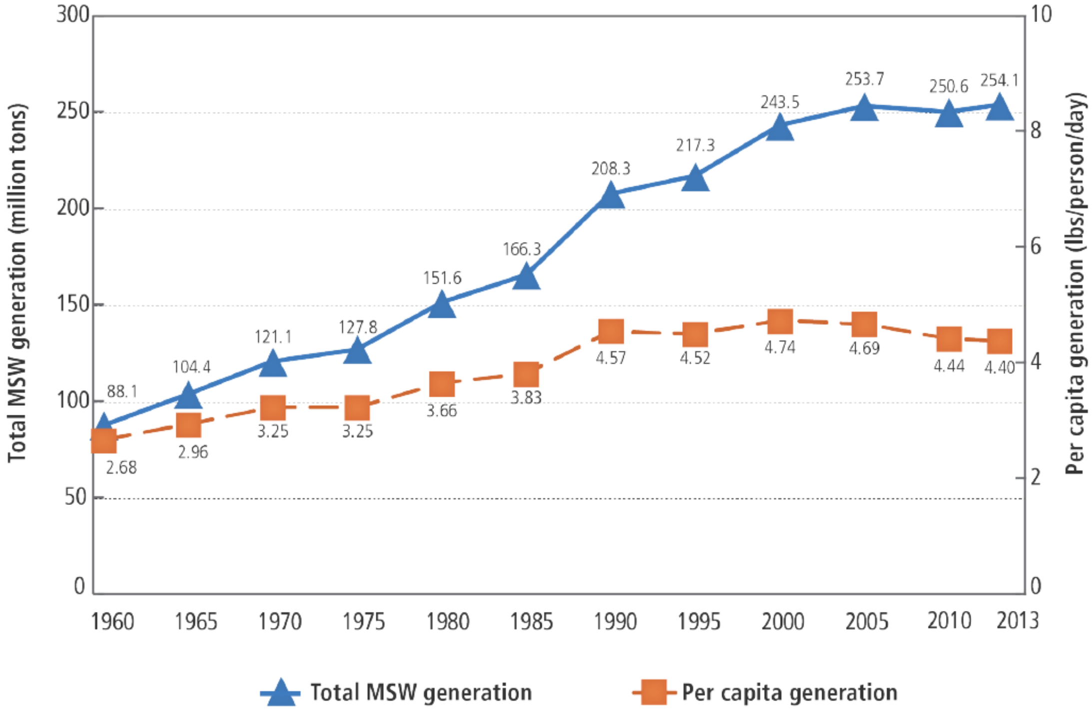

Figure 2.3: US MSW Generation Rates between 1960 to 2013 (USEPA, 2015).

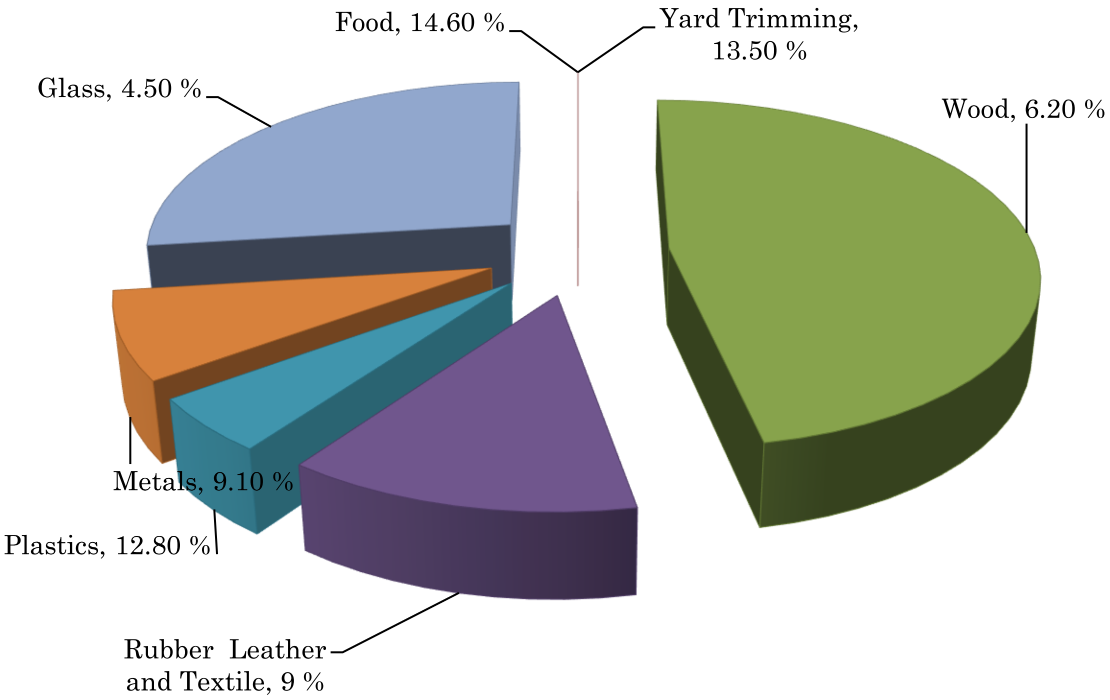

Figure 2.4: Total MSW Generations in US 2013 (USEPA, 2015).

Furthermore, the study of He et al. (2009c) reported that an approximate amount of 900 million tonnes of MSW are generated worldwide each year, with over 220 million tonnes with an annual growth rate of 8 – 10 % (Song et al., 2017) from China alone. There is no doubt that China is a big contributor to the production of global MSW. On average, the annual rate of increase from 1976 to 2006 was 7.1 %. It has been debated that the rapid growth of the urban population and GDP are the major drivers of this increase (Chen et al., 2010, China, 2011). Indeed, the percentage of MSW treated by incineration increased from 2.50 % in 2003 (3.70 million tonnes) to 14.70 % in 2010 (23.2 million tonnes) from 158 million tonnes of MSW (China, 2011). China's per capita waste generation rates have fallen between 0.80 - 1.10 Kg/capita/day, while a typically developed country generates between 1.43 - 2.08 Kg/capita/day (Troschinetz and Mihelcic, 2009, Hui et al., 2006, Tian et al., 2013).

The generation rate of MSW also varies among different cities in China. The cities of Beijing, Shanghai, Chongqing, Lhasa (Tibet) and Hangzhou have per capita waste generation rates of between 0.85 and 1.51 Kg/capita/day while Hong Kong has 1.33 Kg/capita/day (Ko and Poon, 2009, Zhang et al., 2010). Zhang et al. (2010) report a MSW rate of generation range of 0.47 - 1.32 Kg/capita/day for some selected developed countries around the world. It is obvious that the contribution of MSW from China is also very significant because of population growth and living standards and the amount of MSW generated is continually increasing.

In addition to the global MSW generations, India contributed over 17.50 % of MSW to the world population and New Delhi generation rate per capita was 0.50 Kg/capita/day (Singh et al., 2011). The amount of solid waste generated annually was around 48 million tonnes in 1997 with an annual growth rate of 4.25 % and was estimated to exceed 300 million tonnes by 2050 (Gupta and Garg, 2009, Central Pollution Control Board (CPCB), 2004, Singh et al., 2011). The quantity of MSW generated in some Asian countries surpassed one million tonnes/day (Hoornweg and Bhada-Tata, 2012) and it was estimated that by 2025, this figure would have increased to 2.00 million tonnes/day (Norbu et al., 2005, Hoornweg and Bhada-Tata, 2012, Menikpura et al., 2013). The MSW generation rate in New Delhi, India might be lower than that of United State but 17.50 % of MSW is significant.

In South America, Brazil, with the 5th largest population in the world of 196 million in 2011, the MSW was simply discarded in the environment. The quantity of MSW generated is almost 95 million annually, about 99 % of the solid waste generated in the country (Lino and Ismail, 2012). The municipal solid waste generation per capita in Brazil is 0.74 Kg/capita/day (Lino and Ismail, 2012).

The urban population is growing at an alarming rate in Africa. In West Africa, the city of Abuja, Nigeria had the highest growth rate in population between 1991 and 2006, with a 9.30 % increase even though it has the lowest population rate compared to the remaining thirty-six states. The projected population figures for the Abuja capital city predict massive growth with 5.80 million people expected by 2026. Abuja generates 492.17 tonnes of MSW per day. Also, the average solid waste generation rate in Abuja was found to be between 0.550 and 0.634 Kg/capita/day (Imam et al., 2008, Ogwueleka, 2013) while an average Nigerian generates about 0.49 Kg/capita/day from households and commercial activities and carries almost 90 % of the total urban solid waste burden. This is influenced by the time of year, local culture, traditions and personal income, among other factors (Solomon, 2009, Imam et al., 2008). According to Babayemi and Dauda (2009), the estimated waste generation per capita for Nigeria is about 0.58 Kg/capita/day but the studies of Abila (2014) and Somorin et al. (2017) reported another values of 0.53 and 0.80 Kg/capita/day respectively from various states across Nigeria. Though Nigeria is the most populated African country, there is a dearth of data for MSW annual growth rate and MSW contribution to world MSW.

On the contrary, the rates of MSW generation in South Africa in Kg/capita/day are available but not uniformly distributed, ranging from 0.28 to 2.10 Kg/capita/day. Guerrero et al. (2013) report that the rates of MSW generation for Pretoria, Langeberg and Emfuleni are 0.65, 0.65 and 0.60 Kg/capita/day respectively. The estimated values of MSW generated per capita for the Western Cape, Northern Cape, Gauteng and Mpumalanga are higher and they are 1.85, 1.50, 2.10 and 1.42 Kg/capita/day respectively when compared with other provinces (Department of Environmental Affairs, 2012).

However, an average of 0.96 Kg/capita/day was obtained for all the provinces. The study of Nahman et al. (2012) reported a lower estimated value of MSW generated to be 0.52 Kg/capita/day, having considered a different standard of living. South Africa generated approximately 108 million tonnes of solid waste in 2011, of which 90.74 % was disposed of at landfills. The classification of solid waste is not conclusive because 48 million tonnes are still left unclassified. 10 % of all MSW generated in South Africa was recycled in 2011 (DEA, 2102). The global trends of MSW generation require sustainable MSW management. Nevertheless, there are important energy resources that could be derived from this problem of MSW. Sustainable municipal solid waste management that will include adequate classification of MSW and will emphasise pre-treatments required towards ensuring the MSW management sustainability and MSW reused are essential. Moreover, renewable energy potential obtainable from MSW are presented in the next section.

2.3 Renewable Energy Resources: Biomass/Municipal Solid Waste

Renewable energy resources are now in the spotlight. Growing trends are towards a viable and sustainable alternative energy resource to meet the quest for reduction on environmental challenges and degradations suffered as a result of dependence on fossil fuels. Biomass is getting increased attention as a potential renewable energy resource. It has contributed more than 12 % of the world's total primary energy consumption (Li and Suzuki, 2009, Long et al., 2013, Basu, 2013, Halder et al., 2014). Biomass is naturally produced directly or indirectly from plant photosynthesis (Dai et al., 2012). Biomass basically contains non-fossilised biodegradable and organic material originating or derived from plants, animals and micro-organisms. It also includes products, by-products, residues and waste from agriculture, such as forestry, and related industries as well as biodegradable organic fractions of industrial solid waste and MSW (Loppinet-Serani et al., 2008, Long et al., 2013, Halder et al., 2014). Some MSW is derived and obtained from urban waste, wood waste and sawdust, agricultural residue, and putrescible solid waste or miscellaneous food waste and MSW are regarded as a renewable energy source(Song et al., 2017).

According to Corella and Sanz (2005), MSW shows more reactivity than coal because of its fast pyrolysis with very low ash content at lower temperatures. The fast pyrolysis processes and low ash at that temperature are required technical characteristics of MSW for an alternative use for production of syngas. Further processing of MSW and other derivatives of biomass could play a significant role in producing pre-treated MSW as solid fuel chemical feedstock. These characteristics reveal their potential to release energy for various applications (Li and Suzuki, 2009, Corella and Sanz, 2005, Long et al., 2013, Halder et al., 2014).

The virgin biomass and MSW derivative have comparable properties as these are important in bio-energy resources and applications. Lignin-cellulose characteristics of biomass show similar chemical properties with other derivatives found in the substantial combustible constituent of MSW (Long et al., 2013, Basu, 2013, Zhou et al., 2014b). Dai *et al.* (2012) classify MSW as one of the types of renewable biomass resources. The study further emphasises the importance of physicochemical characterisation of biomass to improve feeding reactor performance.

Relatively high quantities of combustible fraction of MSW has been reported in some cities of developing countries like Turkey (43 - 64 %) (Metin *et al.*, 2003), India (40 - 60 %) (Sharholy *et al.*, 2008), Jordan (54 - 78 %) (Abu Qdais, 2007), Nigeria (52 - 65 %) (Imam *et al.*, 2008) and Iran (80 - 88 %) (Alavi Moghadam et al., 2009). Although MSW includes other non-combustible, inorganic and inert waste, the largest (combustible) fraction of the MSW is essential for sustainable energy resources. This substantial (combustible) composition of MSW possesses physicochemical characteristics which are suitable for thermochemical conversion processes.

2.4 Municipal Solid Waste Management and Cape Town Status

Municipal solid waste management methods depend on waste-hierarchy preferential order of solid waste management from optimum minimization of MSW, re-use of MSW, recycle or compost of MSW, energy recovery from MSW and final disposal of MSW (Williams, 2015, Gharfalkar et al., 2015). The level of environmental awareness and technology advancement dictate the choice of municipal solid waste management (Arena, 2012). Landfills, open dumping, and incineration have been traditional methods of disposing of solid waste for centuries. The contemporary challenges have changed the focus towards a better awareness of the environmental implications municipal solid waste management methods (such as various emissions from landfills and incinerators) of disposal methods (Makarenko and Budak, 2017). There is an improved approach to landfill-sanitary landfill. The sanitary landfill involves an advanced engineering method of MSW management that minimize the environmental hazard. The operation sanitary landfill is systemic and guided by a standard procedure that includes surface filling, compacting to smallest volume, and final soil cover on a regular pattern (Youcai and Ziyang, 2017).

However, because of leachates and erosion, geographical location suitability and topography of the land are serious obstacles (Youcai and Ziyang, 2017, de Pauli et al., 2018). Recycling and composting are processes of material waste recovery (Hottle et al., 2015). Recycling involves obtaining substances from MSW (secondary raw materials) and use as a substitution of the primary raw materials in another application. Composting is biochemical decomposition of organic substances found in the MSW into a rich soil known as compost or to produce mainly biogas. On the other hand, energy recovery technologies allow to obtained volume reduction and energy recovery. Incineration was once regarded as a worthy technology for managing MSW because it reduces the volume and weight of the MSW (up to 70 % of the original MSW), generating alternative energy in some cases. There are still ongoing arguments about incineration and landfill treatments as shown in Figure 2.5.

Nonetheless, both incineration and landfill without pre-treatment of the MSW are associated with emissions of pollutants that are dangerous to land, water and atmosphere (Norbu et al., 2005, Assamoi and Lawryshyn, 2012).

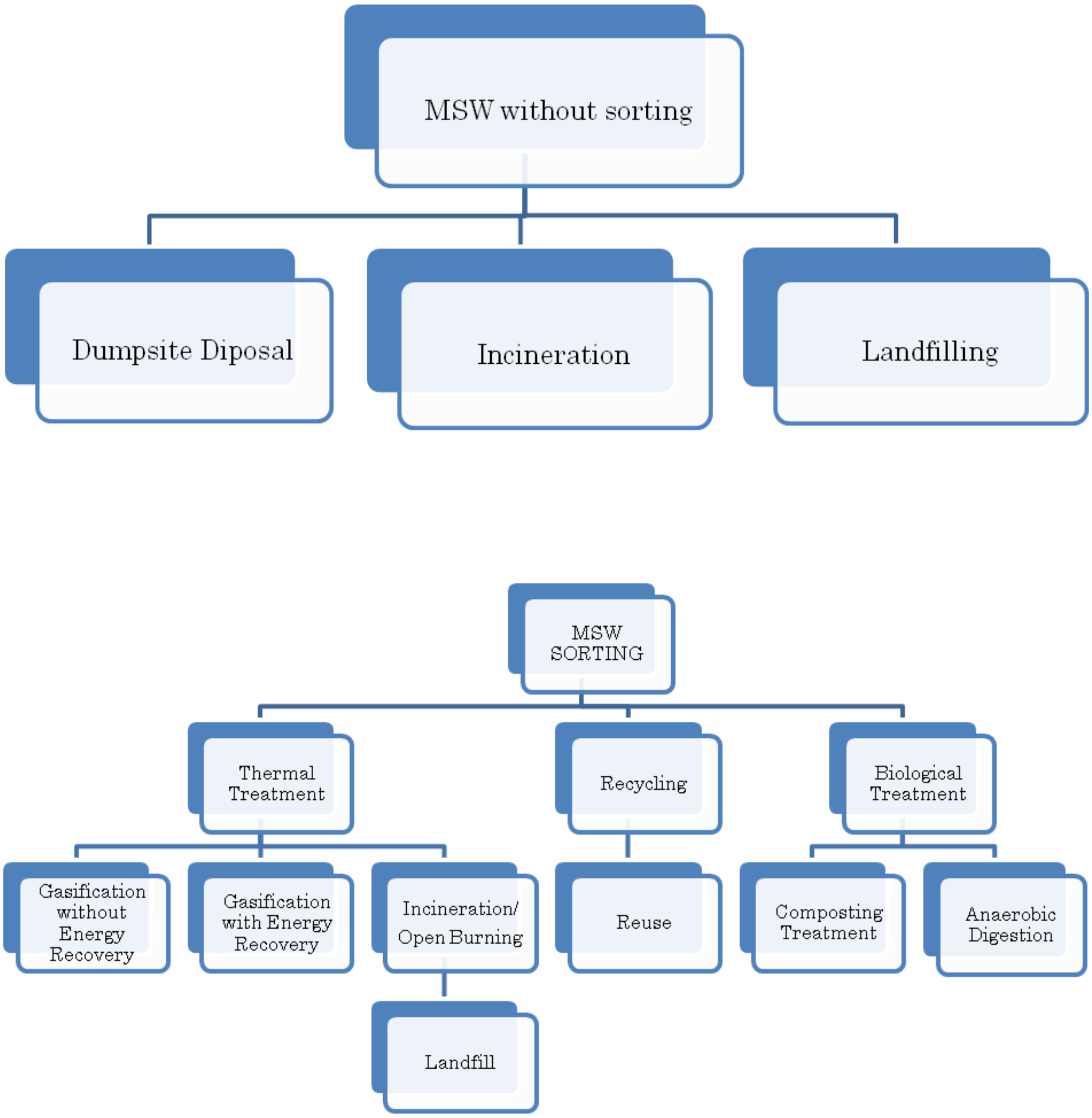

Figure 2.5: Various Technologies for MSW Management

Greenhouse gases (GHG), furan, dioxin and leachate, are some of the pollutants that originate from incineration and landfill. Normally, dioxins and furans are produced during combustion, but researchers used to assume that the high temperatures of thermochemical conversions caused by incineration might have destroyed the compounds. However, studies have confirmed a substantial presence of dioxin and furans in emissions together with others (such as fly ash and GHG,) (McKay, 2002, Cheng and Hu, 2010, Haiying et al., 2010). These methods of MSW disposal are still relevant in some developing countries due to cost implications and a lack of appropriate alternative technology.

Largely in most Africa countries, towns and cities lack regular nor standard waste collection and disposal services. Standard municipal solid waste management (MSW generation, sorting at the source, storage, collection, transfer and transport, pre-treatment/processing and disposal) (Singh et al., 2011) are not common. Poor infrastructure and lack or weak adherence to environment standard legislations are part main factors affecting the MSWM (Scarlat et al., 2015).

Waste landfilling is declining in developed countries due to advanced regulations encouraging waste reduction and recycling unlike developing countries. Landfilling is the main MSWM in South Africa and there are about 1203 landfill sites available in the country while less than 50% satisfies the required legislation and other pollution control requirements (Friedrich and Trois, 2013, Friedrich and Trois, 2010, Godfrey, 2008).
Over 2 million tonnes of MSW are disposed at municipal solid waste facilities annually in the City of Cape Town, South Africa. There were six landfill sites, and several private landfill sites (with or without regulation) responsible for landfilling of the MSW but only three of the six landfill sites are still active. The remaining three sites will soon attain their design capacities.

In order to minimize environmental effects, there is a need for sustainable cleaner technology to solve accumulation of daily generation of the MSW from more than one million households with around 3.7 million people. The MSW management efforts should be directed not only towards collection and disposal but minimization and treatments of MSW.

A number of initiatives (composting and material recovery facilities, awareness programmes on recycle and sorting procedure at source) to diversify the MSWM in Cape Town had been employed. The success rate of these initiatives was not encouraging and landfilling remains the predominant method of MSWM (Nahman, 2011). However, there are not exiting thermochemical technology utilized for MSWM or energy recovery in the City of Cape Town, South Africa.

Environmental-friendly technology should be the main priority where immediate effects of MSW disposal and its future challenges should be considered. Reduction in the amount of MSW used for landfill and the production of harmful emissions might assist in improving MSW management in short-term and particularly long-term prospects. This is because of the environmental implication of a continuous increase in the amount of MSW produced and disposed of. Specific procedures of gasification technology under controlled chemical reaction processes could be the viable technology for achieving the desirable eco-friendly technology and economic feasibility which could promote benefits to the environment, amongst other social considerations.

2.5 Composition and Physicochemical Characteristics of MSW

MSW is a mixture of solid waste from many sources such as households and commercial activities, farmyard waste and waste from educational institutions. The physical appearance of MSW shows its diverse and complex composition.

The physicochemical properties of MSW are an indication of its heterogeneous nature but a comprehensive chemical analysis of most pre-treated MSW confirms the potential trend of a homogeneous chemical composition (Tang et al., 2015, Zhou et al., 2014a).

These homogeneous chemical compositions are reflected in various analyses that measure high heating value, elemental composition analysis, proximate analysis and thermochemical degradation analysis. These procedures establish the inherent potential utilisation of chemical feedstocks and energy resource.

These MSW compositions are categorised into various classes, namely, recyclable solid waste (papers, plastics, glass, ferrous and non-ferrous metals, sawdust, wood waste, bones, debris and ceramics); compostable solid waste (putrescible yard waste, fruit and vegetable waste, bones, household food waste); biodegradable solid waste (paper, bones, putrescible yard waste, fruit and vegetable waste, textiles, leathers, households food waste); textile solid waste (fabrics, all forms of clothing, rubbers, leathers, wool and cotton); inert solid waste (debris, ceramics, sand and soil); non-combustible solid waste (glass, ferrous and non-ferrous metals, moisture content, ashes, debris and ceramics); combustible solid waste (paper, newsprint, corrugated cardboard, mixed cardboard); plastics (PE and PE derivatives); waste with animal, plant, mineral and synthetic sources (sawdust, wood waste, farmyard waste, bones, leathers, textiles); and rubber solid waste (natural and synthetic) (Zhang et al., 2010, Arena 2012, Zhou et al., 2014, Allegrini et al.,2014, Chen et al., 2015a, Czajczyńska et al., 2017). As discussed before, the classification of MSW for this study is mainly to consider two categories of classifications, namely, the combustible and non-combustible content of MSW.

2.5.1 The Non-Combustible Fraction of MSW

Human daily activities (goods and services) and the consumption of all the different forms of edible produce contribute to the non-combustible fraction of MSW. These also include MSW from construction and demolition sites, food packaging, etc. Essentially, they have no energy value as chemical feedstock or to produce direct energy. The non-combustible fraction influences the quality of MSW and they discussed in the following sections.

2.5.1.1 Non-Ferrous and Ferrous Metal Fractions of MSW

These fractions of MSW contain iron, steel, aluminium, tin, zinc, chromium, manganese, nickel, molybdenum, copper and titanium, while aluminium and steel are the only component of the metals that have recycling potential. Other metals are not always available in a significant quantity compared to steel and aluminium used in the production of tin cans. The metal component of the MSW stream is composed mainly of beverage and food cans used to preserve foods. The former is usually made of aluminium and the latter is made of steel and other metals. Generally, tin cans also contribute to the overall ash content of MSW and this may have an implication on the characterisation of combustion and processes of recovery. Large fractions of aluminium found in MSW come from beverage can, foil, and canned food (Diaz and Warith, 2006).

2.5.1.2 The Tin Can

Tin can be used as tinplate in canned food. The tinplate consists of layers of a low-carbon mild-steel base, iron-tin alloy, layer of pure tin and a layer of oxide. The chromium layer is deposited on the surface to prevent oxidation. The tinplate contains 99.75 % of the tin while the remaining steel base contains 0.05 % of manganese, chromium, molybdenum, and 0.04 % of nickel (Board and Vignaroli, 1976, Canned Food Information Service, 1988).

2.5.1.3 Aluminium

Aluminium metal is used for storage of many types of beverages, food, paste and drinks. Aluminium is usually added to iron, copper, zinc, chromium and manganese to produce an alloy which provides special qualities such as strength, improved formability and corrosion resistance (Jimenez and Kane, 1974). It is one of the most attractive materials for recovery from the waste stream. This is because aluminium recycling consumes far less energy (11.7 GJ/ton) than the smelting of aluminium ore (140 GJ/ton). It implies that its recycling and recovery cost implication is very attractive. Furthermore, while processing virgin aluminium, it generates emissions of perfluorocarbons (PFCs), among others, which are potent greenhouse gases.

2.5.1.4 Glass Fractions of MSW

Glass products are used for food and beverage containers, either clear (being transparent about its content) or coloured. It contains 75 % of SiO_2 compounds with other compounds like Na_2CO_3, CaO, MgO, ZnO, PbO and K_2O, Al_2O_3 and BaO (at various percentages for desired applications). The other compounds are for specific purposes such as colour and strength. Most of the glass recovery is from food and beverage containers. This fraction includes both coloured and clear glass bottles. Recycling glass is relatively easy because it involves rinsing, crushing and melting the glass containers. However, the process of glass recycling is an energy-intensive process at 1800 K. (Wang and Pereira, 1980) report on the large contribution made by recycling the glass component in MSW in Cape Town and the contribution that the virgin glass manufacturing process makes to the overall life cycle. Glass recycling reduces the environmental impact. A quantity of glass in the combustion stream may contribute to silicate derivatives present in ash after thermochemical conversion (Friedrich and. Trois 2010, Vossberg et al., 2014). Examples of non-combustible fractions of MSW are shown in Figure 2.6.

Figure 2.6: Several Types of Can and Glass Container Fractions of MSW

2.5.1.5 Ceramics, Debris, Moisture Content and Ashes Fractions of MSW

Ceramics, debris, moisture content and ash fractions are non-combustible components and they reduce the heating value of derived solid waste if they are not separated. Some of these components are inert and are not reactive components of MSW. They cannot produce useful energy. Moisture and ash composition make a significant contribution to the low quality of energy that can be produced from MSW (Narobe et al., 2014). The separation of these components of MSW is essential for the quality of MSW for potential energy resources.

2.5.2 The Combustible Fraction of MSW

The combustible characteristics of MSW prove that MSW has the potential for solid fuel considerations. Putrescible wood waste, leather and textile materials, paper, plastics, biomass/farmyard waste, and leather are examples of common combustible solid waste.

2.5.2.1 Leather and Textile Material of MSW

Both leather and textiles are derived from animal, synthetic fibre and plant sources. The combustion characteristics of leather and textile solid waste are essential though their quantity in MSW is not significant and may not be worth consideration. The elemental composition of leather textiles is generally similar. The HHV of textile materials is relatively high, due to the low ash content. (Zhou et al., 2014b). The contribution of leather in MSW may not be relevant to the required characteristics of potential solid fuel because of their low quantity in MSW.

2.5.2.2 Paper Formation Fractions in MSW

Virgin and recycled paper are processed in essentially the same manner. Paper belongs to the field of polymeric materials (Monica, 2009). A paper typically contains 90 - 99 %

cellulose fibres which are the main structural elements (Zhou et al., 2014b). Paper network is composed of randomly laid fibrous (cellulose) and non-fibrous (fillers) materials, thus it contains a complicated set of cavity pore channels with a variety of capillary dimensions (Sahin and Arslan, 2008). These fibres degrade in the recycling process, so paper cannot be reused indefinitely. Four different kinds of paper are usually considered for recycling, namely, newspaper (largest fraction of paper); the largest fraction of paper recycled (USEPA, 2002); fine paper (printing and photocopying); mixed papers (unsorted paper waste); and cardboard for book binding.

Paper at high temperatures and low relative humidity can become brittle, while paper creeps more rapidly in a moist environment (Monica, 2009). The average HHV of paper is around 15.894 MJ/kg but ranges from13.445 MJ/kg to 19.277 MJ/kg (Zhou et al., 2014b). The importance of paper in MSW cannot be overlooked due to its CHO ratio in its chemical composition. This chemical composition is the sole indicator for energy recovery and recycling purposes though the potential of recycling has a time limit that affects the quality of paper production. Figure 2.7 shows the physical and chemical composition of cellulose which major component of paper.

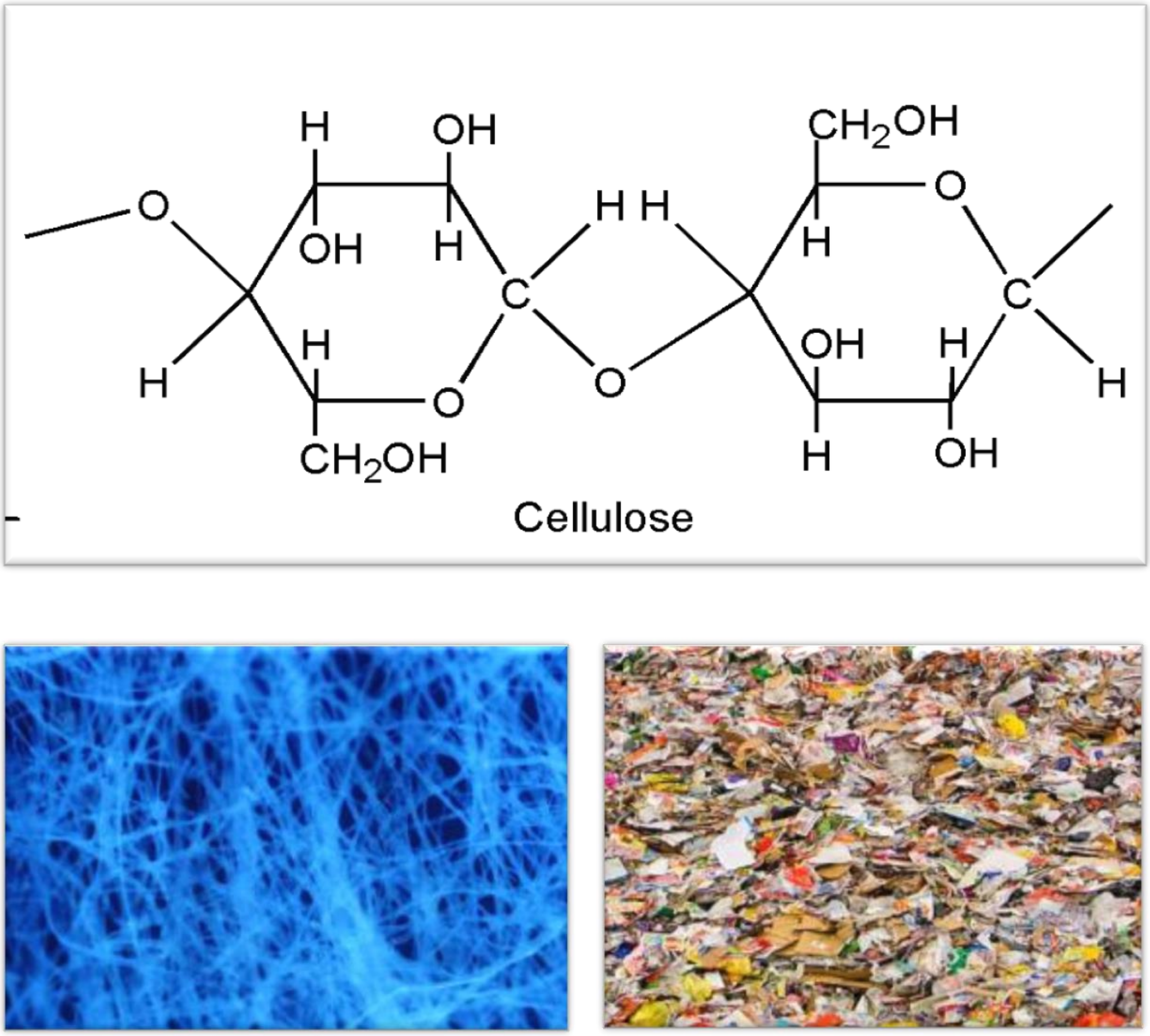

Figure 2.7: Structure of Cellulose, Micrograph and Waste Major Components of Paper

2.5.2.3 Plastics/Polymer Fractions of MSW

Plastics are macromolecules that are products of polymerisation. Often plastics are not properly defined to encompass their various derivatives and are often over-simplified (Zhou et al., 2014b). Plastics can be broadly divided into three categories, such as thermoplastics, thermosets and elastomers (Figure 2.8) Thermo-plastics are affected by difference phases, namely, they become reversible during heating and cooling, solid at room temperature and liquid at elevated temperatures. Examples are polyethylene (PE), polypropylene (PP), high-density polyethylene (HDPE), cross-linked polyethylene (CLPE), low-density polyethylene (LDPE), Polyvinyl chloride (PVC), Polystyrene (PS), Acrylics (PMMA-polymethyl methacrylate), Polyamide (nylon), polyethylene terephthalate (PET) and polytetrafluoroethylene (PTFE).

2.5.2.4 The Broad Classification of Plastics Available in MSW

Thermoset polymers are irreversible in the heating and cooling phase. Examples are melamine formaldehyde (Formica), phenolics (bakelite), unsaturated polyesters, epoxies and resins and other composites. Elastomers are elastic in behaviour when under load, also known as rubber. Typical uses are medical masks, gloves and rubber-substitutes. Synthetic rubber examples are butadiene rubber, butyl rubber, chloroprene rubber, ethylene-propylene rubber, isoprene rubber, nitrile rubber, polyurethanes, silicones, styrene-butadiene rubber (SBR) and thermoplastic elastomers (Kotz et al., 2010).

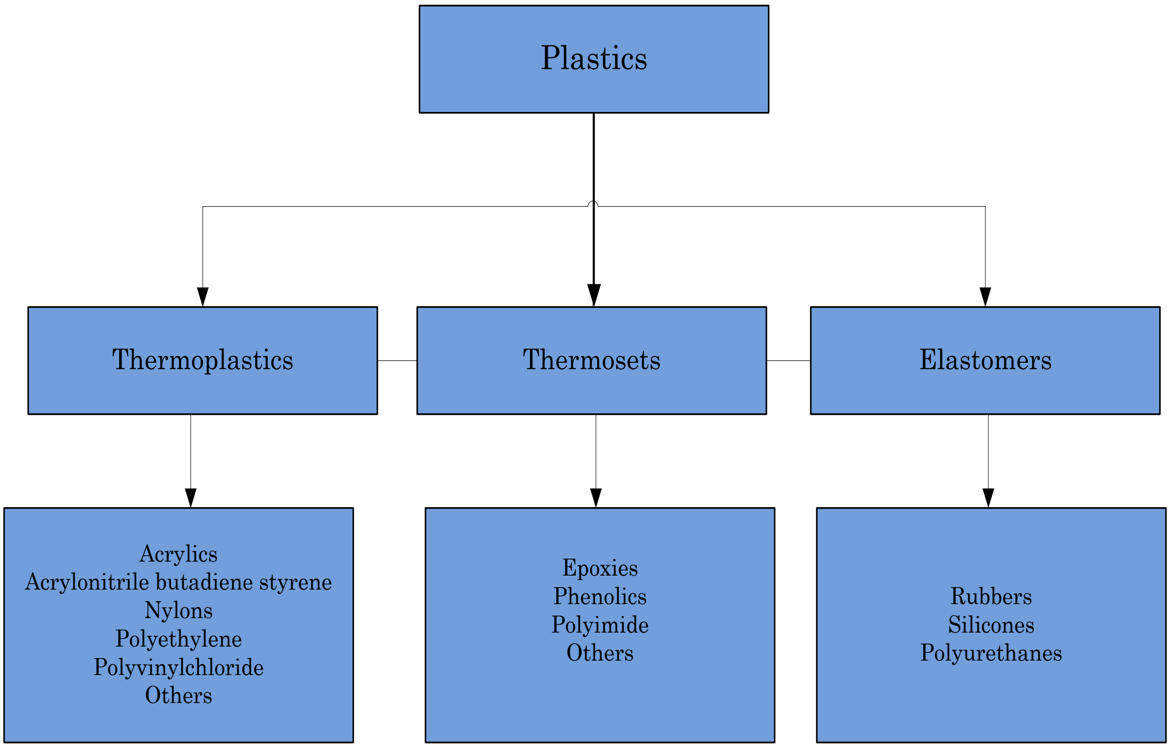

Figure 2.8: The Broad Classification of Plastics Available in MSW

Although the technology to recycle most plastics exists, the sorting and preparation processes are complex. In general, only the most valuable, high-volume plastics are recovered. The process of plastic recycling is very sensitive to contaminants small fraction of different plastic may affect the quality of plastic production (Kelly, 1996).

The default fraction of the total plastics that are recycled is based on the EPA GHG Inventory (USEPA, 2002). PE and its derivatives are commonly used polymers. They are used for wrapping and packaging; HDPE is used in bottles, containers and toys. PET is impermeable to gases and is widely used as a container for carbonated beverages; it is also used to contain other foods and beverages. PS materials are used in containers to insulate foods. PP is used in containers for syrup bottles and yoghurt tubs.

PVC finds application mainly in plastic pipes (Diaz and Warith, 2006). Most recycled plastics are from durable goods non-durable goods and packings. Packings and containers were mostly recovered through recycling up to 15 % of plastic waste in the US in 2013 (USEPA, 2015). More polymer plastics are derived from PE to suit desired and specific purposes like hardness, density, resistance to heat, organic solvent and oxidation and ionisation radiation. All these types of plastic are not equally distributed in quantity in MSW. The physical characterisation of plastic content in MSW reveals LDPE and HDPE which are more than other plastic derivatives. The Figure 2.8 shown general classification of plastics while Figure 2.9 gives examples of plastics and chemical formula indicating the C-H-O ratios.

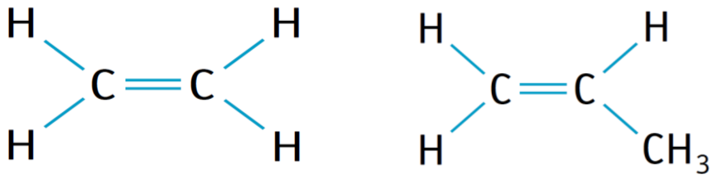

Ethylene

Propylene

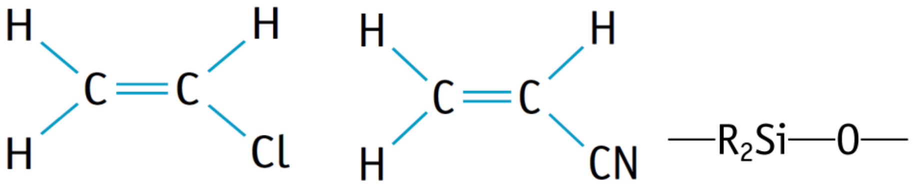

Vinyl Chloride

Acrylonitrile

Silicones

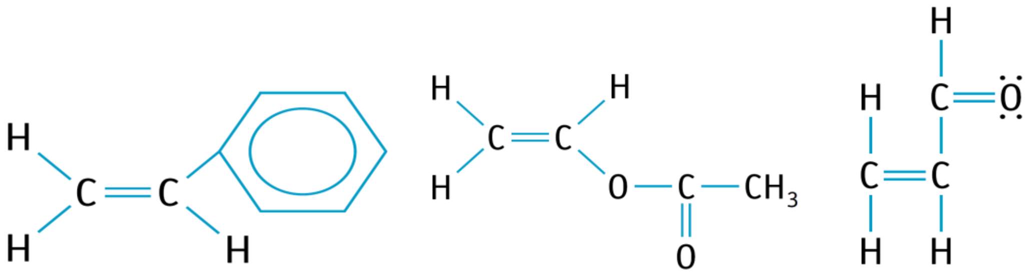

Styrene

Vinyl Acetate

Acrolein

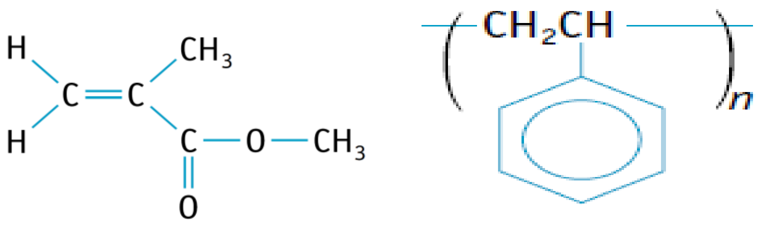

Methyl methacrylate

Polystyrene

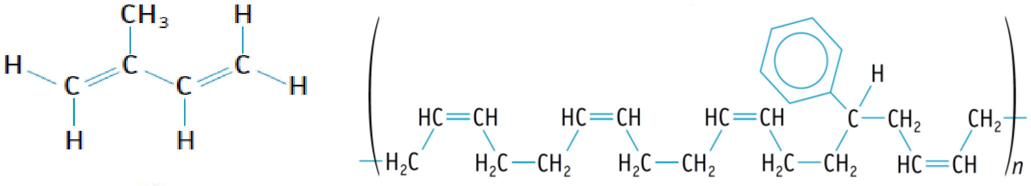

Isoprene

Styrene-butadiene Rubber

Figure 2.9: Structural Formulation of Plastic and Its Derivatives (Kotz et al., 2010)

2.5.3 Biomass and Farmyard Waste Fraction of MSW

Other types of polymer are biomass products. Primary biomass resources are categorised into two main types: virgin and waste biomass. Virgin or fresh biomass is available in natural habitats, but secondary or waste biomass are derived products which are not available immediately. Some species of aquatic biomass are other sources of virgin biomass and are not considered in this study, although they have higher net organic yields compared to most terrestrial biomass. The growth or replacement rate of biomass, it is a renewable resource, is an important parameter in the assessment of its availability. The following are sources of biomass: agricultural and forest products (food grain, bagasse (crushed sugarcane), corn stalks, straw, seed hulls, nutshells and manure from cattle, poultry, trees, wood waste, wood or bark, sawdust, timber slash, mill scrap and hogs) (Fatih Demirbas et al., 2011); biological solid waste (animal waste, aquatic species and biological waste); energy crops (poplars, willows, switch grass, alfalfa, prairie bluestem, corn, soybean, and canola); and MSW (sewage sludge, refuse-derived fuel (RDF), food waste, waste paper and yard clippings and trimmings) (Basu, 2013). Carbohydrates, fats, and proteins are a key complex mixture of organic substances present in biomass while inorganic constituents are small fractions of minerals such as sodium, phosphorus, calcium and iron.

The main physical components of plant biomass are extractives, fibre or cell wall components and ash. Wood and its residues are the principal constituents of the biomass resource base. The composition of wood or forestry biomass cells are a polymeric formation of the cellulose cell walls and other constituents. The composition varies widely but wood or forestry biomass cells are basically made up of three major polymers: cellulose, hemicelluloses and lignin (Basu, 2013). Examples of biomass physicochemical structures are presented in Figure 2.10.

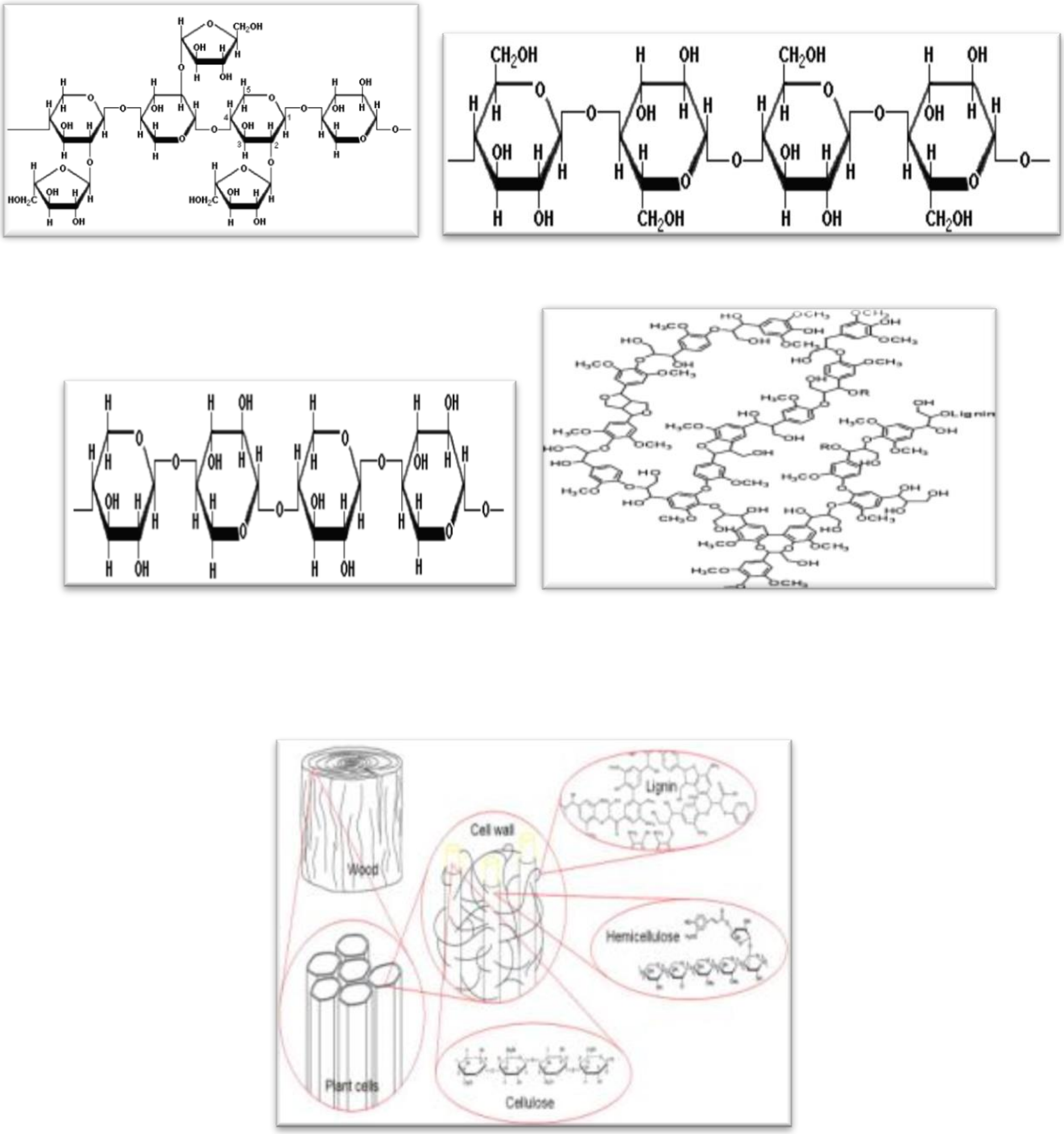

Figure 2.10: Major Compositions of Biomass, Cellulose, Hemicellulose, Lignin and the Distribution of the Compositions of Wood (Basu,2013).

2.5.3.1 Cellulose

Cellulose is the most common and abundant organic compound and is the primary structural component of the cell walls in biomass. Its amount varies from 90 % (by weight) in cotton to 33 % for most plants. Cellulose $(C_6H_{10}O_5)n$ is a long-chain polymer with a high degree of polymerisation (< 10,000 < x< 500,000) molecular weight. Cellulose is a homopolysaccharide composed of b-D-glucopyranose units linked together by (1-4)-glycosidic bonds. The basic repeating unit of the cellulose polymer consists of two glucose anhydride units, called a cellobiose unit (Mohan et al., 2006). This structure (Figure 2.10) gives it high strength, with a skeletal structure of most of the terrestrial biomass. It is highly insoluble, and its carbohydrate polymer is not digestible by humans. It is a dominant component of wood, making up about 40 - 47 % by dry weight (Fatih Demirbas et al., 2011, Basu, 2010, Basu, 2013). Cellulose is a major contributor of tar during the gasification of biomass. The tar formation is critical to the gasification reaction product distributions.

2.5.3.2 Hemicellulose

Hemicellulose is another constituent of the cell walls of a plant which is also known as polyose. Hemicelluloses are derived from chains of pentose sugars and act as the binding material holding together the cellulose, micells and fibre (Fatih Demirbas et al., 2011). It is a group of branched chain carbohydrates and has a lower degree of polymerisation (DP < 100 - 200) unlike cellulose and may be represented by the generic formula $(C_5H_8O_4)n$. Hemicellulose tends to yield more gases and less tar than cellulose (Milne, 2002). It is soluble in weak alkaline solutions and is easily hydrolysed by a dilute acid or base. It constitutes about 20 - 30 % of the dry weight of most wood (Basu, 2013).

Hemicellulose may contribute to reduction in tar, reduce the challenges of gasification processes and enhance syngas productions.

2.5.3.3 Lignin

Lignin is a complex, highly branched polymer of phenyl propane and is an integral part of the secondary cell wall of plants. It is one of the most abundant organic polymers (except for cellulose). The lignin generic polymer structure is $[C_9H_{10}O_5(OCH_3)_{0.9\text{-}1.7}]n$. It is an aromatic polymer synthesised from phenylpropanoid precursors (Fatih Demirbas et al., 2011). It is the cementing agent for cellulose fibres holding adjacent cells together. The dominant monomeric units in the polymers are benzene rings (Figure 2.9). These benzenes rings may have relationships with non-condensable tar. intermediate products of thermochemical conversions. It is similar to glue in a cardboard box, which is made by gluing together papers in a special fashion. Lignin is highly insoluble, even in sulphuric acid. A typical hardwood contains about 18 - 25 % of the dry weight of lignin, while softwood contains 25 - 35 % (Fatih Demirbas et al., 2011, Basu, 2013).

Biomass in the form farmyard waste is the fourth largest source of energy in the world. Accordingly, it has been considered as a possible major source for hydrogen production in the future (Ni et al., 2006, Saxena et al., 2008). Furthermore, these materials can also be very useful for the selective production of higher value-added products, such as light olefins (Artetxe et al., 2012, Alvarez et al., 2014). The C-H-O content of farmyard waste has an insignificant composition of CI because the components of wood waste are very simple. However, the HHV of wood waste has been reported to be approximately 19.461 MJ/kg which is higher than that of food waste because of lower ash content (Zhou et al., 2014b). These important properties show a significant use in thermochemical conversion.

2.5.4 The Miscellaneous Food Waste Fractions of MSW

The average moisture content of some food is usually high (69.85 %) because food residue (a mixture of a number of organic substances) consists of many high moisture components, such as vegetable food waste and fruit peels since fruit and vegetables are usually consumed daily (Zhou et al., 2014b).

Carbon dioxide emission is an indication of potential calories of energy which are available in solid food waste. Food waste is generated largely from the handling and processing of fruit-and-vegetable (Kosseva, 2011). The putrescible and organic fraction of MSW and sludge represents a significant quantity of biodegradable solid waste generated in the European Union (EU) (Righi et al., 2013). The European Commission (2010) reports an estimated amount of about 88 million tonnes of bio-waste derived from municipal solid waste by the member states. Indeed, this is a huge amount of solid food waste.

Historically, a large part of biodegradable waste was landfilled, contributing to air, water and land pollution. Diversion of biodegradable MSW from landfill was the main objective of the Directive 1999/31/EC, which required member states to reduce the amount of biodegradable waste used for landfill to 35 % by 2016 (Righi et al., 2013). The volumes MSW from modern societies have increased out of which, a large fraction is food waste. The annual generation of food waste in Singapore was 542,700 tonnes in 2006 and increased to 570,000 tonnes in 2008 (NEA (National Environmental Agency), 2009).

Proper treatment and management of food waste is a challenge faced by aspiring developing countries as untreated and uncontrolled food waste creates odour, hygiene challenges and causes an adverse environmental impact. Some food waste has been used in co-pelletisation to produce useful pellets which are under consideration for co-gasification (Ryu et al., 2008).

Singapore is highly populated, with limited land area that can be used for landfill though the landfill approach has its environmental demerits (Khoo et al., 2010).

Most solid food waste in Singapore is sent to incinerators (Tan and Khoo, 2006). According to the Singapore Green Plan 2012, up to 30 % of solid food waste recycling has to be achieved by 2012 (MEWR (Ministry of the Environment and Water Resources), 2012).

The major components of food are shown in Zhou et al. (2014b) report that the ash content as dry basis of food residue is 20.98 % lower than that of MSW. The volatile matter of solid food residue is 66.79 %. The elemental composition of food waste follows the sequences: C > O > H > N > Cl > S. The average C content is 47.22 % and the confidence interval is narrow. The nitrogen content of food residue is as high as 3.86 % because meat, fruit, and vegetables contain a high content of protein. The Cl content of food residue is also very high, mainly because of the salt. In China, the average HHV of food residue is 15.386 MJ/kg as a dry basis, higher than the average value of MSW. The HHV of food residue varies greatly, because of the complexity of food residue (Zhou et al., 2014b).

2.6 Solid Fuel Feedstock Chemical Characterisation

The chemical characteristics of MSW should be considered for thermochemical conversion. The main characteristic of combustible MSW substance is the ability to produce chemical feedstock and direct energy production. Physicochemical analyses usually reveal these potentials. The analyses are the following: elemental analysis, proximate analysis, thermal analysis, mass loss analysis or the analysis of vaporisation, the analysis of high heating value distribution and the analysis of some metals distribution.

The chemical characterisation of solid fuel feedstock is an essential analysis and an important part of the determination of the potential of chemical composition of solid fuels (Green and Perry, 2008, Zhou et al., 2014b, Chen et al., 2015b, Soltani et al., Shi et al., 2016, Soltani et al., 2016).

It gives critical information on the solid fuel that is needed for a rational design or better understanding of a process. The pre-treated MSW is usually characterised in order to determine its proximate and ultimate gross heating and thermo-gravimetric value (Basu, 2013, Narobe et al., 2014).

2.6.1 Proximate Analysis

The proximate analysis provides the composition of the fuel feedstock in terms of gross components such as moisture (M), volatile matter (VM), ash (ASH) and fixed carbon (FC). It is a relatively simple and inexpensive process that is carried out in accordance with the ASTM 3172 - 73 (84) (ASTM Standard and ASTM D 3172-73(84), 1989a).

2.6.1.1 Volatile Matter

The volatile matter (VM) of a fuel is the condensable and non-condensable vapour released when the fuel is heated. It consists of a mixture of short and long-chain hydrocarbon and aromatic compounds. Its amount depends on the rate of heating and the temperature at which it is heated. The volatile matter contents are obtained in accordance with the ASTM 3175-89 (ASTM Standard and ASTMD 3147-89, 1989b).

2.6.1.2 Ash

Ash is the inorganic solid residue left after the fuel is completely burned. Its primary ingredients are silica, aluminium, iron and calcium. Small amounts of magnesium, titanium, sodium, and potassium may also be present (Wang et al. (2014b)). These heavy metals have diverse challenges such as slagging, sintering and leaching potentials.

However, ash residue does not represent the initial inorganic components of mineral matter present in the solid fuel, as some of the ash constituents can undergo oxidation during burning which is an important oxidation process.

The ash content of biomass is generally very small but may play a significant role in biomass utilisation especially if it contains alkali metals such as potassium or halides such as chlorine (Mettanant et al., 2009a, Mettanant et al., 2009b). The ash obtained from biomass conversion does not always come entirely from the biomass but also during handling and processing (Basu, 2013). The ash content analysis is carried out in accordance with the ASTM 3174-89 (ASTM Standard and ASTM D 3174-89, 1989c).

2.6.1.3 Moisture Content

High moisture content (MC) is a major characteristic of biomass. The total moisture content of some biomass can be as high as 90 % (d.b). Moisture drains much of the deliverable energy from a gasification plant, as the energy used in evaporation is not recovered. The moisture and ash contents have a great impact on net HHV and the combustion characteristics of MSW. This important input parameter for design must be known when assessing the cost of transportation and energy penalty in drying (Liang *et al.*, 2008). The moisture content is usually obtained in accordance with the ASTM 3173-87 (ASTM Standard and ASTM D 3173-87, 1989d).

2.6.1.4 Fixed Carbon

Fixed carbon (FC) in a fuel is usually determined from the following equation, where M, VM, and ASH stand for moisture, volatile matter and ash, respectively (Basu, 2013).

$$FC = 1 - M - VM - Ash \tag{2.1}$$

This represents the solid carbon in the biomass that remains in the char in the pyrolysis process after devolatilisation. With coal, in the determination of VM, FC includes elemental carbon in the original fuel plus any carbonaceous residue formed while heating (ASTM Standard D- 3175a).

During the determination of VM, a part of the organic carbon is transformed into a carbonaceous material called pyrolytic carbon. Since FC depends on the amount of VM, it is not determined directly. VM also varies with the rate of heating.

In a real sense, then, fixed carbon is not a fixed quantity, but its value, measured under standard conditions, gives a useful evaluation parameter of the fuel. For gasification analysis, FC is an important parameter because in most gasifiers the conversion of fixed carbon into gas determines the rate of gasification and its yield. This conversion reaction, being the slowest, is used to determine the size of the boudouard reaction of the gasifier.

2.6.1.5 Char

Char which is a carbon residue of pyrolysis or devolatilisation is not a pure carbon; neither is it a fixed carbon of the biomass. It is known as pyrolytic char and contains some volatiles and ash in addition to fixed carbon. Biomass char is very reactive. It is highly porous and does not cake. It does partake in further reaction to release useful gaseous products.

2.6.2 Ultimate Analysis

This analysis shows the composition of the carbonaceous fuel in terms of its basic elements except for its moisture, and inorganic constituents, ash. A typical ultimate analysis is:

$$C + H + N + S + Ash + M = 100\ \% \qquad (2.2)$$

Not all solid fuels contain these elements. For example, the clear majority of biomass may not contain any sulphur. The moisture content in the fuel is expressed separately as M. Thus, hydrogen or oxygen in the ultimate analysis does not include the hydrogen and oxygen in the moisture, but only the hydrogen and oxygen present in the organic components of the fuel. Lignin-cellulosic biomass has very relatively high amounts of oxygen and hydrogen, which results in relatively low heating values - low grade solid fuel.

2.6.3 High Heating Value (HHV)

The high heating value (HHV) can be measured in a bomb calorimeter using ASTM standard D-2015-85. The bomb calorimeter consists of a pressurised oxygen “bomb” (30 bar), which houses the fuel. A stirrer stirs the water continuously. Initially, the temperature change is small as the only heat generated is from the stirring of the water molecules. As the product of combustion is cooled below the condensation temperature of water, this technique gives the HHV of the fuel. It is one of the most important properties of energy fuel. Compared to most fossil fuels, the heating value of MSW is usually low. The high heating value is measured in MJ/kg and various predictive measures are used to obtained HHV (Channiwala and Parikh 2002, Zhou et al. 2014, Qian et al., 2016).

2.6.4 Thermo-Gravimetric Analysis

Thermo-gravimetric analysis (TGA) instruments determine a host of parameters categorised into quantitative and qualitative characteristics. These parameters are moisture loss, decarboxylation, ash, thermal stability of substance, sample components, loss of solvent, loss of plasticiser, oxidation, and characteristics of dissociating temperature and decomposition kinetics. The TGA processes involve dehydration, polymorphic stage transitions and solid state and melting transitions (Crouch et al., 2007). The operation of this apparatus is based on the change in weight of the sample with change in temperature (Figure 2.11). Using the TGA method, the mass losses of the sample are monitored over time, while the sample is subjected to a pre-defined heating rate (Basu, 2013).

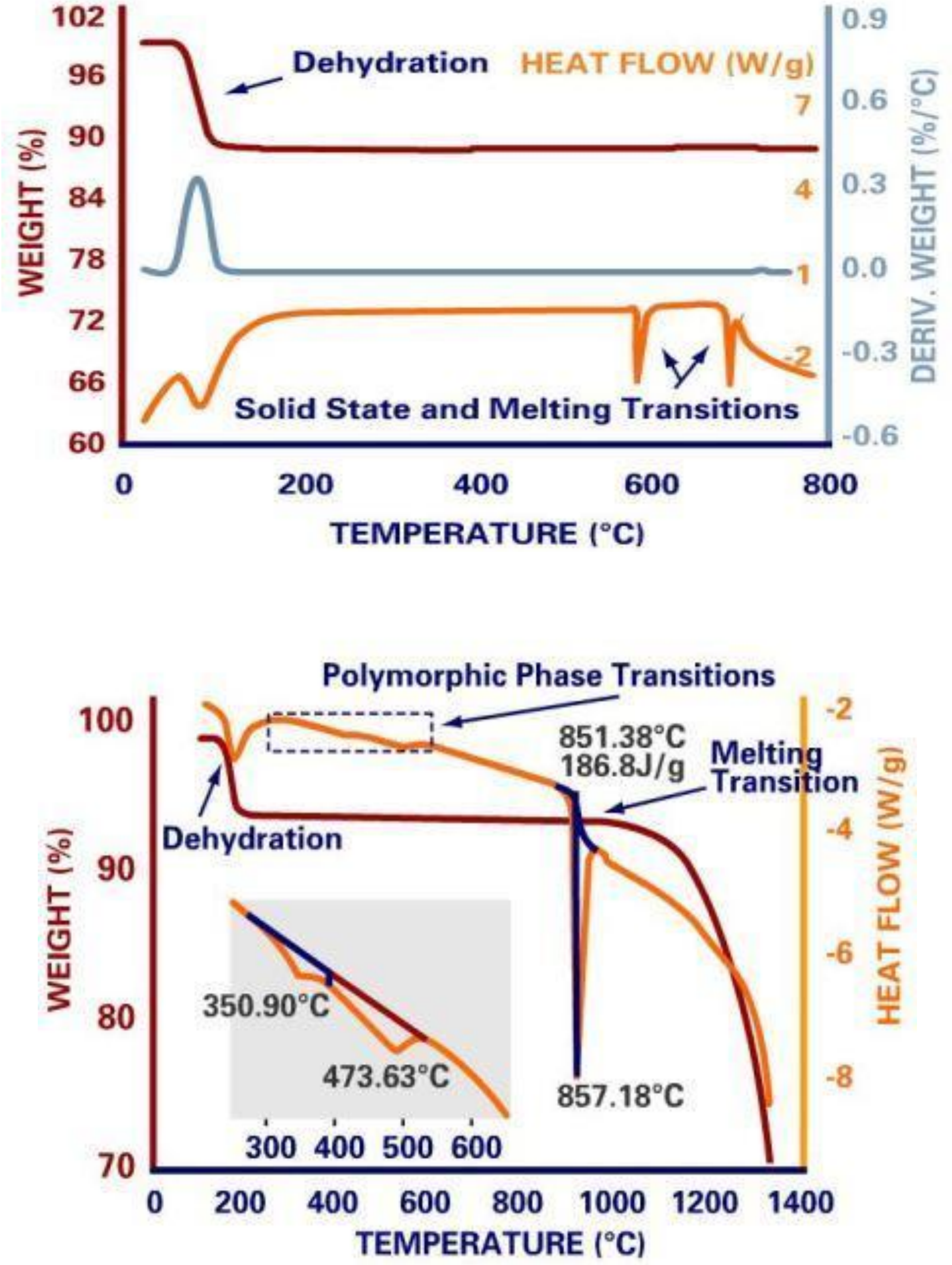

Figure 2.11: A TGA Curve Showing Weight Loss/Weight Derivatives and Temperature (Basu, 2013).

2.7 Effects of Combustible Contents of MSW on Its Thermochemical Conversion

The various combustible compositions (papers, plastics, woody biomass and food waste) of MSW have useful heating values. Several studies and investigations (Mohan et al., 2006, Galvagno et al., 2006, Galvagno et al., 2009, Ahmed and Gupta, 2009a, Ahmed and Gupta, 2009b, Khoo et al., 2010, Arena et al., 2010, Wu and Williams, 2010b, Wu and Williams, 2010a, Artetxe et al., 2012, Long et al., 2013, Chen et al., 2013) have reported thermochemical conversion of these combustible substances (papers, plastics, woody biomass and food waste) when considered together as a composite solid fuel or separately, and that they produce useful energy and chemical feedstock for supplementary applications. In the gasification of composite solid fuel, the presence of plastics contributes to the increased yield of the gaseous fraction and hydrogen. A reduction in CO and CO_2 concentration are obtained when the amount of plastics-polypropylene is introduced up to 20 wt. % in the initial feedstock mixture (Alvarez *et al.*, 2014). Pinto et al. (2002) investigated steam gasification of biomass and PE and concluded that plastic contents up to 20 wt. % in the feed, favoured the production of H_2, with its concentration being at around 50 vol. %, with decreased CO concentration (v/v) yield and 13 % of C_nH_m (C_1 - C_4) in the final gas. The syngas constituent of the product was constant for the higher plastic concentration in the feedstock.

Ruoppolo et al. (2012) performed the gasification of a mixture of plastics and biomass pellets in a catalytic fluidised bed and achieved hydrogen concentration of up to 32 (v/v) %. In addition, Liu *et al.* (2013b) carried out the vapour-catalysed co-pyrolysis of pubescents and LDPE obtained a hydrogen concentration of approximately 62 (v/v) % in the gaseous products. The study of Kannan et al. (2013b) demonstrates the feasibility of energy recovery from waste PE and PET blends through gasification by considering conversion efficiencies and syngas characteristics. The blends showed a significant positive effect on syngas yield and LHV in the absence of external oxidising agents while the energy efficiency of PET blending is much higher than that of PE gasification. The study further emphasised selectivity of the composition of the solid waste feedstock to improve H_2/CO mole ratio in the product gas suitable for various applications.

Janajreh and Al Shrah (2013) investigated the potential of using a small-scale biomass gasifier for thermochemical conversion. They used a commercial downdraft gasifier scaled for 10 - 20 kW batched with wood chips of medium size. The work provided adequate understanding of the limiting factors and the challenges facing the implementation of small-scale downdraft gasifiers for biomass gasification. It was also shown that the density in terms of the heating value and moisture content of the feedstock significantly affects reactivity.

Apart from ash and moisture compositions of MSW and the low solid fuel quality of some species of woody biomass, pellets obtained from these pre-treated, non-homogeneous mixtures of combustible feed from the MSW could serve as an important blend. Plastics, on the other hand, are not renewable sources but are mostly hydrocarbon sources. However, this study considers the inclusion of plastics which are commonly used and found in the MSW. This is because of challenges in recycling prospects and its ultimate environmental problem that may arise from the cradle-to-grave cycle. Plastic solid waste is essential complementary feedstock to improve the quality of gasification gaseous products. Diverse components of MSW, such as paper, plastics, biodegradable, putrescible and forestry and wood waste, have different physicochemical characteristics and potentials for thermochemical conversions.

The study will consider a number of analyses to evaluate possible energy resource potential from heterogeneous MSW. In this view, the study will conduct elaborate analyses of the physicochemical characteristics of a substantial quantity of MSW from solid waste disposal facilities in the City of Cape Town.

2.8 Municipal Solid Waste to Refuse-Derived Fuel Production

Municipal solid waste (MSW) is heterogeneous solid waste consisting of combustible, non-combustible, organic, inorganic and inert materials. It also exhibits a low bulk density and relatively high-water content. Processes must, therefore, be designed to reduce the cost of collection, transportation and storage for any MSW conversion technique to be competitive (Gravitis, 2007, Wright and Brown, 2007). Refuse-derived fuel (RDF) is a result of processing MSW to separate the combustible fraction from the non-combustibles, such as metals, glass and cinders in MSW. The RDF is predominantly composed of miscellaneous paper, plastic, wood and kitchen or yard waste and has a higher energy content than untreated MSW, typically in the range of 12 - 23 MJ/Kg (Galvagno et al., 2006, Galvagno et al., 2009, Burnley et al., 2011, Ryu et al., 2008).

The MSW can be shredded into uniformly-sized particles (pre-treatment procedure) or densified into pellets. Both characteristics facilitate easy handling, transportation and combustion. The economics of the thermochemical conversion processes therefore maybe dramatically improved through the reduced volume of MSW and water content of the MSW. The thermochemical conversion of the RDF with a higher carbon and hydrogen content is advantageous.

Pelletisation of MSW involves the processes of segregating, crushing and mixing high and low heat-value organic waste material and solidifying it to produce RDF. Magnetic separation and eddy current separations could be applied to separate out ferrous and non-ferrous metals while glass and plastics would be separated by an optical scanning system, pneumatic and NIR sensor sorting system. The RDF is prepared by the pelletising machine or compactor after it has been shredded to homogenous particles. The intermediate product that is formed at this stage is referred to as *fluff RDF*. The fluff RDF can be passed through the palletising machine to produce densified RDF.

Various qualities of RDF pellets can be produced, depending on the needs of the user. A high-quality RDF would possess HHV with lower moisture and ash contents. There are two main types of RDF: coarse-RDF (c-RDF) and densified pellets (d-RDF). RDF is produced by processing solid waste into coarse or densified RDF after first mechanically removing the non-combustible materials, such as metal and glass. Another process known as the wet RDF method makes use of a machine called a hydropulper. A hydropulper is essentially a large blender. In this method, raw MSW is fed into the hydropulper where high-speed rotating cutters chop the waste into water slurry. Large items are removed while the remaining suspension is pumped into a liquid cyclone separator which removes the smaller, heavier materials.

A major disadvantage of the wet method is that it requires significantly higher operating costs than the dry technology. Solid fuel improvement is enhanced through densification of the MSW via pelletisation to form RDF. A density increase of up to a factor of three is obtained with the RDF (Deswarte et al., 2007).

Generally, commercial briquettes/pellets have a density of about 800 - 1300 Kg/m^3 compared to loose biomass with a bulk density of 10 - 20 Kg/m^3 (Hedman et al., 2005). The RDF is more homogeneous and has a higher heat content per unit mass than raw MSW (Dalai *et al.*, 2009). Untreated MSW typically has a HHV of around 5.815 MJ/Kg while processed (and dried) MSW has a fuel value as high as 9.304 - 16.282 MJ/Kg. Physicochemical characterisation procedures and sorting of MSW are essential for material and energy recovery from organic-rich MSW.

The following current MSW management methods (landfill, incineration, other thermochemical conversion methods with or without energy recovery, etc.) focus on the conversion of the combustible contents to produce energy and solid fuels. Heterogeneity, characteristic of MSW, is a hindering factor requiring detailed analyses to improve performance of the agglomeration circuit and associated costs of homogenisation are also relevant. A high-quality RDF would possess HHV, with low moisture and low ash contents.

2.9 Thermochemical Conversion

Pyrolysis, torrefaction, incineration and gasification technologies are forms of combustion reactions (thermochemical reactions) with different approaches to combustion mechanisms for several applications. They produce useful energy resources and chemical feedstocks. The choice of product specifies the conditions for the thermochemical processes that have to be considered. Pyrolysis and gasification are thermochemically controlled, but the pyrolysis process is one of the processes in gasification reactions, but their products vary significantly in different phases. Torrefaction is a low temperature process (150 ^{0}C - 600 ^{0}C)(Poudel et al., 2015, Iroba et al., 2017, Siritheerasas et al., 2017, Abdul Samad et al., 2017) and relatively new process that heats the carbonaceous substances in the absence of air to improve its usefulness and its quality of the products as feedstocks (Basu, 2010, Basu, 2013). Torrefaction process improves the quality of MSW combustion characteristic (Iroba et al., 2017). Pyrolysis is another thermochemical decomposition of biomass into an approximate range of useful products such as 75 % liquid tars (pyrolysis oil), 3 % chars while syngas and C_2 - C_4 hydrocarbons constitute less than 22 % (Basu, 2013). The tar produced from pyrolysis of MSW are very complex with considerable moisture content (Chen et al., 2015a, Czajczyńska et al., 2017).

Incineration treatment technology involves conversion of MSW to into product gases that have very low caloric values. The incineration treatment takes place in a fast oxidizing environment giving off heat energy - energy recovery system.

The incineration treatment technology is a traditional waste treatment technique for municipal solid waste disposal (Hwang et al., 2017). The main purpose of incineration system is to effectively reduce the quantity and volume MSW, stabilization of MSW and pathogen elimination (Wu et al., 2014) while energy recovery is an added advantage for WTE technology (Song et al., 2017). The incineration is still very popular and relevant in most developing country till date (Fu et al., 2015, Somorin et al., 2017, Allegrini et al., 2014).

However, gasification technology requires a gasifying medium like steam, air or oxygen to convert the solid feedstock into useful gaseous fuel or chemical feedstocks that can be used as an energy resource or for the production of value-added chemical feedstocks(Thakare and Nandi, 2016). Hydrogen (H_2), carbon monoxide (CO), carbon dioxide(CO_2), methane (CH_4), aliphatic hydrocarbons, benzene and toluene, as well as small amounts of ammonia, hydrochloric acid and hydrogen sulphide are typical products of solid fuel derived from MSW gasification, while CO and H_2 are main valuable compositions of the gasification (Dalai et al., 2009, Basu, 2013, Ramos et al., 2018).

The useful application of these chemical feedstocks ranges from FT technology, ethanol production, CHP systems and fuel cell applications (Lopez et al., 2018). The main content of the produced chemical feedstocks is syngas. Interest in the gasification technology to produce syngas from MSW is increasing.

The gasification process boosts hydrogen content and reduces carbon content MSW to produce useful gases with a higher hydrogen-to-carbon (H/C) ratio, while incineration converts hydrogen and carbon in combustible materials (biomass/MSW) into water, carbon dioxide and heat, respectively. Gasification technology increases production of energy packed chemical feedstocks while incineration treatment technology releases heat energy (Ng et al., 2014).

2.9.1 Gasification Technologies

Biomass/MSW gasification contributes only 0.33 % of the total gasification capacity all over the world. Gasification technology offers remarkable advantages via material conversions and waste-to-energy approaches. Associated problems with landfilling and the conventional open incineration combustion of MSW are avoided (He et al., 2009c, He et al., 2009a, He et al., 2009b). Gasification is a process of converting carbonaceous compounds into a mixture of gaseous species that is predominantly syngas, CO, H_2, with others like CO_2, and CH_4. Other chemical products are also formed in the process of gasification, but their concentrations are mostly negligible. Gaseous products of gasification are utilised for electricity generation. These gases must be pre-treated to avoid a drop in efficiency.

Gasification has the advantage of producing a multi-use product (H_2, CO and CH_4) and when pre-treatment is not considered, its efficiency is sometimes higher than that of incineration (Arafat and Jijakli, 2013). Gasification has significant potential as a waste treatment option for municipal solid waste (MSW) as discussed earlier. Of the MSW categories mentioned earlier, metals and glass are inorganic and thus cannot be gasified. Therefore, the remaining MSW streams are biodegradable organic solid waste and have the potential of gasification. Since 2010, gasification has been a readily available technology with a worldwide capacity of 122,106 thermal MW (Energy, 2010).

Basu (2013) report on a survey of gasifier technology use in Europe, the United States, and Canada showed that downdraft gasifiers are the most common - 75 % are downdraft, 20 % are fluidised beds, 2.5 % are updraft and 2.5 % are of various other designs. The fixed-bed air-blown downdraft gasifier is a simple type of gasifier compared to other fixed-bed types. It is one of the simplest and cheapest biomass/MSW thermochemical conversion technologies. The downdraft fixed-bed gasifier was selected as the best because of low tar formation and removal. The fixed-bed air-blown downdraft gasifier is a simple type of gasifier compared to other fixed-bed types.

The fixed-bed air-blown downdraft gasifier is one of the simplest and cheapest biomass conversion technologies. The downdraft fixed-bed gasifier is suitable for this thermochemical conversion. Though RDF is produced from the combustible constituents of MSW and compressed into pellets, some studies (Dalai et al., 2009, Ahmed and Gupta, 2009c, Wu and Williams, 2010b, Wu and Williams, 2010a) have suggested that including the plastic content of MSW has increased the high heating value of RDF and has also produced hydrogen-rich syngas during the gasification process.

The following studies, namely, (Ruoppolo et al., 2012, Wu and Williams, 2010b, Pinto et al., 2002, Mastellone et al., 2010, Kannan et al., 2013a, He et al., 2009b, Alvarez et al., 2014, Ahmed et al., 2011, Ahmed and Gupta, 2011, Narobe et al., 2014, Moghadam et al., 2014, Park et al., 2016, Jeong et al., 2017, Ramos et al., 2018), have done similar work on co-gasification of some types of plastics that support the use of plastic in co-gasification. Also, RDF often shares some significant characteristics with coal (Dalai et al., 2009, Kannan et al., 2013b, Narobe et al., 2014). Thus, physicochemical characterisation of the RDF will further explain the relevance of MSW as a potential RDF-solid fuel. The valuable composition of the pre-treated MSW for energy recovery is the combustible part which is usually greater than 70 % of the total MSW. In this study, plastics are taken to be part of combustible materials and used in the RDF gasification.

2.9.2 Gasification and Incineration Technologies

Unlike pyrolysis and torrefaction technology, incineration and gasification technologies are characterized with the production of chemicals and energy recovery (Lino and Ismail, 2017, Somorin et al., 2017, Chen et al., 2013, Thakare and Nandi, 2016, Lopez et al., 2018). The incineration and gasification technologies are still relevant for MSW management, GHG gases control, and energy recovery (Wu et al., 2014, Hwang et al., 2017)

Thakare and Nandi (2016) reported extensive work on how MSW was used for energy recovery through gasification. The synthesis gas produced can be used to produce industrial chemicals, or for power generation in gas engines and turbines unlike the gaseous product from incineration treatment technology. The study concluded that gasification is more efficient than incineration treatment while the study of Fu et al. (2015) opined that the MSW incineration is still relevant with potential future prospects in China because of possible co-incineration.

The high moisture content maybe serious challenge for MSW incineration, creating a need for MSW pre-treatment prior to MSW incineration (Fu et al., 2015). MSW incineration treatment technology is not an outdated choice around the world. There are over 1000 MSW incineration plants (large capacities of MSW incineration) with a total global capacity of more than 600,000 Mg/d. China is one the countries with substantial number of incineration plants but lack of adherence to specific standard incineration plant and coordinating emission standard is a major challenge (Lu et al., 2017).

The available WTE potential in Nigeria at various MSW generation rates, collection efficiencies, and energy conversion technologies are essential tools towards the realization of the incineration technology but MSWM lack standard of operational policies. The incineration treatment technology with energy recovery (31- 205 MW) as the preferred choice of thermal treatment.

The operation of WTE facilities for MSW in Nigeria will require standard working policies and enabling regulations (Somorin et al., 2017). Allegrini et al. (2014) reported on resources recovery potential of MSW incineration treatment. The incineration treatment approach may not be viable for some metals of interest and cannot be ideal for resources recovery procedure while gasification lowers the emissions of heavy metals in flue gases and fly ashes, heavy metals in bottom ashes (Wu et al., 2014).

Incineration is traditional municipal solid waste treatment technique developed to WTE technology for energy and power production. Gasification is a renowned chemical process for production of chemical feedstocks, energy resources and electrical energy. As incineration treatment was developed to produce energy so was modification of gasification towards reduction of harmful emissions and heavy metal mitigations.

Gasification technology offers more efficient and cleaner than direct combustion of MSW; lower thermal losses because specified air flowrate; production of less volume of output fuel gas than that from an incinerator and it offers an intermediate step for gas separation. The gasification produces some intermediate products for use (energy generation, liquid fuels and chemicals manufacturing processes), potential for higher efficiency conversion, lower operating temperature and easily adaptable for small scales power generations which are easily obtainable from other methods. Also, the gasification plants are often modular where most emissions from processes are collected as bottom ashes with metals mainly in a non-oxidized form while it reduces atmosphere emissions (Arena, 2012). The considerations reported above indicate that MSW gasification demonstrates several, effective or potential, benefits over traditional open combustion or incineration of MSW. Comparisons between gasification and incineration are presented in Table 2.3 below.

Table 2.3: Comparisons between Gasification and Incineration Technology

Factors	Gasification Technology	Incineration Technology
Reaction	Thermochemical	Thermochemical
Temperature	700 ^{0}C - 900 ^{0}C	> 900 ^{0}C/Very High
Type of Reaction	Incomplete Combustion	Complete Combustion
Major Products	CO, H_2, CH_4	Heat Energy, CO_2 and H_2O
Product Uses	Fertilizer, FT Technology, ethanol production, CHP systems and fuel cell applications	Electrical Energy and Heating
Heavy Metal Control	Effective Control	Not Efficient
Emissions Control	Effective Control	Still hindrance
Quantity and Volume Reduction	Effective	Very Effective
Chemical Reactions	Series of Chemical Reactions	Oxidation Chemical Reaction
Energy Production	Bye Product	Heat Energy via Endothermic reaction
Waste Treatment	Very Effective	Very Effective

2.9.3 The End-Products of Thermochemical Conversions

Hydrogen, carbon monoxide, carbon dioxide, methane, aliphatic hydrocarbons, benzene, and toluene, as well as small amounts of ammonia, hydrochloric acid and hydrogen sulphide are all typical end-products of gasification while CO and H_2 are the main products (Dalai et al., 2009, Basu, 2010, Basu, 2013).

During pyrolysis, large hydrocarbon molecules break down into relatively smaller and simpler molecules of gas, liquid and char. Pyrolysis is similar to and sometimes overlaps with processes like cracking, devolatilisation, carbonisation, dry distillation and destructive distillation but it has no similarity with the gasification process. Pyrolysis of carbonaceous substances is carried out in a relatively low temperature range of 300 to 650 ^{0}C compared to 800 to 1000 ^{0}C for gasification as can be seen in Figure 2.12.

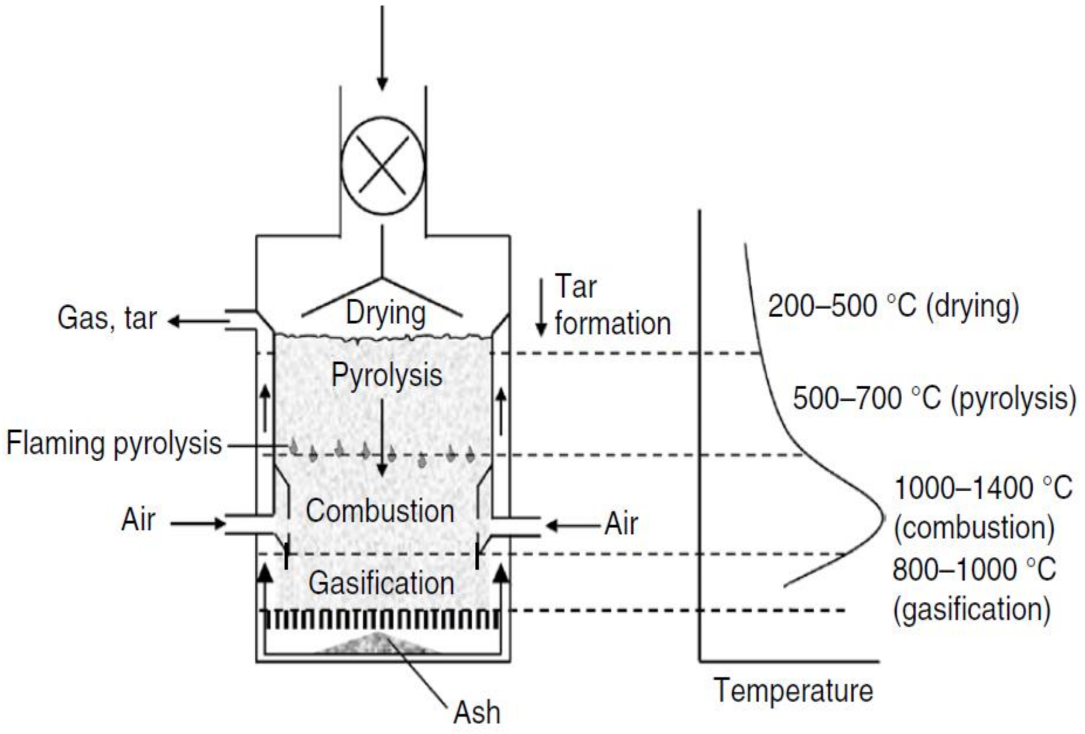

Figure 2.12: Reaction Schemes in an Air-blown Downdraft Fixed Bed Gasifier

Predominant products are more than 75 % liquid tar (pyrolysis oil) with gaseous compounds and chars. The gasification process packs energy into chemical bonds in the product gas; combustion breaks those bonds to release the energy. The gasification process adds hydrogen to and strips off carbon from the carbonaceous feedstock to produce gases with a higher hydrogen-to-carbon (H/C) ratio, while combustion converts most carbonaceous feedstock into water and carbon dioxide. The later products from combustion have very low high heating values (Basu, 2013). The products of thermochemical conversion (gasification) have many energy and industrial uses. It is potentially more efficient than incineration technology and it can be operated at a lower temperature. In the end, fewer pollutants are volatised in gasification than in incineration (Arena et al., 2010, Arena, 2012). Most of the gasification studies found in the literature focus on evaluating the gasification of specific biomass feedstock from specific localities under very specific conditions. This focus requires further extensive studies to broaden the coverage scope of the thermochemical conversion of MSW.

2.9.4 Syngas Production

Syngas (H_2 and CO) is an important and major fraction of gasification products particularly when a suitable gasifier reactor is being considered. Apart from energy sources, gasification and pyrolysis have an important application in the production of chemicals, transport fuels, plastic, resin and fertilizer from biomass. Syngas is a fuel as well as a basic building block for many hydrocarbons. Transport fuel and several chemicals are produced from different syntheses of syngas from gasification processes.

These products are energy feedstock (methane, carbon monoxide, hydrogen); transportation fuels (hydrogen, biodiesel and biogas); and chemical feedstock (glycerol, fumaric acid, methanol, ammonia). Yunus et al. (2010) report that hydrogen production from virgin biomass gasification is more economically viable than pyrolysis.

Biomass/MSW gasification is a promising system for the production of renewable hydrogen, efficient clean large-scale hydrogen production and will become the dominant technology beyond the 21st century (Balat and Kırtay, 2010). However, the choice of an appropriate gasifier is relevant to the yield of desirable products.

2.9.5 The Gasifying Media and Equivalence Ratio

The use of gasifying media is essential to the gasification process. The equivalence ratio (ER) is an important gasifier parameter that shows the limits of various types of thermochemical conversions. The ER is a relevant factor in the design of the gasifier and in the control of the distribution of products in thermochemical conversions. It is the ratio of the actual air-fuel to the stoichiometric (theoretical) air-fuel. Normally, the general term 'oxidant' is used to refer to air, pure oxygen and other gases used for thermochemical conversions.

The ER is expressed in equation 2.3.

$$ER\ (< 1.0)_{gasification} = \frac{Actual\ Air}{Stoichiometric\ Air} = ER\ (> 1.0)_{combustion} \qquad (2.3)$$

The stoichiometric amount of oxidant required could be obtained from the ultimate analysis of the RDF solid fuel.

The ER dictates the performance of the gasifier in terms of useful energy products. The ER requirement for various thermochemical conversions varies because of the desired products intended for it. The useful ranges of ER are shown in equations 2.4 - 2.6.

$$Gasification \qquad 0.01 \leq ER \lll 1.0 \tag{2.4}$$

$$Torrefaction, pyrolysis \qquad 0.0 \leq ER \ll 0.1 \tag{2.5}$$

$$Combustion \qquad ER > 1.0 \tag{2.6}$$

Lower ER values in equation 2.4 usually cause char and tars production. The char produced may be suitable for charcoal production. Some studies have reported a number of values for ER (0.08 - 0.80) and steam fuel ratios (0.40 - 3.35) for gasification to produce various products (Dalai et al., 2009, Chen et al., 2013, Corella and Sanz, 2005, Plis and Wilk, 2011, Skoulou et al., 2008c, Skoulou et al., 2008a, Tinaut et al., 2008, Zhang et al., 2012).

However, an excessive ER value (>> 0.6) may result in the excessive formation of products of complete combustion, such as CO_2 and H_2O, at the expense of desirable products, such as CO and H_2. The ER also has an effect on bed temperatures and carbon conversion efficiency as shown in Figure 2.13 and Figure 2.14 below (Basu, 2013).

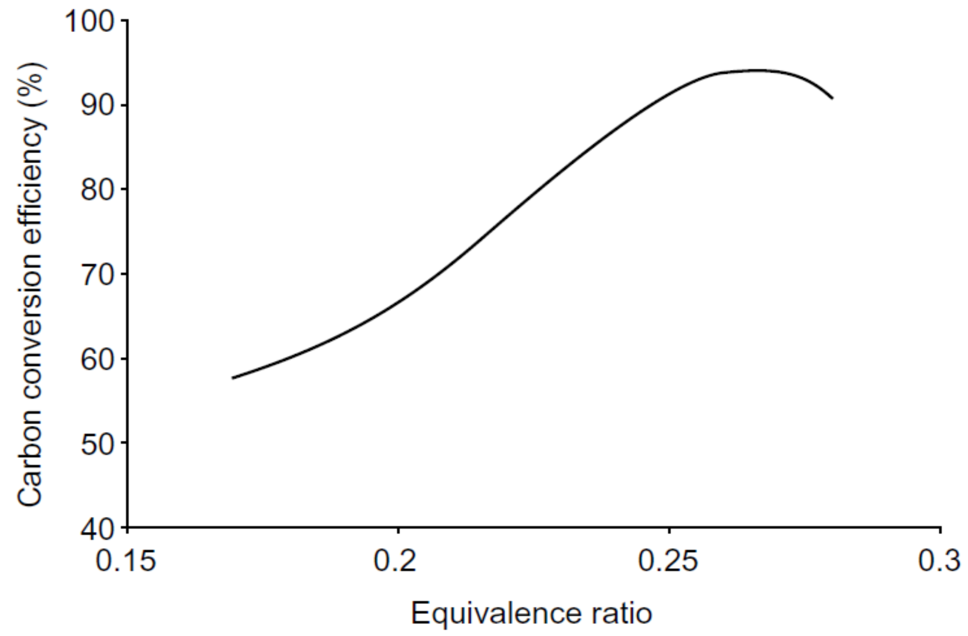

Figure 2.13: Relationships between ER and Carbon Conversion Efficiency (Basu, 2013)

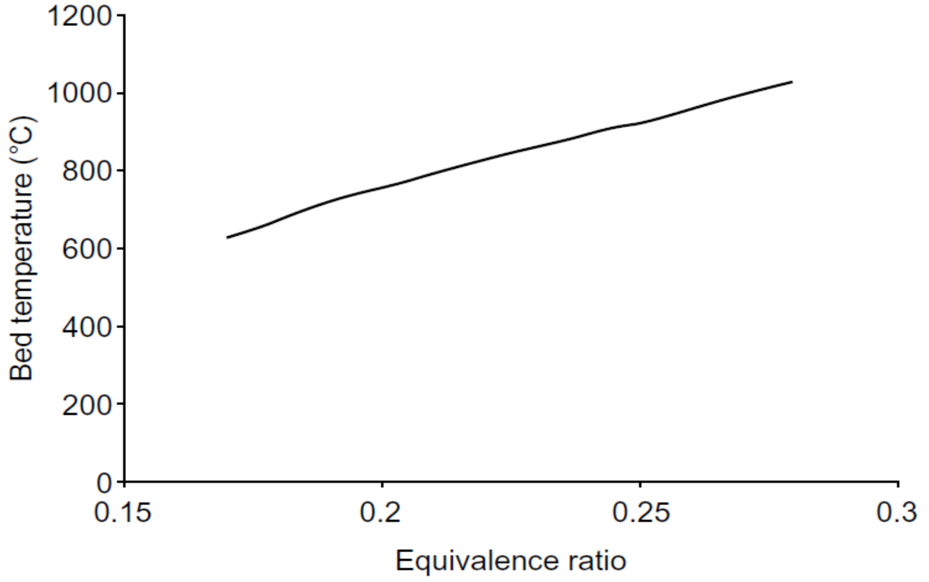

Figure 2.14: Relationships between ER and Bed Temperatures (Basu, 2013)

The optimum value for ER against carbon conversion efficiency is around 0.27, but the ER may not be the only factor responsible for the conversions. However, the bed temperature is strongly associated with a high value of ER.

2.10 Benefits of Municipal Solid Waste (MSW)

The advantages of MSW through gasification technology are relevant for energy and material recovery from MSW. Environmental problems from MSW management could be easily addressed. The following four benefits of gasification of MSW are discussed below.

2.10.1 Gasification Destroys Harmful Pollutants

Gasification is a form of gasification processes under controlled combustion circumstances for enhancing the production of an energy-packed product, namely syngas. Water (steam) is used as the most common gasifying agent to improve the yield and quality of hydrogen in syngas products through reforming processes. A specific type of gasifier operation allows for the reduction in tar and ash production while improving the quality of syngas (Cao et al., 2006). Its operation enhances the reduction of GHG and other harmful emissions (Singh *et al.*, 2011). The formation of light hydrocarbon like the natural gas, methane, is not favoured in any form of downdraft gasification conversion. The global-warming potential is minimised further. The last phase of combustion in the gasifying process produces significantly fewer quantities of furans and dioxins than traditional MSW incineration. In gasification reactions, not only does the oxygen deficit region of the reactions enhance partial oxidation to produce the desired syngas products with an H_2/CO molar ratio, but also prevents the formation of dioxins and furans. The boudouard reactions reduce the amount of CO_2, furans, and dioxins because of reducing environment (low level of oxygen of equivalence ratios between 0.25 and 0.50) of the boudouard reactions inhibit the formation of furans and dioxins (Arena 2012). This accounts for the significant reduction in the production of harmful dioxins and furans (Lopes et al., 2015).

In addition, oxide of calcium (CaO), compounds of nitrogen and sulphur from organic matter origins, have been reported to have inhibitive effects on the formation of furans and dioxins (Cheng and Hu, 2010, Lopes et al., 2015). Carbon dioxide capture in various units during gasification processes can be monitored, unlike open incineration and landfill emissions. The consumption of CO_2 in the boudouard reaction, which will be discussed in Chapter 4, can also reduce the amount of CO_2 released into the atmosphere. To prevent serious health effects from furans and dioxins emissions, abatement measures are essential to control environmental exposure to these harmful compounds. These emissions are not easily biodegradable, and abatement or treatment procedures will incur high costs (Ramos et al., 2018).

2.10.2 Gasification Controls Heavy Metal Mobility into Environment

Apart from the production of dioxins and furans in thermal processes, heavy metal distribution in MSW before, during and after thermochemical conversions, are relevant components of MSW that need to be monitored.

The heavy metal content is found in raw MSW during thermal processes. It contributes towards gasification reactions which leads to the formation of fly ash, bottom ash and even slag (Nzihou and Stanmore, 2013, Wu et al., 2014). This remains important due to the mobility of heavy metal, remediation and the non-destructive nature of the elements and some of its derivatives(Hasselriis and Licata, 1996). Some of the alkaline metals cause the process of ash sintering but, on the other hand, catalyse char oxidation reactions (Sekito et al., 2014). The volume and weight reduction of MSW increase densities of heavy metals that remain in the residue (Nzihou and Stanmore, 2013, Sekito et al., 2014).

The biodegradable and other combustible components of MSW are converted into various products (gaseous products and solid ash) during gasification combustion. Usually, the weight of MSW is reduced by 75 % - 80 % or more. In the process of gasification combustion, the some of the heavy metals remain in the residue. They are highly concentrated, hence very toxic. The MSW weight reduction allows opportunities for easy handling of the toxic heavy metal which can be destroyed or recovered for other uses. The method of the landfill, on the other hand, does not have adequate procedures for handling this challenge (Xiaoli et al., 2007). Studies have shown that most heavy metals is distributed between fly ash and bottom ash. The coefficient of transfer of these heavy metals suggests that most of the heavy metals are transferred to bottom ash. This procedure shall be discussed in Chapter 6. The mobility of the heavy metal during gasification processes allows the reduction of heavy metal by means of gaseous emission into the atmosphere and the heavy metal is also trapped in highly dense bottom ash for better inhibition and management (Yao et al., 2010).

Remediation, recovery and re-use are some of the positive ways in which these toxic heavy metals can be contained and controlled to prevent them from contaminating land, water or atmosphere. Hence, by reducing heavy metal emissions into urban air-shed increases the reduction in environmental cost. Thus, this type of gasification technology allows for an improved approach to monitoring mobility of heavy metal from cradle-to-grave.

2.10.3 Calorific Contents of Some Municipal Solid Wastes

Waste-to-energy technology is another potential application of MSW, though some studies regard the energy potential as low-grade solid fuel. Liang *et al.* (2008) report the high heating value of 10.25 $MJKg^{-1}$ for the United Kingdom (UK) whereas more than an average value of 4.13 $MJKg^{-1}$ has been obtained from some cities in China.

The study of McIlveen-Wright et al. (2011) and other studies, namely (Diaz and Warith, 2006, Galvagno et al., 2006, He et al., 2009b, Zhang et al., 2010, Burnley et al., 2011, Chen et al., 2013, Zhou et al., 2014b), report a range of heating values for biomass, MSW and RDF (6 - 18 $MJKg^{-1}$). However, other studies have suggested values above 10 $MJKg^{-1}$ though this value is low compared to the typically high range of heating values of coal (25 - 35 $MJKg^{-1}$) (McIlveen-Wright *et al.*, 2011). A previous study conducted on three disposal facilities in Cape Town shows an average value of 15.45 $MJKg^{-1}$ (Ikhu-Omoregbe and Mahomed, 2012).

This study conducted further quantification of high heating values on 13 municipal solid waste disposal facilities to quantify and characterise the MSW energy potentials. Over 24 pre-treated samples of MSW were used to determine the high heating values. The high heating values obtained showed that an average of 20 $MJKg^{-1}$ and the HHV value as high as 27 $MJKg^{-1}$ was obtained in one of the solid waste disposal facilities. The details will be discussed in Chapter 4. This result is an indication of the high potential of waste-to-energy opportunities in MSW in Cape Town.

Short and long-term effects of environmental challenges, environmental costs and waste-to-energy significance may enhance effective MSW management. and maybe necessary approach to massive reduction of the amount of MSW going into landfill.

2.10.4 Socio-Economic Benefits of Gasification

The socio-economic benefits of MSW gasification technology are equally substantial. They provide alternative energy resources, reduce environmental emissions, improve MSW management and reduce the burden of the landfill. The technology offers a better eco-friendly environment and generates economic opportunities other than landfill and traditional incineration. The generation of MSW is sustainable because it is neither intermittent nor location-dependent. For an alternative MSW energy-based system to be economically viable, the MSW gasification technology needs to be located close to the community. The development of MSW management needs associated industries for MSW pre-treatment, collection and transport in that local community.

The thermochemical conversions have the capacity to produce an improved MSW gasification technology that can create better locally-based employment even more than that created by a coal/oil-based plant (Koppejan and Van Loo, 2008).

Another very important aspect of MSW-based energy resources, fuel or chemicals is that it reduces the dependence on fossil fuels. The unpredictable global politics has shown that supply and price are subjected to constant fluctuation. Solid fuels produced locally from MSW will be relatively free from such insecurity and the instability of fossil fuel. Utilisation of MSW ensures a stable generation of power and ensures that the power is locally resourced and essentially indigenous for remote districts.

2.11 Fuel Cell System: An Alternative Energy System

As the energy crisis becomes real and pollution regulations become stricter, internal combustion engine-based energy generation technologies (ICE), with a major contribution to climatic change, acid rain, environmental degradation and environmental pollution.

demand feasible alternatives. The ICE processes are the main sources of air pollution such as carbon monoxides, nitrogen oxides, sulphur oxides, volatile organic compounds and particulate matter infiltrating the environment. The cost of energy produced from ICE is relatively low and attractive, but the cost implications of environmental consequences are of grave concern.

Clean energy conversion technologies have gained popularity because of the challenges of fossil fuels. Among these, fuel cells have been receiving great attention as a suitable conversion technology to replace the ICE. The fuel cells can efficiently convert chemical energy to useful electricity without the combustion of fuels.

The fuel cell and the battery share a few similar characteristics such as electrolytes, electrodes and direct current (DC) production through electrochemical reactions. Unlike the battery, the fuel cell requires a continuous supply of fuel, and oxidants and electrodes in the fuel cell do not undergo chemical changes. After use, the battery is often discharged when the reactants participating in electrochemical reactions have been depleted. The fuel cell does not stop producing electricity as long as the reactants continuously flow through the fuel cell and the products are removed properly and immediately.

When compared with traditional technology (internal combustion engine) and fuel cells have advantages in both gravimetric and volumetric energy density in the portable sector; have high efficiencies and capacity factors in the stationary sector; and offer high efficiencies and fuel flexibilities in the transportation sector (Sharaf and Orhan, 2014). This indication of long life and durability make it more suitable for several applications. The diagrams of fuel cell, battery and internal combustion engine and their comparison are shown in Figure 2.15 and Table 2.4.

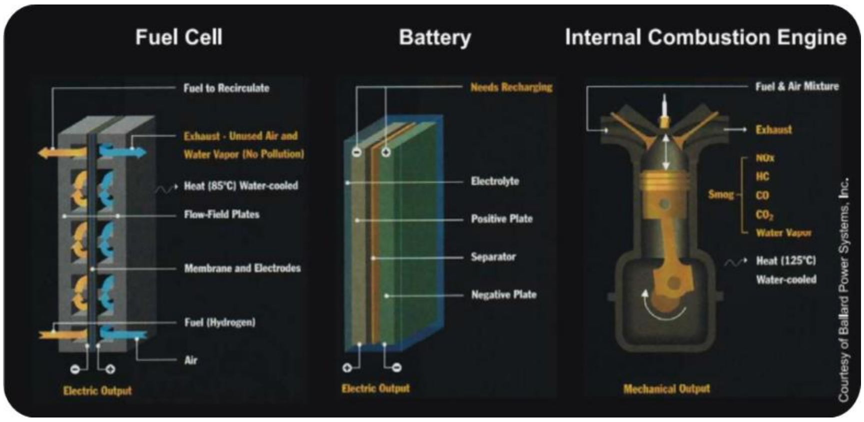

Figure 2.15: Fuel Cell, Battery and Internal Combustion Engine (Sharaf and Orhan, 2014).

Table 2.4: Similarities and Differences between Fuel Cells, Batteries and Heat Engines

Comparison	Fuel cell	Battery	Heat Engine
Function	energy conversion	energy storage and conversion	energy conversion
Technology	electrochemical reactions	electrochemical reactions	combustion
Typical Fuel	usually pure hydrogen	stored chemicals	gasoline, diesel
Useful Output	DC electricity	DC electricity	mechanical power
Main Advantages	high efficiency reduced harmful emissions	high efficiency, high maturity	high maturity, low cost
Main Disadvantages	high cost, low durability	low operational cycles, low durability	significant harmful emissions, low efficiency

2.11.1 Fuel Cell System

Fuel cells are energy conversion devices that convert chemical energy directly into electrical and heat energy by electro-chemical redox reaction (Li et al., 2009, Peighambardoust et al., 2010, Shamardina et al., 2010). Fuel cells offer high energy conversion efficiency, minimised pollutant emission and other advanced features compared to traditional energy conversion technologies.

Fuel cells circumvent the heat and mechanical energy route, traditional Carnot pathway and obtain valuable electrical and thermal energy with almost zero emission characteristics (Moser, 2010, Barbir, 2013). The theoretical conversions of the fuel cells exceed 75 % for directly converting fuel feedstock to energy but practical conversions efficiency range between 35 and 70 % based on HHV value. According to the report of Staffell (2015a), various types of fuels have electrical efficiencies ranging from 42 % to 60 % while their total efficiencies are between 85 % and 90 %.

This efficiency is practical when compared to traditional heat engines (ICE) which are typically below 30 % and approaches 50 % on rare conditions in turbine applications. Obviously, fuel cells are highly attractive, potential energy conversion devices (Moser, 2010, Barbir, 2013). Fuel cells do not require a combustion process but electrochemical redox reactions which have extremely low emissions of nitrogen oxides (NO_x) and carbon oxides (CO_x) and have a higher theoretical and practical efficiency (Zoulias and Lymberopoulos, 2007, Sharaf and Orhan, 2014). Carbon monoxides, nitrogen oxides, sulphur oxides, volatile organic compounds and particulate matter are forms of emissions that can be reduced by using a cleaner conversion technology offered by fuel cell technology.

2.11.2 Overview of Fuel Cell Technologies

Fuel cell technology is attractive, a promising energy conversion technology and has gained more attention globally among other alternatives. This technology is very flexible because of a range of fuels (hydrogen, methanol, carbon monoxide, methane, etc) and abundant oxidant (air/oxygen) that can be used in electrochemical reactions. The flexibility of the fuel-for-fuel cell is another important criterion for reducing over-dependency on fossil fuels. Fuel cells are often categorised based on their operating temperatures, electrolyte component materials and fuels. A further classification of fuel cell technology also considers the following properties, namely, the nature of the catalyst, electrolyte, membrane, proton conductivity, fuel type and operating temperatures. For example, the polymer electrolyte membrane fuel cells are also called proton exchange membranes with their name based on the electrolyte type. They may also be referred to as low temperature fuel cells because of their range of operating temperature. The electrolytes of fuel cells are unique materials which are selective proton conductors and isolators for electrons. The selective characteristics of electrolytes are displayed at different temperatures for different electrolyte materials in fuel cells. The various types of fuel cells are categorised in Tables 2.5 - 2.6. These factors of classification point to various applications of fuel from stationary use to portable and mobile applications. Table 2.5 shows anode and cathode reactions available in different types of fuel cell technologies and their capacities.

Table 2.5: Available Types of Fuel Cell Technology and Redox Reactions

Fuel Cells	Fuel, Charge Carrier	Electrode/Electrolyte	Temperature	Anode/Cathode Reactions
Alkaline Fuel Cell (AFC)	hydrogen, OH-	liquid alkaline	90 ^{0}C- 100 ^{0}C	$H_2 + 2OH^- \rightarrow 2H_2O + 2e^-$ $\frac{1}{2}O_2 + H_2O + 2e^- \rightarrow 2OH^-$
Phosphoric Acid Fuel Cell (PAFC)	hydrogen, H+	liquid phosphoric acid	120 ^{0}C - 200 ^{0}C	$H_2 \rightarrow 2H^+ + 2e^-$ $\frac{1}{2}O_2 + 2H^+ + 2e^- \rightarrow H_2O$
Low Temperature Polymer Electrolyte Membrane Fuel Cell (LTPEMFC)	hydrogen H+	nafion membrane	50 ^{0}C - 80 ^{0}C	$H_2 \rightarrow 2H^+ + 2e^-$ $\frac{1}{2}O_2 + 2H^+ + 2e^- \rightarrow H_2O$
High Temperature Polymer Electrolyte Membrane Fuel Cell (HTPEMFC)	hydrogen H+	acid doped pbi	120 ^{0}C - 200 ^{0}C	$H_2 \rightarrow 2H^+ + 2e^-$ $\frac{1}{2}O_2 + 2H^+ + 2e^- \rightarrow H_2O$

Direct Methanol Fuel Cell (DMFC)	methanol, H+	solid polymer	60 ^{0}C - 80 ^{0}C	$CH_3OH + H_2O \rightarrow CO_2 + 6H^+ + 6e^-$ $\frac{3}{2}O_2 + 6H^+ + 6e^- \rightarrow 3H_2O$
Molten Carbonate Fuel Cell (MCFC)	hydrogen, carbon monoxide, methane, CO_3^{2-}	molten carbonate	650 ^{0}C	$H_2 + CO_3^{2-} \rightarrow H_2O + CO_2 + 2e^-$ $CO + CO_3^{2-} \rightarrow 2CO_2 + 2e^-$ $\frac{1}{2}O_2 + CO_2 + 2e^- \rightarrow CO_3^{2-}$
Solid Oxide Fuel Cell (SOFC)	hydrogen, carbon monoxide, O^{2-}	Yitria Stabilised Zerconia (YSZ)	850 ^{0}C - 1000 ^{0}C	$H_2 + O^{2-} \rightarrow H_2O + 2e^-$ $CO + O^{2-} \rightarrow CO_2 + 2e^-$ $CH_4 + 4O^{2-} \rightarrow 2H_2O + CO_2 + 8e^-$ $\frac{1}{2}O_2 + 2e^- \rightarrow O^{2-}$

Table 2.6: Available Types of Fuel Cell Technology and Operation Characteristics

Fuel Cells	Power Density [$mWcm^{-2}$]	CO Tolerance	Rated Power(KW)	Electrical Efficiency (%)	Fuel Efficiency (%)	Projected Lifetime (H)	Capital Cost ($/KW)
Alkaline Fuel Cell (AFC)	100 - 200	<50 ppm	10 - 100	50	40	>10000	>200
Phosphoric Acid Fuel Cell (PAFC)	150 - 300	< 1 %	100 - 5000	40	40	>40000	1000
Low Temperature Polymer Electrolyte Membrane Fuel Cell (LTPEMFC)	300 - 1000	< 50 ppm	1 - 1000	40 - 50	45	>40000	>200
High Temperature Polymer Electrolyte Membrane Fuel Cell (HTPEMFC)	300 - 1000	> 50 ppm	1 - 1000	40 - 50	45	>40000	>200
Direct Methanol Fuel Cell (DMFC)	1 - 100	< 50 ppm	1 - 100		30	>10000	>200

Molten Carbonate Fuel Cell (MCFC)	100 - 400	fuel	1000 - 100000	45 - 55	50 - 75	>40000	1000
Solid Oxide Fuel Cell (SOFC)	250 - 350	fuel	1000 - 100000	50 - 60	>50	>40000	1500

2.11.3 The Fuel Cells and High Temperature PEM System

Alkaline fuel cells (AFCs) have the best performance when operating on pure hydrogen and oxygen, yet their extremely high sensitivity to impurities (especially carbon oxides), lower power density, highly corrosive electrolyte and short lifetime hinder their role for terrestrial applications (they are predominantly used for extra-terrestrial purposes). Phosphoric acid fuel cells (PAFCs) are possibly the most commercially-developed fuel cells operating at intermediate temperatures. PAFCs are used for combined heat-and-power (CHP) applications with a high energy efficiency. PAFCs are sensitive to contaminants, have a low power density, relatively low start-up time, relatively large system size and low electrical efficiency. Solid oxide fuel cells (SOFCs) benefit from the highest electrical efficiency and greater fuel flexibility but lack dynamic because of its high operating temperature (600 ^{0}C - 1000 ^{0}C) while the start-up and shot-down take up to 720 minutes. Molten carbonate fuel cells (MCFCs) are another type of high-temperature fuel cell which is low in cost because of non-platinum catalyst application, a low lifetime, low power density and material cost. These properties have an impact on costs (Sharaf and Orhan, 2014, Staffell and Green, 2013, Staffell, 2015a).

Molten carbonate fuel cells (MCFCs) and solid oxide fuel cells (SOFCs) are high-temperature fuel cells appropriate for cogeneration and combined cycle systems. MCFCs have the highest energy efficiency attainable from methane-to-electricity conversion in the size range of 250 kW to 20 MW, while SOFCs are best suited for base-load utility applications operating on coal-based gases. The high initial capital costs are associated with MCFCs and SOFCs technologies. Both MCFCs and SOFCs are high-temperature fuel cells (> 650 ^{0}C) with a low power density, relatively low start-up time and high manufacturing costs. Nevertheless, the choice of fuel and high operating temperature make them unsuitable for certain applications and have cost implications (Sharaf and Orhan, 2014).

Polymer electrolyte membrane fuel cell (PEMFC) technology covers a range of applications, for instance in transport and stationary applications, and has a power range of up to hundreds of kilowatts. The PEMFC has contributed around 50 % of sales of fuel cell since 2009. Due to the large size of many stationary MCFC and SOFC units, the dominance of PEMFC is waning and MCFC is expected to become the leading fuel cell type in terms of megawatt in future (Fuel Cell Today, 2013).

The high-temperature polymer electrolyte membrane fuel cell (HT-PEMFC) has emerged to address some challenges of the low-temperature polymer electrolyte membrane fuel cell (LT-PEMFCs). A high operating temperature enhances the electrode tolerance to fuel impurities (carbon monoxides) and simply fuel processing units (Li et al., 2009). It is considered a promising alternative means of exploiting energy with merits including high energy efficiency, minimised pollution emissions, sustainability and reliability (Li e*t al.*, 2009).

Sharaf and Orhan (2014) emphasise the importance of PEMFC as a promising fuel cell for transport applications because of its high-power density, fast start-up time, high efficiency and easy and safe handling which is another factor for portability. However, they point out the cost implications of its competitiveness. It operates by generating electrical energy when the fuel (hydrogen) enters the anode through a flow channel and moves through the porous electrode by convection and diffusion and subsequently splits into proton ions (H^+) and electrons (e^-) in a catalytic reaction. The heat energy is produced because the cathode reaction is exothermic.

When the hydrogen and oxygen ions combine, water is formed in the electro-chemical reactions in HT-PEMFC as shown in equations 2.7 - 2.9 (Li et al., 2009, Shamardina et al., 2010, Peighambardoust et al., 2010, Wang et al., 2011):

$$\text{Anode: } 2H_2 \rightarrow 4H^+ + 4e^- \quad (2.7)$$

$$\text{Cathode: } O_2 + 4H^+ + 4e^- \rightarrow 2H_2O \quad (2.8)$$

$$\text{Overall Electrochemical Reaction: } 2H_2 + O_2 \rightarrow H_2O \quad (2.9)$$

In Figure 2.16 the basic structure and electrochemical in a fuel cell are illustrated.

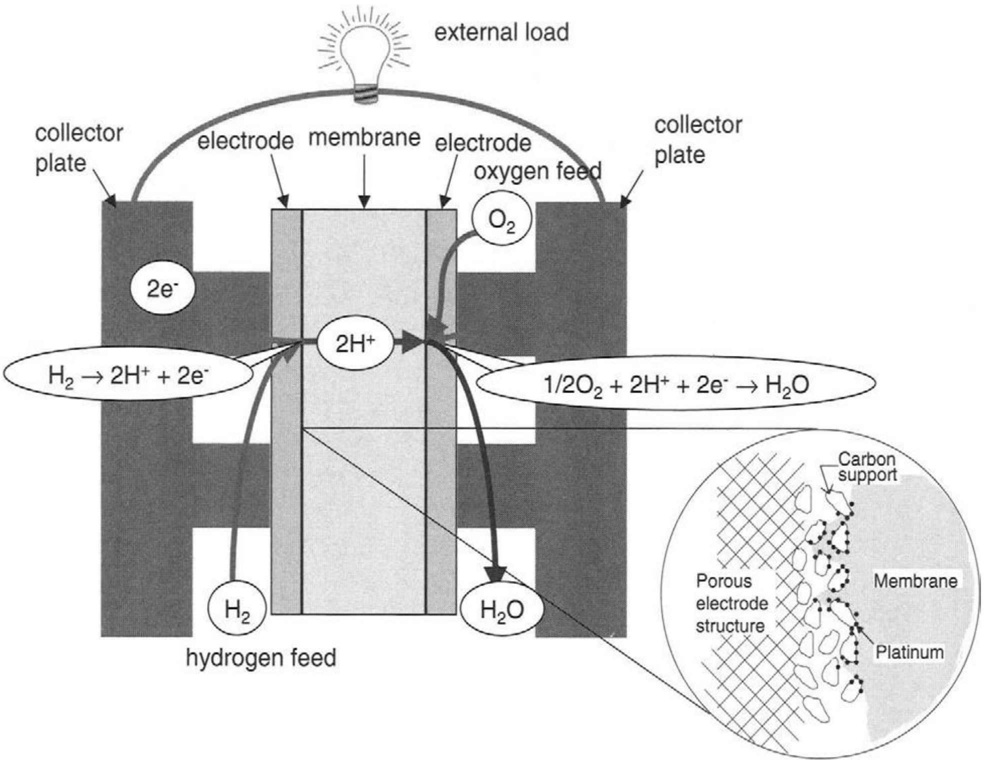

Figure 2.16: The Basic Structure and Electrochemical in a Fuel Cell (Barbir, 2013).

The equations 2.7 - 2.9 showed how hydrogen (chemical energy) was transformed to electron ions (electrical energy) and associated heat energy produced during the redox reactions. The simultaneous generation of electrical energy and heat energy in the HT-PEMFC is regarded as cogeneration. The cogeneration capacity of the HT-PEMFC with moderately high temperatures makes a suitable candidate for the element of CHP system. The operation of HT-PEMFC at high temperatures (120 - 180 ^{0}C) offers several advantages than the low temperatures (< 100 ^{0}C) in terms of fuel cell efficiency, performance (it is more stable than Nafion membranes and has a relatively low cost non-perfluorinated basic polymer), kinetics of electrode reactions, water management and advantage of good carbon monoxide poisoning tolerance of up to 1 - 3 % CO and 10 ppm SO_2 (Korsgaard et al., 2006, Li et al., 2009, Mamlouk and Scott, 2011b, Mamlouk and Scott, 2011a, Rao et al., 2010).

HT-PEMFC, among the five types of fuel cells, is attractive for various applications. Compared to liquid electrolyte systems, solid polymer electrolyte membranes have numerous advantages. The membranes have the following characteristics; low water uptake, reduced crossover, high proton conductivity, good thermal stability, low vapour pressure at high temperature and high mechanical flexibility and strength (Li et al., 2009, Wu et al., 2009). The solid polymer membrane is strong and elastic and constitutes a major structural component in the fuel cell. It makes the handling, sealing and assembling much easier than fuel cells with liquid electrolytes.

The studies of Staffell and Green (2013) and Staffell (2015a) report that alternative hydrogen availability as fuel for HT-PEMFC will greatly assist in overcoming fossil fuel dependence. It will enhance the simplified system and cost, the fuel processor and will increase efficiency. The dual characteristics of the HT-PEMFC (high-quality thermal energy and high electrical efficiency) and use of clean hydrogen energy makes it a suitable candidate for use in CHP systems. The HT-PEMFC attracts interest as a power source. This is because of its high efficiency and low air pollution when compared with internal ICE. The application of hydrogen in high efficiency fuel cells (HT-PEMFCs) and the possible integration of combustion processes (gasification of biomass, MSW) (Pan et al., 2005, Li et al., 2009) makes hydrogen superior to other alternative fuels in a fuel cell-based CHP system. Also, the cost implication is an important factor in which local source materials play a pertinent role. The traditional high-temperature fuel cells (SOFC, MCFC and DMFC) operate at a very high temperature (> 600 ^{0}C).

The operating temperatures of HT-PEMFCs are very low compared with a high temperature fuel cell. This offers an advantage of simple heat management when compared to high-temperature fuel cell systems. Rich hydrogen will be produced from gasification simulation and if it is properly treated to meet the specifications of proposed HTPEM fuel cell. It will present a clear distinction suitable application for cogeneration system.

2.12 Environmental Impact of MSW Disposal

Solid waste management systems include waste collection and segregation followed by one or more of the following options: recovery of secondary materials for recycling, biological treatment of organic waste, production of marketable compost, thermal treatment, for example, incineration to recover energy in the form of heat and electricity, and landfilling (Tian et al., 2013, Yan et al., 2010, Hui et al., 2006, Wang et al., 2015). The rate of production of MSW in developing countries requires paramount attention to tackle the ever-growing challenge of untreated amounts of MSW in most developing and under-developed nations. This is because the impact is becoming serious in terms of lingering environmental challenges on air, land, surface, and subsurface water systems, as well as short and long-time health implications (Othman et al., 2013, Kırtay, 2011, Tian et al., 2013). Solid waste management in South Africa greatly depends on landfill as a solid waste management approach, with 90.74 % of waste generated being disposed off by means of landfill in 2011. South Africa generated approximately 108 million tonnes of solid waste in 2011, of which 90.74 % was disposed of at landfills (Department of Environmental Affairs, 2012).

The classification of solid waste is not conclusive because 48 million tonnes are still left unclassified. In the order of 10 % of all solid waste generated in South Africa was recycled in 2011. Landfill of MSW releases GHGs and volatile organic compounds along with leachable toxic heavy metal to the surrounding environment.

The enormous emission of GHGs from some existing and closed landfill sites in South Africa is calling for serious and thorough solutions (Vossberg et al., 2014, Friedrich and Trois, 2016). Moreover, some of the environmental effects are discussed below.

2.12.1 Effects of Inadequate MSW Disposal and Management on Land

The soil is contaminated by being in contact with municipal solid waste (MSW) and leachate. In a study on a dumpsite in Kariba in Zimbabwe, a concentration of trace metals was found in soil samples collected from the area during 1996 and 1997. The accumulation of copper, lead, iron, and zinc were found at the disposal site (Chifamba, 2007). There is a high frequency of the landfill option while neither the financial nor the environmental implications are considered. However, Assamoi and Lawryshyn (2012) study report that a landfill site appeared to be the better option but only in the short term. Okonkwo and Mothiba (2005) also reported obtaining a high concentration of lead in the Madanzhe and Mvudi Rivers in Thohoyandou, South Africa, which was attributed to the effluent from a nearby sewage treatment plant and a waste dumping site.

These heavy metal contaminants pose severe health implications when released and find their way into the ecosystem. Similar experiences were observed by other authors suggesting actions that might lead to the uncontrolled release of heavy metals into the ecosystem through the disposal of untreated incineration ash and MSW (Kwak et al., 2006, Xiaoli et al., 2007, Yao et al., 2010, Haiying et al., 2010, Zhao et al., 2012, Sekito et al., 2014).

2.12.2 Effects of Inadequate MSW Disposal on Surface and Sub-Surface Water

Both surface and sub-surface water sources close to MSW management (dump sites, incinerators) are prone to heavy metal contaminations. The golden quarry landfill in

Harare pollutes groundwater in the area close to it. The concentration levels of coliforms, cadmium, iron, lead, and nitrates were above the water quality guidelines throughout the nearby suburb of Westlea. In a study of the Mucheke MSW dumpsite in Masvingo, Zimbabwe, Mangizvo (2008) noted that soil within a 50 m radius had been contaminated by trace metals of lead, iron, copper, zinc and phosphorus. There was a temporal migration of heavy metal and concentrations the distribution contaminants that might originate from MSW. Further study is needed to help reduce the infiltration into the ecosystem. About 4.6 million tonnes of total solid waste is being incinerated per year in the US which has led to the generation of a large amount of solid residues including fly and bottom ash, hazardous emissions and GHG that might find their way into community water sources (Ahmed and Gupta, 2009c, Ahmed and Gupta, 2009a, Ahmed and Gupta, 2009b).

The global potable water source is under serious depletion particularly access to potable water. Heavy metal, uncontrolled migration and other contaminants pose a life threat to the well-being of human survival and the availability of potable water.

2.12.3 Inadequate MSW Treatments, Disposal and Air Pollution

Incineration to generate energy is one of the traditional methods of dealing with combustible waste efficiently because it reduces the volume and mass of MSW. Although heavy metals are inert and give off no energy when they are incinerated, the high temperature of an MSW furnace causes metals to partially volatise, resulting in the release of toxic fumes and fly ash. But, incineration has drawbacks as well as particularly hazardous emissions such as NO_x, SO_x and HCl which are harmful organic compounds (McKay, 2002, Liu et al., 2015) and harmful process residues (Hasselriis and Licata, 1996).

Apart from any likely catalytic contribution of some compounds of heavy metal (alkali metals, Al, Ti, Si, Mg, etc.) available in pre-treated MSW, most heavy metal will be concentrated in both fly and bottom ashes. Heavy metals are found naturally in the environment and are released from a range of anthropogenic activities such as combustion processes (Hasselriis and Licata, 1996, Arena, 2012, Liu et al., 2015). Studies have reported larger fractions of heavy metal fractions concentrated in bottom ashes and most of these heavy metals may be recovered (Chimenos et al., 1999, Belevi and Moench, 2000, Forteza et al., 2004, Chang and Wey, 2006, Yao et al., 2010, Long et al., 2013, Sekito et al., 2014, Allegrini et al., 2014).

Generally, bottom ashes contain SiO_2, CaO, Al_2O_3, Fe_2O_3 Na_2O, K_2O and MgO (Chimenos *et al.*, 1999, Forteza *et al.*, 2004, Chang and Wey, 2006). The study of Yao et al. (2010) on distribution of heavy metals between fly and bottom ashes using transfer coefficient procedures, concludes that the average range of transfer coefficient for As and Mn out of the range of these heavy metals Cu, Cr, Mn, Ni, Cd, Co, As, Mo, Pb, and Zn, were between 0.533 and 0.947 respectively. The study of Belevi and Moench (2000) also investigated a group of eighteen heavy metals and non-metals and observed a range of transfer coefficients of 0.120 - 0.989 for heavy metals and for non-metals However, the transfer coefficients of Hg for studies mentioned above are significantly low or negligible (almost not detected). This shows that Hg has been completely transferred to fly ashes.

The studies of (Chimenos et al., 1999, Song et al., 2004, Song et al., 2013, Forteza et al., 2004, Chang and Wey, 2006, Yao et al., 2010, Tozlu et al., 2016, Sekito et al., 2014, Allegrini et al., 2014) used incineration towards waste-to-energy technology with untreated MSW.

However, incineration of MSW generates fly and bottom ash which release leachable toxic heavy metal, dioxin, furans and volatile organic compounds (Quina et al., 2008, Haiying et al., 2010, Zhao et al., 2012). Dioxin compound, which contains the dibenzo-p-dioxin nucleus, and furan are other compounds that contain the dibenzofuran nucleus.

Dioxin emission from incinerators attracts much attention from the public owing to its serious high health risk and the challenges required for a sustainable approach (Cheng and Hu, 2010, Chang and Wey, 2006, Liu et al., 2012). Dioxins and furans are emitted into the atmosphere from a wide variety of unregulated combustion processes. Their contribution to air pollution may impact on neighbouring communities in the order of such magnitude that could exceed the contribution of emissions from domestic activities to air-shed, especially in small communities. Most of the studies recommend pre-treatment in the form of source re-classification of MSW (Norbu et al., 2005) to enhance the quality of bottom ash residue for effective heavy metals recovery. According to Yao et al. (2010) report that a heavy metal concentration distribution in an MSW thermochemical conversion plant was mostly concentrated in the bottom ash residues during the incineration process. The reports indicated heavy metals, like As, Fe, Cu, Cr, Pb, Co, Ni and Zn, were highly concentrated mainly in the bottom ash residues with up to an average of 80 %. However, special attention should be paid to these metals, Cd, As, Cu, Cr, Pb and Zn, because of proven high toxicity to the environment.

However, little attention had been given to gasification emissions. In contrast to conventional wood-fired boilers, these systems operate at high temperatures and were much more versatile in achieving high reductions of both dioxins and PAHs, and in providing energy recovery options (Cheremisinoff and Rosenfeld, 2010, Quina et al., 2008).

Therefore, gasification technology conversion may be a very promising remedy for controlling the dangerous emission of furan, dioxin and other harmful emissions.

2.12.4 Efforts on Regulation of Environmental Impact of Inadequate MSW Disposal

Stringent environmental regulations are being imposed to control the environmental impact of MSW and incinerator residues. In China, advanced disposal technologies, effective laws, standards and regulations, as well as public awareness education have been proposed to prevent problems resulting from air pollution from MSW disposal processes and their adverse effects (Zhang *et al.*, 2012, Tian *et al.*, 2013). In addition, in the study of Wang and Geng (2015), they analysed carbon emissions from sanitary landfills, simple landfill, composting and open incineration. It was also reported that carbon emissions from sanitary landfills were more than double the amount of the emissions of composting and open incineration. The study emphasised the importance of the systematic MSW handling procedure as a fundamental tool to accrue economic and environmental benefits. The landfill is a long-term thermochemical, biochemical reactor producing several contaminants and pollutants into the air, water and land (Wang *et al.*, 2015). Policy towards ensuring the regulation of MSW treatment requires an enormous effort through contemporary research to balance the conflict between the priorities of cost and environmental implications (Fodor and Klemeš, 2012).

2.13 Combined Heat Power System and MSW Gasification

A combined heat power (CHP) system is also regarded as a co-generation system used to recover and make use of wasted heat (which would otherwise have been released into the atmosphere) or it is the simultaneous generation of electrical and thermal energy in a decentralised manner. The CHP system improves the overall efficiency of conversion processes (Farzaneh-Kord et al., 2016, Patuzzi et al., 2016). The increase in fuel (fossil fuel) utilisation is achieved by capturing the 'waste heat' released by the combustion of the fossil fuel to produce hot water in domestic CHP or steam in industrial CHP. There is also a reduction in power lost through transmission to the end-user in centralised power generation. The main components of the CHP system are an electrical energy generator, a supplementary thermal recovery system, heat exchangers and control instruments (Mikalsen et al., 2009). The types of commercially available and widely researched CHP generation are classified according to their prime mover and sources of energy.

The micro CHP system (fuel cell) pre-commercial project has been initiated for the implementation of micro-CHP systems on a large scale. According to Ren and Gao (2010), five countries (Japan, Germany, the UK, the Netherlands and the USA) are the most active in the research and development of micro CHP fuel systems. Japan deployed more than 10,000 cumulative units in 2010, providing home power and heating (Fuel Cell Today, 2013).

These include the ICE-based CHP system, the micro gas turbine-based CHP system, the fuel cell-based CHP system and the Stirling engine-based CHP system (Rovas and Zabaniotou, 2015, Pantaleo et al., 2015, Bartela et al., 2017).

Most of the heat generated through electricity production are mostly from non-renewable carbon-based sources (Mongibello et al., 2016, Mikalsen et al., 2009, Farzaneh-Kord et al., 2016). In this regard, the application of CHP systems with renewable option could be of a great advantage, not only in the efficiency of the electricity production but environmentally and for economic benefits (Torchio, 2015, Bianchi et al., 2014, Adams and McManus, 2014, Nazari and Ardehali, 2017, Kanematsu et al., 2017, Patuzzi et al., 2016). Some researchers had done some studies describing how MSW gasification (Kanematsu et al., 2017, Patuzzi et al., 2016, Salomón et al., 2011, Farzaneh-Kord et al., 2016) could be resourceful technology for renewable and sustainable CHP system.

The contribution of solid waste biomass to produce energy at reduced costs using thermochemical technology is attracting research interest (Dornburg and Faaij, 2001, Farzaneh-Kord et al., 2016). According to Bridgwater et al. (2011), the trend of small-scale MSW CHP in the UK and entire Europe is growing.

The study of Arafat and Jijakli (2013) utilized a modelling tool to produce energy from MSW (from UAE, USA and Thailand) gasification. The gasification system focused on energy production from municipal solid waste management (MSWM) though the heat and energy are still a challenge, co-generation potential is limited. The authors suggested that the gasification technology may offer a better technique to MSWM system and WTE technology than traditional incineration treatment technology despite the limitations.

The investigations of Chacartegui et al. (2015) and Farhad et al. (2010) presented a number of analyses on biogas fuelled CHP where generation economic feasibility of the CHP system and environmental implications of leachates were evaluated. The CHP system considered was fuel by biochemical processes producing landfill gases.

The CHP system had negative impact on the performance of power generation while new legislation has introduced constraints to the biogas and operation time. The management of final solid residue of MSW gasification was not considered in their study. The configuration of integrated CHP system and energy, economic and environmental performance were studied with a robust optimization design model developed by (Wang et al., 2014a). The study was able to minimise annual total cost and optimum MSW gasification in the CHP system was around 45 % and almost 90 % of CO_2 emissions reduction was achieved.

Another evaluation of biomass gasification integrated CHP system was performed by means of the micro-power optimization model HOMER Energy (Montuori et al., 2014) considering a micro-grid. The study generated scenarios to create a balance between consumption and generation. Thus, he suggested that demand response consumption in not only viable but more profitable than other conventional technologies using fossil fuels.

The ECLIPSE model was used to simulate techno-economic analysis of systems - combine biomass gasification with solid oxide fuel cell SOFC stacks (Ud Din and Zainal, 2016). The choice of air blown down-draft gasifier was because simple operation and low capital cost. The performance efficiencies were around 30 % which was more than similar solid waste fired electricity plant within the same scale (McIlveen-Wright et al., 2011, McIlveen-Wright et al., 2013).

The techno-economic study was done to measure feasibility of some biomass-fuelled CHP systems operated in the community. An economic modelling developed was used and several operational scenarios were analysed to determine the viability of specific systems and the sensitivity of the results to a range of technical and economic parameters.

The CHP system demonstrated positive net present value (NPV) without the need for starting or working capital subsidies (Wood and Rowley, 2011). The sensitivity conducted implied that there was a very diverse to input parameters (Wood and Rowley, 2011).

A CHP system-based fuel cell offers high efficiency, low emission (if not zero), a decentralised or stand-alone power, and heat generation and supply for mostly domestic (Pellegrino et al., 2015) and stationary use (Najafi et al., 2015, Ren and Gao, 2010, McMahon, 2015). The fuel cell is cogeneration CHP system ranging from low temperature (Gandiglio et al., 2014), medium temperature (Li et al., 2009, Chandan et al., 2013, Bujlo et al., 2013, Najafi et al., 2015), moderate temperature (Hamad et al., 2014) and high temperature fuel cell(Farhad et al., 2010) but they mostly depend on fossil fuel(Mikalsen et al., 2009). The studies of (Korsgaard et al., 2006, Korsgaard et al., 2008a, Korsgaard et al., 2008b, Hawkes et al., 2009, Hawkes et al., 2006) established the prospects of fuel cell for CHP applications.

Among the other benefits of fuel cell-based systems are reliability, availability and a reduction of energy cost on a long-term basis and improvement of overall system efficiency (Hinnells, 2008, Staffell, 2015b, Staffell, 2015a, Najafi et al., 2015).

South Africa is one of the largest deposits of Platinum Group Metal (PGM) resource in the world. The availability of this abundant natural resources has led to initiation of hydrogen and fuel cell technologies (HFCT) research development and innovation (RDI) strategy which was officially launched in 2008 by the Department of Science and Technology (DST)(Pollet, 2013). The programme was Hydrogen South Africa (HySA) based upon the beneficiation of the country's large PGM resources for production of catalyst(Barrett, 2013b, Barrett, 2013a) while one the area of research is on high temperature proton exchange membrane fuel cell (HT-PEMFC) (Pollet et al., 2014).

In this line, hydrogen fuel production (Bessarabov et al., 2012) is very important from renewable resources will be an added advantage over environmental impacts of fossil fuel. This study merges two distinct systems (fuel processor via gasification of MSW for HT-PEMFC stack) together to enhance cogeneration. This system exploits the availability of MSW, a moderate temperature range and low emission of GHG from the system (Patuzzi et al., 2016).

The system thus requires a viable technical, economic and environmental assessment and analysis in order to become viable cost-effective systems. The cost and durability of HT-PEMFC (Najafi et al., 2015) appear to be the lingering obstacles for HT-PEMFC-based systems.

2.14 Techno-Economic Analysis Models and Tools

Several tools are employed in evaluating a techno-economic analysis. The HOMER (Hybrid Optimisation Model for Electric Renewables) simulation package was applied by (Zoulias and Lymberopoulos, 2007, Karakoulidis et al., 2011)). Korsgaard et al. (2008a) used the Matlab Simulink Package with EES Package; the ECLIPSE simulation package was used by (McIlveen-Wright et al., 2011) which was developed by Williams and McMullan (1996), and Aspen Plus Package was used by (Klimantos et al., 2009)). These models are all prominent tools used in various techno-economic assessments and analyses.

Secanell et al. (2011) conducted a sensitivity analysis to deal with the change of output variable with respect to variation in input variables.McIlveen-Wright et al. (2011) conducted a detailed techno-economic analysis on an integrated biomass gasification integrated with a solid oxide fuel cell-based CHP system at high and intermediate temperatures. They reported a high rate of efficiency with significantly low emissions relative to their small-scale operation compared to other CHPs of the same capacity. However, a high investment cost is imminent due to the fuel cell cost and lifespan of the system/investment. The study concluded that the challenges of these costs may be overcome in the foreseeable future.

Also, TeymouriHamzehkolaei and Sattari (2011) conducted a detailed study on the economic analysis of a micro-CHP system in different zones in Iran with climatic variations. They developed a model using sensitivity analysis to find the optimum value of fuel and price of electricity for profitability. Their study shows both electricity price and duration of heat use are sensitive to profitability. However, the environmental analysis was not done. Besides, greater economic merit was achieved due to the incentive policies of the government and private sectors.

The model developed by Williams and McMullan (1996) incorporates a number of stages of technical and economic analysis embedded in the eclipse model. The model's financial parameters are total capital investment, net present worth and break-even point or payback time. The model prescribes various options of evaluating some factors in investments such as the influence net present value (NPV), discounted cash flow rate of return (DCFRR), return on Investment (ROI), break-even point (BEP) and payback time (PT). All these financial parameters mentioned can give enough of an analysis of an energy-generating system.

Sen and Bhattacharyya (2014) use HOMER. developed by NREL (National Renewable Energy Laboratory, USA), as a preferred tool for renewable technologies (including PV, wind, hydro, fuel cells and boilers) and perform hourly simulations. HOMER is a good tool for deciding the system configuration for decentralised systems. The model can perform techno-economic analysis and compares a range of equipment with different constraints and sensitivities to optimise the system design. The analysis is done on the technical properties of the system and the life-cycle cost (LCC) of the system.

The model minimises the total net present cost (NPC). Since the cost of the supply of renewable energy-based electricity may not always be a cost-effective option for remote applications, there is a need for support (transportation) by the government. Also, different groups of researchers have applied the model to evaluate economic by means of the micro-power optimisation model, HOMER Energy.

The outcome of their study shows that the cost of supplying the variability of renewable resources with other traditional resources is more expensive than requiring the participation of customers to reduce the total load in the micro grid.

Nevertheless, micro grids may improve the global efficiency of the power system, reducing the energy losses with the subsequent reduction in the carbon footprint (Montuori et al., 2014).

The study of Huang et al. (2011) applies the ECLIPSE model to a trigeneration (heat + cooling +electricity) system to evaluate the economic analysis of a biomass-based system. Their study concludes that the high capital cost of the system hinders the economic performance and viability of small system application. The model actually considers economic, technical and environmental analysis. The break-even point was used to evaluate the economic analysis but the total capital cost of investment is very high.

McIlveen-Wright et al. (2013) used the ECLIPSE model to evaluate the technical, environmental and economic analysis of large-scale biomass combustion systems and system efficiencies for generating electricity and CO_2 emissions. These are evaluated and compared with a traditional, large coal-fired plant. The specific investment (SI) and Break-Even Electricity Selling Price (BESP) were calculated and compared with the coal-fired plants. The study further carried out economic sensitivity analyses. The break-even electricity selling price (BESP) was determined, based on the net present value (NPV), for a range of biomass buying prices (at 30 % Moisture Content). They opined that the system could only compete with the traditional coal-fired power plants at low wood costs. However, the issue of the cost of biomass transportation, moisture content and costs of wood were factors that need further investigation.

Overall, environmental merits, cost implications, transportation, medium/small-scale application and government intervention policy are challenges that require further studies, particularly for decentralised applications. This research investigated the MSW (biomass type) gasification/HTPEM fuel cell-based CHP system to evaluate the techno-economic analysis while the environmental impact was not excluded.

It is highly improbable that approval will be given to investment into the development of a process without some indication of the likely positive economic impact, as well as technical advantage, were the process to prove successful. Thus, an economic evaluation or analysis usually comprises an estimate of the capital and operating costs and an indication of other financial parameters such as return on investment, net present value, discounted cash flow rate of return, payback time and break-even point and sensitivity analysis (Smith, 2005, Sinnott and Towler, 2012, Peters et al., 2013). These are economic analysis indicators which prove useful for measuring the viability of the process. The financial indicators are further narrowed down to profitability standard and economic potential.

The Aspen Plus Model Package is one of the most widely accepted models in chemical industry design. The modelling tool is used for a steady-state simulation, modelling chemical, power generation design, performance monitoring, optimisation and business planning for chemicals, specialty chemicals, petrochemicals and metallurgy industries.

The Aspen Plus Model can solve challenging engineering and operating problems that arise throughout the lifecycle of a chemical process, such as designing a new process, troubleshooting a process unit or optimising operations of a full process. It caters for the deficiencies of other models (Schefflan, 2011).

The Model criteria of Aspen Plus are preferred for this study. Aspen Plus modelling tools are characterised by tools such as the Aspen Plus economic evaluator; Aspen capital cost estimator; Aspen plus In-plant cost estimator and the Aspen plus process economic analyser.

2.15 Chapter Summary

The characteristics of municipal solid waste (MSW), MSW management and the renewable potential of MSW are reviewed in this chapter. Physicochemical characterisation methods and gasification technologies and their relevant processes are also discussed; possible effects environmental effects of MSW management and the choice fuel cell application in a combined heat power system is reviewed, as well as the cost implications of the overall system. The next chapter will present methodology of the research.

CHAPTER THREE

3 MATERIALS AND METHODOLOGY

3.1 Materials and Methodology

The materials and methodology section of this study involves a brief description of locations and sampling of municipal solid waste (MSW) from municipal solid waste facilities in Cape Town, followed by pre-treatment and pelletisation of pre-treated MSW. The physicochemical characterisation of pre-treated MSW, gasification procedures, quantification of heavy metal concentration and costing procedures will also be discussed.

3.1.1 Description and Characteristics of Sampling Area

Cape Town is in the Western Cape, a region in the southern part of South Africa. It has a coordinate of latitude 33.55° S and longitude 18.25° E with a land mass area of 2,455 km^2. It is a port city located on South Africa’s southwest coast as shown in Figure 3.1.

In 2014, the city was ranked 10th most populous city in Africa and home to 64 % of the Western Cape's population. It is one of the most multicultural cities in the world, reflecting its role as a major destination for immigrants and expatriates to South Africa. According to the South African National Census of 2011, the population of the Cape Town metropolitan municipality is over 3.7 million. The settlements in Cape Town are classified as follows: formal residential, informal residential, farming and collective living quarters. It has industrial and commercial areas. These factors mentioned above contribute to the economy and municipal solid waste distributions across the city. There are over one million households in the municipality with an average annual household income of US$14,706.

Cape Town is the provincial capital, administrative centre and economic hub of the Western Cape Province, South Africa's second main economic centre and Africa's third main economic hub. Cape Town is an important centre for the industry on the continent with the highest number of successful information technology companies in Africa. Growing at an annual rate of 8.5 % and an estimated worth of R77 billion in 2010 nationwide, the IT industry in Cape Town is becoming increasingly important to the city's economy.

The Western Cape is an important tourist region in South Africa; the tourism industry accounts for 9.8 % of the GDP of the province and employs 9.6 % of the province's workforce. The City of Cape Town is a metropolitan municipality. The city is governed by a 221-member city council. The city is divided into 111 electoral wards. The solid waste management of the city is expected to be a continuous challenge.

A map showing the geographical location of Cape Town as well as sampling locations follows in Figure 3.1 and Table 3.1 respectively.

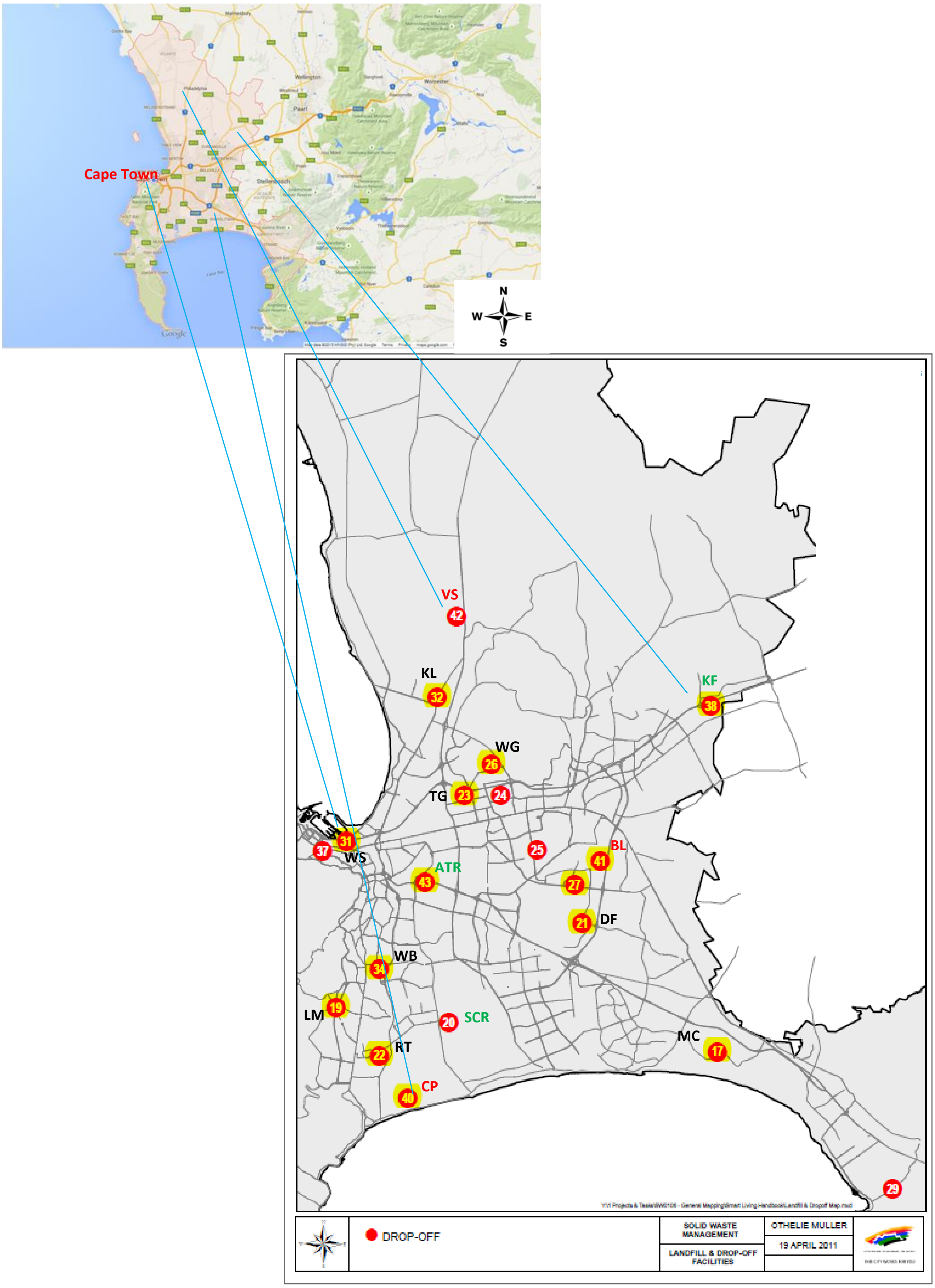

Figure 3.1: Map of City of Cape Town and Sampling Locations

Table 3.1: Municipal Solid Waste Disposal Facility Sites around Cape Town

Municipal Solid Waste Disposal Facility	GPS Location (S' E')	Tonnes/day
Ladies Miles (DO)	-34.030072, 18445121	150 - 500
Belhar (DO)		> 50
Killarney (DO)	-33.829811, 18.526669	> 220
Welgelegen (DO)	-33.8735374, 18.5696545	200 - 400
Delft (DO)	-33.978125, 18.642142	20 – 40
De Grendel (DO)	-33.8939147,18.5767901	> 80
Woodstock (DO)	-33.9263086, 18.4332658	> 242
Tygerdal (DO)	-33.9390663, 18.4528555	> 100
Kraaifontein (IWM & TS)	-33.9163982, 18.4461799	> 800
Athlone (DO & TS)	-33.949205, 18.516379	> 1980
Bellville South (LS & TS)	33.9356509, 18.6552615	
Coastal Park (LS & TS)	-34.0170711, 18.3298305	1000 - 2500
Vissershok (LS & TS)	-33.773931, 18.545786	

DO = Drop Off

IWM = Integrated Solid Waste Management

TS = Transfer Station

LS = Landfill Site

3.1.2 MSW Sampling and Pre-treatment

The MSW samples were collected from selected municipal solid waste disposal facilities (MSWDF) spread around the settlements in Cape Town. Thirteen solid waste disposal facilities (drop-off sites, transfer stations and landfill sites) were selected for raw MSW sampling, namely, Kraaifontein, Athlone, Woodstock, Tygerdal, Belhar, Killarney, Wynberg, Macassar, Delft, Welgelegen Ladies' Mile, Retreat and Coastal Park (KF, ARTS, WS, TG, BL, KL, WY, MC, DF, WG, LM, RT and CP). Among them, KF, ARTS, and CP are transfer stations, while others are drop-off sites and landfill site. This includes ten drop-off sites and one landfill site (refer to Table 3.1 and Figure 3.1).

In each MSWDF, the MSW samples were randomly collected in order to achieve a representative sample. Subsequently, all sub-samples from every location were manually mixed completely and immediately placed in an airtight plastic bag. Certain amounts of MSW, varying between 3.0 Kg and 5.0 kg, were finally collected from each MSWDF. The MSW samples were made up of a mixture of five different components of kitchen garbage, paper, textiles, wood, garden waste, metallic and glass cans, and plastics. The percentage of distribution of the different components of MSW were obtained

The MSW samples were dried under the sun for a period of three days to reduce the moisture content. The inorganic components (non-combustible) of MSW samples such as ferrous and non-ferrous metals, glass and plastics were separated manually. This procedure enabled a physical characterisation of the MSW samples. The plastics content was initially removed during sorting and returned to the MSW after drying. The combustible materials (including the plastics) were shredded and pulverised to form a fluffy material after the separation.

The organic fraction of the MSW samples was first dried at 105 ^{0}C for 2 h, then shredded into particles in sizes of approximately < 5 mm (see Figure 3.2) and mixed before performing the experiments to obtain representative MSW samples from the different sources (Narobe *et al*., 2014).

Furthermore, the MSW were shredded again, milled and sieved with a specific mesh to ensure that MSW was properly homogenised (Figure 3.2). The pre-treated MSW samples were divided into more than six portions for each sampling location for various determinations and chemical analyses.

Figure 3.2: The Pre-treated and Shredded Samples of MSW for Chemical Analysis.

3.2 Physicochemical Characterisation

The physicochemical characterisation was carried out on pre-treated MSW otherwise referred to as potential solid fuel. The physicochemical characterisations were relative bulk density, proximate analysis, ultimate analysis (elemental compositions), high heating value, and thermo-gravimetric analysis (Basu, 2013, Narobe et al., 2014).

3.2.1 Determination of Bulk Density

Both types of bulk density are measured in Kg/m^3, both packed bulk density and loose bulk density which are considered for the handling of solids. Loose bulk density is also known as aerated bulk density or un-compacted bulk density, while packed bulk density is also called compacted bulk density. The determination of packed bulk density requires a sort of compression or packing, while loose bulk density is determined as received. The determination of bulk densities is to show the quantity of air entrained in the void spaces between the particles, improve the power density of the solid fuel and the degree of compressibility of the solid fuel. Refuse-derived fuel (RDF) pellets were prepared at room temperature with an improvised single pellet press unit. Packed bulk density is an important factor in storage and transport and is a more realistic quantity to use.

3.2.2 Determination of High Heat Values (HHV)

The E2K Combustion Calorimeter System was used to determine high heating values (HHV). It is a "dry" static jacket isothermal calorimeter system with an isothermal design using a waterless patented vessel. The E2K Combustion Calorimeter System has the following accessories: bomb calorimeter, vessel, cooler and filing station (Figure 3.3). The calorimeter has a temperature resolution of 0.000001 ^{0}C; net HHV resolution 0.001 MJ/Kg and operating temperature from 0 to 60 ^{0}C. The vessel has the capacity to determine the high heating value of samples of 0.200 g and 1.999 g.

The E2K Calorimeter Air Cooler Station

The Filling Station The Vessel (A Bomb)

Figure 3.3: The Bomb Calorimeter System

The E2K Combustion Calorimeter System is in compliance with the following international standards: ASTM-E711-87 (HHV of RDF by Bomb Calorimeter) and DIN 51900-2 (Determining the Gross High heating value of solid and liquid fuels using 2003 Yes isoperibol or static jacket calorimeter and calculation of net HHV).

To perform this measurement, the equipment used a controlled combustion of the sample under an oxygen atmosphere and measured the calorific power very carefully, based on information obtained during combustion. The HHV was obtained in MJ/Kg. Certain weights between 0.249 g and 0.501 g of the MSW sample were weighed and put into the crucible and placed in the vessel, and then taken to filling station where the vessel was filled up with oxygen measuring up to 3 MPa (3000 KPa).

The filled vessel and pressurised vessel were transferred to the bomb calorimeter for the determination of the actual high heating value. After preparation of the vessel in the calorimeter, the vessel was put through four distinct cycles, waiting for stabilisation for one minute so that the vessel could equalise outside the calorimeter. The actual determination of the sample was then carried out for two minutes in the bomb calorimeter. Thereafter, the vessel was allowed to cool for an approximate period of one hour, before subsequent determination of MSW HHV. These procedures were carried out in triplicate for all the samples from various locations and other general MSW samples totalling 53 samples.

3.2.3 Determination of MSW Composition

The elemental composition of pre-treated MSW was limited to a few elements. The ultimate analysis of the pre-treated MSW samples was obtained with a CHNS/O analyser (Vario Micro cube, Elementar) (Figure 3.4).

Figure 3.4: The CHNS/O Analyser (Vario Micro-cube Elementar)

The analysis gives the weight percentage of carbon, hydrogen, oxygen, nitrogen and sulphur in the samples simultaneously and the weight percentage of oxygen is determined by the difference.

The total amount of carbon and nitrogen was determined by the elemental analyser truspec micro (LECO). The samples were dried at 60 ^{0}C. The samples were then milled using a Retch ball mill to a fineness of ca. 50 µm. 2 to 4 mg of sample were then weighed into a tin cup and sealed. The sample was then introduced into an auto sampler and the C, H, N, S and O were determined (simultaneously).

The Leco TruSpec Micro is a system that determines C, H, N and S in organic materials using Windows-based software to control the system and data management. The analysis is done in several steps. The first step occurs prior to the analysis when 2 mg of the samples are precisely weighed into weightless tin capsules. The analysis itself is realised in three steps: purge, combustion and analysis.

First, the purge phase involves removing excess atmospheric gases (which contain C and N and which entered the system during sample loading or standby) in the instrument. The entire system (tubing, column and crucible) was kept clean from any atmospheric contamination with a constantly maintained stream of helium.

The second step is the combustion phase. Just prior to the sample introduction, the helium stream was dosed with a precise volume of pure oxygen. When the sample entered the combustion tube (kept at 1075 ^{0}C) it burned instantaneously, followed by intense oxidation of the tin capsule (flash combustion). The products of combustion were swept through the system by the Helium carrier gas, then sent through a secondary furnace (850 ^{0}C) for further oxidation (any oxides of nitrogen are reduced to nitrogen), reduction and particulate removal.

The method is based on the oxidation of the sample by 'flash combustion' which converts all organic and inorganic substances into combustion gases (N_2, NO_x, CO_2, and H_2O). The products of combustion thus separate into nitrogen, carbon dioxide and water vapour which are quantitatively measured by a thermal conductivity detector.

The third step is the analysis of the gas phase. The combustion products (gases) were measured quantitatively by means of a non-dispersive infra-red absorption detection system, except for the nitrogen which was determined via a thermal conductivity detector.

The combustion gases passed from the secondary furnace through a heated manifold to the water infrared detector for hydrogen analysis. From the carbon dioxide detector, the combustion gases passed through a column filled with lecosorb and anhydrone to remove carbon dioxide and water after which the nitrogen is measured by thermal conductivity.

The final result was expressed as a percentage. Before calibration and analysis, blanks were analysed and a blank area was set. The analysis was carried out on the LECO Micro Truspec analyser, using the method 'CSG Sulfamethazine'. Control standards were also analysed with the samples to evaluate the precision and accuracy of the measurement.

3.2.4 Determination of Ultimate Analysis

The TGA instruments system (SDT Q600 V20.9 Build 20 Module DSC-TGA Standard) was used to obtain a proximate analysis of the pre-treated MSW samples (moisture, volatile matter, fixed carbon and ash content of the MSW). The SDT Q600 provides simultaneous measurement of weight change and true differential heat flow on the same sample from ambient to 1500 ^{0}C (Figure 3.5).

Figure 3.5: TGA Instruments System (SDT Q600 V20.9 DSC-TGA Standard)

It features a field-proven horizontal dual beam design with automatic beam growth compensation, and the ability to analyse two TGA samples simultaneously. DSC heat flow data is dynamically normalised using the instantaneous sample weight at any given temperature. The instrument has the following features: sample capacity of 200 mg (350 mg including a sample holder); a balanced sensitivity of 0.1 µg; temperature range from ambient to 1500 ^{0}C; heating rate – ambient to 1000 ^{0}C; heating rate ranges from ambient to 1500 ^{0}C at 0.1 to 25 ^{0}C/min. Additionally, the furnace cools forced air (1500 to 50 0C in < 30 min, 1000 0C in 50 0C in < 20 min) with DTA sensitivity at 0.001 0C and a mass flow controller with automatic gas switching included.

3.2.5 Thermo-gravimetric Analysis Methodology

This experiment was performed with the SDT Q600 V20.9 Build 20 Module DSC-TGA Standard, similar to the above procedure, but could achieve a maximum temperature of 1500 ^{0}C and heating rates from 2 to 30 ^{0}C /min. The experiments were conducted under an inert flow of nitrogen air at a rate of 50 mL/min to prevent the samples from oxidising and to determine the concentration of moisture and volatile material. Subsequently, dry air (50 mL/min) was used to determine the ash content. The experimental procedures were divided into three steps to obtain moisture contents, volatile matter and ash content respectively. A fifteen-step temperature program was used

Steps 1 to 4 (Mass flow 50 mL/min, Isothermal for 1 min, Ramp 30 ^{0}C /min to 70 ^{0}C , Ramp 15 ^{0}C /min to 90 ^{0}C , Ramp 2 ^{0}C /min to 105 ^{0}C) were conducted to determine the moisture content.

Steps 5 to 11 (Isothermal for 30 min, Ramp 10 ^{0}C /min to 145 ^{0}C, Isothermal for 10 min, Ramp 10 ^{0}C /min to 500 ^{0}C, Isothermal for 60 min, Ramp 20 ^{0}C /min to 600 ^{0}C, Isothermal for 10 min) were performed to determine the concentration of volatile material.

Lastly, steps 12 to 15 (Mass flow 50 mL/min, Isothermal for 40 min, Ramp 20 ^{0}C /min to 700 ^{0}C, Isothermal for 10 min, Mass flow 5 mL/min) were conducted to determine the ash content of the MSW samples and adapted same temperature programme used by Pazó et al. (2010).

Starting from room temperature, the sample was observed to dry if the sample contained moisture. A small weight (moisture or gas desorption) was lost of up to about 150 ^{0}C. Between 200 ^{0}C and 500 ^{0}C, there was thermal oxidative decomposition leading to a very rapid loss of weight due to the evolution of additives and volatile materials. After the release of these materials, there was slow loss of weight at temperatures above 600 ^{0}C as the residual char (metallic oxides and inorganic salts) decomposed. The conversion of the sample in inert atmosphere nitrogen is a function of temperature (Jenkins et al., 1998).

3.3 Thermochemical Theoretical Processing and Reaction Schemes

Thermochemical conversion of a carbon-containing material through the addition of heat in an oxidant-controlled environment was employed using gaseous compounds such as water, air, oxygen and their mixtures, producing largely gaseous products as suggested by these authors Basu (2013) and Huang et al. (2011). A downdraft fixed-bed gasifier was selected because of low tar formation (Chen *et al.*, 2013), pellet fuel compatibility, moisture content tolerance, low gasification temperature and a suitable power range.

The air blown downdraft fixed-bed gasification processes involved the following reaction schemes: drying (dehydration and decarboxylation), thermal decompositions, char combustion/tar reforming, and gasification and char gasification reactions (Pinto *et al.*, 2002). The sequences of reaction schemes follow the downdraft fixed-bed gasifier presented in Figure 3.6. The theoretical calculations were based on stoichiometry ratios of all reactions which were used to examine the schemes of the reactions. The Aspen Plus Model process tool was employed to investigate the reactions (exothermic and endothermic) in the downdraft gasification and WGS reactions. A detailed process flowsheet diagram (PFD) is shown in the Aspen Plus Model interface in Figure 3.7.

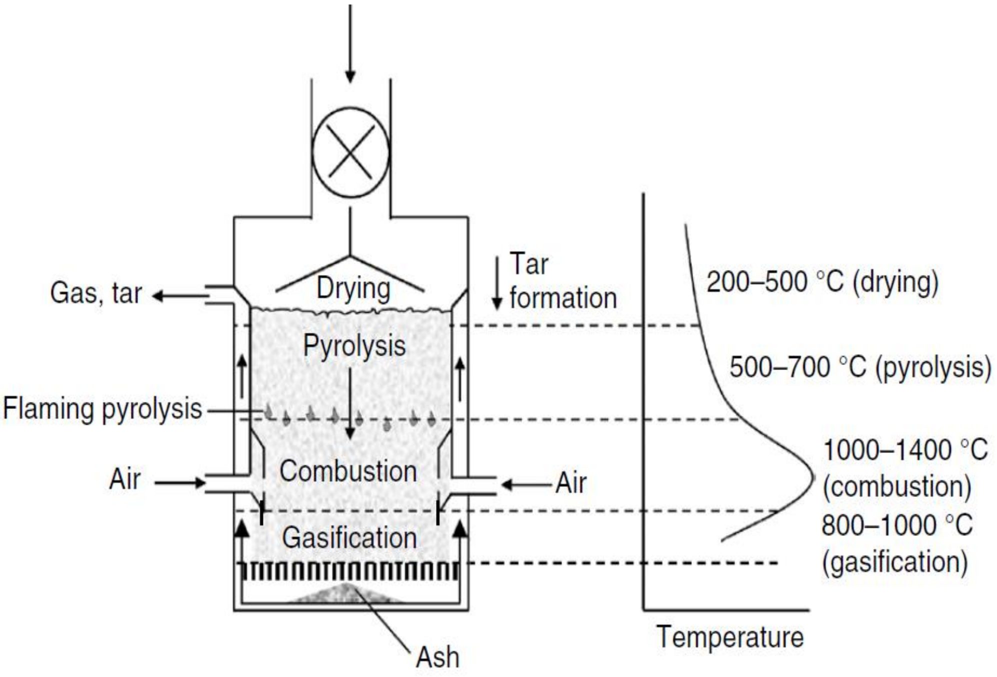

Figure 3.6: Reactions Schemes in Downdraft Fixed-bed Gasifier (Basu,2103).

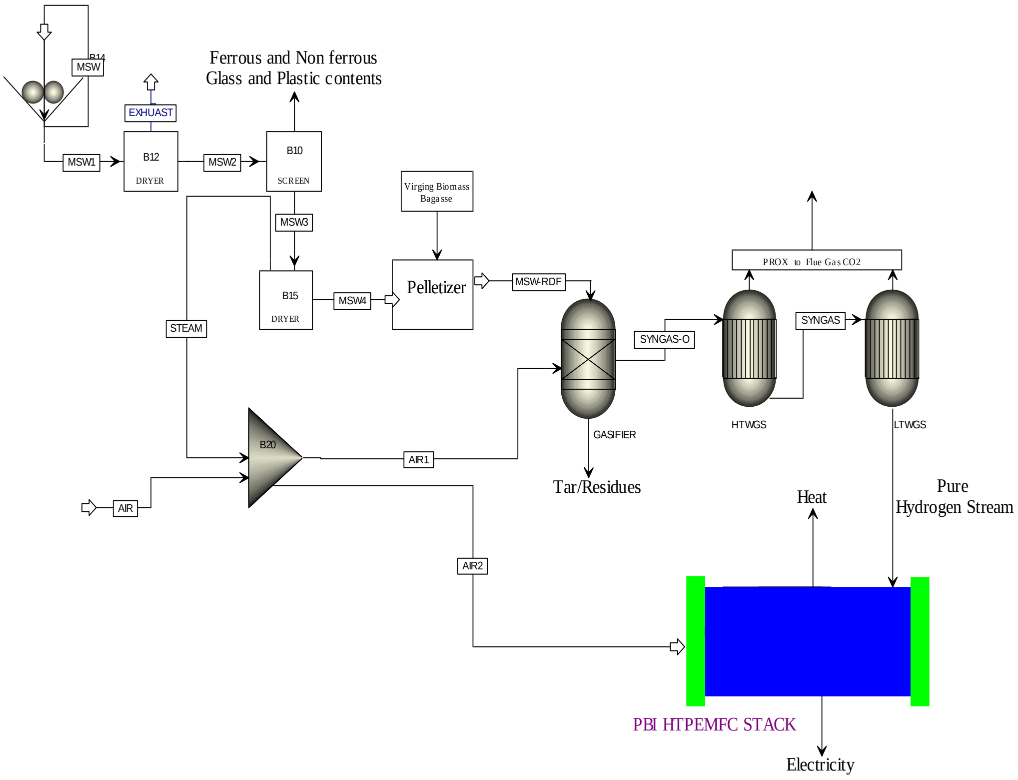

Figure 3.7: Aspen Plus Process Flow Diagram of the System (Own Source).

3.3.1 Modelling Protocol

One of the most widely accepted models in chemical industry design kits is Aspen Plus. ASPEN (Advanced System for Processing Engineering) is a process-modelling tool for steady-state simulation, modelling chemical, power-generation design, performance monitoring, optimisation and business planning for chemicals, specialty chemicals, petrochemicals and metallurgy industries. Aspen Plus solves the critical engineering and operating problems that arise throughout the lifecycle of a chemical process, such as designing a new process, troubleshooting a process unit or optimising operations of a full process. This study considered a number of Aspen Plus reactor models (Sotudeh-Gharebaagh et al., 1998). This simulation approach presented a model approach to obtain a process simulation programme for RDF gasification in a fixed-bed downdraft gasifier. A number of chemical reactions are involved in the gasification reactions as shown in equations 3.1 - 3.14.

The Aspen Plus Model simulated the following processes in a sequence of operations (Bell et al., 2011, Basu, 2013), such as:

Drying (dehydration and decarboxylation);

Thermal Decomposition;

Char Combustion and Reforming;

Gasification and Char Gasification.

First, the drying (Dehydration and Decarboxylation) reactions:

$$C_m H_n O_q \rightarrow C_m H_{n-2q} + qH_2O \tag{3.1}$$

$$C_m H_n O_q \rightarrow C_{m-\frac{q}{2}} H_n + \left(\frac{q}{2}\right) CO_2 \tag{3.2}$$

Second, the thermal decomposition reactions:

$$C + 0.5O_2 \rightarrow CO \tag{3.3}$$

$$C + H_2O \leftrightarrow CO + H_2 \tag{3.4}$$

$$C_n H_m + \left(\frac{n}{2}\right) O_2 \rightarrow nCO + \left(\frac{m}{2}\right) H_2 \tag{3.5}$$

Third, the char combustion and reforming reactions:

$$C + O_2 \rightarrow CO_2 \tag{3.6}$$

$$2CO + O_2 \rightarrow 2CO_2 \tag{3.7}$$

$$C + CO_2 \rightarrow 2CO \tag{3.8}$$

$$C + H_2O \leftrightarrow CO + H_2 \tag{3.9}$$

$$C_n H_m + \left(\frac{n}{2}\right) O_2 \rightarrow nCO + \left(\frac{m}{2}\right) H_2 \tag{3.10}$$

Fourth, gasification and char gasification reactions:

$$C_n H_m + nH_2O \leftrightarrow nCO + \left(n + \frac{m}{2}\right) H_2 \tag{3.11}$$

$$C_n H_m + nCO_2 \rightarrow 2nCO + \left(\frac{m}{2}\right) H_2 \tag{3.12}$$

$$C_n H_m + xH_2O \rightarrow yCO + zH_2 + wC_p H_q \tag{3.13}$$

And, finally, the water-gas shift reaction (WGS):

$$CO + H_2O \leftrightarrow CO_2 + H_2 \tag{3.14}$$

3.3.2 Modelling Procedure

Selectivity of syngas production towards High H_2/CO molar ratio was the main target of the modelling to make the product a suitable fuel source for HT-PEMFC. The HT-PEMFC possesses a high tolerance to CO-poisoning in the HT-PEMFC base system. RYield, RStoich, REquilb and RGibbs (Schefflan, 2011) were considered for these reaction schemes in the Aspen Plus Model environment and operating parameters as illustrated in Table 3.2 and Table 3.3.

Table 3.2: The Aspen Plus Reactor Model Required for the Simulation

Reactor Model in Aspen Plus Model	Rector Model Descriptions
RYield	A reactor-based yield. It is applied when the distribution of products is known. No reaction stoichiometry is required.
RStoich	A stoichiometry-based reactor with specified extent of reaction It allows the use of several reactions with the molar extent of conversion or fractional conversion of a component.
REquilb	A rigorous equilibrium reactor based on reaction stoichiometry. It is used when reaction stoichiometry and some of the reactions reach equilibrium.
RGibbs	A rigorous reactor that includes phase equilibrium using Gibbs' free energy minimisation. The RGibbs block can be used to establish the equilibrium composition between reactants and products.

The model approach was similar to the study of (Sotudeh-Gharebaagh et al., 1998, Corella and Sanz, 2005) but there were variations in the choice of processes, reactions and operating parameters as can be seen in Table 3.3.

Table 3.3: List of Operating Parameter Inputs Used in RDF Gasification Simulation.

Parameters	Value	Unit
Gasifier Temperature Block	700 - 950	^0C
Equivalence Ratios	0.02 - 0.60	-
Steam Temperature	110	^0C
RDFs Flow Rate	5/10	Kg/h
Gasifier Agent Flow Rate	5 - 20	Kg/h
Inert	50	m^3/h

The following assumptions are considered for the simulations. All the chemical reactions were assumed to have reached equilibrium within the air-blown downdraft fixed-bed gasifier. These assumptions are as follows: a steady state condition is assumed and adiabatic and isobaric are assumed for the first process. The reactions occur in sequence. sulphur and nitrogen were not considered in the reactions but char is assumed to be 100 % for the last gasification processes. The product gases of RDF gasification are hydrogen, carbon monoxide, carbon dioxide and methane. Tar formation is assumed to be negligible in the air-blown downdraft fixed-bed gasifier (Bell et al., 2011, Basu, 2010, Basu, 2013). Ash is considered inert.

Lists of some assumption regarding the conversions and selectivity of pyrolysis, gasification and other reactions are presented in Table 3.3. The selectivity of various reactions is restricted to the major components (H_2 and CO) of syngas fuel.

Table 3.4: Some Required Assumptions for Mass and Energy Balances

Reactions	Conversion	Selectivity to high H_2/CO
Pyrolysis	75 %	75 %
Gasification	60 %	75 %
WGS	75 %	65 %
Carbon Conversions	80 %	75 %

3.4 Calculation Procedure of Mass and Energy Balance for Gasification

The global balance of all the reactions were considered (equations 3.1 - 3.14) containing all the steps and phases (drying, dehydration and decarboxylation) as well as thermal decomposition, char combustion and reforming, and gasification and char gasification required in the air-blown downdraft gasifier. There were a number of assumptions regarding reactants, intermediate products, product distribution and all the chemical reactions (major and minor). The obtained formula for enthalpy calculations are presented in APPENDIX F. A unit mass in kg of pre-treated MSW basis for an hour was assumed for all the balances.

The various balances were distributed into the following; stoichiometry oxygen/air requirement; standard stoichiometry steam requirement and steam produced; stoichiometry CO_2 requirement and produced; standard syngas production; standard stoichiometry steam requirement and produced for WGS; standard stoichiometry O-C, S-C and equivalence ratios.

3.4.1 Standard Stoichiometry Oxygen/Air Requirement

The reactions from the second phase (thermal decomposition and char combustion and reforming) were considered in the determination of oxygen-air required for the gasification process. Char and tar combustion were considered based on the works of (Corella and Sanz (2005), Li and Suzuki, 2009, Kotz et al., 2010). The reactions are presented below. Equations 3.15 - 3.18 were introduced to account for tar conversion.

The products of these reactions are mainly syngas component gases with a negligible amount of tar in the downdraft gasifier.

$$C + 0.5O_2 \rightarrow CO \qquad \Delta^\circ H_{r,773} = -103.6412\ KJ/Mol \qquad (3.15)$$

$$C\,H_{1.14} + 0.5O_2 \rightarrow CO + 0.57H_2 \qquad \Delta^\circ H_{r,773} = -189.1009\ KJ/Mol \qquad (3.16)$$

$$C\,H_{0.8} + 0.5O_2 \rightarrow CO + 0.4H_2 \qquad \Delta^\circ H_{r,773} = -254.1860\ KJ/Mol \qquad (3.17)$$

$$C_{0.54}H_{0.54} + 0.27O_2 \rightarrow 0.54CO + 0.27H_2 \qquad \Delta^\circ\ H_{r,1123} = -25.6824\ KJ/Mol \qquad (3.18)$$

3.4.2 Standard Stoichiometry Steam Requirement and Production

The reactions from phase three (drying dehydration, char combustion and reforming and char gasification) were considered in the determination of the steam required and produced for the gasification processes (see APPENDIX F). Char combustion and gasification were considered based on the works of (Corella and Sanz (2005), Li and Suzuki (2009)). The reactions are presented below.

$$C + H_2O \leftrightarrow CO + H_2 \qquad \Delta^\circ H_{r,1123} = +212.6505\ KJ/Mol \qquad (3.19)$$

$$CH_4 + H_2O \leftrightarrow CO + 3H_2 \qquad \Delta^\circ H_{r,1123} = +326.4565\ KJ/Mol \qquad (3.20)$$

$$CH_{0.2}\,H_{0.13} + 0.87H_2O \rightarrow CO + 0.97H_2 \qquad \Delta^\circ H_{r,1123} = +166.5928\ KJ/Mol \qquad (3.21)$$

$$C_m\,H_nO_q + H_2O_{(l)} \rightarrow C_mH_{n-2q} + H_2O_{\ (g)} \qquad \Delta^\circ\ H_{r,380} = +21.4900\ KJ/Mol * \qquad (3.22)$$

3.4.3 Standard Stoichiometry CO_2 Required and Produced

Also, the reactions from the three stages (thermal decomposition, char combustion and reforming and char gasification) were considered in the determination of the CO_2 required and produced for the gasification processes. Char combustion, thermal decomposition and gasification were considered based on the general assumption that char is 100 % carbon (Corella and Sanz, 2005).

The reactions are presented below.

$$C + CO_2 \rightarrow 2CO \qquad \Delta^\circ H_{r,1123} = +178.4130 \text{ KJ/Mol} \quad (3.23)$$

$$C + O_2 \rightarrow CO_2 \qquad \Delta^\circ H_{r,1123} = -376.2210 \text{ KJ/Mol} \quad (3.24)$$

$$CO + 0.5O_2 \rightarrow CO_2 \qquad \Delta^\circ H_{r,1123} = -554.6342 \text{ KJ/Mol} \quad (3.25)$$

3.4.4 Standard Stoichiometry Steam Requirement for WGS

Water-gas shift process is required to promote the quality of hydrogen concentration in syngas produced from the gasification processes. The water-gas shift process reaction is the last stage for producing the desired syngas for fuel cell application. The reactions are presented below.

$$CO + H_2O \leftrightarrow CO_2 + H_2 \qquad \Delta^\circ H_{r,628} = +10.4000 \text{ KJ/mol} \quad (3.26)$$

3.5 Heavy Metal Concentration Quantification and Analysis Procedure

The concentration of heavy metal in pre-treated MSW was measured to evaluate the environmental implications in, during and after thermochemical conversion. This quantification of heavy metal can reduce emissions by retaining alkali and heavy metal (except mercury and cadmium) within the thermochemical conversion process residues and with its disposal (Basu, 2010, Huang et al., 2011).

3.5.1 The ICP-MS Solution Method

The ICP-MS solution method was used to determine heavy metal (Al, Fe, Li, Be, Ti, V, Cr, Mn, Fe and etc) concentration in MSW. The 7700 Series quadrupole ICP-MS from Agilent Technologies provides an unmatched combination of high performance and simplicity of operation, redefining the benchmark for ICP-MS. Comprising three models, the powerful semiconductor-configured 7700s and the simple, streamlined 7700e, the 7700 Series provides good performance.

All components were optimised for a high throughput routine analysis of samples with a TDS of up to 0.2 % (2000 ppm). A hyperbolic profile quadrupole provides superior ion transmission, resolution and abundant sensitivity at standard settings, thereby eliminating the need for multiple resolution settings to separate adjacent peaks. The following are its features: mass range: 2 - 260 amu; mass scan speed: slew rate (Li to U, no intervening peaks): 56.6 million amu/s; scan speed (Li to U, plus data collection at 40 intervening masses): > 3000 amu/s; Mass resolution: variable from < 0.3 amu to > 1.0 amu; typical mass calibration stability < 0.05 amu per day, < 0.1 amu per 6 months; abundant sensitivity (at Cs): low mass side: 5×10^{-7}, high mass side: 1×10^{-7}.

3.5.2 Quantification of Heavy Metals in Pre-treated MSW

Pre-treated MSW samples (0.25 - 0.40g) were first digested using the USEPA standard procedure for digestion. The procedure normally uses acid and heat to break up organo-metallic bonds and free ions for analysis.

Where samples had undergone a digestion, the results were corrected for the dilution factor resulting from the digestion procedure. Heavy metal elements (Al, Fe, Li, Be, Ti, V, Cr, Mn, Fe, Co, Ni, Cu, Zn, As, Se, Sb, Mo, Cd, Pb, Hg) were then analysed with an Agilent 7700 quadrupole ICP-MS.

The instrument was calibrated using NIST (National Institute of Standards and Technology, Gaithersburg MD, USA) traceable standards to quantify selected elements. Thereafter, a prediction of projected quantification of heavy metal that might be found in bottom ash, as the remaining residue from the thermochemical conversion processes, was calculated.

The Agilent 7700x ICP-MS is illustrated in Figure 3.8.

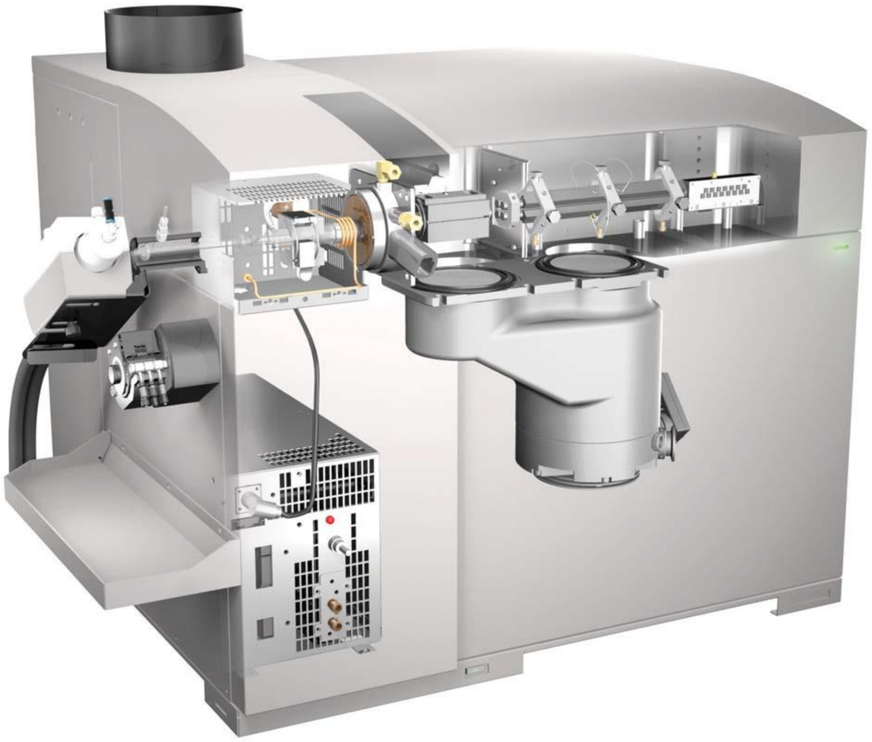

Figure 3.8: The Agilent 7700x ICP-MS

3.5.3 Quantification of Heavy Metals in Bottom Ash

The model of (Belevi and Moench, 2000, Yao et al., 2010) as shown in equation 3.5 was used among other assumptions to predict the quantity of heavy metals that will be transferred to bottom ash residue.

$$K_{ij} = \frac{C_{BAij} * R_j}{C_{wij} * (1 - y_j)} \qquad 3.5$$

Where $K_{i,j}$ is the transfer coefficient of the heavy metal i from the input MSW to the bottom ash of location j; $C_{BAi,j}$ is the content of the heavy metal i in the bottom ash of the city location j (mg/kg dry weight); $C_{W\,i,j}$ is the content of heavy metal i in the input MSW of location j (mg/kg dry weight); R_j is the bottom ash mass production ratio of the incinerator in location j, which is about 0.2 - 0.3; and y_j is the water ratio of the input MSW of the incinerator in location j.

The possible environmental effects will be measured through distribution of the following heavy metals present in various municipal solid waste disposal facilities (MSWDF) in Cape Town: Al, As, Ba, Cd, Co, Cr, Cu, Fe, Hg, Mg, Mn, Mo, Ni, Pb, Sb, Se, V and Zn. These heavy metals were considered for the following purpose; hazardous or toxic properties (Song et al., 2004, Quina et al., 2008, Sekito et al., 2014), great environmental concerns (Allegrini et al., 2014, Quina et al., 2008) and most of the heavy metals (Al, Si, As, Cd, Cr, Cu, Fe, Hg, Mg, Pb, Se, and Zn) are found in bottom ash which may lead to disposal problems and leaching (Quina et al., 2008). Gasification may enhance recovery of some heavy metals (Allegrini et al., 2014, Belevi and Moench, 2000, Sekito et al., 2014).

3.6 Procedure for Costing Evaluation on Gasification System

The profitability standard is a measure of profit with respect to the investment required to generate that profit. Profit is the goal of any investment, but maximising profit must be judged relative to the investment among other intangible factors (social, political, environmental and safety). The profitability estimate attempts to quantify the desirability of taking risk in a project investment. This profitability measure puts the emphasis on value-for-money in the near future (Green and Perry, 2008, Peters et al., 2013).

The economic indicators for assessment are total capital costs (working capital + fixed capital cost), specific capital investments, operational and maintenance costs and cash flow analysis etc. Equipment capital costs were estimated as a power law of capacity as shown in equation 3.1(Sinnott and Towler, 2012).

$$C_E = C_B \left(\frac{Q}{Q_B}\right)^M * F_M * F_P * F_T \qquad 3.1$$

Where:

C_E - Equipment cost with capacity Q;

C_B - Known base cost for equipment with capacity Q_B;

M - Constant depending on equipment type.

F_M - Material factor

F_P - Pressure factor

F_T - Temperature Factor

For the estimation of operational and maintenance costs, the mass and energy balances were used. Operational and maintenance costs are generally allocated as variable and fixed costs while variable operating costs are directly proportional to the amount of energy produced (raw materials, chemicals, solvents, waste disposal etc).

3.6.1 Economic Potential Indicators and Profitability Measure and Standard

According to Smith (2005), the economic potential is simply a function of fixed and variable costs as shown below:

Economic potential = Revenue – fixed cost - variable costs - taxes 3.27

The study further emphasises time-value for money through the cash flow, as shown by(Green and Perry, 2008, Towler and Sinnott, 2013), to be measured with the net present value (NPV), discounted cash flow rate of return (DCFROR), payback time and return on investment (ROI). NPV and DCFROR are key factors because of the measurement of profitability and efficient use of capital respectively.

The project cash-flow diagram is illustrated in Figure 3.9 below.

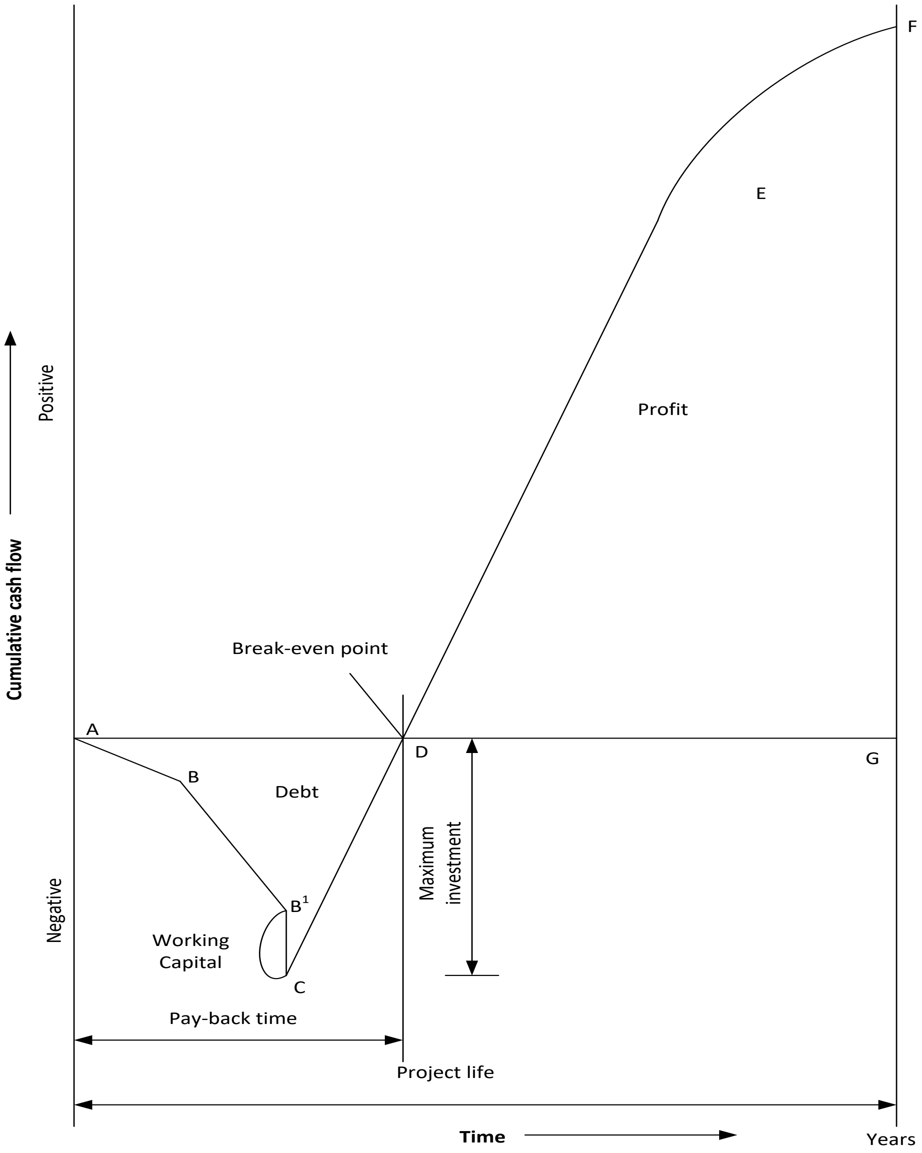

Figure 3.9: Project Cash-flow Diagram (Sinnott and Towler, 2012)

Green and Perry (2008) suggest a quantitative and qualitative determination measurement of profitability. The net present value (NPV), discounted cash flow rate of return (DCFROR) and pay out time plus interest are quantitative tools while qualitative measures are intangible factors such as environmental impact, legal constraints, employee morale, employee safety, product liability, government policy, etc., which are difficult to measure. A sensitivity analysis is recommended to cater for any risk that may be encountered due to variation or uncertainty of the factors.

The profitability of the project is dependent on cash flow as it is related to the time value for money. ROI, payback period and net return do not consider the time value of money (depreciation, interest and inflation) while the present value (NPV) and discounted cash flow rate of return (DCFROR) methods do consider the time value of money. They conclude that the two methods are very viable in evaluating the economic potential of the project and are always applied together. Not much emphasis was placed on other aspects of risk analysis (Peters *et al.*, 2013). Below are measures of a profitability standard (time value for money, cash flow and risk analysis).

3.6.2 Rate of Return on Investment

The rate of return on any investment is the annual average return on the total investment for the total lifespan of the project. It is usually expressed in percentages and is one of the parameters used to evaluate the performance of the project without considering the time value for money.

$$ROI = \frac{(1/N)\sum_{J=1}^{N}(N_{P,j})}{FT} = \frac{N_{p,ave}}{FT} \qquad 3.28$$

3.6.3 Payback Period

The payback period is the minimum time required to break even in terms of the volume of products sold to keep afloat before earning real profit for a given project.

This is another profitability measure parameter to evaluate the performance of the investment without considering the time value for money.

$$PBP = \frac{0.85^{*}}{m_{ar} + 0.85/N} = \frac{1}{1.18m_{ar} + 1/N} \qquad 3.29$$

3.6.4 Net Return

The net return profitability measure is the amount of cash flow over and above that required to meet the minimum acceptable rate of return and recovery of the total investment.

$$R_{n,ave} = N_{p,ave} - m_{ar}FT \qquad 3.30$$

The 0.85 in equation 3.29 value is obtained from the assumption that the working capital is 0.15FT (Sinnott and Towler, 2012, Towler and Sinnott, 2013)

Where:

ROI = return on investment

N_p, ave = average value of net profit per year over the evaluation period

FT = the total capital investment

m_{ar} = minimum acceptable rate of return

N_p = the annual net profit

N = evaluation period in years

Rn = the net return

rec_j = recovery from working capital and sale of physical assets

$R_{n,ave}$ = average rate of return per year

3.6.5 Net Present Value

The net present value is the total of the present worth of all cash flows minus the present worth of all capital investments as defined by:

$$NPV = \sum_{j=0}^{N} PWF_{cf,j}[(S_J - c_{oj} - d_j)(1-\emptyset) + rec_j + d_J] - \sum_{j=-b}^{N} PWF_{v,j}\, FT_j \qquad 3.31$$

3.6.6 Discounted Cash Flow Rate of Return

This is the return obtained from an investment in which all investments and cash flows are discounted. NPV = 0 and determines the discount rate that satisfies the result relation.

$$NPV = 0 = \sum_{j=0}^{N} PWF_{cf,j}[(S_J - c_{oj} - d_j)(1-\emptyset) + rec_j + d_J] - \sum_{j=-b}^{N} PWF_{v,j}\, FT_j \qquad 3.32$$

NPV = net present value,

$PWF_{cf,j}$ = selected net present value for cash flow, year j, sj,

J, c_{oj} = the total product cost not including depreciation in year j,

$PWF_{v,j}$ = appropriate present value factor for investment occurring in year j,

FT_j = the total investment in year j

3.6.7 Minimum Acceptable Rate of Return (MARR)

The value of MARR is usually set as the lower limit for investment which is acceptable to an individual or a company. The lower boundary for the MARR is generally set at the cost of capital, which reflects the expense of obtaining funds for a given project. How much higher the MARR is above the cost of capital depends on some factors for a project. Also, the prevailing interest rate needs to be considered in choosing MARR (Smith, 2005).

The minimum interest rate that can earn by investing money is MARR and it would consider being a success. The DCFROR will be greater than the MARR used Thus, the MARR value used is a good starting point.

When the NPV is favourable the DCFROR will necessarily also be favourable and will be the actual earning rate of the investment. The two methods are always used together. This is regarded as a very good method for making economic decisions because not only does it include all the other relevant information of other methods, but it takes into account the time value for money.

3.6.8 Sensitivity Analysis: Break-even Analysis

This is associated with unforeseen risks that are usually involved in undertaking any project. The possibility of success or failure of a project is important. Thus, quantification of risk and its analysis are essential in project evaluation and decision-making. The break-even point is a function of demand and the volume of demand to pay back the total investment where NPV = 0. Cash flow is a function of the total investment while the cash flow depends on other factors such as the cost of raw materials, operating costs, sales volume and prices. Not only is break-even important, but profit-making is equally essential. This type of sensitivity analysis shows some of the details of responses to change.

While it affords the opportunity to maximise risks and minimise losses, it also gives some ideas on the degree of the risk involved in making judgments about the forecast of the performance of the project. Figure 3.10 illustrates the break-even plot.

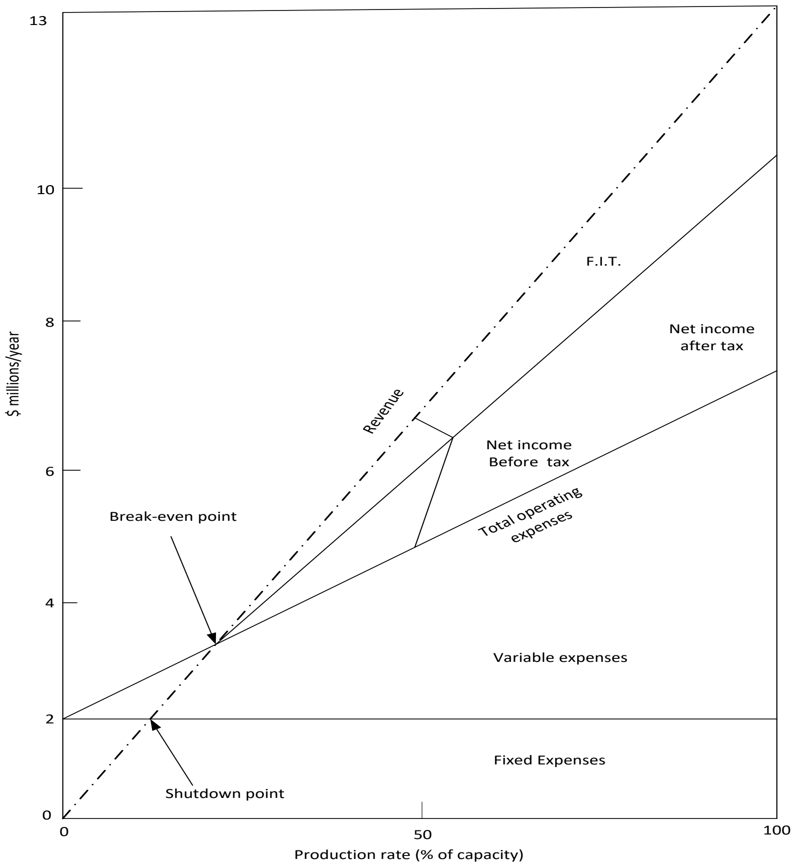

Figure 3.10: Break-Even Plot (Green & Perry, 2008)

3.7 Chapter Summary

The methods used for physicochemical characterisation of pre-treated MSW, thermochemical procedures, quantification of heavy metal concentrations and costing procedures are presented in this chapter. The result of the physicochemical characterisation of RDF from MSW are presented in chapter four while other results are presented in following chapters (chapter five, chapter six, and chapter seven).

CHAPTER FOUR

4 PHYSICOCHEMICAL CHARACTERISATION OF RDF FROM MSW

4.1 Physicochemical Characterisation of RDF from MSW

The results of the pre-treatment of municipal solid waste (MSW) are presented in this chapter. The Pre-treated MSW was characterised to obtain bulk and loose densities, HHV, proximate and ultimate analysis values and thermo-gravimetric analysis for further procedures.

4.2 Results and Discussion

4.2.1 Bulk Density

The physical characterisation parameter describes a variation in specific volume granular material per unit weight. The parameter could be used to determine the compressibility factor that will enhance handling before any thermochemical treatment. The production of RDF pellets may improve quality appreciably compared to raw MSW. The bulk densities were calculated from their defined dimensions and weights.

The loose densities, packed bulky densities and compressibility factor (CF) of refuse-derived fuel (RDF) obtained are presented in Table 4.1 while the comparisons and mean and coefficient of variation of densities are presented in Table 4.2.

Loose densities of pre-treated MSW in Table 4.1 showed that loose densities of samples obtained from KL and WY were over 230 Kgm^{-3} while other samples obtained from CP and ATR were less than 100 Kgm^{-3}. The difference in densities (between 70.4 Kgm^{-3} and 148 Kgm^{-3}) showed the heterogeneous characteristic of MSW.

Table 4.1: Loose Bulk and Packed Bulk Density of Pre-treated MSW in Cape Town

MSWDF	Loose Density (Kg/m^3)	Packed Bulk Density (Kg/m^3)	CF
KF	114	367.8	0.3100
ATR	96.8	324.2	0.2986
WS	98.4	296.2	0.3322
TG	106.2	284.2	0.3737
BL	147.2	333.0	0.4420
KL	239.2	515.0	0.4645
WY	310	389.8	0.7953
WG	122	351.6	0.3470
RT	168.6	407.2	0.4140
CP	70.4	320.8	0.2195
LM	168	425.6	0.3947
GMM	138.8	396.6	0.3500
Min	70.4	284.2	0.2477
Max	310	515	0.6019
Ave	148.3	367.7	0.4035

In addition, the packed densities of pre-treated MSW in Table 4.1 had increased and packed densities of KL, RT and LM were good. The packed densities from theses KL, RT and LM contained high content of organic matter, wood wastes, garden wastes and waste paper while other samples obtained from TG, WS and CP were lower than those obtained from KL, RT and LM. The low packed densities obtained from TG, WS and CP may be associated little content of organic matter and high inert materials.

Table 4.2: Comparison of Densities from Literatures with the Results of this Study

Municipal Solid Waste/Biomass	Density (Kg/m^3)	Status
KF, WS, KL and LM	367.8, 296.2, 515.0, 425.6	This Study
MSW and Biomass (Commercial Pellet)	223.09^a, 400^b , 20 - 800^c , 733^d, 280.05^e	Lit. Data

a = Vyas and Singh (2007)

b = Montuori et al. (2015)

c = Hedman et al. (2005)

d = Moghadam et al. (2014)

e = He et al. (2009a)

Table 4.3: Mean and Coefficient of Variation of Densities of MSW in Cape Town

Density	Range of Density	Mean	Standard Deviation	Coefficient of Variations
Loose Bulk Density	70.4 - 310.0	148.3	67.5230	46 %
Packed Bulk Density	284.2 - 515.0	367.7	64.3660	18 %

4.2.2 Pelletisation of RDF

As described earlier in the previous chapter, non-combustible components of MSW were removed before the reaming combustible components shredded, milled and densified. These could be technically described as size reduction (shredding and milling) and size enlargement (pelletisation). The whole procedure showing how raw MSW collected from municipal solid waste facilities are pre-treated to RDF is shown in Figure 4.1.

RDF Solid fuel pellets were produced from the raw samples of MSW. The MSW samples were collected from thirteen municipal solid waste disposal facilities (MSWDF) spread around the settlements in Cape Town. Pre-treatment Procedures were drying, separation, grinding (size reduction), sieving (uniform size of MSW), and size enlargement as required standard procedure from these authors (Green and Perry, 2008, Liu et al., 2014).

The inorganic components (non-combustible) of MSW samples such as ferrous and non-ferrous metals and glass were separated and sorted manually as shown in Figure 4.1. This procedure was carried out to enhance the combustible composition of raw MSW. The MSW samples were then shredded and pulverised to form a fluffy material after the separation into particles size < 5 mm using a hammer mill. Furthermore, the MSW were shredded again, milled and sieved (pre-treated as shown in Figure 4.1) with a specific mesh to (200 mm in diameter and a mesh size of 0.5, 1, 2.8 and 5 mm) ensure that MSW was properly homogenised (Stelte et al., 2012, Stelte et al., 2011b).

The RDF pellets from MSW in this study were then produced using improvised single pellet press units. The MSW samples were compressed with a pressure less than 10 MPa. The improvised nature of the pellet press energy requirements may not exceed energy of 15 KWh/t and 18 MJ respectively (Puig-Arnavat et al., 2016).

The bulk densities of RDF have improved from 70.4 Kg/m^3 to – 515 Kg/m^3 and similar trend were obtained for energy density increased from 4142.07 MJ/m^3 to 10735.8 MJ/m^3. The pelletization procedures have added more value to RDF pellets (pre-treated MSW) by increasing the density, energy content density, homogenous shape and structure - energy-dense homogeneous solid RDF (Figure 4.1).

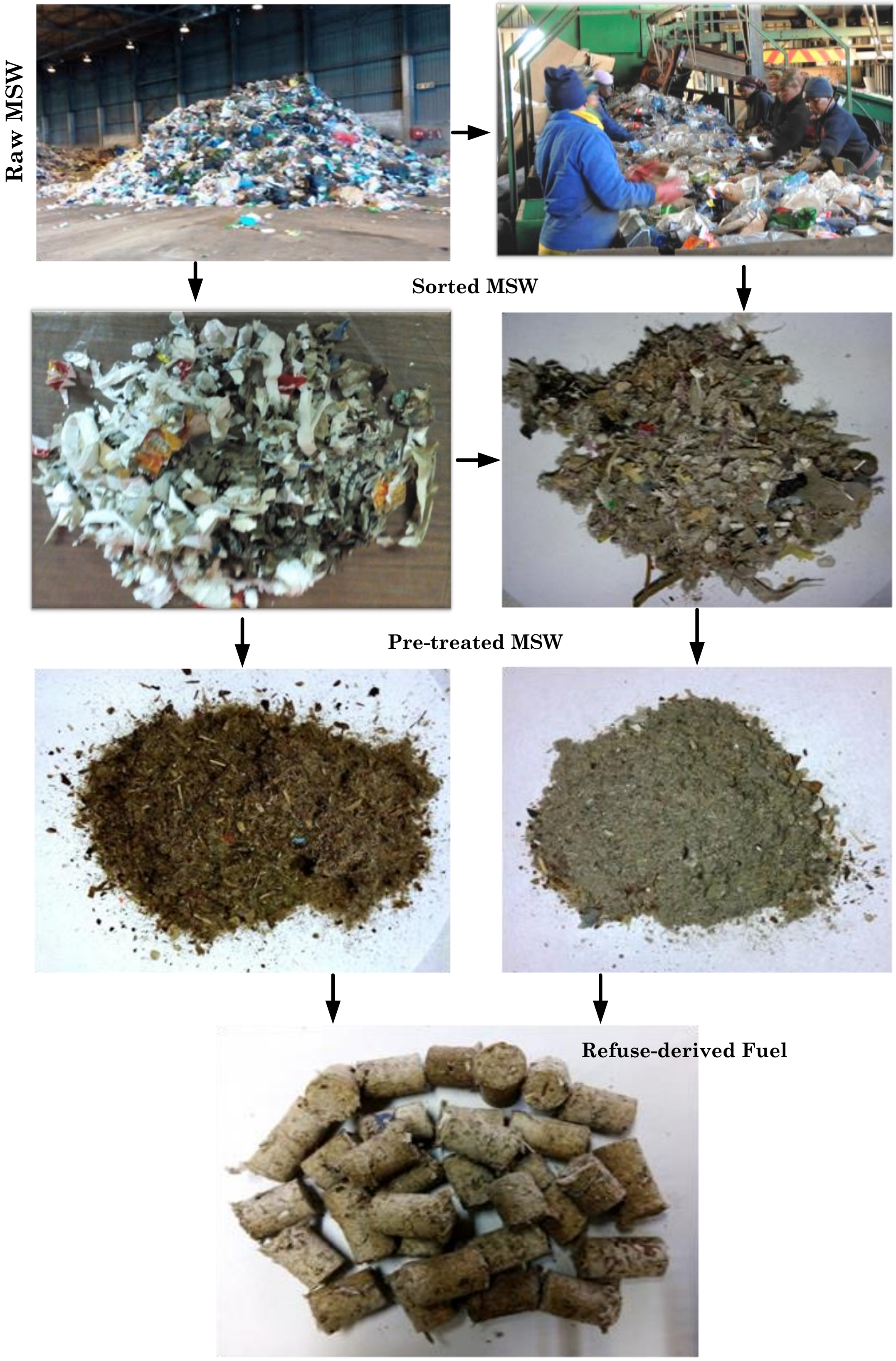

Figure 4.1: Production of Refuse-derived Fuel (RDF) from Raw MSW

Packed bulk density is an important parameter, which determines the energy density per volume and the stability of the RDF pellets. Densification through pelletisation increases the mass energy density of MSW and volume energy density. Loose bulk densities were also measured to understand the compressibility ratios of the RDF. The densities of the samples were calculated based on the measured RDF mass and RDF volume. The loose bulk densities of pre-treated MSW produced were between 70.40 Kg/m^3 and 310.00 Kg/m^3 with a mean value of 143.00 ± 67.52 Kg/m^3 while the packed bulk densities were between 284.20 Kg/m^3 and 515.00 Kg/m^3 with a mean value of 367.67 ± 64.37 Kg/m^3 (Table 4.1). According to the study of Li et al. (2012a), who made reference to a report that general loose bulk densities of biomass were found to be between 40 - 200 kg/m^3. The findings in Li *et al.*'s as well as Hedman et al. (2005) study were both lower than the range (70.40 Kg/m^3 and 310.00 Kg/m^3) obtained in this study, though, after pelletisation of the biomass, the densities improved. The values reported by Stelte et al. (2011), Moghadam et al. (2014), Veki et al. (2011), Sharma (2009) and etc are attributed to thermochemical pre-treatments (Ramos et al., 2018) which enhance the quality of the of biomass/MSW.

The relative difference between the values of packed bulk densities obtained from KF, KL, LM and GMM samples were higher compared to the initial loose bulk densities. The relative difference between loose and packed densities was more than 250 Kg/m^3 for KF, LM and GMM samples while KL samples differed between loose (239.2 Kg/m^3) and packed density (515.00 Kg/m^3), which was well over 270 Kg/m^3. This characteristic may be considered as significant for RDF quality though the production of pellets was carried out with an improvised device. The KL drop-off site sample of packed bulk density was another good product for the pelletisation of pre-treated MSW.

The values of KF and LM municipal solid waste disposal facilities showed that there might be links with the ongoing procedure (integrated MSW system) with the facility that might be responsible for the quality of pre-treated MSW in the KF facility while the LM site sample was characterised by a large quantity of organic materials, hence these might have a profound effect on the RDF formation.

The packed bulk densities of RDF from ATR, WG, CP and RT are equally important as the previous densities because the relative difference between the two types of densities was over 200 Kg/m^3 as well. However, the potential of other remaining packed bulk densities was not high, especially the bulk density of the WY site because RDF packed bulk was the least of them, though the packed bulk density was still good value when compared to one biomass product (Adapa *et al.*, 2009).

Generally, the loose density values are relatively low compared to the packed density for the same MSWDF. The compressibility factor was normal compared to the loose and packed bulk densities and this factor was used to measure the pellet-production potential even before considering the relevance of binder.

The values of GMM and average value (250 Kg/m^3 and 219 Kg/m^3) proved that RDF produced from MSW from the city of Cape Town has a high potential of producing good quality RDF. On the other hand, without considering the loose bulk densities, the packed bulk densities of KL, LM and RT are 515 Kg/m^3, 425.6 Kg/m^3 and 407.2 Kg/m^3 respectively. The KL site has the highest value of the density of 515 Kg/m^3 and the reason for this could be attributed to the heterogeneous nature, relative high difference between loose and bulk densities and high compressibility ratio.

The studies carried out by Li et al. (2012a) and Stelte et al. (2011a) show that torrefied biomass pellet densities were higher than those obtained in this study and this was because the biomass samples had undergone partial thermochemical processes. The higher value of densities could be attributed to the torrefaction process. In another study, however, results are well above the bulk densities obtained from another biomass RDF product (Adapa *et al.*, 2009).

All these features discussed above contribute to the good quality of the pre-treated MSW from the sites even though some are low-quality substitutes for RDF production.

Any deviation from the mean value of the bulk densities seems close for both loose and packed bulk densities but the coefficient of the variations of loose bulk density and packed bulk density are 46 % and 18 % respectively.

These account for the heterogeneous characteristics of pre-treated MSW. This packed bulk density parameter provides indications of particle size, shape, uniformity and cohesion, and thus the overall flowability of the samples. Bulk solids with a compressibility ratio less than approximately 0.18 percent are considered free-flowing and non-yielding to compaction and thus might not be suitable for RDF production to promote syngas production during thermochemical conversion. The overall average compressibility (volumetric energy density) ratio was more than 0.20. This proved the high potential of converting pre-treated MSW to RDF without considering binders.

4.2.3 High Heating Values (HHV) of Pre-treated MSW

The MSW is extremely non-homogeneous but equally enriched with substantial combustible substances mainly from organic sources. The HHV determination of various pre-treated MSW from MSWDF in the city of Cape Town are shown in APPENDIX A.

As mentioned earlier in previous chapters, more than fifty pre-treated MSW samples were prepared for the determination of high heating values from thirteen MSWDF (drop-off sites and transfer stations) (See Figure 4.1). The HHV determinations were performed three times for all the samples while the other twenty high-heating value determinations were also carried out on all mixture of pre-treated MSW from all sampling locations.

It was carried out because of the extreme heterogeneous characteristic of MSW and to ensure a good representation of HHV of MSW from the City of Cape Town. The literature HHV data and the summary of the HHV determinations are shown in Table 4.4 and Table 4.5 respectively.

Table 4.4: The Typical HHV Distribution across MSWDF in Cape Town

MSWDF	HHV (MJ/Kg)	HHV (MJ/Kg)
Drop-off Sites	Range	Mean ± SD
Belhar (BL)	14.5090 - 18.6010	16.5047 ± 2.0479
Delft (DF)	-	-
Killarney (KL)	16.4560 - 28.6480	20.8463 ± 6.7742
Ladies Mile (LM)	21.8889 - 28.9070	24.6553 ± 3.7387
Retreat (RT)	17.7110 - 18.9510	18.1693 ± 0.6803
Tygerdal (TG)	20.1030 - 27.5030	22.7723 ± 4.1081
Welgelegen (WG)	12.4680 - 20.5750	16.7213 ± 4.0683
Woodstock (WS)	13.8490 - 16.2000	14.8453 ± 1.2158
Wynberg (WY)	14.8230 - 16.4380	15.6870 ± 0.8134
Transfer Stations	Range	Mean ± SD
Athlone (ARTS)	15.4310 - 25.5900	20.7623 ± 5.0982
Coastal Park (CP)	14.1140 - 19.3330	15.9697 ± 2.9179
Kraaifontein (KF)	21.2720 - 23.3700	22.1043 ± 1.1141
	Range	Mean ± SD
General MSW Mixture (GMM)	13.5120 - 25.8720	20.1691 ± 2.9815
Total Average	12.4680 - 28.9070	19.4433 ± 3.9056

SD = Standard deviation

Table 4.5: Comparison of Densities from Literatures with the Results of this Study

Municipal Solid Waste/Biomass	HHV (MJ/Kg)	Status
KF, WS, KL and LM	22.1043, 14.8453, 20.8463, 24.6553	This Study
MSW(RDF) and Biomass	15.00[a], 17.67[b] , 13.08[c] , 16.80[d], 10.80[e]	Literature Data

a = Evangelisti et al. (2015)

b = Kocer et al. (2017)

c = Chen et al. (2013)

d = Burnley et al. (2011)

e = Tsai and Kuo (2010)

Having discussed the RDF production potential in the previous section, it will not be sufficient not to analyse the HHV results of various pre-treated MSW samples further. This analysis was to examine the significance of RDF derivable solid fuel from MSWDF in the city of Cape Town. The determination of HHV added value to the preliminary assessment of MSW and was complementary to the RDF produced. The carbonaceous content of solid fuel RDF and the caloric values are useful indicators of numerous applications.

The overall results showed the extent of the heterogeneous composition of MSW. This was responsible for the variation of the range of the HHV (12.4680 - 28.9070 MJ/Kg). From the result obtained from all the drop-off sites, the HHV obtained from WG, WS and WY drop-off sites were very low compared to other drop-off site (Table 4.4). WS and WY drop-off sites were characterised by a high content of garden weed waste, wood and similar biomass. The nature of the origin of the MSW might be the reason for this low value; however, the value was higher than that obtained by these authors (Ahmed and Gupta, 2011, Lopes et al., 2015, Mastellone et al., 2010). Their values were less than other drop-off sites. The HHVs did not have a wide range as it was reflected in the mean value and their deviations (Table 4.4). Another low HHV (12.00 MJ/Kg) was obtained from the WG drop-off site but with a wider range because a high value of 20.60 MJ/Kg was also obtained unlike the WS and WY drop-off sites with less than 16.50 MJ/Kg. These confirmed the extent of the non-homogeneous nature of MSW. However, none of these HHVs falling below 12.00 MJ/Kg. High HHVs were obtained from TG, KL and LM while TG and LM have good averages (Figure 4.2). The LM drop-off site had the highest gross and average high heating values. A high rate of organic matter was solely responsible for such HHV while the TG and KL drop-off sites had components such as plastics, paper, wood and other combustible substances. These high heating values exceeded that of the typical biomass and some commercial RDF (18.00 MJ/Kg and 19.88 MJ/Kg) (Channiwala and Parikh, 2002, Parikh et al., 2005, Galvagno et al., 2006, Galvagno et al., 2009).

GMM represents a general mixture of all the pre-treated MSW (20 samples) from the transfer stations and drop off sites and the high heating values obtained from these samples range from 13.51 to 25.87 MJ/Kg with an average of 20.17 MJ/Kg. This lowest HHV 13.51 MJ/Kg is higher than some literature data presented in Table 4.4.

The results showed that the HHV values obtained were higher than those suggested in the literature (Galvagno et al., 2009, Galvagno et al., 2006) and a previous study (Ikhu-Omoregbe and Mahomed, 2012) conducted on a few MSW disposal facilities. These demonstrated the quality of the pre-treated MSW from the city of Cape Town. These HHV values were higher than suggested above and the previous study of the HHV values.

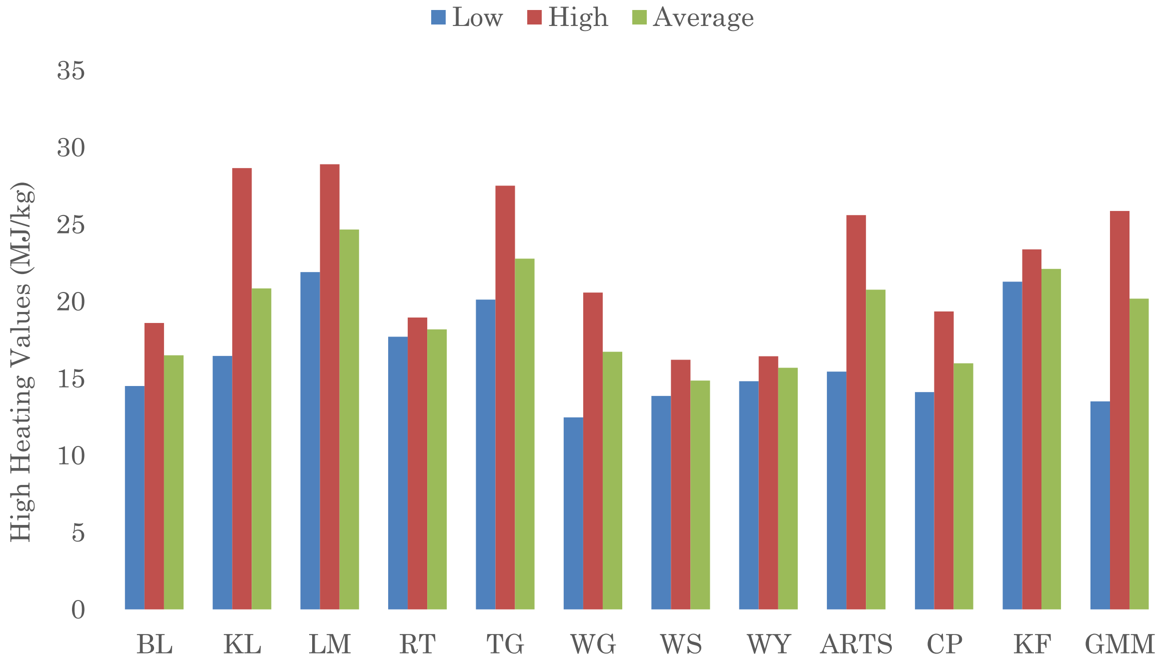

Figure 4.2: The Distributions of HHV from Municipal Solid Waste Disposal Facilities.

Having considered various drop-off sites, transfer stations ARTS, CP and KF are also transits for solid waste handling and disposal. Large quantities of MSW are received, pre-treated and transfer to their final destinations such as landfills. Most of the MSW is sorted at the transfer stations but only KF transfer station has effective separating facilities and this might contribute to the good HHV result obtained from the transfer station. The KF transfer station was named an integrated solid waste management facility because of the functioning of the facility. This facility may enhance the quality of pre-treated MSW for potential waste-to-energy technology.

The HHV (23.37 MJ/Kg) obtained from the KF transfer station is of a good quality for solid fuel from MSW (23.37 MJ/Kg) when compared with the results from literature (Table 4.5) and its average high heating value - 22.10 MJ/Kg was the highest compared to the other two transfer stations. The ARTS and CP transfer stations had a lower average of 15 MJ/Kg and 20 MJ/Kg respectively. The CP transfer station's HHV was the lowest amongst the transfer stations because of ineffective sorting. This transfer station is dedicated to rubbles, inert and other construction solid waste. However, the results showed that quality are still better than the quality reported by these following authors Evangelisti et al. (2015), Fu et al. (2015), Burnley et al. (2011) and Jeong et al. (2017).

The KL site showed the highest deviation in values obtained (20.85 MJ/Kg ± 6.77 MJ/Kg) but still has a relatively high HHV while other results from LM, TG and WG were also of a relatively high deviation but with non-uniform values of HHV (Table 4.4). The others (WS, WY, RT and BL) show HHV values with a low deviation, lower HHV but with otherwise relatively uniform results, especially the values obtained from the RT and WY sites. For the transfer stations (ATRS, CP and KF) HHV values were presented in Table 4.4. The KF transfer station had the best HHV among the others while HHV at the CP station was the lowest of the transfer stations.

The CP station's low HHV values may be attributed to the nature of MSW, consisting of rubble, inert substance and other construction solid waste which was usually accepted at the station while the main factor for the HHV value of KF station has been discussed earlier. The average high heating values of 20.76 and 22.10 MJ/Kg were obtained for the ATR and KF transfer stations. These values are higher than those obtained in the previous study because of the pre-treatment that was introduced (Ikhu-Omoregbe and Mahomed, 2012).

From the results analysed above, the Cape Town RDF produced from MSW could be used in co-blending, co-pelletising, co-pyrolysis and co-gasification, which is of greater significance to this study. These may be considered as an alternative supplement for a contemporary fossil fuel-powered system. Co-firing of pre-treated MSW with the existing boiler (coal/gas) could also generate economic and environmental benefits though it may not be an ultimate and sustainable system for the desired eco-friendly system (Melikoglu, 2013a, Bing et al., 2016, Jeong et al., 2017, Park et al., 2016).

Apart from environmental challenges, these values of HHVs are further proof for promoting the opportunity of solid fuel producing energy from pre-treated MSW. Solid fuel is a practical alternative energy fuel and one of the prime substitutes for fossil fuels for cogeneration applications.

4.2.4 Proximate Analysis of Pre-treated MSW

Based on the HHV obtained from the pre-treated MSW, further analysis is required to generate another analysis to complement the assessments of the MSW and provide an estimate of the pre-treated MSW compositions. A proximate analysis is a rough estimate of ash, volatile matter (VM), fixed carbon (FC) and the moisture content (MC) of solid fuel. The results of the analysis are very important for the consideration of thermochemical reactions. The proximate analysis results if some of the MSWDFs are presented below in Table 4.1 and Figure 4.3.

Table 4.6: The Proximate Analysis of Pre-treated MSW from MSWDF in Cape Town

MSWDF	MC (wt. %)	FC (wt. %)	VM (wt. %)	Ash (wt. %)	BD (g/cm^3)
Drop-off Sites					
BL	-	-	-	-	0.3678
KL	10.7008	11.1194	74.1680	4.0012	0.3242
TG	-	-	-	-	0.3330
WG	-	-	-	-	0.5150
WS	9.0906	28.2188	40.8804	21.8101	0.3898
WY	-	-	-	-	0.3516
ARTS	-	-	-	-	0.4072
CP	5.1008	29.9818	48.3225	16.9722	0.3208
KF	-	-	-	-	0.4256

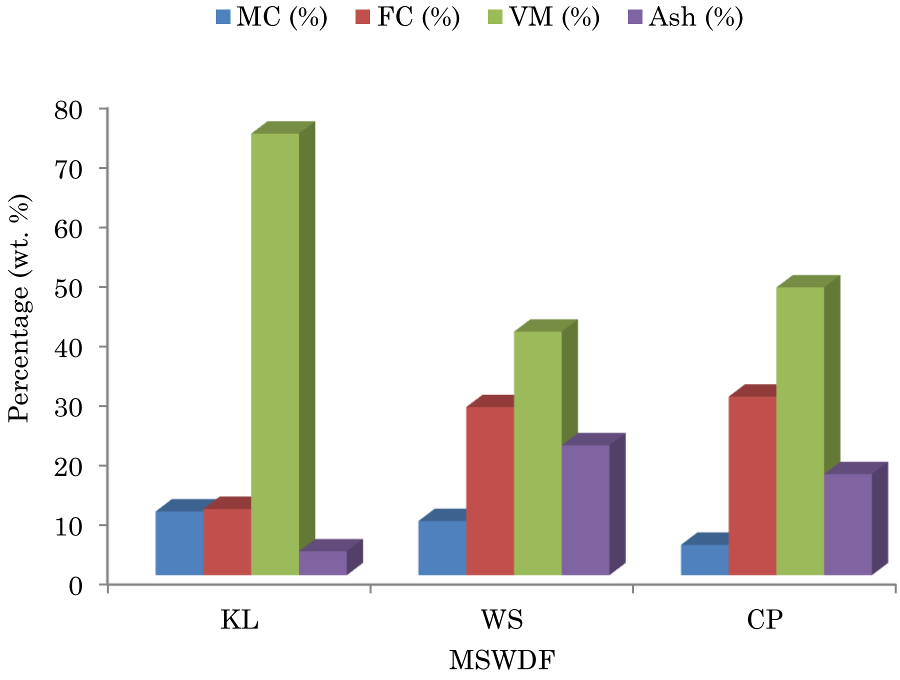

Figure 4.3: Proximate Analysis of Pre-treated MSW from MSWDF in Cape Town

As a sequel to the previous physicochemical determination towards the analysis of RDF production potential, an additional chemical characterisation of pre-treated MSW samples was considered to obtain an approximate analysis of the distribution of the chemical contents which are relevant to the thermochemical properties of the potential solid fuels under consideration. The implication of RDF-derivable solid fuel from MSWDF in the City of Cape Town also had to be examined. The proximate analysis determination is preliminary assessments of the density ash, as related to slagging, and sintering during thermochemical conversion. Heavy metal distributions in MSW, environmental implications, the carbonaceous non-carbon content of the solid fuel, RDF and caloric values are useful indicators of numerous applications.

Proximate analysis is a compositional analysis carried out for the determination of the MC, VM, FC and ash content of the potential solid fuel in pre-treated MSW, expressed in percentages compositions of MC, VM, FC and ash. The analysis is used to show the ratio of combustible to non-combustible constituents of solid fuel.

The volatile matter (volatile hydrocarbon) generally contributes to the fraction that evolves (non-condensable compounds) by means of thermal decomposition. The fixed carbon, together with the ash, represents the theoretical solid residue (char) of a possible pyrolysis/gasification process. Generally, MC reduces the re-use potential of solid fuel because of the low HHV and the syngas quality is affected by MC (Plis and Wilk, 2011). The less the composition of MC, the better the quality of RDF. All the pre-treated MSW samples presented high volatile contents (40 - 74 %) especially the KL sample with respect to ash composition (1 - 20 %) (remember the KL had a very good HHV with a relatively high deviation from the mean). Ash composition has a lot to do with decomposition and others chemical interactions in gasification scheme conversions and a low amount of ash is vital for thermochemical conversions (Alvarez et al., 2014, Galvagno et al., 2009).

These values were indications of the non-homogeneous characteristics of MSW. The GMM ash value is a good value to be considered because the ash content was 1.0 %, thus also being a packed bulk density value and HHV.

The data showed that the fixed carbon content was 11 - 30 % (Table 4.4) while the CP station had the highest fixed carbon content which could be due to the nature of the CP station and other attributes of the samples. This contributed to the combustible and non-combustible content of the pre-treated samples as emphasised earlier and the high fixed carbon in the sample may have contributed to the formation of char. As mentioned before, this analysis is an approximate compositional analysis of solid fuel to show the rank and possible composition of combustible pre-treated MSW.

The VM, FC and ash constituents had presented some patterns of combustion characteristics. Nonetheless, there is a need for further comprehensive elemental analysis particularly of the element that may have effects on the combustible properties of the pre-treated MSW. The analysis is presented in the next section of the physicochemical characterisation of the pre-treated MSW.

4.2.5 Ultimate Analysis of Pre-treated MSW

The ultimate analysis is another chemical characterisation for obtaining the elementary composition of pre-treated MSW. The molecular formula of MSW can be obtained from the ultimate analysis value(s). The formula and the stoichiometric ratio of elements in compounds are part of the necessary input required for a detailed analysis of gaseous yield during thermochemical conversion processes. This analysis focus is on the determination of the C-H-O elemental composition of solid fuels or derived solid fuels. Literature data and Elemental compositions of MSW are presented in Table 4.7 and Table 4.8 respectively.

Table 4.7: The Ultimate Analysis of Biomass/RDF/PE/Coal/MSW from Literatures

Carbon (wt. %)	Hydrogen (wt. %)	Oxygen (wt. %)	Nitrogen (wt. %)	Sulphur (wt. %)	Ash (wt. %)	References	Type of Solid Waste
16.45	2.12	10.51	0.35	0.05	16.04	Xu et al. (2017)	MSW
30.30	3.40	35.80	1.40	2.934	29.1	Thakare and Nandi (2016)	MSW
51.43	6.72	39.59	1.74	0.52	20.78	Fernandez-Lopez et al. (2017)	Biomass
22.82	3.45	18.56	0.76	0.19	-	Wissing et al. (2017)	MSW
14.06	1.99	7.95	0.36	0.37	27.85	Fu et al. (2015)	MSW
41.80	5.10	35.30	1.00	0.25	15.80	Evangelisti et al. (2015)	MSW
42.00	5.00	35.00	1.00	0.30	16.00	Evangelisti et al. (2015)	MSW
24.14	3.27	15.75	0.35	0.24	-	Tsai and Kuo (2010)	MSW
44.30	6.17	49.50	-	-	0.07	Wu et al. (2017)	Biomass/Coal
49.50	8.10	41.20	0.08	0.02	1.10	Jeong et al. (2017)	Biomass/Coal
44.83	5.96	63.912	0.35	0.15	1.49	Zheng et al. (2016)	Biomass/PE
30.70	4.62	17.30	0.77	0.39	46.15	Chen et al. (2013)	MSW
50.50	5.60	30.70	1.10	0.30	11.70	Zhang et al. (2012)	MSW
52.50	6.90	40.50	0.11	-	0.20	Park et al. (2016)	Biomass/PE
48.78	7.76	29.22	0.74	-	13.50	Galvagno et al. (2006)	RDF

Table 4.8: The Ultimate Analysis of Pre-treated MSW from MSWDF in Cape Town

MSWDF	Carbon (wt. %)	Hydrogen (wt. %)	Oxygen (wt. %)	Nitrogen (wt. %)	Sulphur (wt. %)	Ash (wt. %)
Drop-off Sites						
Belhar (BL)	29.404	3.835	51.000	1.046	3.123	14.6701
Delft (DF)	34.979	4.603	-	-	2.934	
Killarney (KL)	32.049	4.048	56.460	-	2.908	4.0118
Ladies Mile (LM)	39.283	4.817	34.539	0.959	2.719	20.4016
Retreat (RT)	34.080	4.396	52.823	1.194	2.851	7.5072
Tygerdal (TG)	36.877	4.872	44.961	0.991	2.786	12.2992
Welgelegen (WG)	15.546	2.185	68.062	0.469	3.449	13.7378
Woodstock (WS)	33.891	4.239	38.877	1.183	3.04	21.8101
Wynberg (WY)	35.125	4.230	42.457	-	2.488	18.1885
Transfer Stations						
Athlone (ARTS)	19.592	2.421	73.444	0.892	2.567	3.6503
Coastal Park (CP)	22.316	2.624	58.088	-	2.469	16.9722
Kraaifontein (KF)	23.912	2.751	63.912	-	2.831	9.4248
GMM	38.081	4.750	54.996	1.075	3.1717	1.0977
Total Average	30.395	3.8285	52.820	0.9761	2.8721	11.9809

The ultimate analysis presented in Table 4.5 was of the elemental composition of pre-treated MSW, especially of those relevant to the gasification processes. The analysis presented were carbon (15 - 39 %), hydrogen (2 - 5 %), oxygen (42 - 68 %), nitrogen (0.4 - 1.1 %) and sulphur (2 - 3 %) while overall averages were carbon (30 %), hydrogen (4 %), oxygen (52 %), nitrogen (0.9 %) and sulphur (2 %).

The empirical formulas were computed from the result of the analysis. The C-H-O ratios are important to thermochemical conversion computation in modelling the reactions as highlighted in the previous chapter and would be discussed and analysed in the following chapter.

The carbon and hydrogen composition of solid fuel have an impact on the gasification characteristics. The carbon composition was highest in the LM 's data results followed by those of GMM, TG and WY, while oxygen and ash constituents usually contribute to the non-combustible properties of solid fuels. The same patterns were observed in previous physicochemical characterisation for the TG site data. The carbon-hydrogen ratios (C/H) for all the data were also considered and compared to the previous relevant literature. The ratios of C/H were in the range of 7 to 8 but the study of Galvagno *et al.* (2009) using RDF and Jiang *et al.* (2016) using sludge reported carbon-hydrogen ratios of 6 while the HHV showed some kind of relationship. This study obtained ratios between 7.11 and 8.90.

The C/H ratio from the data results obtained for BL, DF, KL, RT and TG were below the value of 8 which was quite similar to values obtained by (Alvarez et al., 2014, Janajreh and Al Shrah, 2013, Galvagno et al., 2006, Galvagno et al., 2009) using sawdust, woodchips, RDF and virgin biomass which have shown to be excellent for gasification application.

C/H ratios results obtained from the other facilities, LM, WS, WY, GMM and all the transfer stations (ARTS, CP KF) were more than 8 while an overall average was approximately 8. These C/H ratio result were quite similar to values obtained by (Li et al. (2012a), Muresan et al. (2013), Jiang et al. (2016), Chen et al. (2015b)) using biomass wood, paper, straws and cabbage waste. It was also reported that their HHVs were in the range of 15 to 20 MJ/Kg while average values obtained in a number of sites in this study were higher than 15 - 20 MJ/Kg. The total average of the data results for the elemental composition and ratio (C - 30 %, H - 4 %, O - 52 % and S - 3 %, N - 0.9 %, C/H - 8) were generally good values. In addition to these results, low nitrogen (~1 %) together with high HHV which are similar to the study of Alvarez et al. (2014), as elaborated earlier, was another feature that boosted the quality of RDF produced from MSW in Cape Town.

However, the GMM results in the analysed data for the elemental composition (C - 38 %, H - 5 %, O - 55 % and S - 3 %, N - 1 %, C/H - 8) were good values on average compared to studies of (Lopes et al., 2015, Alvarez et al., 2014) using MSW derived RDF. The molecular formulas derived from the pre-treated MSW for the averages of GMM and LM are $CH_{1.45}O_{1.85}$, $CH_{1.49}O_{1.19}$, and $CH_{1.43}O_{1.02}$, respectively. Other elemental compositions were considered insignificant as shown in Table 4.8.

The molecular formulas are essential requirements for gasification reactions, particularly in gasification through the model application. Some qualities are expected from the potential solid fuel. The chemical characterisation done so far for this study on pre-treated MSW for RDF has a good quality of packed bulk density (which could still be upgraded), low ash composition, low nitrogen and a considerably high HHV. These physicochemical characterisation results presented in Table 4.8.

showed that the properties of RDF produced from MSW in Cape Town was of suitable which could be very useful in co-pelletising with other solid fuels and exploited for co-blending in co-pyrolysis and co-gasification processes. Indeed, from the values obtained for HHV, it could be used alone with or without co-blending for thermochemical conversion to produce a high hydrogen content syngas.

4.2.6 Thermo-gravimetric Analysis of Pre-treated MSW

The characteristics of thermal degradation profiles of pre-treated MSW solid fuel were monitored by thermo-gravimetric analysis (TGA). The TGA is an essential technique to understand the combustibility of solid fuels for application in thermochemical conversions. The graphs of thermal degradation profiles of the RDF from MSW were presented where the most pertinent combustion characteristics of RDF were shown. The decomposition profiles of TGA, DSC and derivative weight results were reported in Figure 4.4 to Figure 4.6.

The TGA of the TWS (TGA for WS sample), TKL (TGA for KL sample) and TCP (TGA for CP sample) pre-treated MSW samples revealed that four stages were observed in the thermal degradation or decomposition as demonstrated in the studies of (Jiang et al., 2016, Janajreh and Al Shrah, 2013, Cao et al., 2006, Cao et al., 2015, Li et al., 2015, Yan et al., 2010, Chen et al., 2015b). The four stages were characterised by various gasification reactions (drying, dehydration and decarboxylation), thermal decomposition, char combustion and reforming, gasification and char gasification as presented in previous sections. The stages are discussed below.

The first stage of the thermal degradation of the pre-treated MSW samples was essentially the release of moisture content (MC) or dehydration/drying.

The MC of the pre-treated MSW samples was mostly released between 20 and 110 ^{0}C (Figure 4.4) and that was not the actual gasification reaction but represented the initial removal of non-combustible constituents (water) before the decomposition of the samples commenced. The total removal of MC from the pre-treated MSW was the predominant activity in this stage. No real chemical reaction took place, but it was more of an endothermic process which consumed some energy. The energy consumed at this stage might be reflected in the overall net energy. However, the dehydrating and decarboxylation stage was required and essential for the overall thermochemical conversion.

Slight degradation was observed just before the second stage but the mass loss was not as significant as that of the first stage. All three samples of TGA showed a similar thermal degradation trend though the value for MC might be different as shown in Figure 4.5, while a slight variation was observed in the thermal degradation profile for the CP facility. The actual decomposition started at around 250 ^{0}C, but there was a slight stability in temperature changes between 110 and 250 ^{0}C. Thereafter, there was a relative stability in mass loss just before the second stage when a series of chemical reactions began.

The second stage took place between (250 - 550 ^{0}C) which might represent the beginning of decomposition (devolatilisation processes) of volatile matters (VM) to produce volatiles and non-condensable compounds (pyrolysis products) (Figure 4.4). The largest mass volatilisation compared to other stages occurred at this stage. The DSC graph also showed an endotherm profiles that reflect production of volatile compounds. This was the usual combustion characteristic for most combustible solid fuels where biomass materials (Cao et al., 2006, Cao et al., 2015) were decomposed into high energy gases (CO, H_2 and CH_4)

and tar (Mettanant et al., 2009b, Basu, 2013). The TKL sample had a good degradation mass loss that may be high energy gaseous products (CO, H_2 and CH_4).

The result of TCP thermal degradation reflected previous HHV results and the nature of the transfer station (which only allowed inerts and rubbles solid waste). The oxidant (air/O_2) was part of the reaction and was quickly consumed due to the relatively high kinetics of the volatile reactions (Janajreh and Al Shrah, 2013), which facilitated the production of more products unlike those in the previous stage.

The third stage (500 - 600 ^{0}C) showed continuous thermal degradation of the samples though the mass gradient which was different for all the samples with the highest observed in the KL sample, while the TCP pre-treated MSW sample showed a different trend as shown in Figures 4.5 and 4.6 respectively. The samples showed an increased decomposition rate till 600 ^{0}C. Most of the previous products underwent further chemical reactions as the temperatures surges from the pyrolysis region to the gasification region. The following Figures 4.4 to Figure 4.6 show the trend mass loss in thermochemical degradation processes.

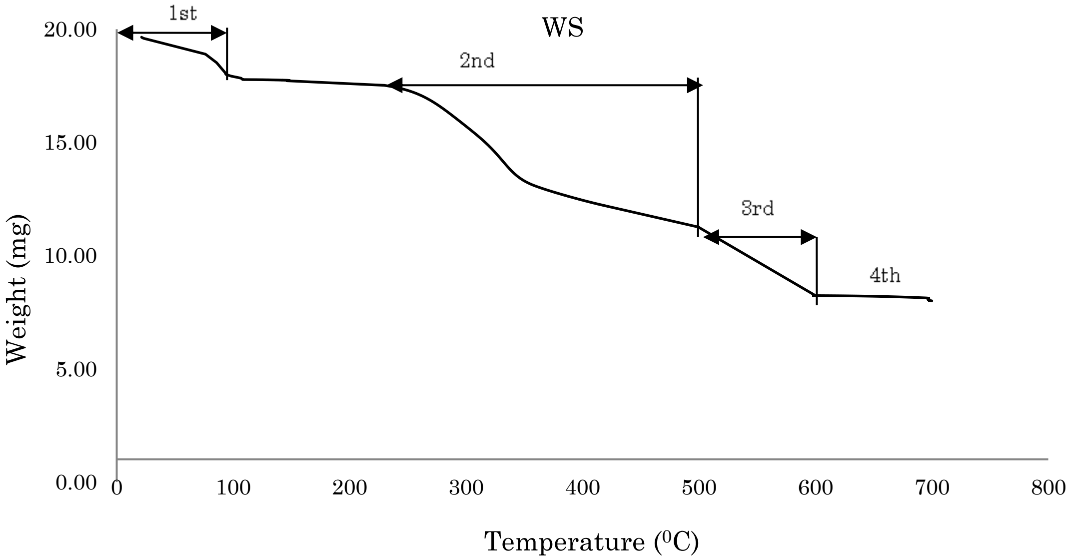

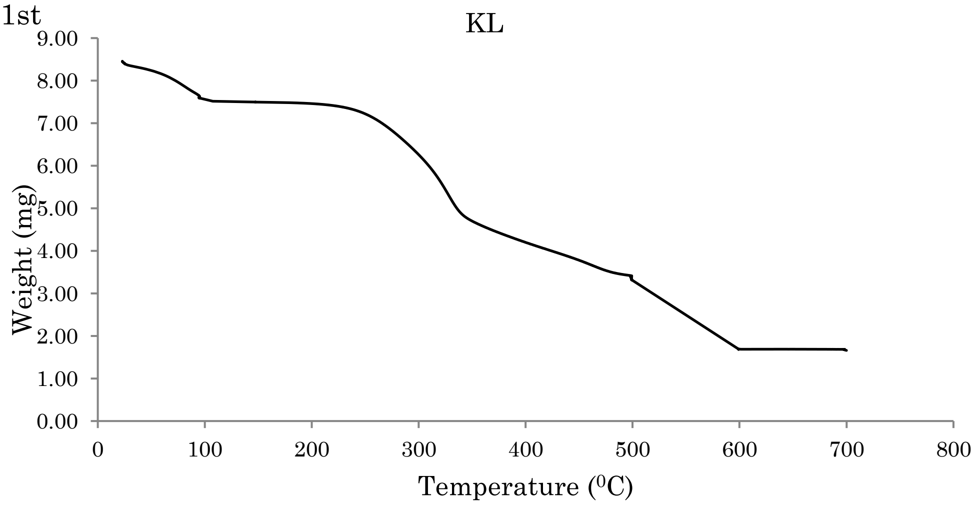

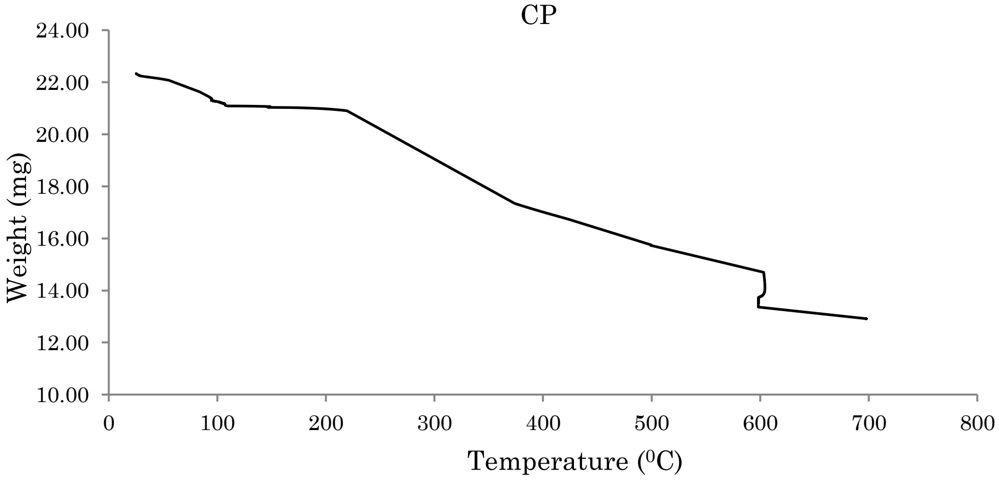

Figure 4.4: The TGA of WS, KL and CP Pre-treated MSW Samples

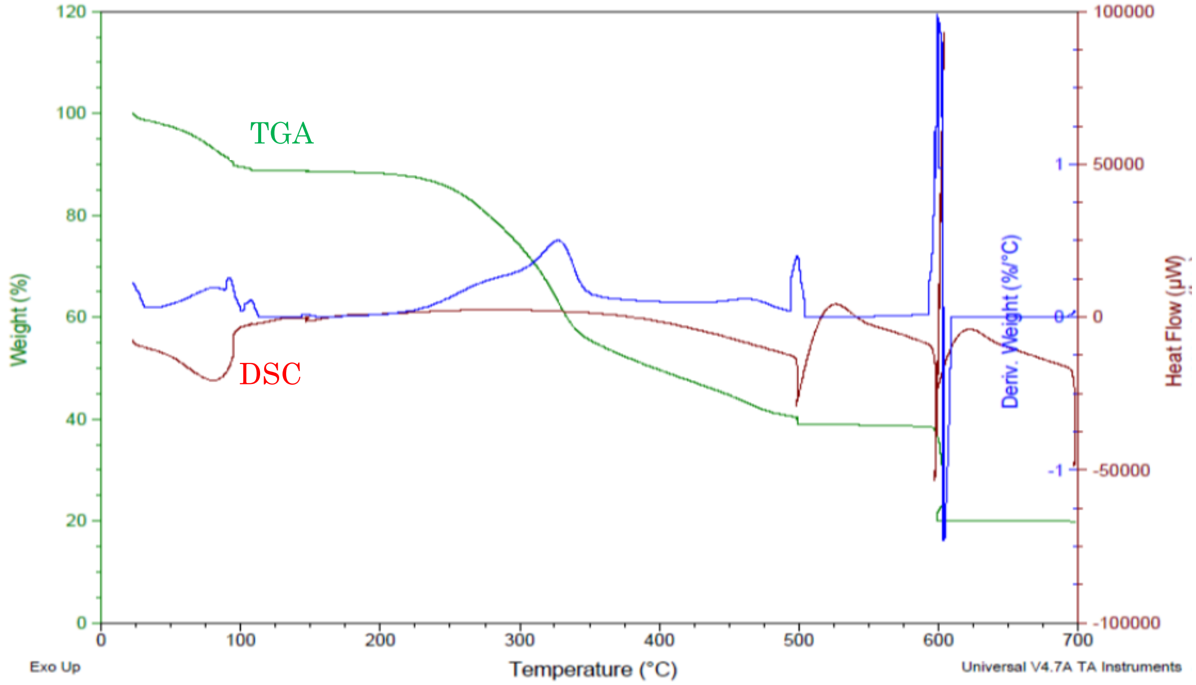

Figure 4.5: The Thermal Analysis of TKL Showing TGA, DSC and DTG

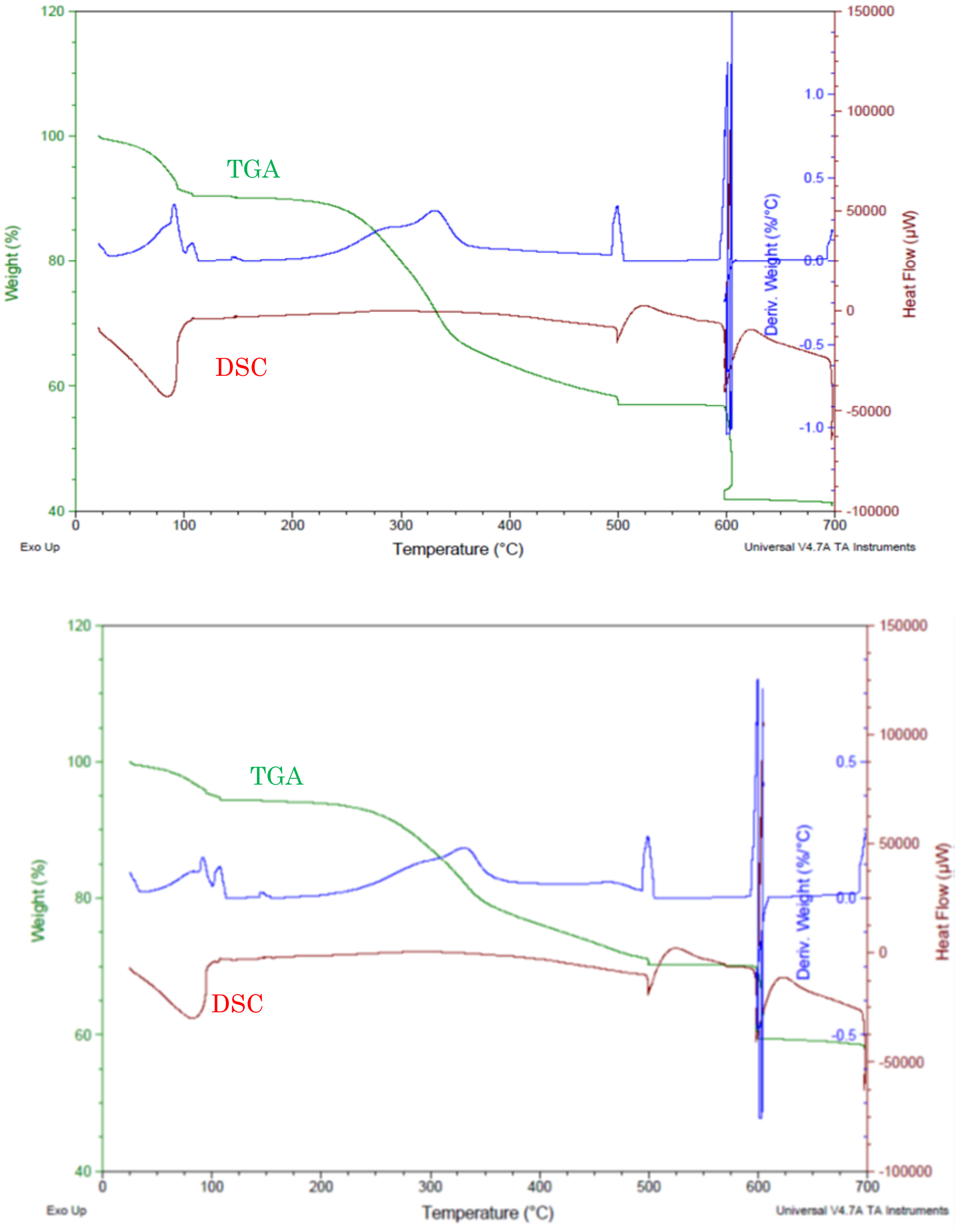

Figure 4.6: The Thermal Analyses of TWS and TCP Showing TGA, DSC and DTG

After the gasification stage, char was gradually being produced and the char gasification reaction began because of the availability of hot gases and hot steam present in the reaction environment (Janajreh and Al Shrah, 2013). The char gasification reaction produces a set of compounds (CO, H_2 and C_xH_y) which are very important products of gasification for some applications. These were shown earlier in the second stage with a differential mass loss. There was partial combustion at a higher temperature under a controlled quantity of oxidants. Flaming pyrolysis was experienced just before 600 ^{0}C for all the sample species (Figures 4.6 - 4.7). This was another indication of secondary reactions and high kinetics. Also, the condition (temperature) of thermal degradation at this stage favoured a Boudouard reaction (reaction between char and CO_2) where CO_2 was involved in the production of CO and it was an endothermic reaction (Chen et al., 2015b). This CO_2 consumption in this stage might facilitate further production of a molar volume of CO and H_2 even beyond this stage up to the fourth stage.

The Final stage (fourth stage) did not show any significant thermal degradation but char gasification that might continue to produce CO. The Boudouard reaction was initiated at about < 700 ^{0}C which led to a further decrease of char composition. This was the stage where ash was the main constituent. Ash and a fraction of FC are also found in this residue after completion of the thermal gradation processes. The percentage of ash in the samples is an important precursor in thermochemical conversion processes because they contribute to the energy potential of solid fuel. The trend observed for this analysis indicated that the samples were stable for thermal degradation except for samples from the CP facility for the same reason (disposal of rubbles and inert materials) mentioned earlier.

In the previous stage, the stage was uniform for the whole sample because the processes were just dehydration and decarboxylation unlike other stages, particularly the last stage, where the trend of degradation of the CP station was totally different.

4.3 Chapter Summary

A physicochemical characterisation was carried out on some pre-treated MSW samples from MSWDFs in Cape Town. The daily generation of MSW from more than 1 million households with 3.7 million people is approximately 1800 tonnes with 5 - 7 % growth per annum of MSW in Cape Town, South Africa. These quantities of MSW come from residential, commercial and industrial activities in these fractions: 2:1:1. More than 40 % of the MSW is from organic matters while combustible contents are approximately 70 % of all MSW generated in the city.

The results are summarised in Table 4.9. The need for proper handling of the pre-treated MSW was addressed through a demonstration of improvised RDF production.

The RDF pellets were produced from pre-treated MSW and packed bulk densities obtained and compared with RDF pellets of the same origin. The packed bulk densities were relatively good for thermochemical conversion though they may be improved upon. The energy density increased from 4142.07 MJ/m^3 to 10735.8 MJ/m^3. The packed bulk density characteristics could serve as an alternative solid fuel, among other alternatives.

In addition, the results of various analyses have shown the useful potential of MSW if pre-treated. The HHV obtained compared better to normal products of RDF pellets produced from MSW in the market or virgin biomass with a value around 16 - 18 MJ/Kg.

The ultimate and proximate analyses showed distinction between the combustible non-combustible potential of the RDF solid fuel and C/H ratio content of the RDF. The proximate analysis reflected that combustible composition of 78 % and non-combustible of 14 %. Their analyses demonstrated another opportunity for an alternative solid fuel application. The average result data for the ultimate analysis and C/H ratio were good values while a low nitrogen composition together with good HHV were positive indicators of solid fuel.

Table 4.9: Summary of Physicochemical Characterisation of Pre-treated MSW Samples

Analyses	KL	LM	CP	WS
Moisture Content (wt. %)	10.7008	9.0906	5.1008	9.0906
Volatile Matter (wt. %)	74.1680	40.8804	48.3225	40.8804
Fixed Carbon (wt. %)	11.1194	28.2188	29.9818	28.2188
Ash (wt. %)	4.0012	21.8101	16.9722	21.8101
Heating Values (MJ/Kg)	20.8463	24.6553	15.9697	14.8453
Packed Bulk Density (g/mL)	0.5150	0.2962	0.3208	0.3898
Ultimate Analysis	LM	GMM	Average	WS
Carbon (wt. %)	39.2830	38.0810	30.3950	33.8910
Hydrogen (wt. %)	4.8170	4.7500	3.8285	4.2390
Oxygen (wt. %)	34.5390	54.9960	52.8200	38.8770
Nitrogen (wt. %)	0.9590	1.0750	0.9761	1.1830
Sulphur (wt. %)	2.7190	3.1717	2.8721	3.0400
Ash (wt. %)	4.0012	21.8101	16.9722	21.8101
High Heating Values (MJ/Kg)	24.6553	20.1691	19.4433	14.8453
Packed Bulk Density (g/mL)	0.4256	0.3966	0.3677	0.2962

The molecular formula ($CH_{1.45}O_{1.85}$) of the pre-treated MSW from LM was selected for gasification simulation because of its high HHV, relatively low ash content, and good C/H ratio when to others. The proximate analysis showed the percentage compositions of MC, VM, FC and ash.

The contribution of VM and FC were significant compared to MC and ash. The VM, FC and ash components had presented similar patterns of combustion characteristics. The TGA analysis showed the preferred degradation profiles which were uniform for all the samples analysed. In theory, the temperature profiles for all the samples considered the net effect of the endothermic and exothermic reactions and these matched the expected trend and matched the expected temperature evolution.

The relevance of the values of bulk density, proximate analysis, proximate analysis, high heating values, and TGA obtained were that they will be used in gasification simulation. All these analyses provide indications of using Cape Town MSW for alternative solid fuel. The focus of this study is to exploit the thermochemical conversion of pre-treated MSW for syngas production and later to produce hydrogen for a fuel cell-based CHP system. The next chapter will embark upon a brief discussion on the need for alternative energy resources and consider the analyses of thermochemical conversion through preferred thermochemical conversion technology.

CHAPTER FIVE

5 SIMULATION OF THE GASIFICATION OF RDF

5.1 The Refuse-Derived Fuel Gasification Simulation

This chapter presents results of gasification simulation of refuse-derived fuel (RDF). It also discusses how operating parameters of gasification affect the results of the simulation.

5.2 Standard Syngas Production

The chemical reactions from the three stages (thermal decomposition, char combustion and reforming and char gasification) were considered to produce syngas (CO and H_2), the main product of an air-blown downdraft gasifier produced from the gasification processes. Char (equation 5.8) and tar (equations 5.5 - 5.7) combustion were considered, based on the works of (Corella and Sanz (2005), Li and Suzuki (2009), Kotz et al., 2010). Table 5.1 listed the summary of important input parameters for gasification modelling while the essential chemical reactions (exothermic and endothermic reactions) relevant for production of syngas are presented below.

$$\mathrm{C} + 0.5\mathrm{O_2} \rightarrow \mathrm{CO} \qquad \Delta^\circ H_{r,773} = -103.6412 \text{ KJ/mol} \quad (5.1)$$

$$\mathrm{C} + \mathrm{H_2O} \leftrightarrow \mathrm{CO} + \mathrm{H_2} \qquad \Delta^\circ H_{r,773} = +150.2474 \text{ KJ/mol} \quad (5.2)$$

$$\mathrm{C} + \mathrm{CO_2} \rightarrow 2\mathrm{CO} \qquad \Delta^\circ\ H_{r,1123} = +178.4130 \text{ KJ/mol} \quad (5.3)$$

$$\mathrm{CH_4} + \mathrm{H_2O} \leftrightarrow \mathrm{CO} + 3\mathrm{H_2} \qquad \Delta^\circ H_{r,1123} = +326.4565 \text{ KJ/mol} \quad (5.4)$$

$$\mathrm{C\,H_{1.14}} + 0.5\mathrm{O_2} \rightarrow \mathrm{CO} + 0.57\mathrm{H_2} \qquad \Delta^\circ H_{r,773} = -189.1009 \text{ KJ/mol} \quad (5.5)$$

$$\mathrm{C\,H_{0.8}} + 0.5\mathrm{O_2} \rightarrow \mathrm{CO} + 0.4\mathrm{H_2} \qquad \Delta^\circ H_{r,773} = -254.1860 \text{ KJ/mol} \quad (5.6)$$

$$\mathrm{C_{0.54}H_{0.54}} + 0.27\mathrm{O_2} \rightarrow 0.54\mathrm{CO} + 0.27\mathrm{H_2} \qquad \Delta^\circ\ H_{r,1123} = -25.6824 \text{ KJ/mol} \quad (5.7)$$

$$\mathrm{CH_{0.2}\,O_{0.13}} + 0.87\mathrm{H_2O} \rightarrow \mathrm{CO} + 0.97\mathrm{H_2} \qquad \Delta^\circ H_{r,1123} = +166.5928 \text{ KJ/mol} \quad (5.8)$$

5.3 Summary of Enthalpy and Energy Balances for Gasification

All gasification conversion reactions (drying, thermal decomposition, char combustion and reforming, char gasification and water-gas shift) were considered in the determination of energy content for reactions to produce syngas (CO and H_2) in a downdraft gasifier gasification process and WGS. All the thermochemical reactions are detailed in APPENDIX F. The summary of the distributions of reactions is presented in Table 5.1.

Table 5.1: Summary of Heat of Chemical Reaction

Reactions	No	$\in \Delta^\circ \mathbf{H_r}$
Exothermic Reactions	Six	-1503.4834 KJ/Mol
Endothermic Reactions	Seven	+1066.2502 KJ/Mol
Net Energy of Reactions	Thirteen	-437.2332 KJ/Mol

5.4 Results and Discussion

Gasification technology offers the production of energy-packed gaseous products, essentially syngas. The choice of the right gasifier and operating parameters were very useful to produce the desired syngas composition to suit the end use of the required gaseous products. The bulk density, HHV, proximate and ultimate analyses of RDF1 (literature), RDF2 (KL sample) RDF3 (LM sample) results to be used in gasification simulation are presented in Table 5.2. RDF1 sample data was obtained from literature (Galvagno et al., 2006) while RDF2 and RDF3 samples were produced in this study.

Table 5.2: Bulk Density, HHV, Proximate and Ultimate Analyses of RDF Samples

Proximate Analysis	RDF1$^+$	RDF2 (KL)	RDF3 (LM)	Average
Moisture Content (wt. %)	-	10.7008	9.0906	8.2947
Volatile Matter (wt. %)	79.70	74.1680	40.8804	54.4543
Fixed Carbon (wt. %)	6.80	11.1194	28.2188	23.1067
Ash (wt. %)	13.50	4.0012	21.8101	14.2612
Heating Values (MJ/Kg)	19.88	20.8463	24.6553	19.4433
Bulk Density (kg/m^3)	270	515.0	425.6	367.7
Ultimate Analysis				
Carbon (wt. %)	48.80	32.049	33.891	30.3950
Hydrogen (wt. %)	7.80	4.048	4.239	3.8285
Oxygen (wt. %)	29.20	-	38.877	-
Nitrogen (wt. %)	0.70	-	1.183	0.9761
Sulphur (wt. %)	0.00	2.908	3.04	2.8721

The quality of syngas is a very important factor that decides the relative feasibility of the gasification process towards a sustainable CHP system. One of the main parameters in determining the quality of syngas is hydrogen to CO molar ratio (H_2/CO) and the molar ratios indicate the syngas end-use applications (F-T synthesis, methanol production, hydrogen production and fuel cell application). These various applications require different H_2/CO molar ratios for specific end-use.

This study requires a high H_2/CO molar ratio for a fuel cell-based CHP system. This requirement has been demonstrated in the entire process of gasification technology from the choice of the gasifier to the appropriate reaction modelling to produce the desired high hydrogen syngas product mixture. The equations 29 - 43 as shown in APPENDIX F were selected to represent all the possible reactions in the gasification processes where tar oxidation and reforming were introduced to selectively account for the reduction in tar formation, but not beyond stages 2 and 3 (Figure 5.6). Tar chemical compositions were addressed by selecting common tar as most tar is largely condensable and with aromatic intermediate products (Kotz *et al.*, 2010). The selected gasifier adequately dealt with the minimisation of tar, which is an unwanted product as discussed earlier. The equations 5.5 - 5.7 were introduced to the model equations to show the thermochemical conversion of tar during the flaming pyrolysis and contributed to the production of syngas.

A Boudouard reaction (equation 5.2) generated CO to enhance the quality of syngas at elevated temperatures in the combustion stage of the gasification reactions while technically reducing carbon emissions.

The generated CO product in the syngas products was then sent to the Water-Gas Shift reactor to improve the high hydrogen content in syngas by a reasonable percentage.

As discussed previously, pyrolysis is one of the gasification processes which involves the decomposition of the $C_xH_yO_z$ composition of pre-treated MSW into condensable and non-condensable gases with high energy values. Pyrolysis products play a significant role in determining the char and tar cracking and reforming.

The basis of these balances is 5 Kg/hr of RDF1 from the data contained in the literature (Galvagno *et al.*, 2006) which was produced by pre-treated MSW. The distribution of the product stream from the gasification simulation are H_2 (3.6435 Nm^3), CO (2.902592 Nm^3), CO_2 (2.1770 Nm^3) and H_2O (0.1120 Nm^3), while char and light hydrocarbon are assumed negligible based on the choice of the gasifier for the modelling of the reaction schemes. The equivalence ratio (ER) played a prominent role in these reactions before the air becomes very deficient while steam and other primary products constitute the reactant for subsequent reactions in the reaction schemes.

The oxidants (H_2O/steam and Air) were determined based on the assumed basis of the reactions with an amount of $3.5770 \text{ X } 10^{-2}$ kmole and $6.1142 \text{ x } 10^{-2}$ kmole for steam and air respectively. The choices of air depend on the cost implication while the quality of hydrogen could be compromised if raw air is utilised without an air separation unit. The reactions involving air/oxygen are all exothermic which tend to increase the temperature of the whole gasification processes while other steam gasification and Boudouard reactions are endothermic reactions (APPENDIX F).

The endothermic reactions tend to complement the entire initial process. However, as the gasifying agent is being depleted and the gasifier bed temperatures are increased, other subsequent reactions (combustion and gasification equations) (equations 5.1 - 5.8) follow. The ER values chosen were between 0.02 and 0.60 for this, unlike the previous model reaction schemes.

This range was contrary to other studies (0.08 - 0.80) because of the introduction of char and tar components from the stage two products which are involved in combustion and gasification to produce useful syngas products.

Other parameters such as the choice of temperature in some of the gasification reactions are very close to the combustion zone (Chen et al., 2013, Plis and Wilk, 2011, Skoulou et al., 2008c, Skoulou et al., 2008a, Zhang et al., 2012, He et al., 2009a).

Tar reforming and char gasification also complement the gasification product with a sudden peak (flaming pyrolysis) wherein almost all the tar and char are converted to valuable non-condensable gaseous products. The reduction in ER values was found to improve the quality of syngas distribution to improve the desired fuel cell application. The impact of these oxidants is discussed later in this chapter.

This was the reason for selecting the specific gasifier that would minimise tar formation (through flaming pyrolysis) in the last combustion zone of the gasifier.

However, the selectivity of the high hydrogen concentration in the syngas is of interest in the overall application. A few studies have reported syngas molar ratios between 1.33 and 3.15 for biomass, MSW and industrial RDF (Galvagno et al., 2006, Galvagno et al., 2009, He et al., 2009b, Skoulou et al., 2008c, Skoulou et al., 2008a, Chen et al., 2013). The syngas molar volume ratio for product H_2 and CO is approximately 7:3 (v/v) for this study.

Based on the assumption that tar productions were expected to be minimal, this could lead to an overall increase of high-energy syngas production, especially hydrogen concentration. Syngas production is favoured by endothermic reactions though demand the need to maximise the heating value and high H_2/CO molar ratio of syngas by driving the endothermic gas-forming reactions as much as possible with the efficient choice of ER values and SFR (steam-fuel-ratio) values. Also, the exothermic reaction at the early stage is required to boost the temperature of reactant activities by providing the minimum required energy to achieve the desired gasification level that provides heat for the endothermic reactions to enhance gas-forming reactions. Hypothetically, the temperature is usually controlled by varying the ER /SFR balance, but the temperature was fixed at 1123 K.

The reactions involving oxygen (equations 3.15 - 3.18) are all exothermic reactions which tend to increase the gasifier temperature while steam gasification (equations 3.19 and 3.22) is an endothermic reaction which tends to reduce the temperature. The endothermic reactions would be complemented by reducing the gasifier's bed temperature.

The theoretical net energy implication of the reaction is shown in Table 5.1 which indicates there are mostly exothermic reactions.

5.4.1 Discussion of Preliminary Aspen Plus Modelling Results

The RDF1 was used to conduct the thermochemical conversion to generate the desired high hydrogen content of the syngas mixture. The overview of the model result was briefly discussed in the previous chapter. The detailed discussion of the RDF1 simulation was analysed for the purpose of this study and the analysis is shown in this report (Adefeso et al., 2015). As discussed earlier, pyrolysis usually precedes gasification which involves the thermochemical conversions of the $C_xH_yO_z$ component of RDF1 (Galvagno *et al.*, 2006) into condensable and non-condensable gases with no significant chemical reactions with a gasifying medium (air and steam). These processes include drying, dehydration, decarboxylation and thermal decomposition (equations 4.1 - 4.14) and other minor reactions are available in APPENDIX F. The equivalence ratio (ER) played a prominent role in these reactions before the air becomes very deficient, while steam and other primary products constitute a reactant for subsequent reactions in the reaction schemes. The reactions involving air/oxygen (Zhang et al., 2012, Chen et al., 2013) are all exothermic which tend to increase the temperature of the whole reaction processes while other steam gasification and Boudouard reactions are endothermic reactions. The endothermic reactions tend to complement the whole initial process. However, as the gasifying agent is being gradually depleted and the consumption of the gasifying agent leads to the gasifier bed temperatures increasing, other subsequent reactions (combustion and gasification equations) follow.

As a result, the temperature ranges may have an impact on the quality of the high heating value of syngas while also considering the choice of a gasifier reactor. The reduction in ER was monitored to improve the quality of syngas distribution to favour the production of syngas with a high hydrogen content to suit the final desired application.

This was another reason for selecting the specific gasifier that will optimally minimise tar formation (flaming pyrolysis) and efficiently promote secondary cracking of tar to generate more syngas content and simultaneously, a Boudouard chemical reaction consumed some CO_2 to produce more CO which facilitates more syngas production in the last combustion zone of the reactions (equation 5.3). At the same, the emission of GHG CO_2 into the immediate urban air was minimised. However, a high hydrogen concentration in syngas is of interest to the overall application. A few studies have reported experimental data for syngas H_2/CO molar ratios of between 1.33 and 3.15 for biomass, MSW and industrial RDF (Galvagno et al., 2006, Galvagno et al., 2009, Skoulou et al., 2008c, Chen et al., 2013). On the other hand, the work conducted by (Kannan et al., 2013a) using Aspen Plus on PET/PE blending yielded significantly high molar ratio H_2/CO though the solid waste was purely hydrocarbon.

Based on the assumption of minimal tar production, the air-blown downdraft gasifier may enhance an overall increase in the hydrogen content of the syngas mixture in the production stream. However, syngas production favoured by endothermic reactions demand the need to maximise the heating value and high H_2/CO molar ratio of syngas by driving the endothermic gas-forming reactions as much as possible. Nevertheless, these endothermic reactions do not occur spontaneously.

The temperature is usually controlled by varying the ER/SFR balance. The reactions involving oxygen (equations 4.9 - 4.11) are all exothermic reactions which tend to increase the gasifier temperature while the steam gasification (equations 4.12 and 4.14) is another endothermic reaction which is complemented by reducing the gasifier bed temperature. The performance of the gasifier reaction requires an adequate balance of ER values (air flow rates) and SFR values (steam flow rates) as shown in Figure 5.2 to Figure 5.29.

The molar ratio of H_2/CO of 17.3 and low hydrogen-carbon ratios were obtained from the gasifier processes but the overall syngas yield from the RDF was low - less than 20 % of MSW. The syngas was then sent to the Water-gas Shift (WGS) to increase the H_2/CO molar ratios, to enhance purity and to maximise the high production of hydrogen with a tolerance level of CO for HT-PEMFC application.

The net H_2/CO molar ratios could be within the tolerance limit of HT-PEMFC. The compositions of the syngas are 20 % of CO; 10 % of CO_2 and 70 % of hydrogen (Adefeso *et al.*, 2015). The detailed results of the Aspen Plus model for all RDFs, including RDF1, will be presented and discussed in the following sections describing the effects of ERs, SFRs and quality of RDFs.

5.4.2 Effects of Equivalence Ratios

The equivalence ratios (ER) used in the Aspen Plus Modelling for gasification of various types of RDF were in the range of 0.02 and 0.60 (corresponding to the air flow rate of 1.00 to 30 Kg/hr). RDF1 (from literature), RDF 2 and RDF 3 (produced in this study) were used as feed for the gasification process. The importance of steam during gasification processes was examined thus the steam fuel ratios (SFR) during the gasification processes were set between 1.00 and 3.90 (corresponding to the steam flow rate of 2.10 to 8.20 Kg/hr).

The complete process flow diagram for the high hydrogen syngas production from the gasification of RDFs (RDF1, RDF2 and RDF3), including the two-stage water-gas shift system, is shown in Figure 5.1.

The parameters for the steam flow rate (SFR) value (1.00, 1.50, 1.80, 2.00, 2.10, 2.80, 3.90) were fixed while the ER were varied for every run for RDFs simulation with equivalence ratio (ER) values of 0.01, 0.02, 0.04, 0.1, 0.2, 0.4 and 0.60 respectively as can be seen in Table 5.3 while raw samples of Aspen Plus Model streams results were shown in Table 5.4.

Table 5.3: The Steam Flow Rate (SF) and Equivalence Ratios

RDF 1		RDF 2		RDF 3	
ER	SFR	ER	SFR	ER	SFR
0.15	2.1	0.1	2.1	0.1	2.1
0.2	3.1	0.15	3.1	0.15	3.1
0.3	3.8	0.2	3.8	0.2	3.8
0.35	4.2	0.29	4.2	0.3	4.2
0.4	4.8	0.3	4.8	0.35	4.8
0.45	5.2	0.35	5.2	0.4	5.2
0.5	5.9	0.42	5.9	0.46	5.9
0.55	6.3	0.44	6.3	0.5	6.3
0.60	6.9	0.46	6.9	0.55	6.9
0.65	7.3	0.50	7.3	0.60	7.3

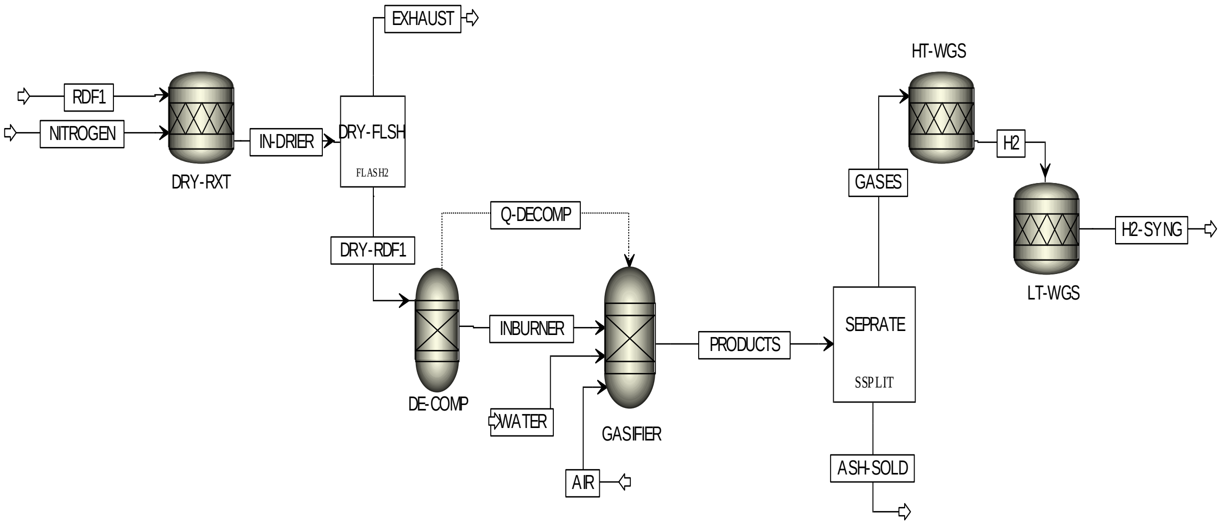

Figure 5.1: The Process Flow Diagram of RDF Gasification in Aspen Model Interface

Table 5.4: Raw Samples of Aspen Plus Model Streams Results

SFR = 2.1				
ER	H_2 Kmole	CO Kmole	CO_2 Kmole	H_2O Kmole
0.1	0.071	0.001	0.001	5.061
0.15	0.137	0.103	1.456	4.458
0.2	0.266	0.25	3.536	3.317
0.3	0.588	0.535	7.561	1.149
0.35	0.533	0.806	8.576	0.928
0.4	0.46	0.606	8.576	1.584
0.45	0.386	0.606	8.576	2.239
0.5	0.313	0.606	8.576	2.895
0.55	0.239	0.606	8.576	3.551
0.6	0.164	0.63	8.59	4.221

The syngas productions are usually enhanced with ER not exceeding 0.6 with a sufficiently elevated temperature to crack the tar and promote the Boudouard reaction. Previously, in the preliminary discussion, the entire process of gasification was discussed and how various parameters play a vital role in the production of a hydrogen-rich syngas mixture from gasification. The effects of ER on RDF1 RDF2 and RDF3 are discussed below.

5.4.2.1 Effects of Equivalence Ratios on RDF1

The product distribution of H_2, CO and CO_2 at different combinations of ER (0.15 to 0.60) and SFR (1.50 to 3.80) were studied. These gaseous products from the simulation are shown in Figure 5.2 to Figure 5.26. The temperature was fixed at a moderately high temperature at 1123 K as Yan *et al.* (2010) and Chaudhari *et al.* (2003) established that temperature in that range has a high indication of the production of a good quality of syngas.

Between the ER values of 0.10 and 0.35, at the constant, high temperature in the gasifier, the syngas (H_2 and CO) content increases steadily but the hydrogen molar concentration is higher compared to others. The molar concentrations of CO and CO_2 was relatively stable at between 0.30 and 0.49 ER for almost all the SFR values run for RDF1, but the molar concentrations began to decrease after the ER value of 0.50 for all the values of SFR using the Aspen Plus model. The molar concentration of CO_2 was relatively stable and higher than that of other products just after the ER value of 0.45 for all cases of SFR, although a slight decline was noticed towards the end of the simulation (Figure 5.2 and Figure 5.5). This might have been due to the effect of the water-gas shift (WGS) and the consumption of CO_2 in the Boudouard reaction at the elevated temperature. At the ER value of 0.35, for most of the models, the highest hydrogen flow rate (0.534 Kg/hr) was produced for RDF1 but the co-product (CO) concentration was also very high at that ER value. The mixture of H_2 and CO could meet up to the required yield of the H_2/CO molar ratio for the fuel cell application.

The H_2 and CO molar ratios obtained could avoid CO-poisoning of the fuel cell by reducing the efficiency of the fuel cell. These values are higher than similar experimental products of char H_2/CO molar ratios (6.80 and 14.80) by (Chaudhari et al., 2003). It was observed at high ER and SFR levels, the model produced an equal molar concentration H_2/CO ~ 1.00 which was not desirable for application in the fuel cell system. Cold gas efficiency was also obtained for RDF1, RDF2 and RDF3 to complement the performance of the gasification of the RDFs. The cold gas efficiency of RDF1 was presented in Figure 5.6. The efficiency was lower compared to RDF2 and RDF3. The cold efficiency obtained for RDF3 gasification simulation was in between 9 % - 37 % as shown in Figure 5.6.

However, RDF1 gasification produced H_2/CO molar ratio of 18.81 for the ER value of 0.15 and the SFR value of 2.80 (Table 5.5). The corresponding value of hydrogen in the mixture of the molar ratio was less than that obtained at the ER value of 0.35, but a corresponding H_2/CO molar ratio for the ER value of 0.35 was less, hence the molar ratio of 18.81 is the optimum value for this RDF1. Nonetheless, the focus of the study is to produce a high hydrogen concentration in the syngas mixture in the products stream and minimise CO concentration.

Table 5.5: The H_2/CO Ratios for RDF1, RDF2 and RDF3 Simulation Gasification

RDF 1							
SFR	H_2/CO Ratios						
ER	**1.50**	**2.30**	**2.50**	**2.80**	**3.00**	**3.50**	**3.80**
0.15	18.5	16.6	**18.71**	**18.81**	**18.66**	**18.57**	**18.57**
0.20	**14.78**	**14.78**	14.78	14.73	14.73	14.68	14.68
0.30	13.27	13.33	13.36	13.39	13.89	13.39	13.39
0.35	12.22	12.22	12.21	12.22	12.22	12.22	12.22
0.40	10.54	10.54	10.54	10.54	10.54	10.54	9.31
0.45	8.85	8.85	8.85	8.85	8.85	8.85	8.85
0.50	7.17	5.48	5.48	5.48	5.48	5.48	5.48
0.55	5.48	2.23	3.62	3.62	3.62	3.62	3.62
0.60	1.84	1.18	1.27	1.27	1.22	1.26	1.27

RDF 2					
SFR	H_2/CO Ratios				
ER	**1.00**	**1.50**	**1.80**	**2.00**	**2.30**
0.10	2.39	4.2	7.34	11.72	**17.17**
0.15	3.07	6.47	**15.45**	**14.34**	16.85
0.20	4.33	**14.91**	12.98	12.98	15.6
0.29	**11.97**	10.89	10.87	10.85	14.07
0.30	11.05	9.91	9.86	9.83	12.98
0.35	10.05	8.99	8.9	8.84	10.82
0.42	8.81	7.96	7.83	7.76	9.78
0.44	8.52	6.53	6.35	6.07	8.78
0.46	8.17	5.07	5.43	5.01	7.67

RDF 3							
SFR	H_2/CO Ratios						
ER	**1.50**	**1.80**	**2.00**	**2.30**	**2.50**	**2.80**	**3.00**
0.10	1.88	2.48	2.94	3.93	4.92	8.12	12.2
0.15	2.24	3.07	3.72	5.41	7.33	**16.45**	17.27
0.20	2.76	4.03	5.22	8.66	**15.37**	15.77	**18.15**
0.30	5.09	10.47	**14.73**	**13.72**	13.79	13.7	17.53
0.35	8.57	**13.14**	12.72	12.7	12.69	12.68	15.77
0.40	**12.49**	11.78	11.75	11.71	11.69	11.66	13.69
0.46	10.75	10.68	10.63	10.58	10.54	10.49	12.66
0.50	10.08	9.98	9.92	9.85	9.84	9.74	11.65

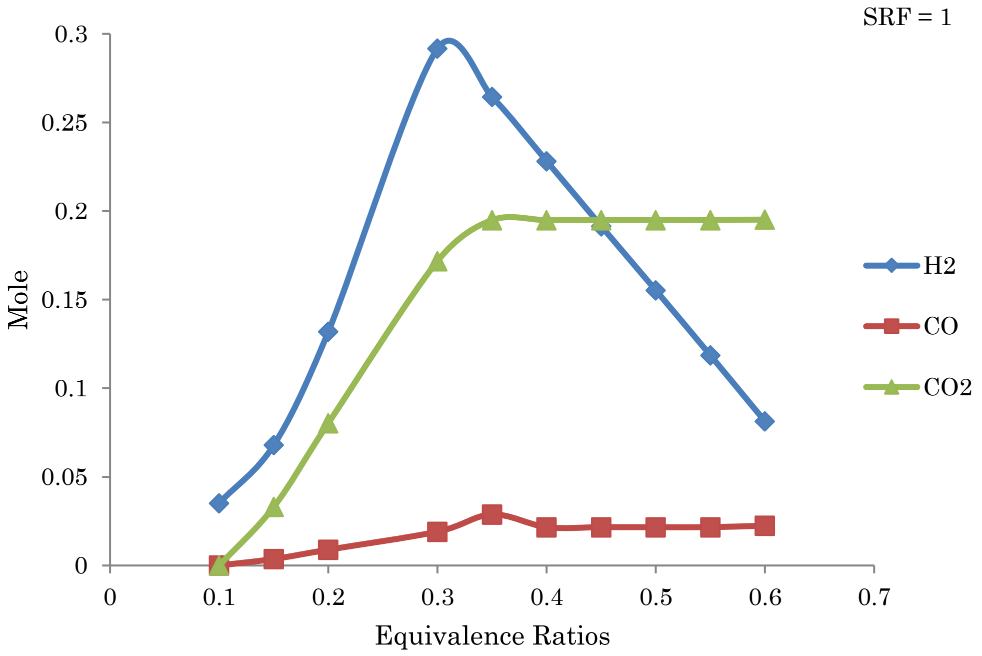

Figure 5.2: Molar Distribution of Desired Products at SFR 1.00 (RDF1)

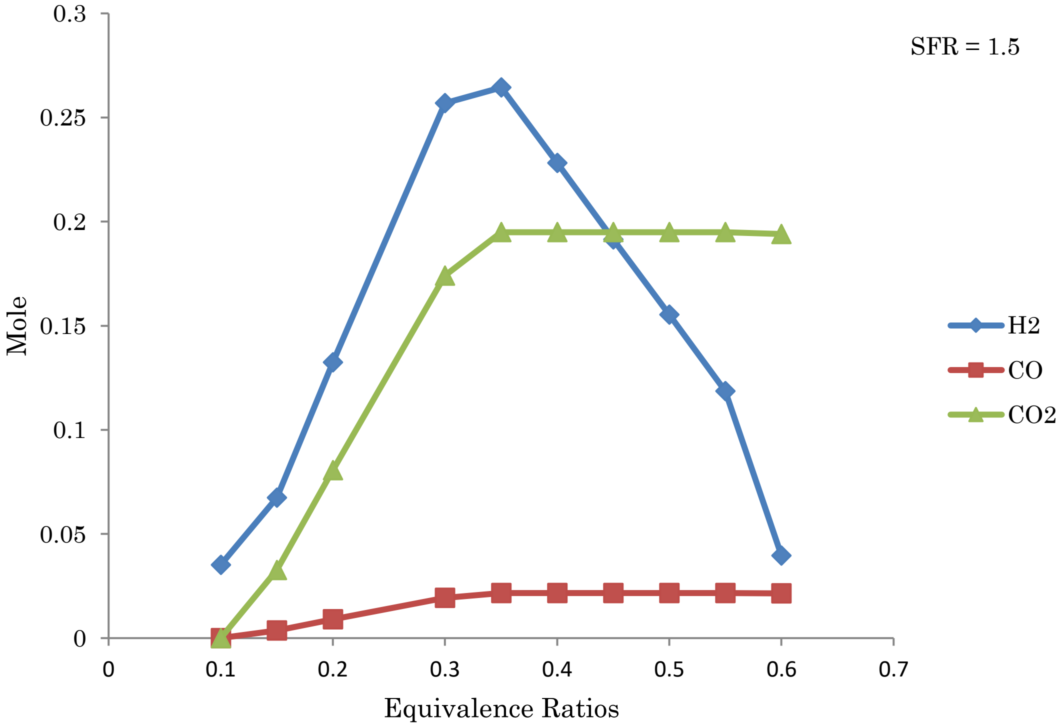

Figure 5.3: Molar Distribution of Desired Products at SFR 1.50 (RDF1)

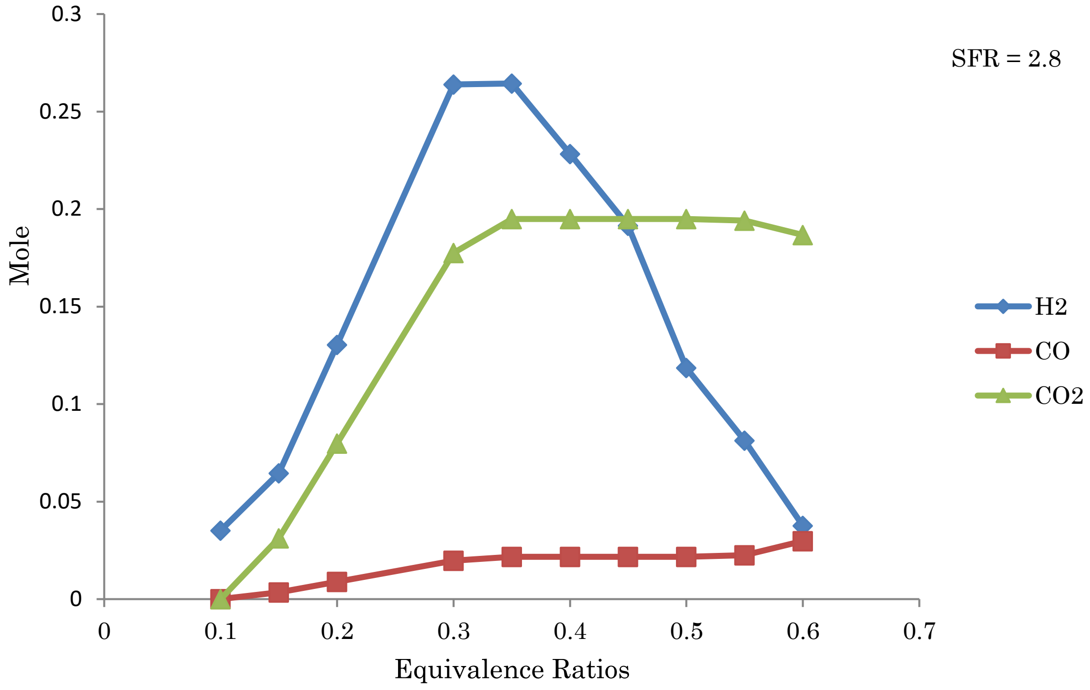

Figure 5.4: Molar Distribution of Desired Products at SFR 2.80 (RDF1)

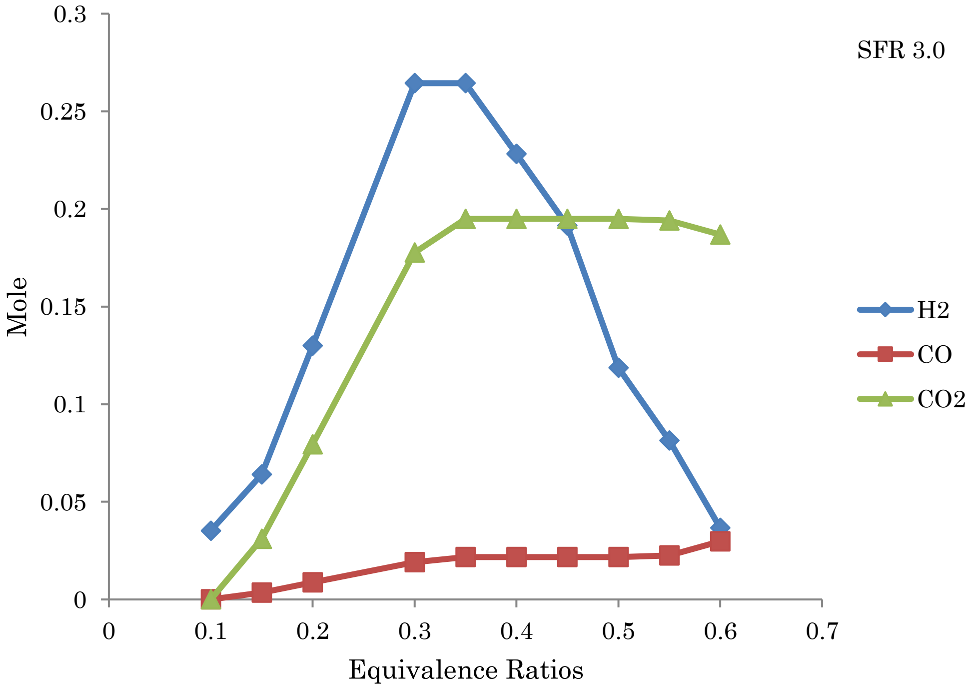

Figure 5.5: Molar Distribution of Desired Products at SFR 3.00 (RDF1)

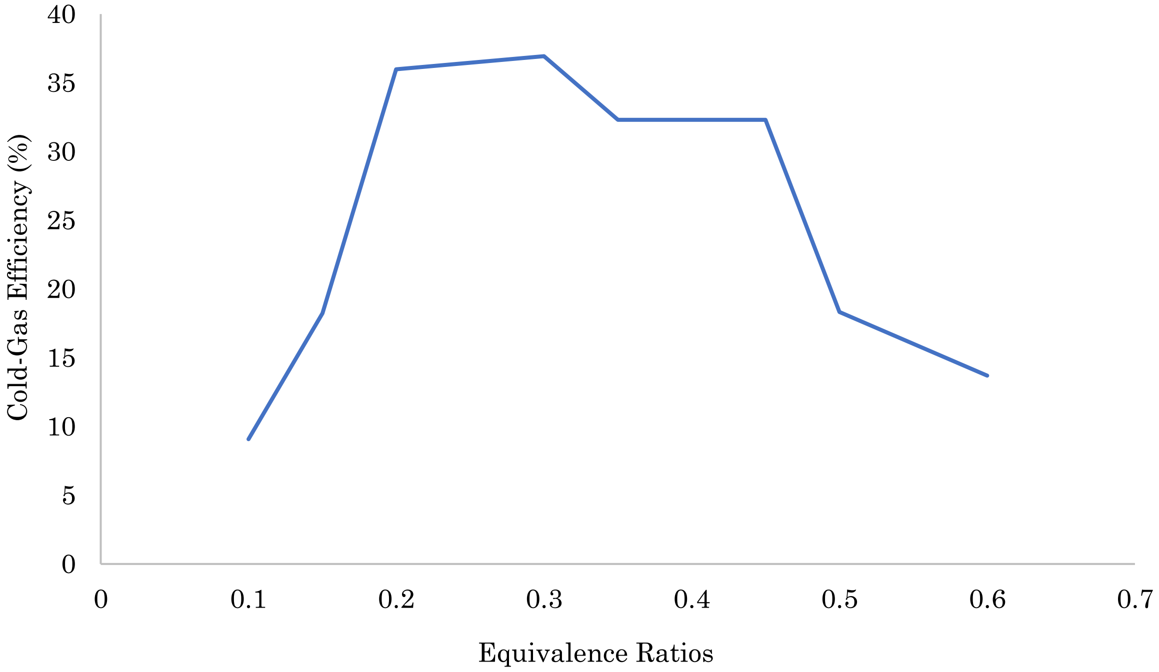

Figure 5.6: Efficiency of Syngas Production for RDF1

5.4.2.2 Effects of Equivalence Ratios on RDF2

The RDF2 was prepared for the thermochemical conversion to hydrogen. Also, the product distribution of H_2, CO and CO_2 at different combinations of ER (0.10 to 0.46) and SFR (1.00 to 2.30) were studied. These gaseous products from the Aspen model are shown in Figure 5.7 and Figure 5.8. The temperature was fixed at a moderately high temperature at 1123 K having established that temperature in that range has a high indication of producing a good quality of syngas while 10 Kg/hr was used for RDF2 mass flow rate in the modelling procedure.

The results obtained from RDF2 were different from RDF1 gasification, although the molar hydrogen concentrations were higher than that of RDF1 the H_2/CO molar ratio was lower. This is because of the effect of high SFR being effective at low ER values. The molar quantities of hydrogen, produced from RDF2 gasification for values of ER values (0.10, 0.20 and 0.30) as shown in Figure 5.7 and Figure 5.8, were higher when compared to the other co-products at a constant, high temperature in the gasifier. These concentrations reduced as the ER values increase for all SFR values. This trend shown by co-products, CO and CO_2, was not similar to that of the hydrogen concentration particularly evident in Figure 5.7 and Figure 5.8, where the increase for CO_2 and decrease for CO were observed respectively. The distribution of the CO and CO_2 concentrations distribution was similar to the results from the catalytic fixed-bed reactor in an experiment conducted by (Ruoppolo et al., 2012). The remaining figures show that co-products were stable enough to change in SFR. The syngas (H_2 and CO) content increased steadily but the hydrogen molar concentration was higher compared to others (Ruoppolo *et al.*, 2012).

The hydrogen molar concentration trend was also similar to the studies of Chen *et al.* (2013), Yunus *et al.* (2010) and Dalai *et al.* (2009) which also involved gasification simulation studies.

The Boudouard reactions and high SFR were responsible for these high concentrations of hydrogen in the syngas (H_2 and CO). On the other hand, the molar concentrations of CO and CO_2 were relatively stable for the SFR value of 2.00.

The relative stability of the molar concentrations of CO and CO_2 observed showed a relationship which might be attributed to the Boudouard reaction at a later stage of the ER values (where CO and CO_2 are actively involved) while the initial relationship might be the influence of the complete combustion of RDF2 gasification as mentioned earlier in the discussion. Besides, this might be the net effects of water-gas shift reaction (WGS) and the consumption of CO_2 in the Boudouard reaction at high temperatures. The high concentration of the higher hydrogen content of syngas (H_2 and CO) could be attributed to a high SFR, Boudouard reaction and WGS.

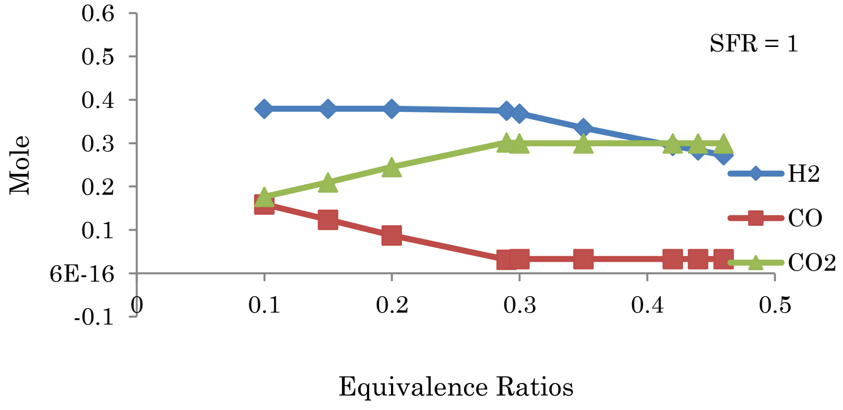

Figure 5.7: Molar Distribution of Desired Products at SFR 1.00 (RDF2)

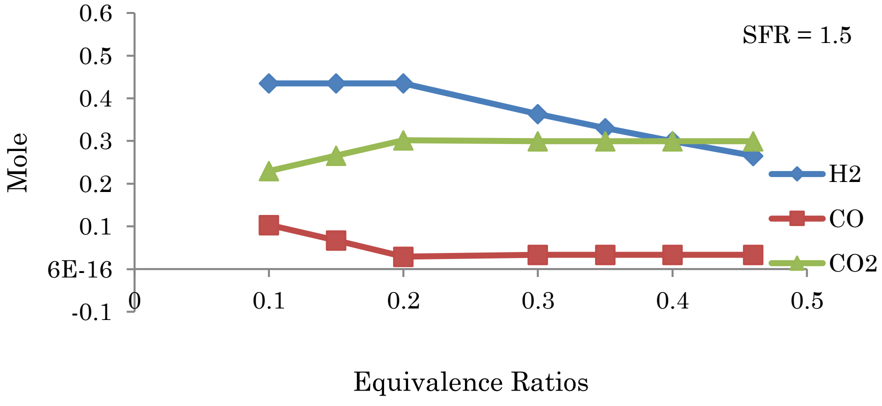

Figure 5.8: Molar Distribution of Desired Products at SFR 1.50 (RDF2)

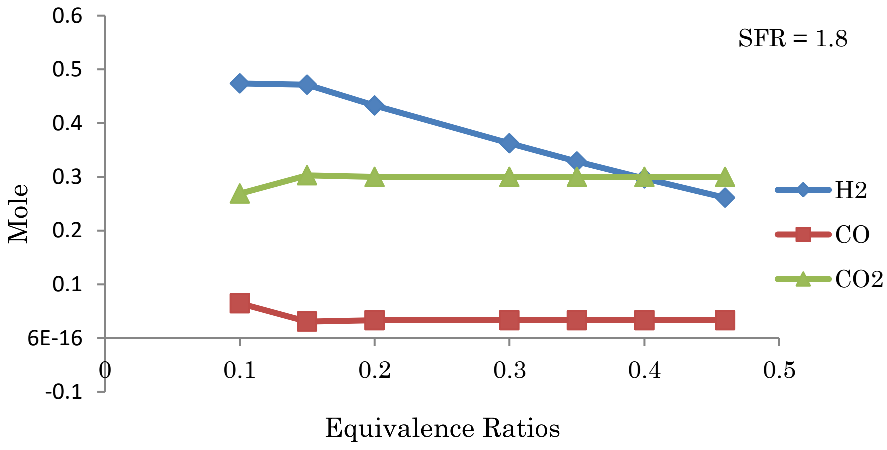

Figure 5.9: Molar Distribution of Desired Products at SFR 1.80 (RDF2)

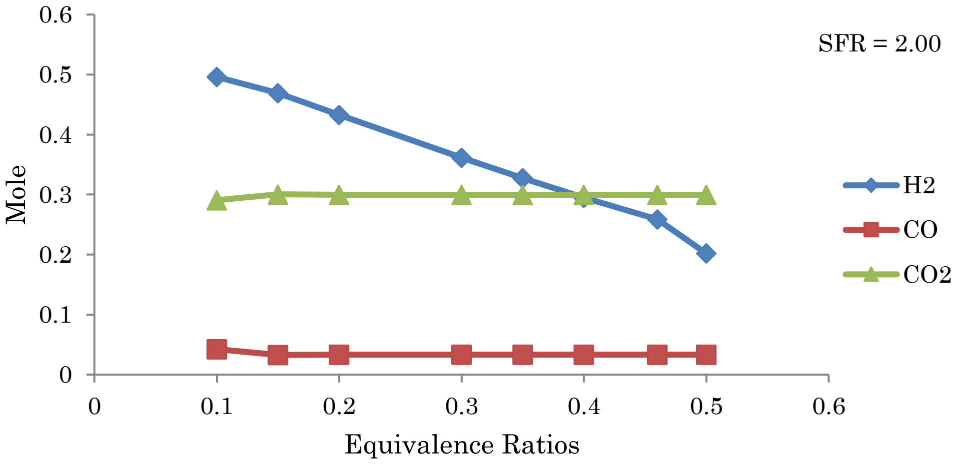

Figure 5.10: Molar Distribution of Desired Products at Various 2.00 (RDF2)

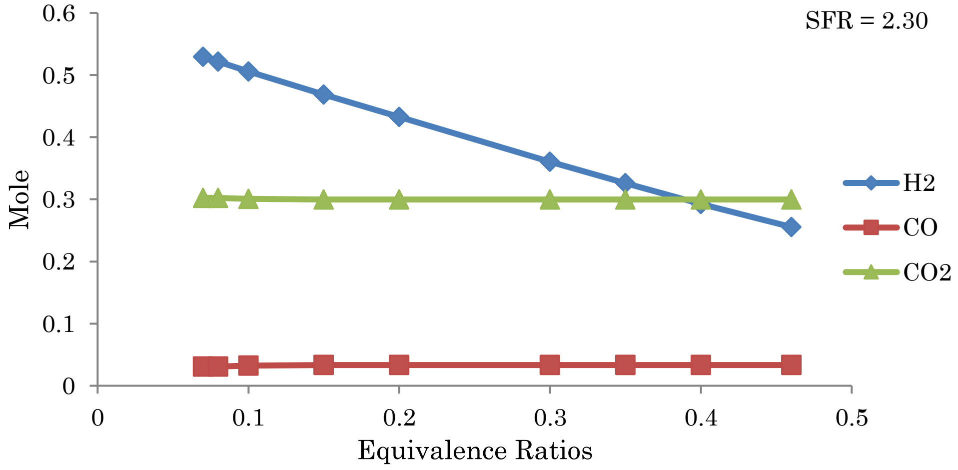

Figure 5.11: Molar Distribution of Desired Products at SFR 2.30 (RDF2)

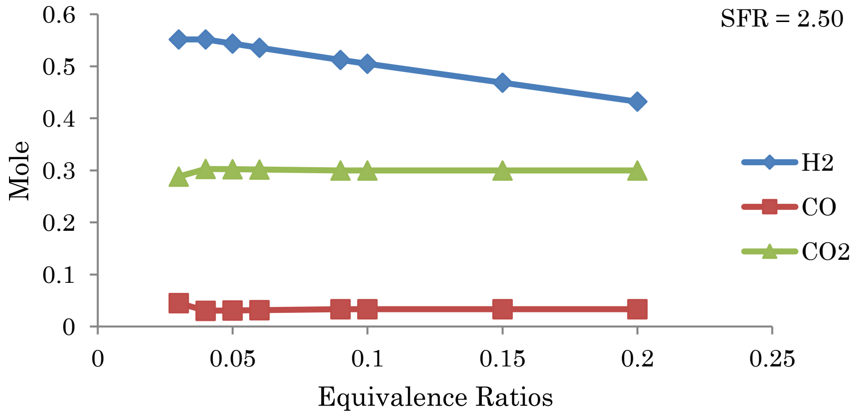

Figure 5.12: Molar Distribution of Desired Products at SFR 2.50 (RDF2)

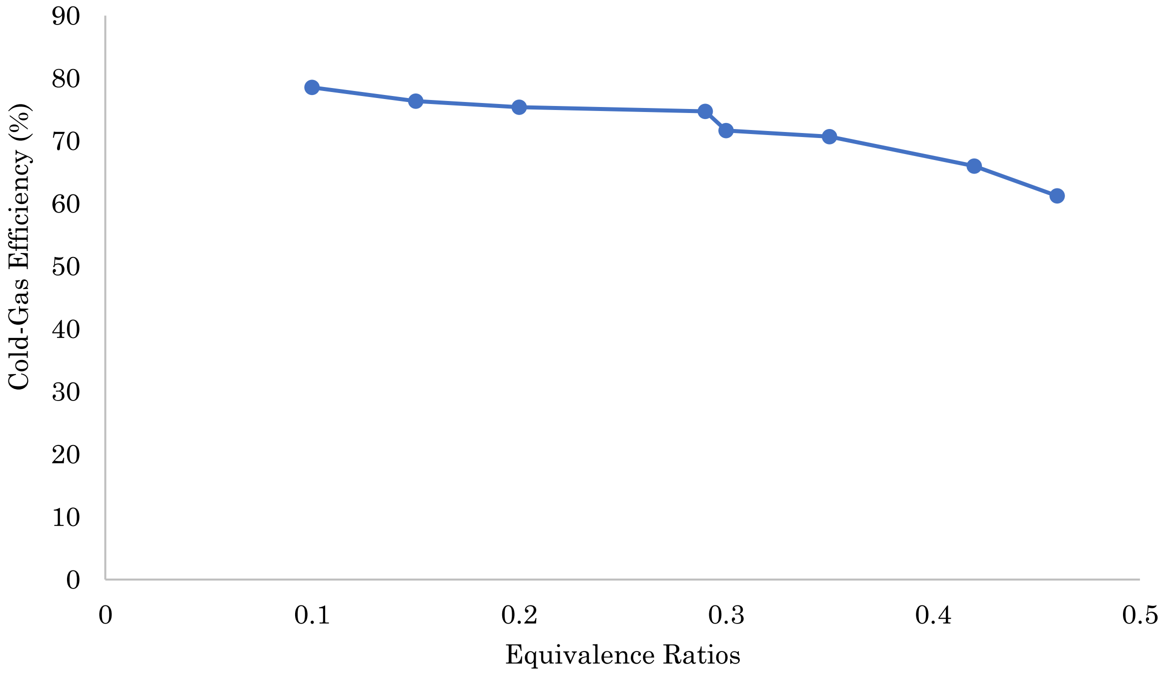

Figure 5.13: Efficiency of Syngas Production for RDF2

At ER values of 0.29, 0.20, 0.15, 0.07 and 0.03 in most of the simulations for RDF2 gasification, the highest hydrogen concentrations (0.756, 0.877 0.955 1.0, 1.067, 1.112 Kmole) was observed for RDF2 but the concentration of the co-product (CO) was also very high at SFRs (2.1, 3.1, 3.8, 4.8 and 5.2) respectively. The mixture of H_2 and CO could not sufficiently meet up to the required yield of the H_2/CO molar ratio for fuel cell application. It was observed at a low ER and SFR that the model produced the same molar concentration $H_2/CO \sim 1.00$ which was not desirable for the application of a fuel cell system. Cold gas efficiency was obtained for RDF2 to complement the performance of the gasification of the RDF. The cold gas efficiency of RDF2 was presented in Figure 5.13. The cold efficiency obtained for RDF3 gasification simulation was in between 61 % - 86 % as shown in Figure 5.13.

However, the RDF2 gasification Aspen model produced 18.12 of H_2/CO molar ratio for the ER value of 0.04 and the SFR value of 5.20. This was a direct influence of SFR as demonstrated by study of (Wu and Williams, 2010b) in the thermochemical conversion involving a two-stage pyrolysis-gasification of plastic waste which improved the quality of syngas sufficiently though the plastic composition was around 15 %. The corresponding value of hydrogen in the mixture was 1.112 Kg/hr. The trend of results showed the influence and dependency of ER values on the desired product and co-products. The focus of the study was to produce high hydrogen concentration in a syngas mixture for application in a fuel cell system.

5.4.2.3 Effects of Equivalence Ratios on RDF3

The distribution of H_2, CO and CO_2 in RDF3 products with different combinations of ER (0.02 to 0.50) and SFR (1.00 to 3.50) was studied. The gaseous products from the model were shown in Figure 5.14 to Figure 5.19. The temperature was fixed at a moderately high temperature at 1123 K (Chaudhari et al., 2003, Yan et al., 2010). 10 Kg/hr was also used in the RDF3 as the mass flow rate in the modelling.

The results obtained for RDF3 were similar to RDF2 gasification though the molar hydrogen concentrations were slightly higher than that of the RDF2 and the H_2/CO molar ratios were also higher. All the molar quantities of hydrogen produced from RDF3 gasification for all the initial values of the ERs were higher when compared to the other co-products at a constant, high temperature in the gasifier. These molar concentrations of hydrogen were relatively stable and began to reduce as the ER values increased to a maximum of 0.50 for all values of SFR. From Figures 5.14 to Figure 5.19, the reduction in the molar concentration of hydrogen was noticed at the ER value of 0.30 to 0.1 0 respectively.

However, there were increases in the molar quantities of hydrogen produced as SFR values increased to the required maximum. Also, the trend showed by the co-products (CO and CO_2) was not like that of the hydrogen molar concentrations particularly in where Figure 5.14 to Figure 5.19 initial increase for CO_2 and a decrease for CO were observed respectively, as can be seen in Figure 5.14 to Figure 5.19. These hydrogen molar concentrations were like the RDF2 trend produced in the previous section.

The remaining figures showed that other co-products were relatively stable to change in SFR. The syngas (H_2 and CO) content increased steadily but the hydrogen molar concentration was higher compared to others as shown in all the figures. The molar concentrations of CO and CO_2 were relatively stable for the SFR values of 3.00 and 3.50. The molar concentrations of CO and CO_2 was relatively stable and showed kind of relationship which might be attributed to the Boudouard reaction at a later stage of ER values while the initial relationship might be the influence of the complete combustion of the RDF3 gasification as mentioned earlier in the discussion.

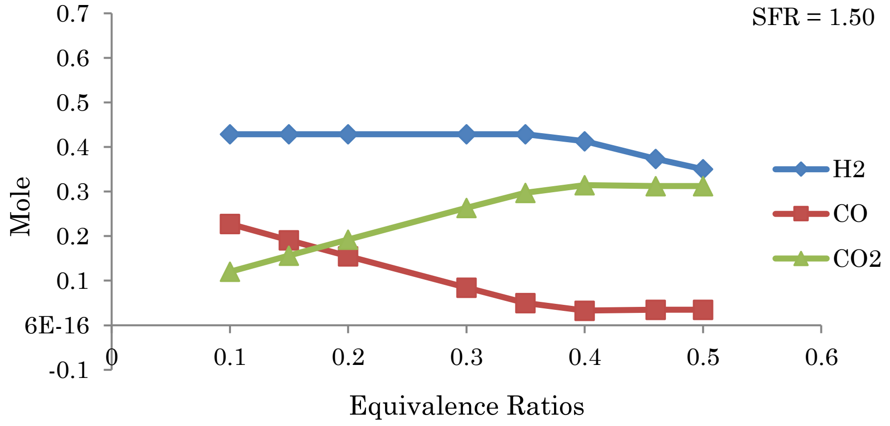

Figure 5.14: Molar Distribution of Desired Products at SFR 1.50 (RDF3)

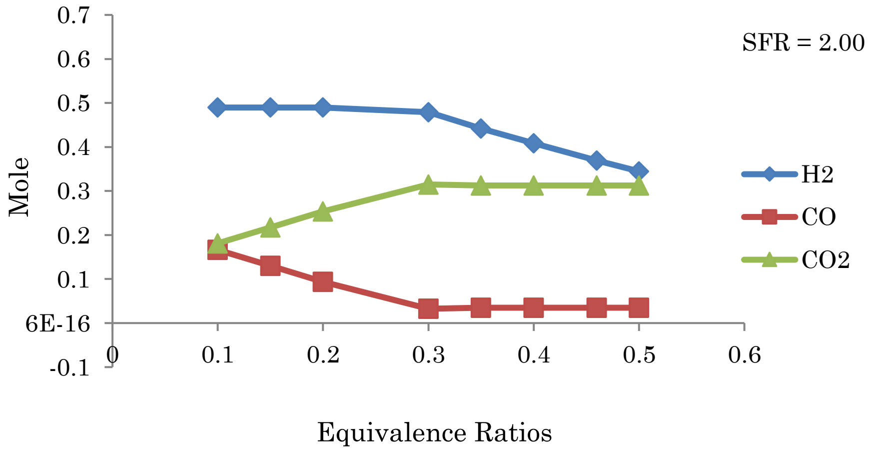

Figure 5.15: Molar Distribution of Desired Products at SFR 2.00 (RDF3)

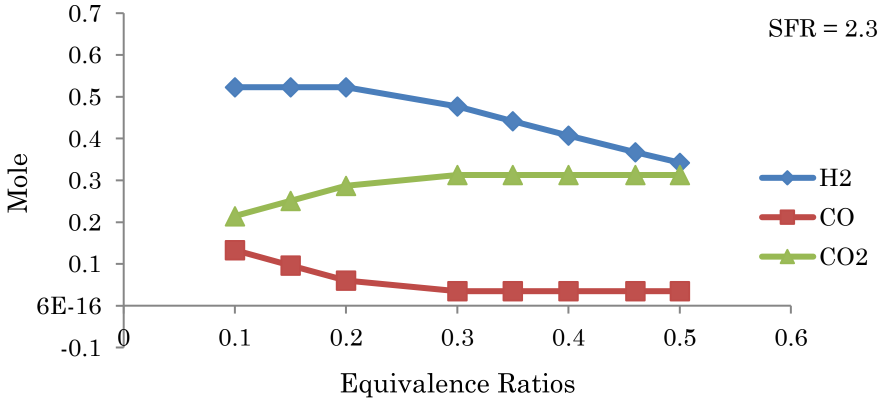

Figure 5.16: Molar Distribution of Desired Products at SFR 2.30 (RDF3)

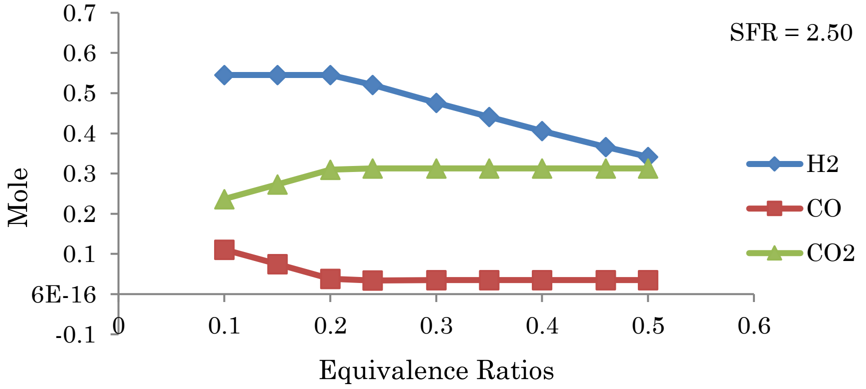

Figure 5.17: Molar Distribution of Desired Products at SFR 2.50 (RDF3)

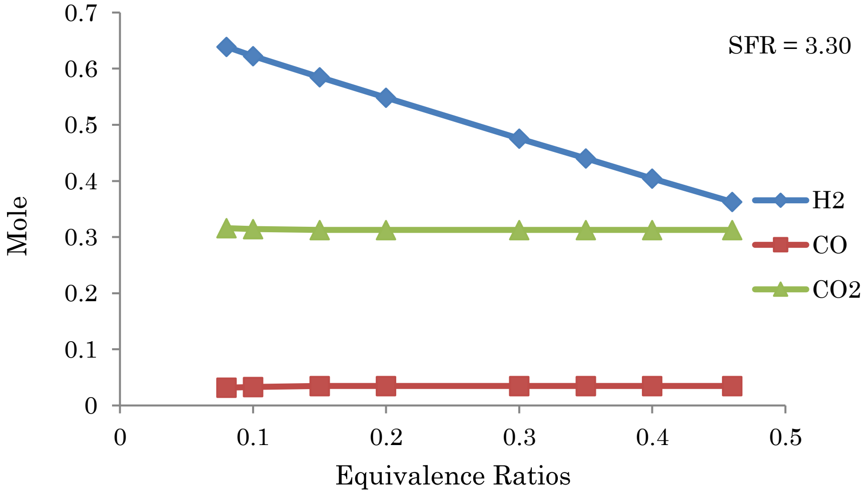

Figure 5.18: Molar Distribution of Desired Products at SFR 3.00 (RDF3)

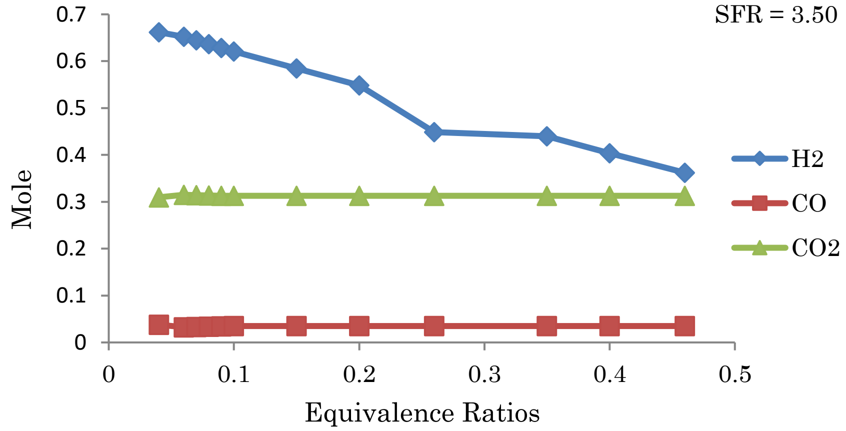

Figure 5.19: Molar Distribution of Desired Products at SFR 3.50 (RDF3)

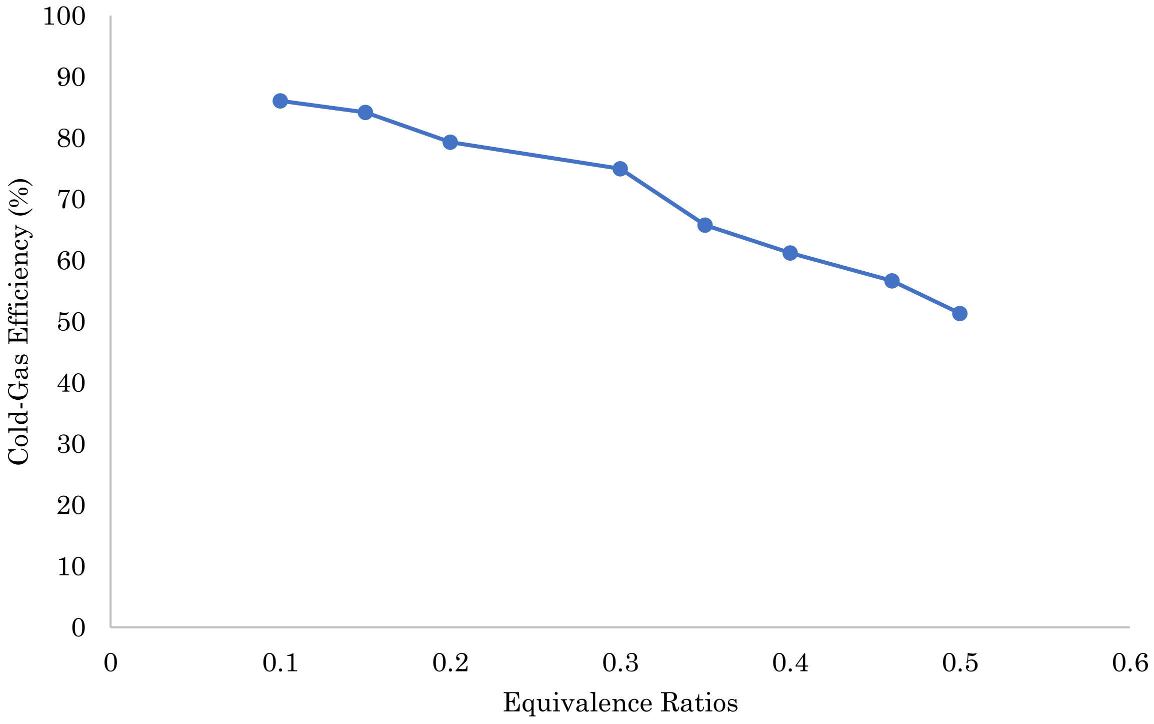

Figure 5.20: Efficiency of Syngas Production for RDF3

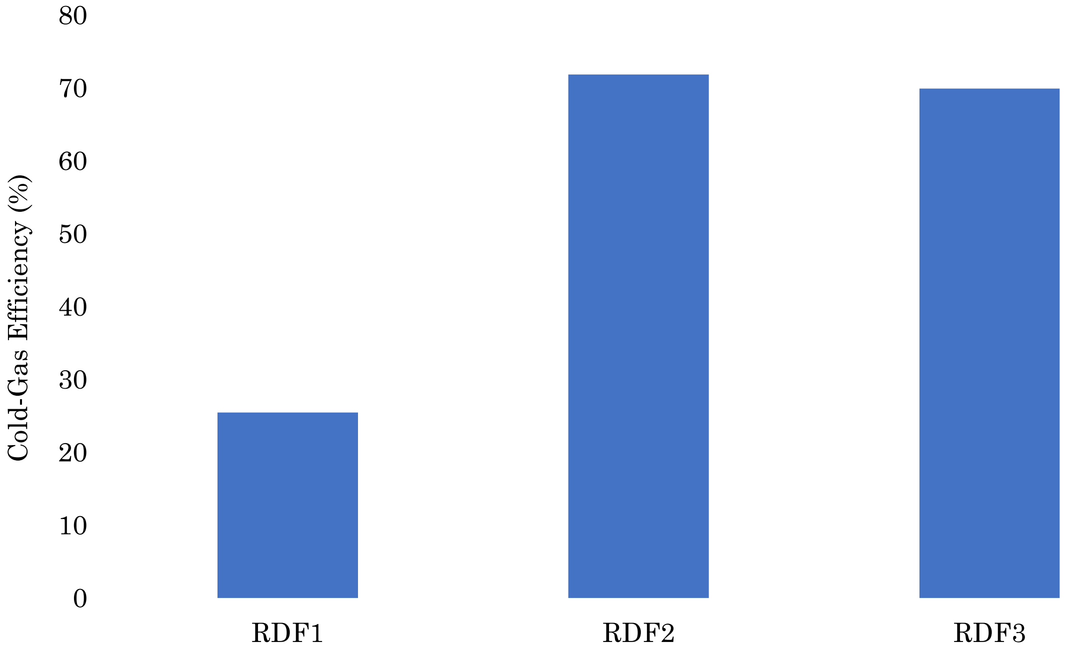

Figure 5.21: Efficiency of Syngas Production for RDF1, RDF2 and RDF3

These results were consistent with the RDF2 trend of results although their proximate and ultimate data were not similar. Furthermore, as discussed earlier, it might be the net effects of WGS and the consumption of CO_2 in the Boudouard reaction at a high temperature.

At ER values of 0.10, 0.10, 0.10, 0.10, 0.12 and 0.04, the simulation runs also gave highest hydrogen concentrations as follows: 0.864, 0.987 1.054 1.099, 1.2227 and 1.334 Kmole for RDF3 at SFRs 3.1, 4.2, 4.8, 5.2, 6.3 and 7.3 respectively. The mixture of H_2 and CO could not sufficiently meet up to the required yield of H_2/CO molar ratio for the application of a fuel cell system because of CO poisoning the fuel cell. It was observed at a low ER and high SFR that the model could produce the same molar concentration, $H_2/CO \sim 1.00$, which was not desirable for application in a fuel cell. Cold gas efficiency was obtained for RDF3 to complement the performance of the gasification of the RDF. The cold gas efficiency of RDF2 was presented in Figure 5.20 while Figure 21 presented averages of the cold gas efficiencies of RDF1, RDF2 and RDF3 respectively. The cold efficiency obtained for RDF3 gasification simulation was in between 51 % - 86 % as shown in Figure 5.20.

However, RDF3 gasification simulation produced the highest molar quantities of hydrogen in the syngas mixture compared to RDF1 and RDF2. The RDF3 gasification model produced a molar ratio of 20.16 of H_2/CO for ER value of 0.08 and a SFR value of 3.30.

The corresponding value of hydrogen mass flow rate in the mixture was 1.288 Kg/hr. At a SFR value of 3.50 and a 0.10 ER value, a higher value mass flow rate of hydrogen (1.334 Kg) was obtained but the corresponding H_2/CO molar ratio was 17.5 which was lower than the one obtained with less CO syngas mixture. The trend of results demonstrated the influence and dependence of ER values on desired product and co-products. This is supported by the work of (Couto et al., 2015). The molar ratios were very consistent with the focus of the study which is to produce a high hydrogen concentration in a syngas mixture for application in a fuel cell system.

5.4.3 Effects of Steam Solid Fuel Ratios

The effect of a steam solid fuel ratio on the RDFs gasification process was also studied in the range of 1.00 to 3.90 (corresponding to steam flow rates of 2.10 to 8.20) with 5 Kg/hr for RDF1 and 10Kg/hr for RDF2 and RDF3 feed rates respectively. Usually, during gasification reactions, steam can contribute to oxidation reactions.

The oxidation reactions would dominate the resulting increased temperatures. A significant contribution could be more relevant at a high temperature during the cracking of tar and secondary tar, particularly spark pyrolysis, that leads to reforming the reaction at that high temperature. A minimum production of tar during the last stage of combustion in the gasification process was probably another indication of the influence of steam that enhances more hydrogen production.

The following figures (Figure 5.14 to Figure 5.19) demonstrate the variation of the product stream molar composition as it varied and influenced the production of hydrogen in the syngas mixture. Similar characteristics were reported by the studies (Chaudhari et al., 2003),(Wu and Williams, 2010b, Zhang et al., 2012).

The SFR contributed immensely to the generation of the high hydrogen concentration in the syngas mixture as discussed earlier in the previous sections. The gasification of RDFs revealed that SFR values, 2.85, 2.80 and 3.30, produced good H_2/CO molar ratio for ERs, 0.04 and 0.15 (Table 5.5) while the SFR values more or less do not yield the required H_2/CO molar ratio. The illustration of RDF1 products in Figure 5.22 shows that the molar content of steam in product distribution presents a unique U-curve which shows the counter-effect of ER. On the contrary, the RDF2 and RDF3 presented different patterns in the molar quantity of steam in the product distribution which increased uniformly with the ER values.

The steam in the product stream mixture was a result of the unreacted steam entering and exiting the reactor. As expected, the temperature of the reactor remains constant at around 1123 K, possibly balanced by the complicated endothermic and exothermic gasification reactions. The SFR contributed to the RDF2 and RDF3 gasification products especially in the production of a good yield of H_2/CO molar ratios for both RDF2 and RDF3.

The steam injection contributed largely to the quality of hydrogen, shown by the molar ratio of H_2/CO in the gaseous product during the gasification. The following figures show various molar concentrations of hydrogen, carbon monoxide and other co-products.

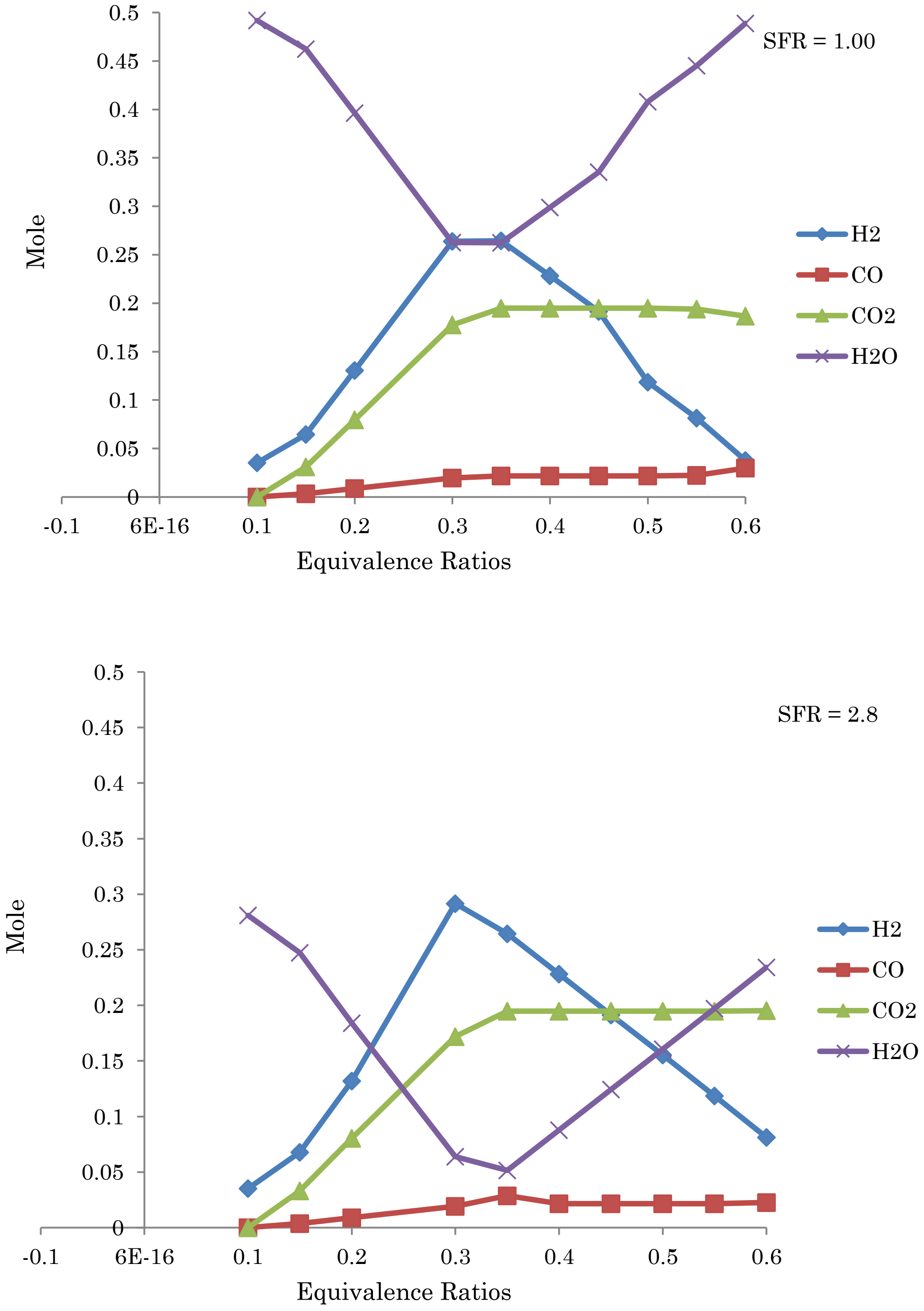

Figure 5.22: Molar Distribution of Desired Products and Steam (RDF1)

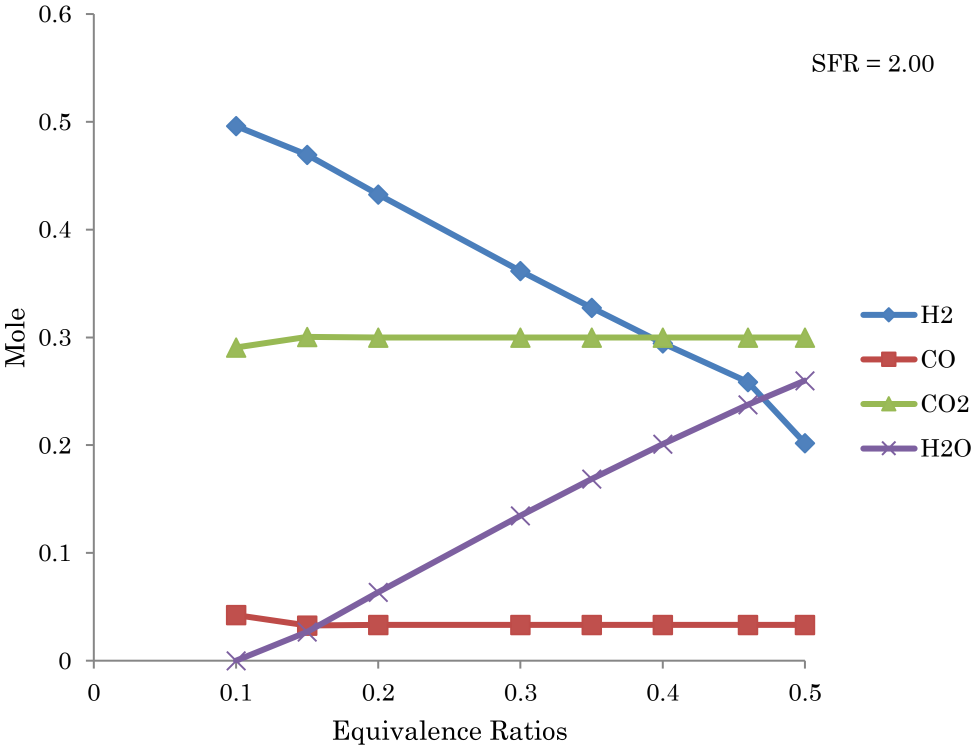

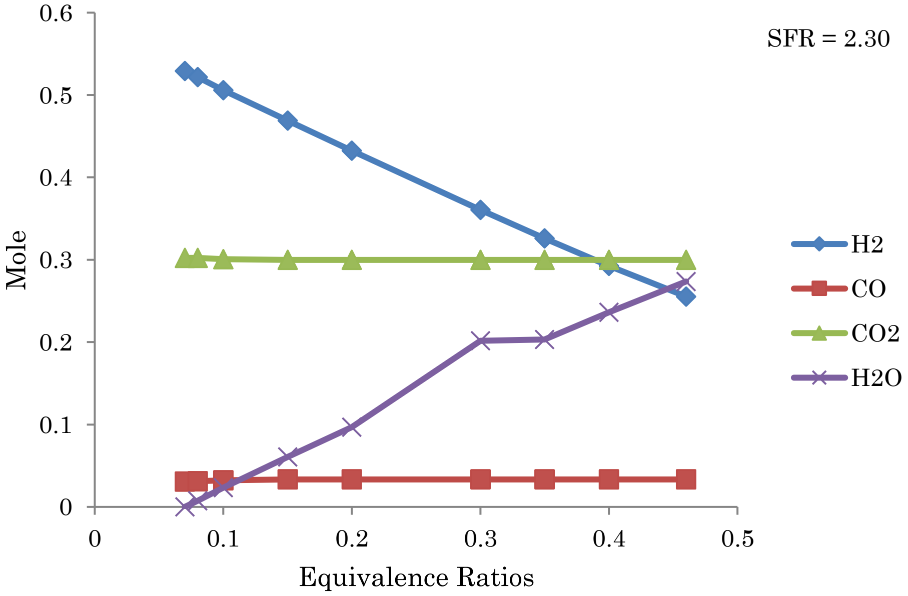

Figure 5.23: Molar Distribution of Desired Products and Steam (RDF2)

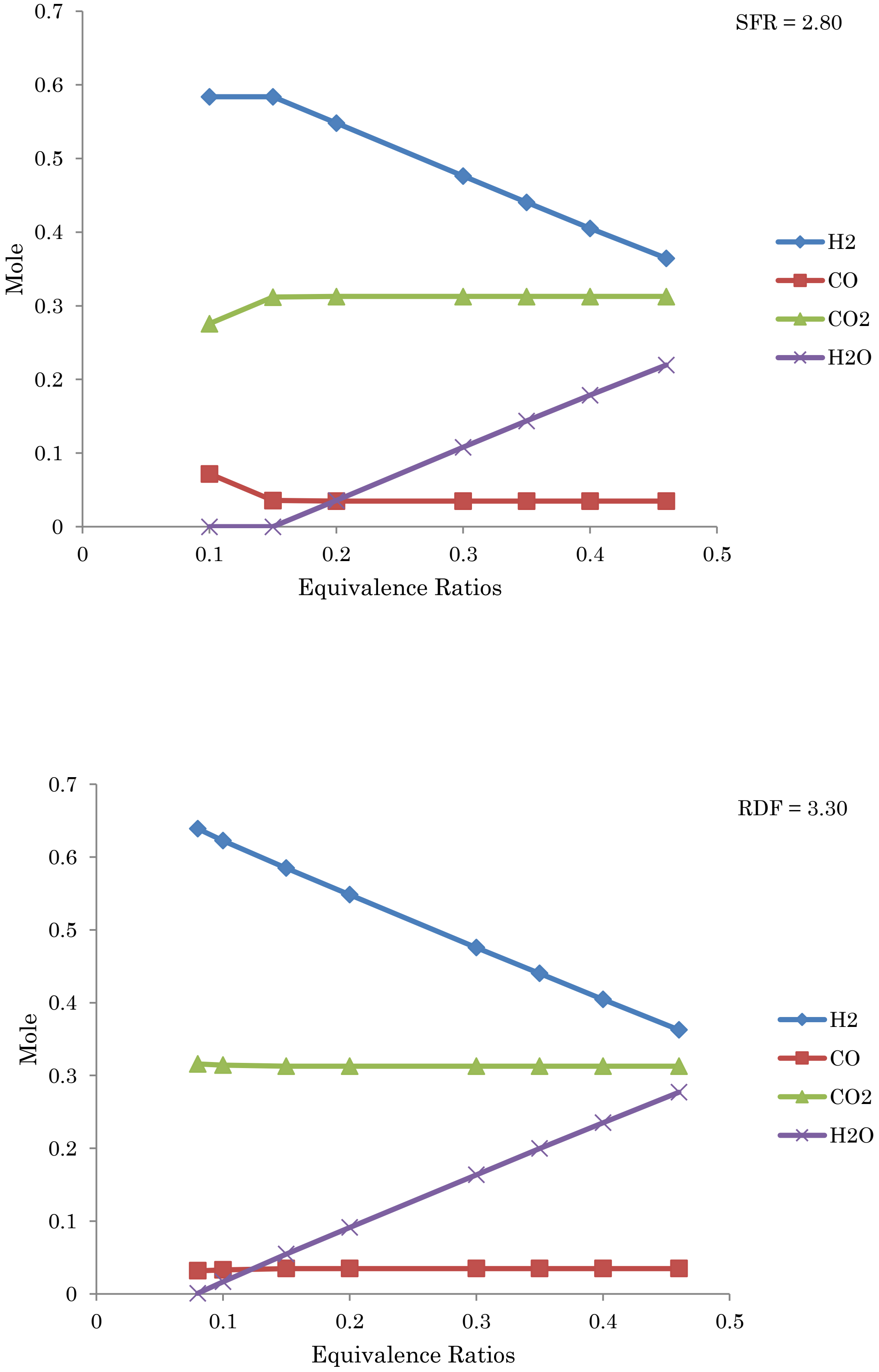

Figure 5.24: Molar Distribution of Desired Products and Steam (RDF3)

5.4.4 Effects of the Qualities of RDF

It has been emphasised all along that the main goal of this study is to carry out gasification simulation to obtain hydrogen-rich syngas for fuel cells. In this last part of the chapter, the effects of ER, SFR, H_2/CO are compared with the response from RDF1, RDF2 and RDF3 (Figures 5.251 to 5.27) respectively.

The combination steam flow rate (SFR) and equivalence ratios (ER) contribute to the high molar ratio of H_2/CO in the products stream for RDFs. The effects of the Boudouard reaction, tar cracking, tar reforming and influence of downdraft reaction schemes contributed to the yield obtained. The WGS reactor converted significant amounts of CO to hydrogen. This favoured a substantial yield of H_2/CO in the product stream.

Figure 5.25 for RDF1 shows the molar ratio of H_2/CO in the product stream between a peak of 18.12 and 18.82 with low values between 1.27 and 3.62. This was a wide margin showing the impact of SFR and ER on the molar ratio of H_2/CO. However, the RDF2 and RDF3 (these RDFs were prepared for this study) showed an entirely different curve. The curve further demonstrated how a combination of SFR and ER affected the distribution of H_2/CO in the product streams. Also, for RDF2 and RDF3, the molar ratio of H_2/CO in the product stream shows peaks for RDF2 (11.97 and 18.13) and RDF3 (12.49 and 20.16) with low values between (2.39 and 6.06) and (1.31 and 10.42) respectively. This was another wide margin demonstrating the impact of SFR and ER on the molar ratio of H_2/CO. With a higher steam supply, the oxidation of CO would be favoured, resulting in a steady increase of carbon dioxide during the gasification process. The quality of syngas was presented in Figure 28 and Figure 29 respectively. The ratio of hydrogen to carbon monoxide is an essential indication for good performance in fuel cell applications. The Figure 28 showed that RDF2 and RDF3 produced higher mole of hydrogen in syngas. The high content of hydrogen was responsible for high HHV of the syngas mixture produced from RDF2 and RDF3 gasification simulations. Similar trend was observed for efficiencies of the gasification as mention earlier in sections 5.4.2.2 and 5.4.2.3 and presented in Figure 5.13 Figure 5.20 and Figure 5.21 respectively.

Besides the high molar ratio of H_2/CO produced with the contribution of steam in the gasification reactions, this ratio was increased further during the water-gas shift reaction system for the removal of CO.

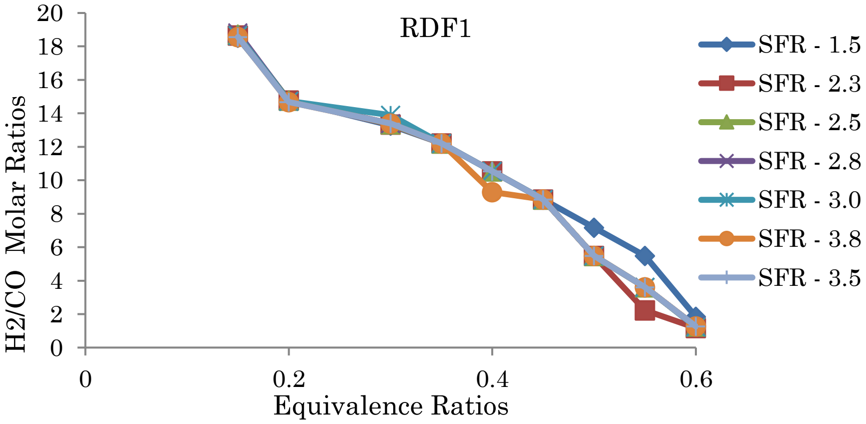

Figure 5.25: H_2/CO Molar Ratio Distribution from RDF1 Gasification

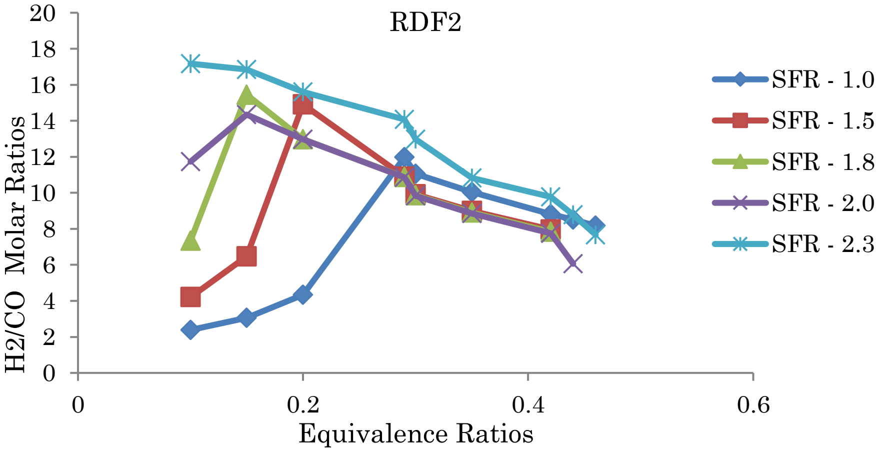

Figure 5.26: H_2/CO Molar Ratio Distribution from RDF2 Gasification

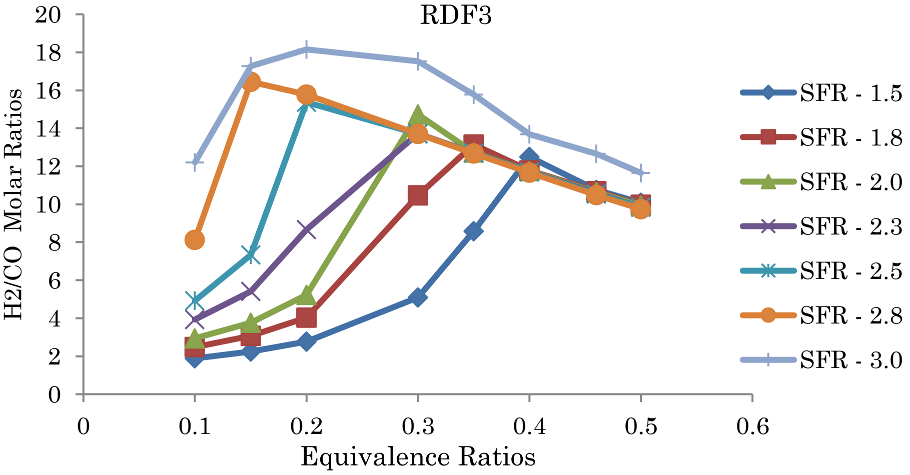

Figure 5.27: H_2/CO Molar Ratio Distribution from RDF3 Gasification

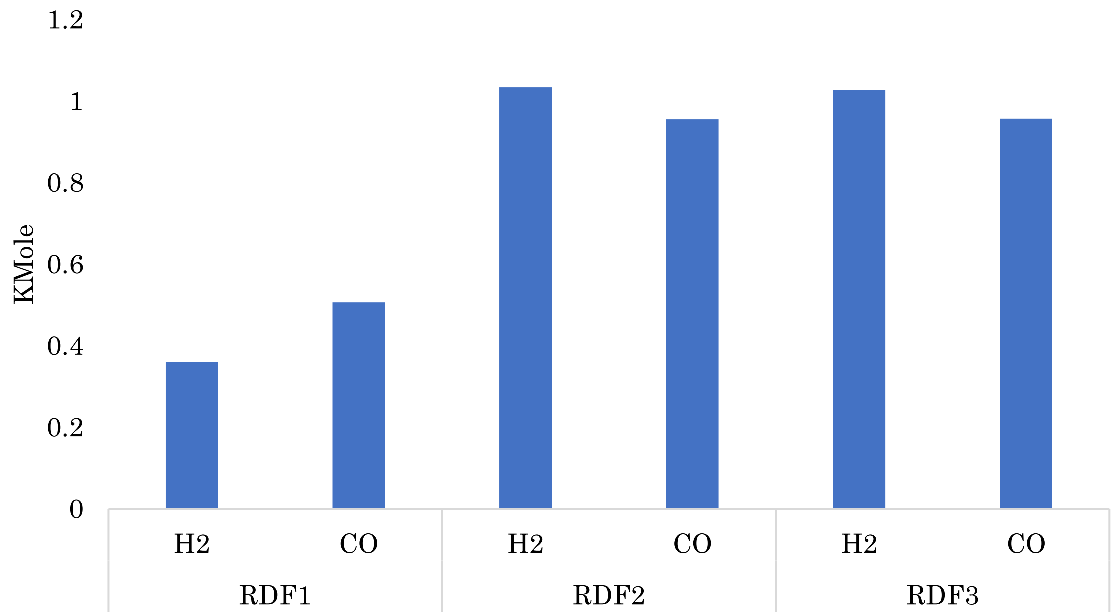

Figure 5.28: Molar Quality of Syngas Production for RDF1, RDF2 and RDF3

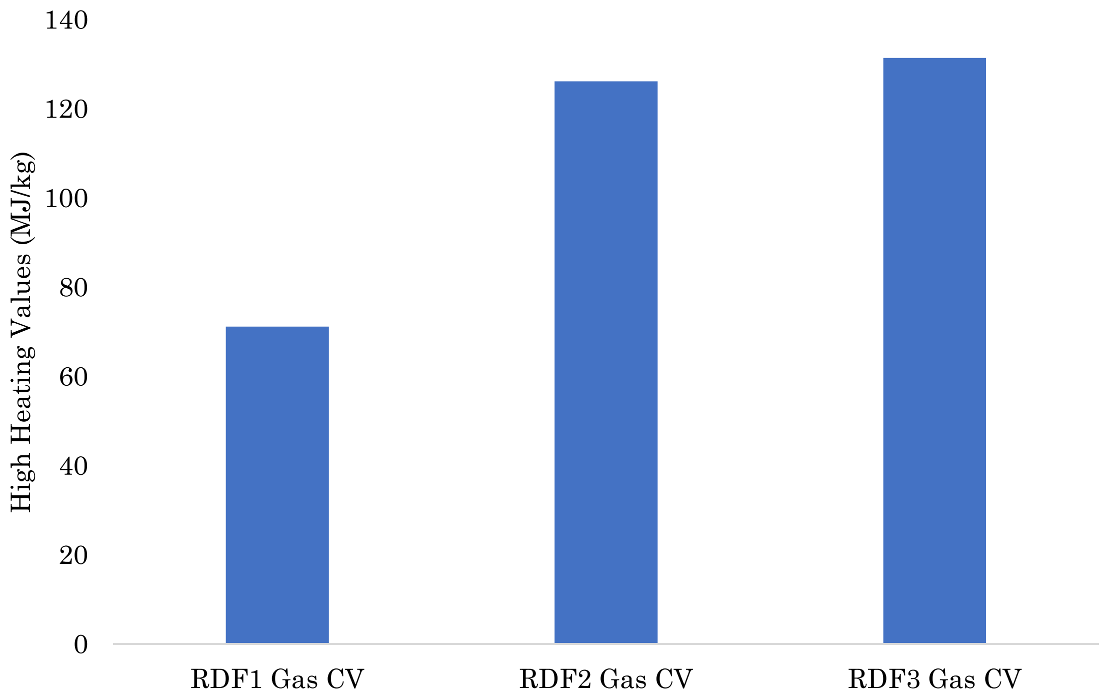

Figure 5.29: High heat Values of Syngas Production for RDF1, RDF2 and RDF3

5.5 Chapter Summary

The gasification process simulation of RDF1, RDF2 and RDF3 were carried out using a combination of various unit operation modules available in the Aspen Plus Model simulation package. The gasifier used in the modelling to investigate the gasification reactions of the RDF gasification in an air-blown downdraft gasifier because of its specific characteristics. The model developed enabled one to predict the feasibility of the behaviour of the gasification of RDFs under various operating parameters in an air-blown downdraft gasifier. Although temperature contributed a vital role in controlling the conversion and product composition, it was kept constant for the gasifier unit in the modelling (Table 5.3). Other parameters were varied to achieve the desired syngas mixture.

The molar product distributions of H_2, CO, and CO_2 were the result of rigorous and competing for simultaneous gasification reactions mainly controlled by the ER and the SFR at a fixed gasifier temperature. High temperature produces a higher hydrogen concentration in syngas (H_2 and CO) and this higher temperature promotes thermal cracking reactions (equation 3.12), steam-reforming reaction (equation 3.11), secondary cracking of tar (equation 3.10) and the Boudouard reaction (equation 3.8), the main reactions that promote higher H_2/CO molar concentration ratios.

Moreover, carbon dioxide capture in the processes and boudouard reactions in gasification prevent the uncontrollable release of these dangerous compounds which reduce the cost of making separating unit for treating those harmful emissions. Thus, the significant reduction in the formation of furans, dioxins and consumption of CO_2 during boudouard reactions may be instrumental to cost savings, sustainable MSW management and the potential of an environment-friendly atmosphere.

The effects of the ERs and the SFRs on the gasification were modelled in the range of 0.02 to 0.60 and 1.00 to 3.90 respectively. Based on the model results, the effects of ER, SFR and the quality of RDFs on the gasification's simulation process are responsible for the high molar ratios of H_2/CO.

The model results were summarised. The optimum SFR values for RDF1, RDF2 and RDF3 were determined to be between 2.8, 2.5 and 3.5 respectively and the optimum ER values for RDF1, RDF2 and RDF3 were also determined to be between 0.15, 0.04 and 0.08 at a fixed gasifier temperature respectively. Under these conditions for all RDFs, the molar ratio of H_2/CO yield in syngas mixture in the product stream reached a maximum. Due to the lack of detailed experimental data on Cape Town's MSW gasification for various process conditions, the data results could not be validated.

The RDF1 gasification Aspen model produced 18.81 of H2/CO molar ratio for the ER value of 0.15 and the SFR value of 2.80; RDF2 produced 18.12 of H_2/CO molar ratio for the ER value of 0.04 and the SFR value of 2.50; and RDF3 produced the highest molar quantities of hydrogen in the syngas mixture compared to RDF1 and RDF2. The H_2/CO concentration molar ratios of Galvagno *et al.* (2006) (2.39 - 3.80), He *et al.* (2009a) (2.89 - 3.15) and Skoulou et al. (2008b) (1.7) are lower than the simulation results for this study. The main factors for those studies were temperature and catalysts but this study considered ER and SFR specifically because of their influence on various reactions in the gasifier.

The RDF3 gasification Aspen model produced 20.16 of H_2/CO molar ratio for the ER value of 0.08 and the SFR value of 3.30. In addition to this, the efficiency of the simulation gasification was around 71 %. This value can satisfy the requirements of the fuel cell application. The trend of results showed the influence and dependence of the ER and the

SFR values on the desired product and co-products. The focus of this study is to produce a high hydrogen concentration in a syngas mixture for fuel cell system application.

In the next chapter, the results of heavy metal distributions in the pre-treated MSW will be presented and evaluated for the possible environmental impacts and possible effects on gasification processes.

CHAPTER SIX

6 QUANTIFICATIONS OF HEAVY METALS IN MSW

6.1 Heavy Metals Quantification in MSW

In this chapter, quantifications of heavy metals and possible thermochemical implications are discussed. The results of the concentration of heavy metal in pre-treated MSW will be presented and discussed. The theoretical spatial distribution of model heavy metal in bottom ash residues was obtained by using the model used by the studies of Belevi and Moench (2000) and Yao *et al.* (2010). This model was used to quantify any possible heavy metal in bottom ash residue.

6.2 Results and Discussion

The heavy metal concentration in pre-treated MSW measurement was considered to evaluate the environmental possible theoretical implications after model thermochemical conversion. This was necessary in preparation of mitigation procedures as a result of corrosion and emissions that may be exposed to the environment after the disposal of residues containing heavy metals with regard to the thermochemical conversion process residues and its disposal. In this study, non-combustible components were separated to remove all ferrous and non-ferrous metals, glass, inert, and rubbles.

However, some trace amounts of heavy metals are still associated with combustible components of MSW particularly trace amount of heavy metals in organic salts and organic substance additives. Heavy metal found in MSW have fundamental implications to produce fly and bottom ash and their disposals. They might also be responsible for fouling effects, corrosion and pollutant emissions during gasification reactions.

Some heavy metals (Fe, Ni and V) may promote some reactions during thermochemical processes. The quantity of heavy metal in pre-treated MSW and predictive heavy metals in bottom ash and fly ash are presented.

6.2.2 Heavy Metal in Pre-treated MSW

The overall concentrations of the heavy metals in pre-treated MSW obtained from the municipal solid waste disposal facilities (MSWDF) in Cape Town were summarily presented in Table 6.1 and Figure 6.1. Al and Fe concentrations data from MSW were the highest for obvious reasons and like the range usually obtained in most soil samples. Al is non-ferrous metal with a very significant concentration in raw MSW. This concentration is like Al profile in soil and could be a reasonable resource recovery for Al likewise Fe (Belevi and Moench, 2000, Allegrini et al., 2014, Sekito et al., 2014). Both concentrations showed a wide range of high concentration of heavy metals which were very significant for MSW. These concentrations may not affect gasification processes but contribute to the baseline earth natural heavy metal concentrations which might be the point of concern (see Figure 6.1).

Table 6.1: Concentrations Distribution of Heavy Metals in Pre-treated MSW in Cape Town

Heavy Metals	Concentrations Range (mg/Kg)	Mean Concentrations (mg/Kg)	Standard Deviation
Al	593.44 -13508.10	5220.651	3403.408
Ti	59.54 - 149.70	94.955	24.784
V	2.68 - 98.70	12.981	23.799
Cr	66.44 - 312.60	171.694	69.576
Mn	57.96 - 199.10	109.169	38.603
Fe	788.01 - 10230.40	4978.294	2731.064
Co	6.12 - 100.00	26.743	21.764
Ni	27.03 - 122.50	72.727	27.406
Cu	15.81 - 134.40	50.563	33.588
Zn	67.76 - 316.10	156.154	62.249
As	2.23 - 103.50	12.616	25.490
Se	0.33 - 93.70	7.068	23.982
Mo	2.78 - 100.20	10.754	24.807
Cd	0.13 - 96.30	7.720	24.779
Sb	0.18 - 3.00	1.390	0.799
Ba	37.97 - 159.80	74.264	35.630
Hg	0.04 - 105.30	7.173	27.151
Pb	9.41 - 97.50	35.256	26.811

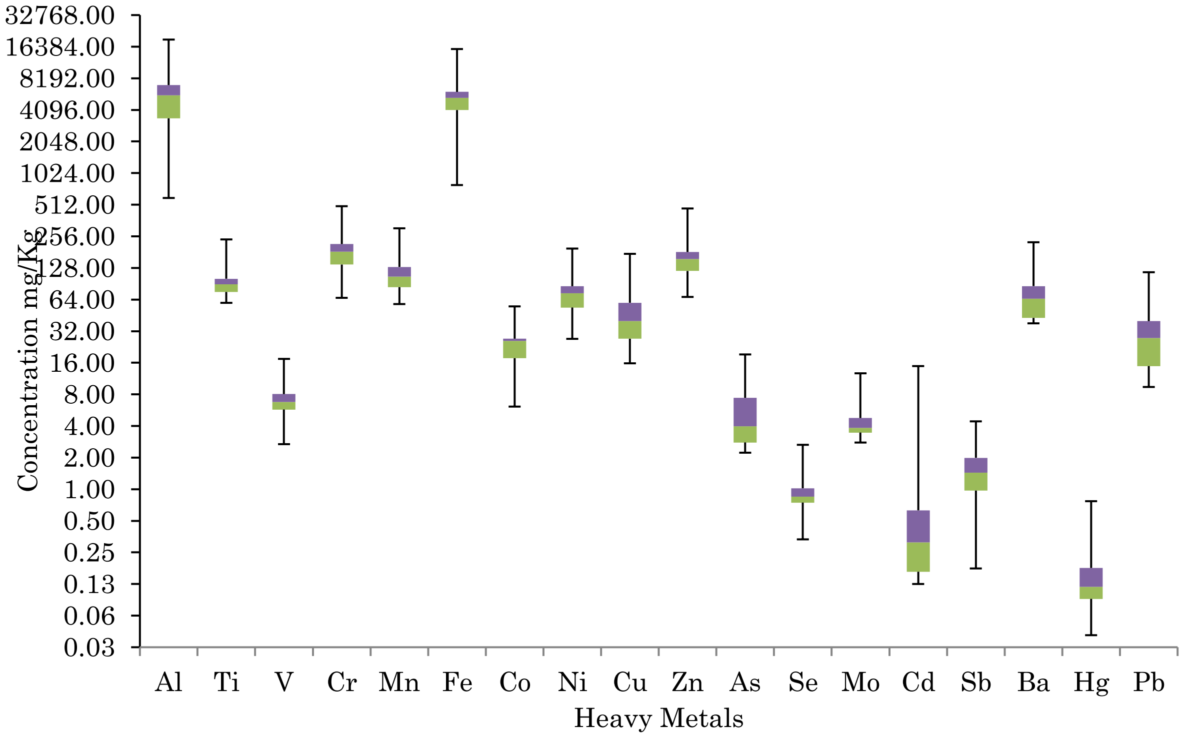

Figure 6.1: Log Plot Distributions of Heavy Metals Concentrations in Pre-treated MSW from MSWDF in Cape Town

Both Al and Fe concentrations in the pre-treated MSW were very relatively high compared to other heavy metals as shown in Figure 6.1 but may not lead to any challenges during thermochemical processes except at certain high temperatures. Disposal of both heavy metals may not pose any threat even thermochemical processes but Fe contributes to the nutrient value of the soil (Wuana and Okieimen, 2011) or possible recovery potentials. The concentrations of both Al and Fe are presented in Figure 6.2 with CP and ATR showing highest and lowest values respectively.

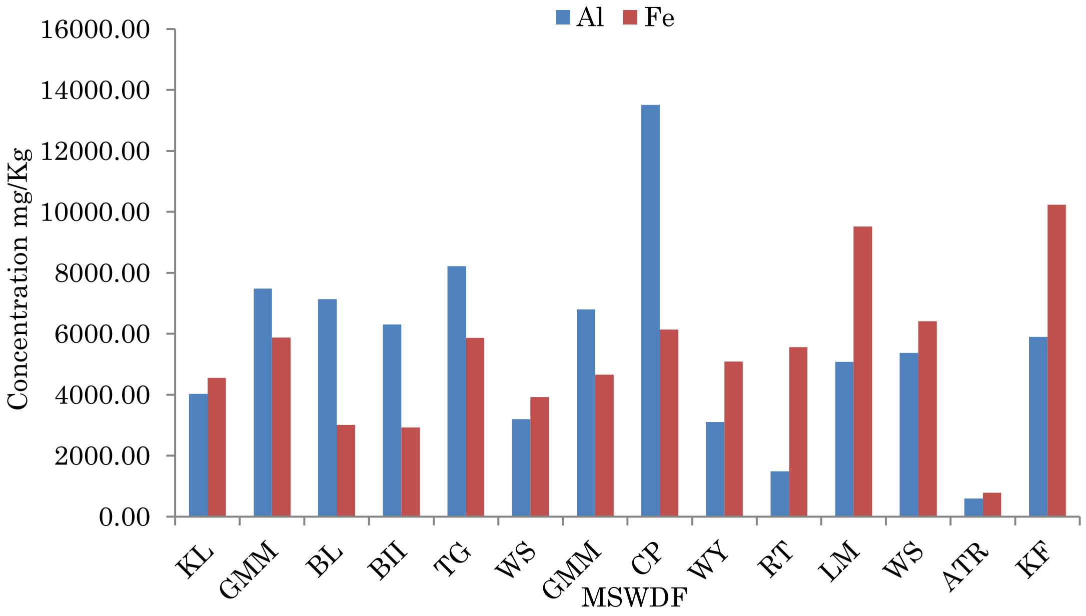

Figure 6.2: Al and Fe Concentrations in Pre-treated MSW from MSWDF in Cape Town.

Zn and Cu were prominent and found in high concentrations across all the MSWDF in Cape Town as shown in Figure 6.3. These two heavy metals are also ranked highly hazardous according to this study (Vodyanitskii, 2016). These high concentrations of Cu and Zn (134.40 mg/Kg and 316.10 mg/Kg) exceeding the standard limit. Zn had a strong link with coal and solid waste combustion and may be leaked to the atmosphere (Wuana and Okieimen, 2011). Both heavy metals have biological relevance but in certain concentration, they become toxic and hazard to plants and human (Tóth et al., 2016).

The following heavy metals (Pb, Mo, As, V and Co) concentrations around below 100 mg/Kg as presented in Figure 6.4 though their environmental impacts may not be similar. The grouping was only on the weight of all the heavy metals around 100 mg/Kg. However, according to the previous classification of highly hazardous heavy metals, it included Pb and As. Both Pb and As are also from anthropogenic sources and some serious health concerns are linked to both heavy metals (Singh and Kalamdhad, 2011, Tóth et al., 2016).

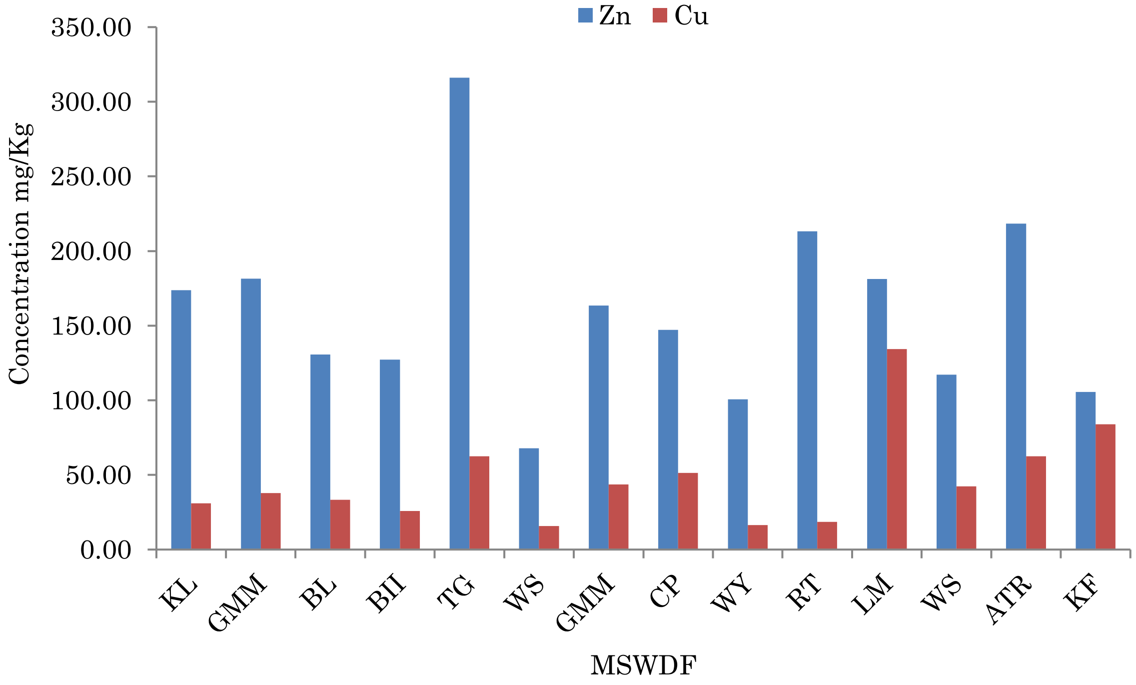

Figure 6.3: Zn and Cu Concentrations in Pre-treated MSW from MSWDF in Cape Town.

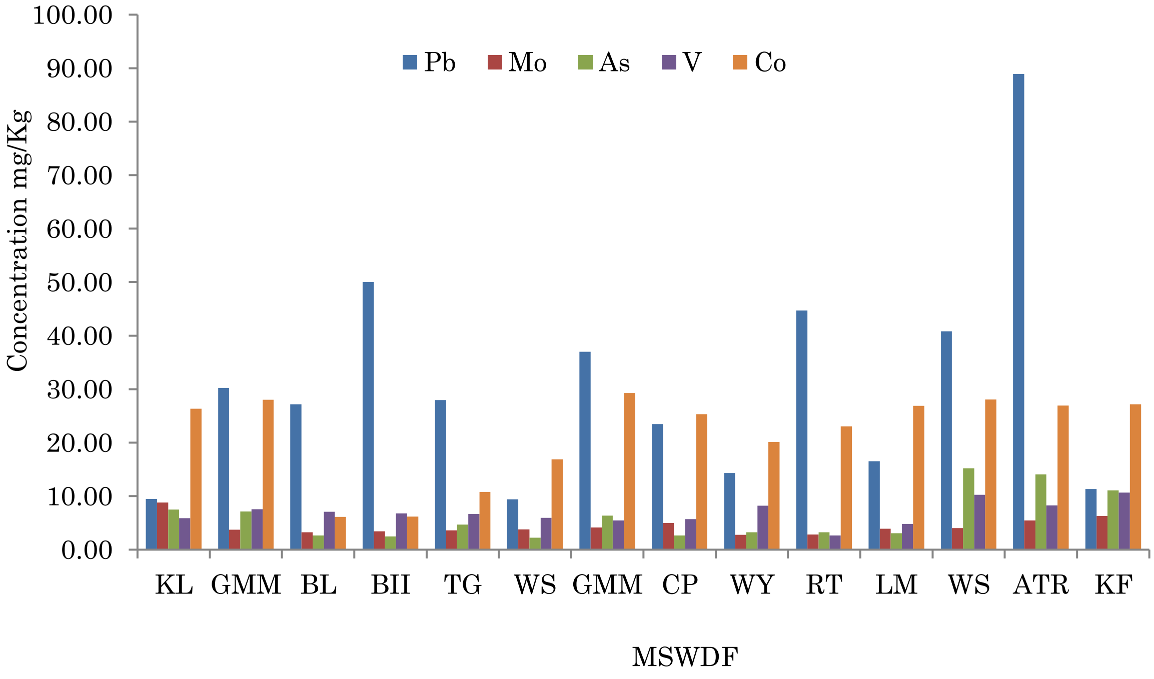

Figure 6.4: Pb, Mo, As, V and Co Concentrations in Pre-treated MSW from MSWDF in Cape Town.

The Pb concentration obtained in this study is less than the value of Pb obtained from compost (material recovery approach) made from MSW (Sharifi and Renella, 2015). The concentration of As of this study was slightly higher than that of the standard presented in this study (Tóth et al., 2016). Both metals are very important because of hazardous potential. These heavy metals (Ti, Ni, Mn, and Ba) concentrations (149.70 mg/Kg, 122.50 mg/Kg, 199.10 mg/Kg and 159.80 mg/Kg) were below 200 mg/Kg as presented in Figure 6.5 though their environmental impacts may not be the same. Similarly, the grouping was only on the weight of all the heavy metals around 200 mg/Kg. Most of the heavy metals in this category do not have serious health concerns except Ni. Nonetheless, the Ni concertation (122.50 mg/Kg) obtained from KF was lower than the value from this study (Tóth et al., 2016) and higher than this study (Sharifi and Renella, 2015). The Ti, Mn, and Ba concentrations are also relevant, but Ba value was within the standard prescribed by this author (Vodyanitskii, 2016). In addition, these heavy metals (Se, Cd, Sb, and Hg) concentrations (93.70 mg/Kg, 96.30 mg/Kg, 3 mg/Kg and 105.30 mg/Kg) were around 100 mg/Kg except Sb though their environmental concerns may not be of the same threat. Similarly, the grouping was only on the weight of all the heavy metals around 200 mg/Kg. According to the classification of Vodyanitskii (2016) Cd is classified among other heavy metals (As, Hg, Se, Pb, Zn and Cu) as highly hazardous heavy metals. The Cd values obtained from CP may be associated with nature of the disposal facility. The Cd concentration was noticed to have had the widest range of concentrations as shown in Figure 6.1, but this concentration affects only one facility having an extremely high concentration of Cd compared to the others. This high Cd concentration might be contamination from batteries, fertilizer, PVC, and detergents disposals from households (Tóth et al., 2016, Wuana and Okieimen, 2011, Singh and Kalamdhad, 2011).

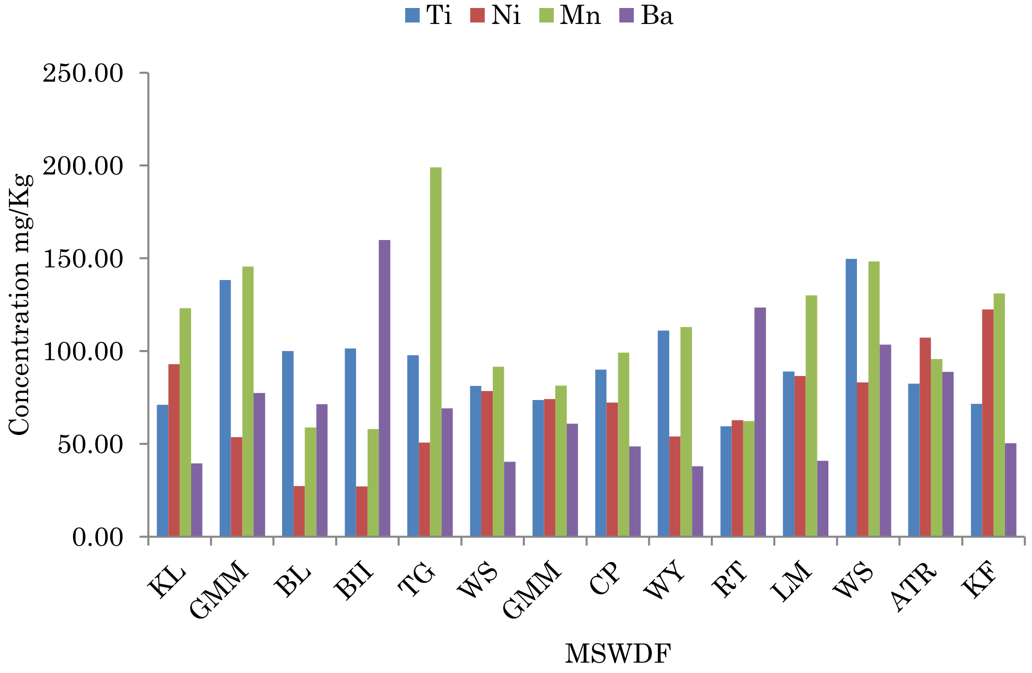

Figure 6.5: Ti, Ni, Mn, and Ba Concentrations in Pre-treated MSW from MSWDF in Cape Town.

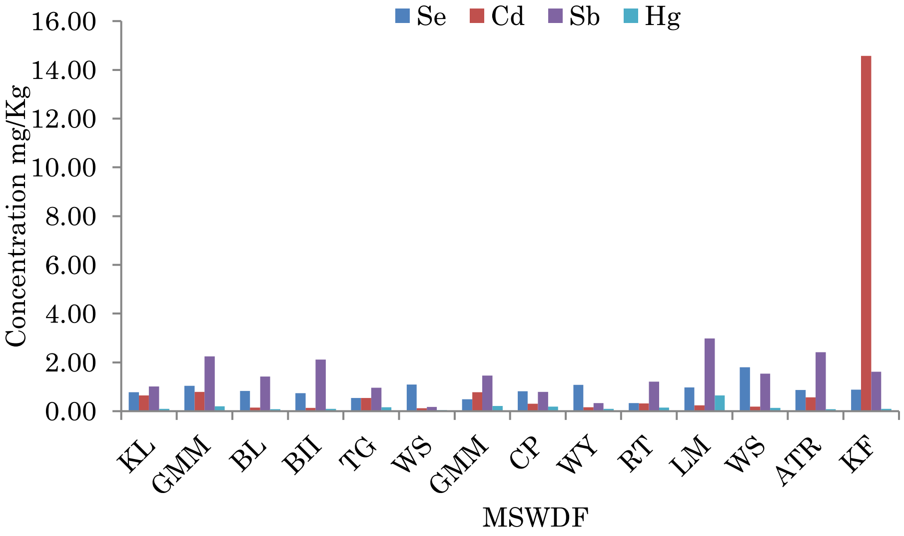

Figure 6.6: Se, Cd, Sb, and Hg Concentrations in Pre-treated MSW from MSWDF in Cape Town.

The Cd concentration exceeded the standards presented by these authors (Smith, 2009, Tóth et al., 2016). It easily binds strongly with soils organic matters (Balkhair and Ashraf, 2016), thus finds its. The concentration of Cd in MSW could find a way to the food chain and environment. The concentrations of Se, Sb and Hg were considered but more emphasise was put on Hg because of various health problems such as a threat to kidney, liver and reproductive system (Tóth et al., 2016). However, the study of Vodyanitskii (2016) presented a different degree of hazardous degree of heavy metal ranking Se as the highest heavy metal of critical concern.

The average concentrations of heavy metal for pre-treated MSW samples were in the following order of concentrations: Al > Fe > Cr > Zn > Mn > Ti >Ba > Ni > Cu > Pb > Co > V > As > Mo > Sb > Cd > Se > Hg. These concentrations are unlike the study of Haiying *et al.* (2010) who reported that the order of heavy metals from an MSW incineration plant showed that the content of heavy metals follows the sequence of Zn > Pb > Cu > Cr > As > Ni > Cd. Also, the study of presented another order of heavy metals: Cr > Zn > Ni > Cd > Mn > Pb > Cu > Fe as environmental health concerned though the order of this study was based on increase order in concentrations of heavy metals in pre-treated MSW.

The highest concentration of heavy metals were Al, Fe, Zn and Cr, which were 13508.10 mg/Kg (CP), 10230.40 mg/Kg (KF), 316.14 mg/Kg (TG) and 312.60 mg/Kg (KF) respectively. As discussed Al and Fe may not be of serious environmental concerns, but Zn and Cr should be noted. These heavy metal quantifications are shown in Table 6.1 while the other remaining quantifications of heavy metals are presented in Figures 6.1 to 6.6.

A relatively high standard of deviation was observed among all the heavy metal content of pre-treated MSW except for Sb as shown Figure 6.1 and Figure 6.6, while Al and Fe (Figures 6.2 and 6.6) were unusually high compared to other heavy metals as observed earlier for apparent reason. This might be due to the heterogeneous distribution of the heavy metals in all the sampling locations.

The heavy metal concentrations from the pre-treated MSW were compared with that of the soil. The concentrations of heavy metals obtained were well below that recommended for residential, industrial and commercial locations in China (Yao *et al.*, 2010). The results indicated that the average values of all the heavy metals from all the pre-treated MSW were within the standard limits (USEPA, 1993). However, the useful application of the possible recovery of these heavy metals may be considered, depending on the quantity of MSW, among other factors.

6.2.3 Heavy Metals in Bottom Ash

The results obtained for predictive quantification of heavy metals in bottom ash residue through model was presented in Table 6.2 above. Using the coefficient of the transfer method from the studies of Belevi and Moench (2000) and Yao *et al.* (2010), the quantity of heavy metal obtained had substantially decreased and been transferred to bottom ash (Tables 6.2 - 6.3). Lithophilic characteristics made some heavy metals (Al, Cr, Cu and Fe) remain in bottom ash. All the heavy metal has a significant presence in the bottom ash except Sb and Hg. This is similar to previous studies mentioned early in the discussion. The result presented in Table 6.2 is substantially lower than that of Yao e*t al.* (2010) and Jung et al. (2004) for a set of heavy metal except for Co, Mo and Ni. Heterogeneity of the raw MSW was expected to be the main factor for this wide difference in concentration. The heterogeneous characteristics were reflected with a high concentration of some heavy metal such as Cr, Cu, Mn and Zn

Table 6.2: Calculated Heavy Metals Concentrations in Bottom Ash Residue

Heavy Metals (HM)	HMC_{BAIJ} Min (mg/Kg)	HMC_{BAIJ} Max (mg/Kg)	HMC_{BAIJ} Average (mg/Kg)
Al	1890.106	43023.29	16627.77
Ti	183.3932	460.9264	292.4624
V	-	-	-
Cr	218.5813	1028.547	564.8735
Mn	188.6588	648.0553	355.3447
Fe	2727.698	35412.6	17232.37
Co	18.85146	307.9555	82.3698
Ni	90.82455	411.6455	244.36
Cu	53.11093	451.5965	169.8929
Zn	101.9803	475.789	235.0111
As	5.922989	275.2099	33.55791
Se	-	-	-
Mo	8.370719	301.7468	32.36865
Cd	0.043768	33.70738	2.70181
Sb	0.073834	1.254428	0.583633
B	118.2868	497.9187	231.3325
Hg	0.002848	7.372194	0.502091
Pb	14.48866	150.0975	54.29484

Table 6.3: Heavy Metals Concentrations in Bottom Ash from the Literature (Jung *et al.*, 2004)

Heavy Metals (HM)	HMC_{BAIJ} Min (mg/Kg)	HMC_{BAIJ} Max (mg/Kg)	HMC_{BAIJ} Average (mg/Kg)
Al	10600	147000	71377
	43420	68060	54675
Cr	6.6	2260	375
	60	256	112
Fe	500	200000	45874
	22000	86800	44421
Sn	53	1364	359
Cu	77	13200	2818
	414	3720	2081
Zn	500	33000	4229
	1280	4800	2446
As	0	93	6
	0.1	3.5	1.3
Se	0.1	2	0.6
	0.5	4.5	2
Cd	0.04	91	15
	0.8	14	5.5
Sb	5	306	67
	37	192	98
Hg	0.001	5.5	0.7
Pb	8	10900	1288
	140	1320	673

The high transfer coefficients indicate the heavy metals are mainly transferred to the bottom ash. Though Hg has a potential environmental health risk, the amount is expected to be below the required standard for emissions because most of Hg remained in the bottom ash. Also, some bottom ash heavy metals (Cd, Cu, Pb, and Zn) are regarded as relatively unstable, thus it will be crucial to conduct further studies for the recovery and reuse of the heavy metals to avoid contamination of the immediate ecosystem and bio-toxicity.

6.3 Chapter Summary

The accumulation of the high concentrations of some heavy metals out of 18 species of heavy metals in bottom ash residue from thermochemical conversion could be a good remedy for the control of heavy metals. Most active heavy metals have been considered in the basic quantification of heavy metals in samples of MSW under consideration. Some heavy metals (Fe, Ni and V) actively promote boudouard reaction and they facilitate production of syngas. These heavy metals (Pb, Zn and Hg) emissions were technically monitored and controlled from escaping into the atmosphere and prevented from their consequential secondary environmental and health implications. The gasification technology prevents the uncontrolled emission of the heavy metals from open-air incinerations and the like. This study pre-treated all the samples of MSW used for heavy metal quantification and it was shown that the from the theoretical modelling that concentrations of heavy metals found in all the samples was much less than all those obtained from thermochemical processes containing unsorted MSW that had not been properly pre-treated. If the raw MSW or the bottom ashes residue without pre-treatment are not disposed of properly there will be grievous environmental implications to the whole eco system and health implications on humans.

However, before disposal or reuse of the bottom ash residue, the residue will require further study of its potential environmental impact. This will be helpful for crucial considerations for policy and by decision making about heavy metals mobility in MSW thermochemical conversion technology from cradle-to-grave.

CHAPTER SEVEN

7 ECONOMIC EVALUATION ANALYSIS

7.1 The Economic Evaluation of the System

The modelling and simulation of the rich hydrogen production process through the gasification of RDF obtained from MSW were developed using Aspen Plus chemical process simulation software. The water-gas shift system was also incorporated into the overall processes for further enrichment of the hydrogen content in the syngas mixture. This chapter presents the results of the hydrogen production economic evaluation of the RDF gasification process. The economic assessment used Aspen Plus criteria and other standard references from (Towler and Sinnott, 2013, Sinnott and Towler, 2012, Peters et al., 2013, Demis et al., 2015). The system's economic assessments are associated with the total capital costs to assess the cost-effectiveness of the system. The total capital costs (TCC) depend on the direct plant costs, which were estimated through sizing all major equipment pieces according to the gasification simulations with 5 Kg/h as a basis. The unit operations are shown in the process flow diagram and other assumptions are presented in chapter three. The mass balances are also shown in section 3.4. The costs were estimated with the same cost functions for the system with reasonable accuracy. The economic evaluation considered total capital costs, working capital and operating cost as the required costs to evaluate the performance of the system.

7.2 Total Capital Cost and Working Capital Estimation

The major elements of the estimation of costs considered in the evaluations were total capital cost (TCC), working capital costs and total operating cost. Hence, other economic assessment parameters were derived from the major elements of cost estimations.

The reference scale factors for the estimation were obtained from relevant studies and standard handbooks. The feedstock MSW was \$0.30 per kg (this amount includes transportation and collection fee of MSW), labour at 3 shifts/day, the utilities were 0.15(TCC), the project lifespan was 10 years, the capacity factor of 0.82, the interest rate a nominal 15 % and start-up costs were 0.10(TCC). The plant maintenance costs account for 0.025(TCC) and the plant overheads are 0.025(TCC) (Towler and Sinnott, 2013, Sinnott and Towler, 2012, Peters et al., 2013, Demis et al., 2015). The selling price of H_2 gas was \$10.00 per kg while the selling price of CO_2 was obtained from (Li et al., 2012b). The total capital cost for the system was estimated to be \$1.5349 million which included the total fixed capital cost of \$1.3023 million and working capital cost of \$0.2326 million annually.

7.3 Results and Discussion

The total capital cost for the system was \$1.5349 million less than that of (Li et al., 2012b) which included a total fixed capital cost of \$1.3023 million and working capital cost of \$0.2326 million. The total revenue from the system was \$7.1587 million for the entire project lifespan with an annual average of \$0.7159 million. The economic assessment parameters below were used for a further analysis the feasibility of the system.

7.3.1 The Economic Evaluations with/without Time Value for Money

The profitability evaluation standard is crucial and usually considers both quantitative and qualitative measurements. The quantitative economic measurements (NR, ROI, PBP, NPV and DCFROR) focused on desirability on risk taking in investments while the qualitative economic evaluation measurements of safety and morale of employee, environmental and legal constraints etc. are not tangible and have an indirect link to profitability measures. The focus was on the rate of return on investment, net return, payback period, net present value and discounted cash flow rate of return.

7.3.2 Rate of Return on Investments (ROI)

The ratio of profit to TCC does not consider the time value for money but it is an assessment to show the brief economic outlook for the investment. The comparison between the minimum acceptable rate of return (MAR) (assumed for this study to be 15 %) and the ROI demonstrates the acceptability of the investment on the project if ROI is more than 15 %. MSW waste management should have the input of government because of the environmental cost for MSW (Wood and Rowley, 2011). The MSW handling (MSW pre-treatments) cost is the responsibility of the government to make environments clean. The MSW handling costs for this study include the cost of cleaning MSW in the municipality, cost of transportation of MSW, collection fees of MSW separation and pre-treatment cost, and the cost of producing RDF. The MSW handling costs are significant costs because they are associated with operational costs. This is important to the overall economic assessment of this project. Introduction of MSW handling costs from concerned institutions will improve the investment outlook. A thorough adjustment of the operational MSW handling costs gives a better outlook; thus, it could be viable and sustainable. If equation 7.1 below is satisfied, ROI is neither a desirable nor acceptable investment.

$$\frac{\mathrm{N_{p,ave}}}{\mathrm{TCC}} \leq \mathrm{m_{ar\,(15\,\%)}} = \text{Not Accepatable ROI} \qquad \frac{\mathrm{N_{p,ave}}}{\mathrm{TCC}} \geq \mathrm{m_{ar\,(15\,\%)}} = \text{Acceptable ROI} \quad (7.1)$$

However, with the consideration and implementation of the environmental cost, the ROI value was 27.88 %, unlike the negative value of – 50.00 % obtained when there was no environmental cost consideration (Figures 7.1 and 7.2).

Figure 7.1 and Figure 7.2 show trends of cumulative cash flow effects throughout the full life cycle of the project which is similar to the typical cumulative cash flow as shown in

Figure 7.9. Figure 7.1 and Figure 7.2 show the same trend in the initial stages of the project when money is spent and there is no production nor sale in the project. The money spent here is usually regarded as negative on the cumulative cash flow graph. Figure 7.1 continues to show a downward movement, despite production which began three years after the beginning of the project.

The payback period (PBP) is not seen in Figure 7.1, which has the economic potential of also being negative. This is because of the effects of MSW handling costs which are continuously being incurred in the operational costs. However, without the MSW handling costs as part of the daily operational cost, Figure 7.2 shows a typical cumulative cash flow that is economically feasible with ROI 27.88 % and a payback period (PBP) of 2.3 years. The payback period, another economic indicator as shown in Figure 7.2, will be discussed in the next section.

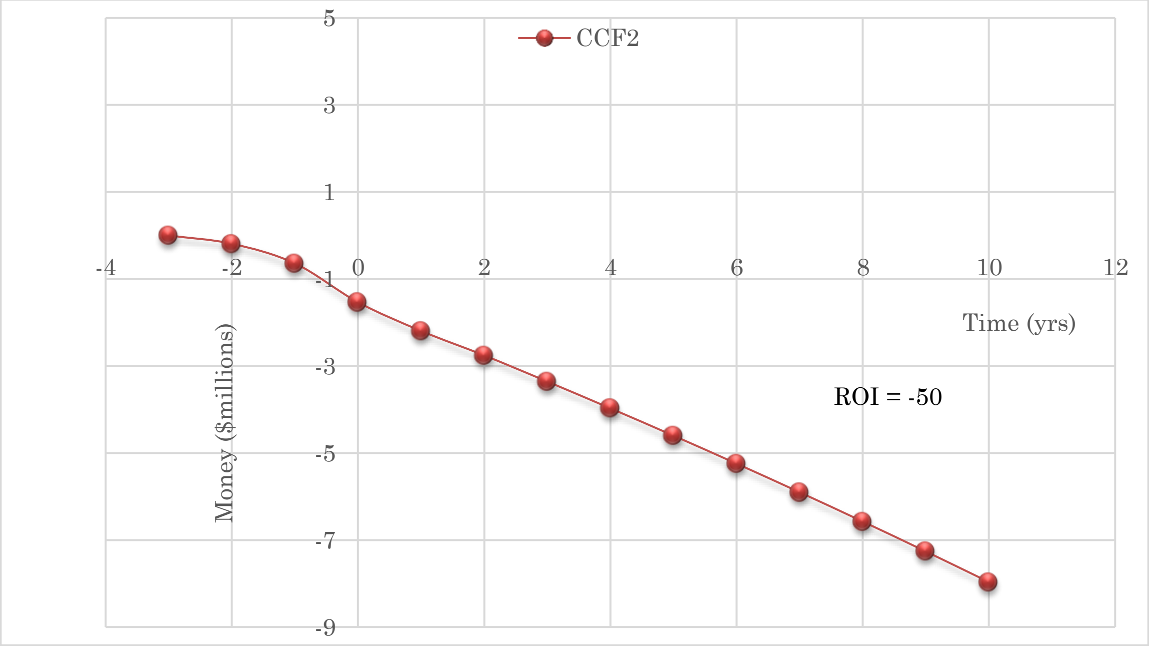

Figure 7.1: Cumulative Cash Flow without MSW Handling Input

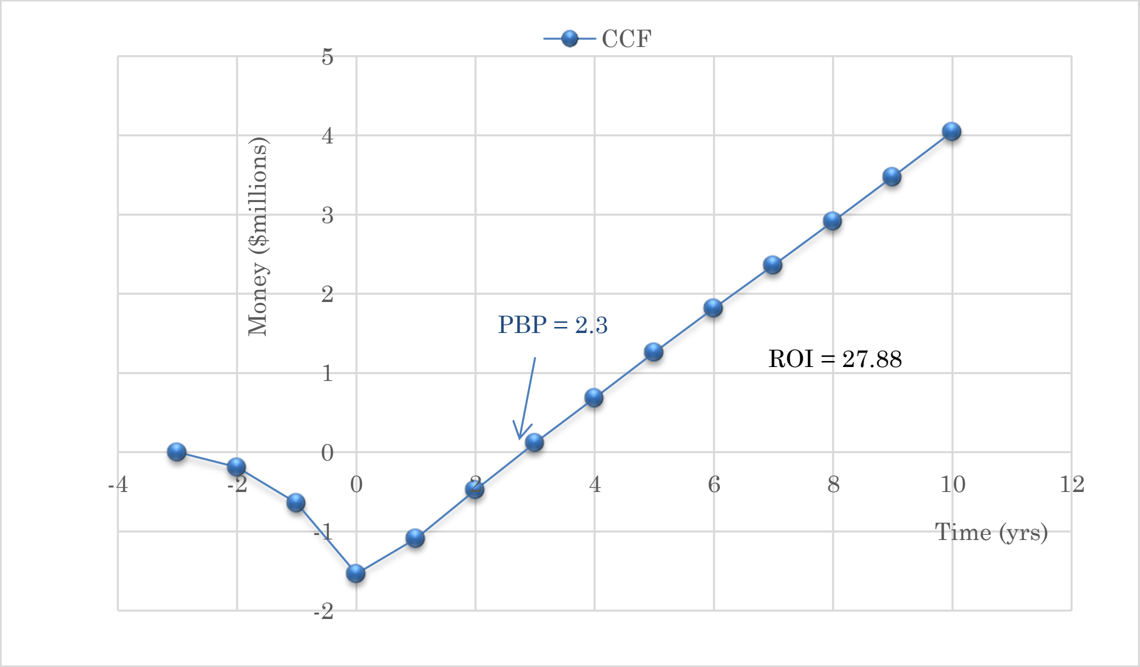

Figure 7.2: Cumulative Cash Flow with MSW Handling Costs Input

7.3.3 Payback Period (PBP)

The results were presented in Figure 7.2, wherein PBP = 2.3 yrs. This reference of PBP (PBP_{ref}) in equation 7.2 obtained 3.62 yrs. The PBP was feasible because of the input of MSW handling costs while the other PBP, without the input of MSW handling cost, is not feasible and cannot reasonably be considered. The PBP obtained allows a swift return on investment. The PBP-PBP_{ref} relationship was satisfied as expressed below (Peters *et al.*, 2013):

$$\mathrm{PBP} = \frac{\mathrm{V} + \mathrm{A_x}}{\mathrm{A_{Jav}}} \leq \mathrm{PBP_{ref}} = \frac{0.85}{\mathrm{M_{ar}} + 0.85\mathrm{N}^{-1}} \qquad (7.2)$$

This PBP value of 2.3 yrs (less than 3.62 yrs) is less than the PBP reference value which shows the potential of the investment. The breakeven point (BEP), as shown in Figure 7.9, is another measure similar to PBP but the price of the product to attain the PBP of 2.3 yrs. The hydrogen selling price is $10 per Kg of hydrogen. The market price of hydrogen varies between $7.00 and $13.00 per Kg of hydrogen. The lower prices of hydrogen are usually obtained from non-renewable sources. The PBP obtained in this study was lower than these values (4.19 years and 5.05 years) presented by (Basu,2013) in a supercritical water gasification with efficiency of 64.8 %.

The focus of this study is to promote the exploitation of sustainable renewable energy resources. This is also useful for assessing the lifespan of a project, how quickly the investors can recover their money and improvement of the project performance similar to this study (Athanassiou and Zabaniotou, 2008).

7.3.4 Net Return (NR)

The positive, conservative result for the value of net return obtained was $0.20 million annually. The net return showed that the annual cash flow is more than the cost required to pay off the capital investment. This ensures the return satisfied a minimum acceptable rate.

Net return with a zero value indicated the project was just paying back the investment, while a negative net return from the other option without MSW handling cost for this study, is not acceptable for the project. It showed the plant net return was not favourable for the project. Figure 7.3 shows the relationship between the two types of annual cash flow for both cases under consideration. Figure 7.3 shows annual cash flows for both environmental cost considerations. It is clearly shown that the flow of income is positive for without MSW handling cost while it is negative for with MSW handling cost.

The graph of the annual cash flow without MSW handling cost continues to move downward towards the end of life of the project. This is a serious implication for costs. The effective area between then the two demonstrates the extent of the impact of environmental cost incorporated into the economic evaluation.

7.3.5 Net Present Value (NPV)

The continuous NPV for the project is $1.1143 million at a discounted rate of 15 % per year with respect to equation 3.31. This is regarded as an acceptable NPV because it is positive, unlike the scenario when the environmental cost was not considered as shown in Figure 7.4. The annual average of NPV is $ 0.08 million which is an equally positive value regarded as the required criteria for investment acceptability (Wood and Rowley, 2011). Both NPV values are good values for the project, both NPV continuous values being higher than the NPV annual economic evaluation and their difference is significant ($1.1143 million and $ 0.08 million). Figure 7.4 illustrates both scenarios which tend to close the gap as time goes by, but this may take a very long time to achieve because of the depreciation factor, and other factors that may occur.

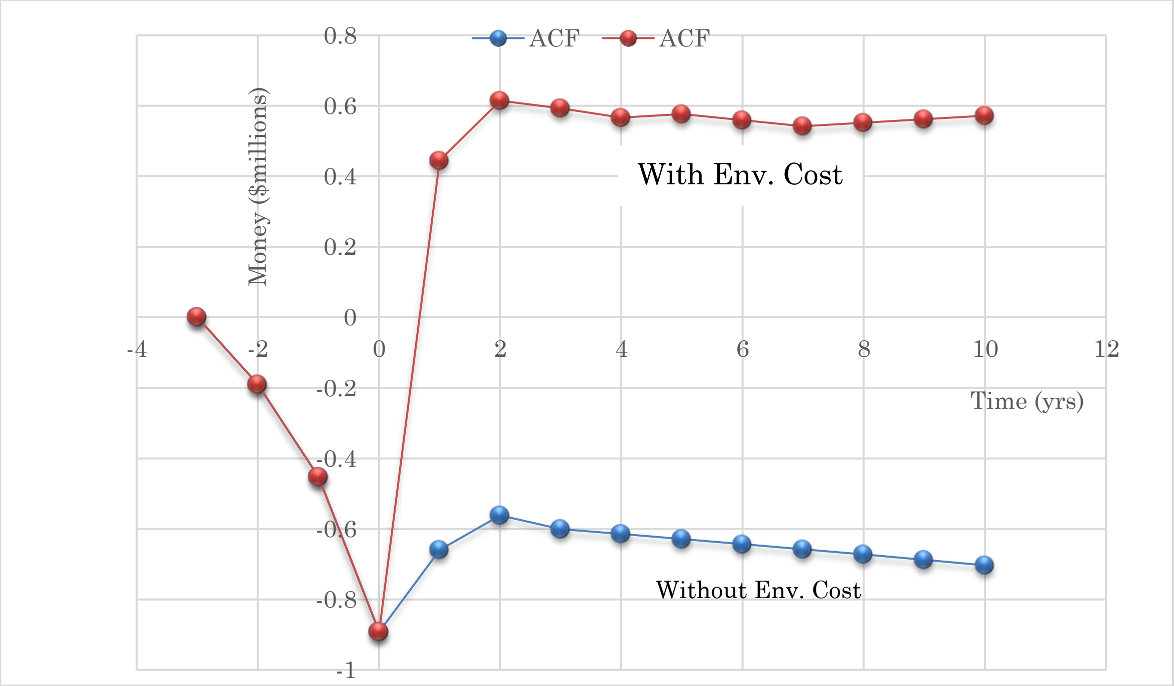

Figure 7.3: Annual Cash Flow with and without MSW Handling Costs Input

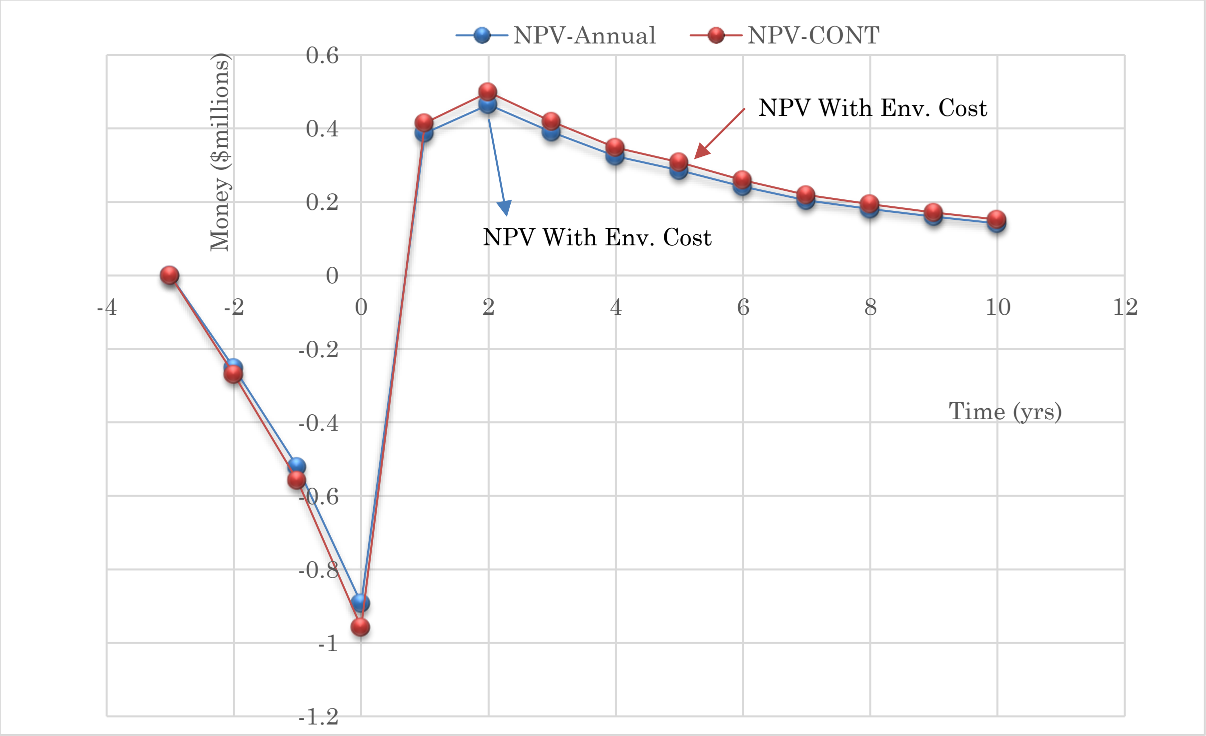

Figure 7.4: NPV Annual Cash Flow with and without MSW Handling Costs Input

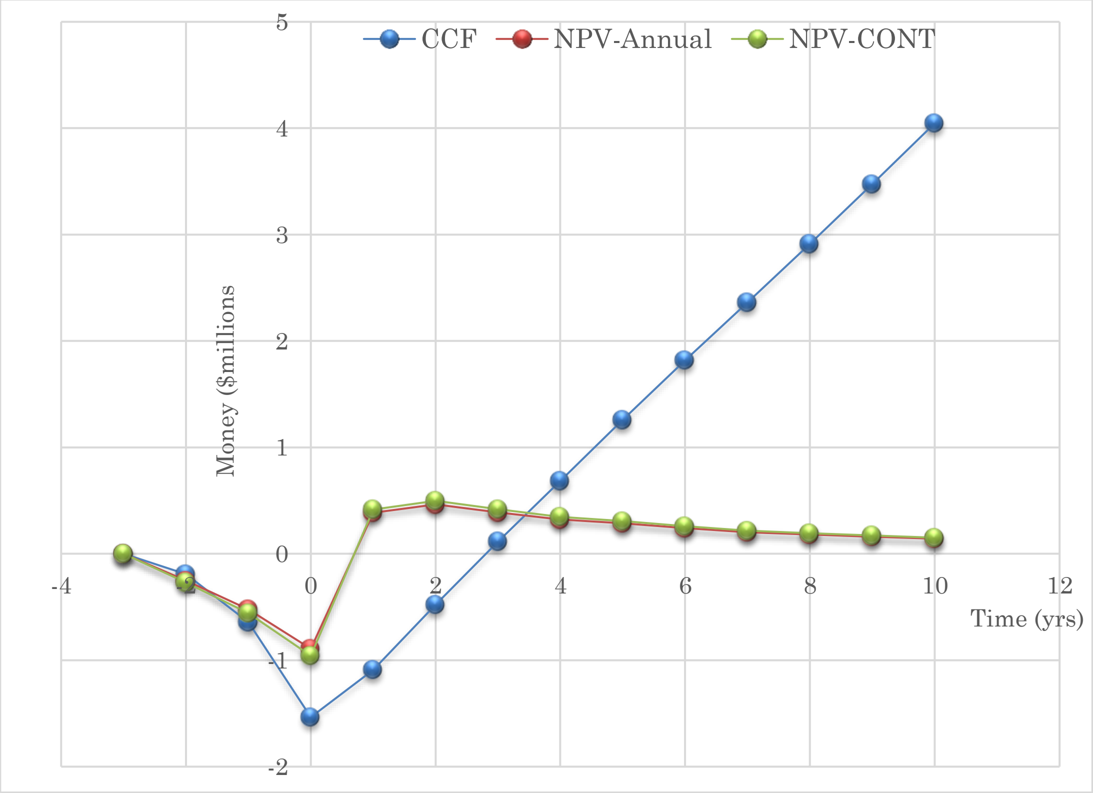

Figure 7.5: CCF, NPV Annual Cash Flow with and without MSW handling Costs Input

7.3.6 Discounted Cash Flow Rate of Return (DCFROR)

The Discounted Cash Flow Rate of Return (DCFROR) was achieved at the discounted rate of 28.20 % when NPV = 0 as expressed in equation 3.32 and the graph is shown in Figure 7.6, while Figure 7.7 shows a negative trend which is not good for potential investment. Several values of rate were iterated, preferably those greater than 15 %, as indicated earlier until NPV = 0 was satisfied at a rate of 28.20 %. DCFROR is a useful tool when comparing a number of projects evaluations. The rate is satisfactory, and the investment earns a discounted cash flow rate of return of 28.20 % annually.

The NPV indicates the monetary return, while the DCFROR value depends on the base lifespan of the project. The higher the value of NPV and DCFROR for a project, the more attractive to investment it becomes.

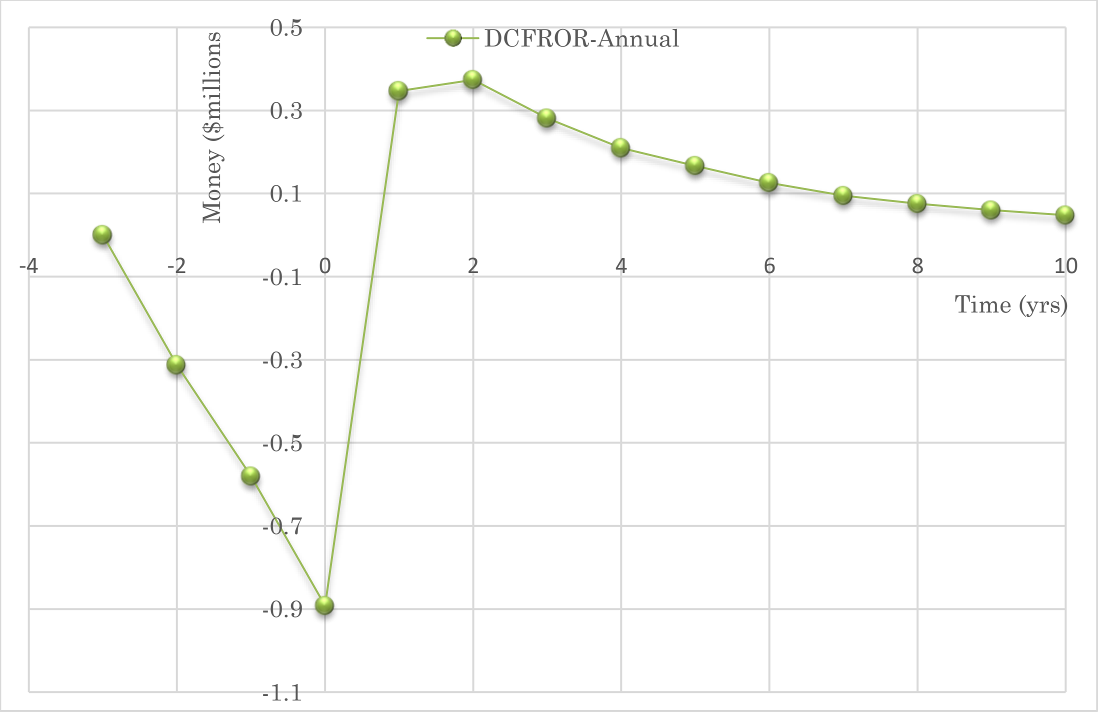

Figure 7.6: DCFROR Annually with MSW Handling Costs Input (NPV = 0)

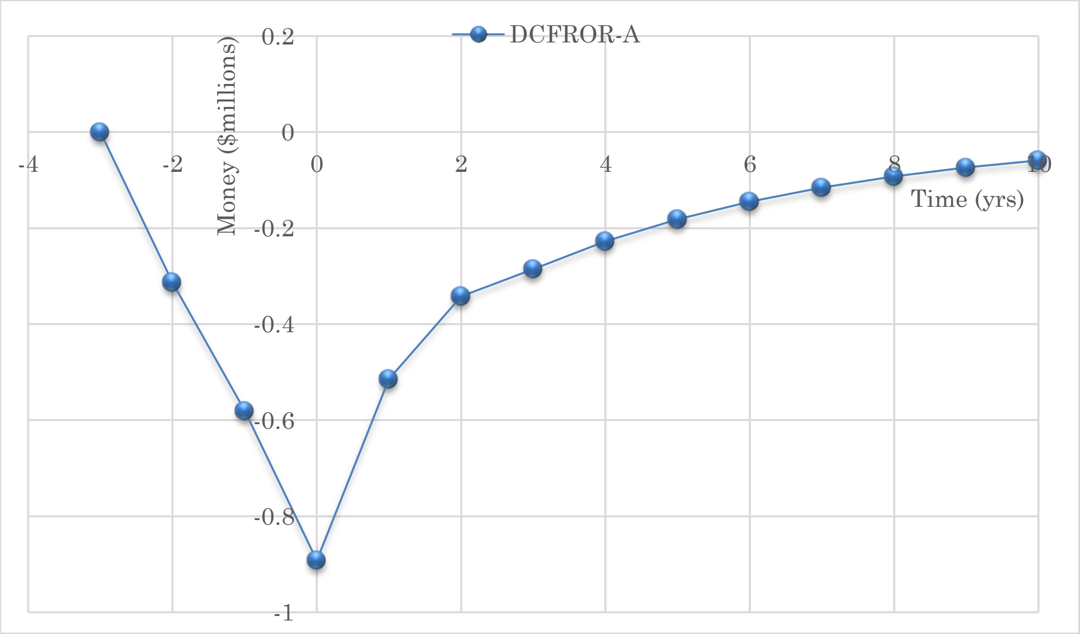

Figure 7.7: DCFROR Annually without MSW Handling Costs Input

The iterated value of 28.20 % DCFROR obtained, implies that 28.20 % per year will be earned on the investment, in addition to which the project generates sufficient money to repay the original investment plus any other expenses. This rate of value could be an effective profitability index for the project. Both NPV and DCFROR economic profitability measures could characterise the economic values of a project in term of capital efficiency and effectiveness of the project. The cash flow for the later years are discounted to a greater extent (Figure 7.6) than the cash flows for the earlier years, the latter having less effect on the overall estimation.

Nevertheless, the challenge of predicting cash flow in later years and the lack of certainty in these predictions are disadvantages of the DCFROR method. Hence, the NPV will complement the challenge because it is calculated annually for the project. Thus, a favourable NPV in the early years is reliable. One way of overcoming the disadvantages of the DCFROR method is to estimate the time required to reach certain values of DCFROR. However, other economic evaluation measurements are complementary to the success of the project. It will be inadequate to make a comprehensive judgement on the profitability of the project after only one or two evaluations.

7.3.7 Analysis of NPV and DCFROF

The shape of the cumulative-cash flow and cumulative-discounted-cash flow curves, both before and after the payback period, are key factors as shown in Figure 7.8 and Figure 7.9. The equivalent maximum investment period (EMIP) is a time in years for the recovery of interest as shown between point A, B and C. The higher the EMIP, the more attractive the project (Green and Perry, 2008). The areas beyond point C are regarded as the interest period.

The larger the area beyond C and the shorter the time between A and C will guarantee desirable investment. The break-even point C is good, as is the flowing area after point B. The collection of various economic assessment parameters was plotted on a single graph (Figure 7.9). The accumulated cash flow (ACF), net present value annually and continuously (NPV-Annual and NPV-CONT) and the discounted cash flow rate of return (DCFROR-Annual and DCFROR-CONT) are illustrated in Figure 7.8. The ACF represents the raw cash flow before any deductions and the continuous increase in the area between the ACF and other cash flows. This area (X) indicates other necessary operational costs. This is an initial indication of economic potential demonstrated by the investment. Also, the return on investment is slightly different for the net present value, annually and continuously, and the discounted cash flow rate of return. The continuous return on investment from the net present value (NPV-CONT) and the continuous discounted cash flow rate of return (DCFROR-CONT) are minimal towards the end of the project. Figure 7.8 also shows that the NPV annual and continuous values are higher than the DCFROR annual and continuous values are both good values for potential project profitability. Both are constituent economic measures because a large number of factors affecting profitability are considered in their determination. Figure 7.9 shows the difference between PBP (at point C) and ACF from revenue at point E. Point E shows where the revenues start coming in but not enough until PBP was achieved at point C (2.3 yrs), though production and sales commenced from point D.

The return on investment from the continuous net present value (NPV-CONT) was \$1.196 million (higher than \$1.114 million for NPV-Annual) but the continuous discounted cash flow rate of return (DCFROR-CONT) was 24.80 %, lower than 28.20 % for the annual DCFROR (Figure 7.8).

The return on investment primarily focuses on investment and cash flows relationships while cash flows are functions of raw materials costs, operating costs, sale revenue and price. These factors may now lead to consumer behaviour patterns. It gives some idea of the degree of risk involved in making judgements on the performance of a project.

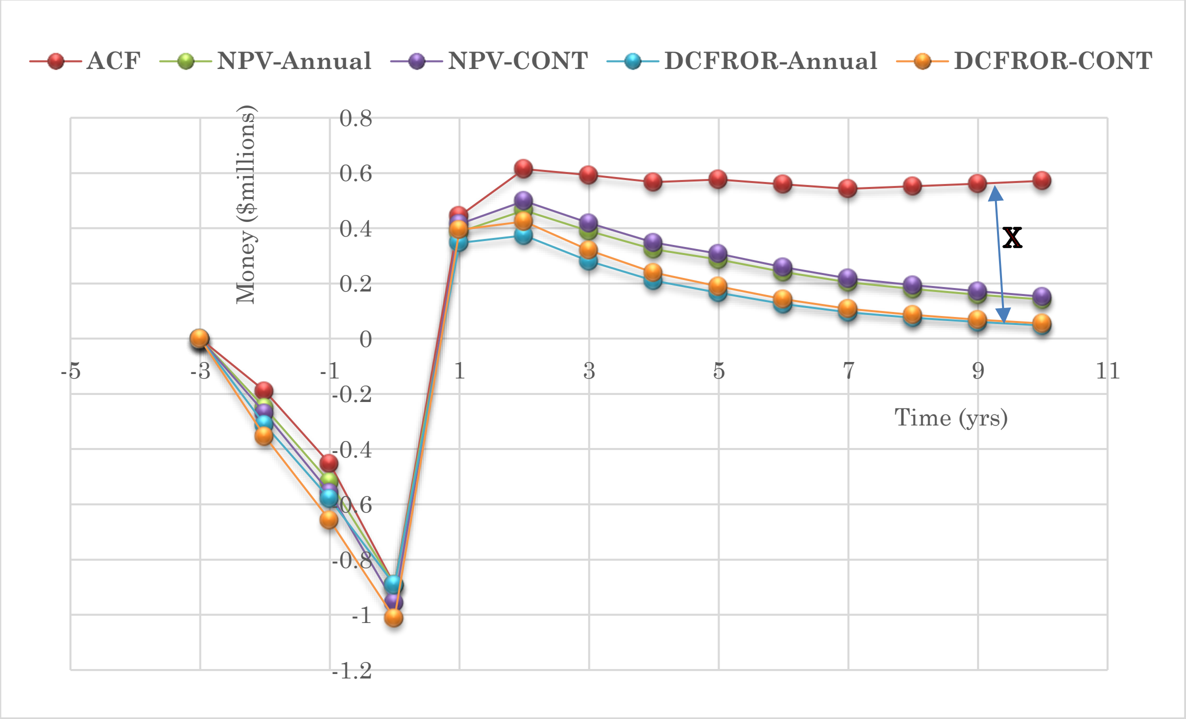

Figure 7.8: All Cash Flow Indicator Diagrams

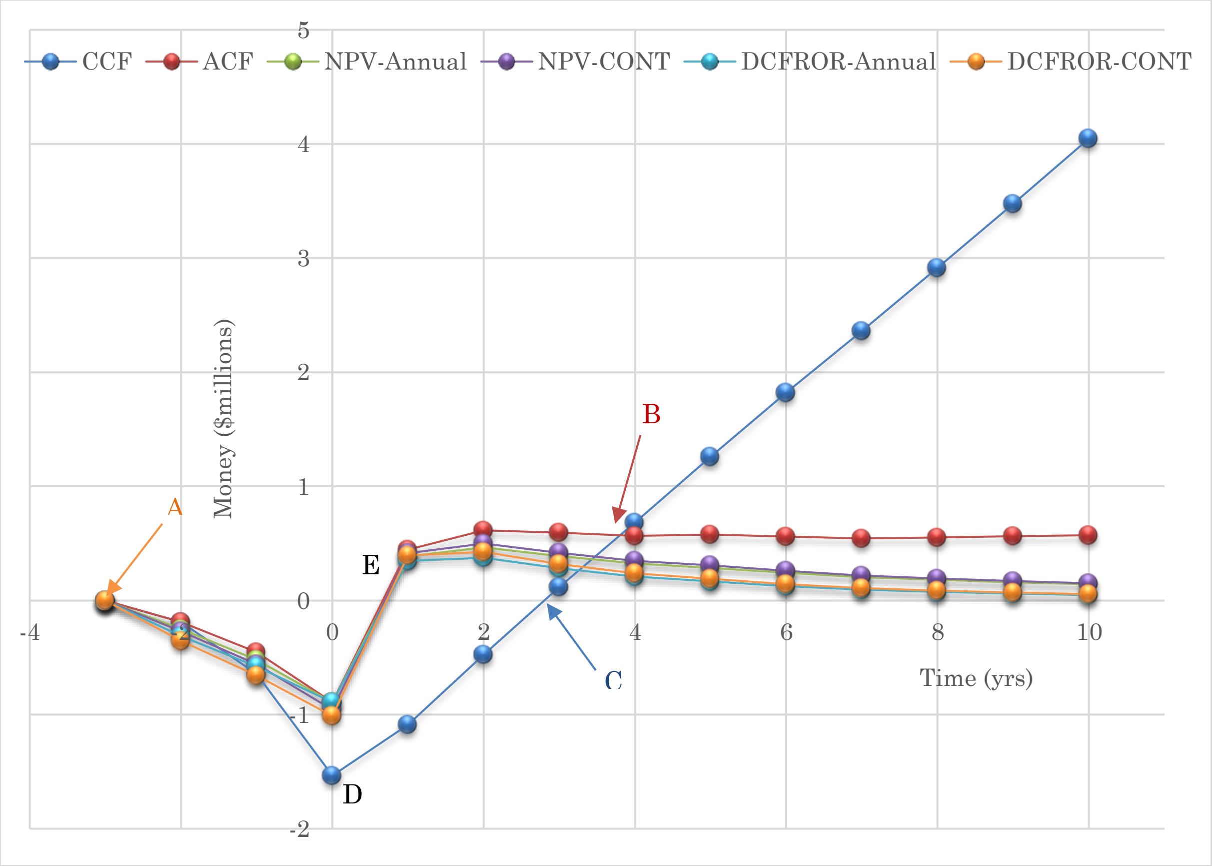

Figure 7.9: All Cash Flow Model Diagram Indicator

7.4 Chapter Summary

The future prospect of hydrogen fuel as an energy carrier is gaining more acceptance worldwide. The processes and technologies requirement should be economically feasible and environmentally friendly while ensuring the quality of the hydrogen. Hydrogen production costs from MSW gasification is very important because of crucial procedures that are required to meet up with eco-friendly technology while minimising the effects of the disposal of MSW. The identification of certain components of the cost evaluation, where the trade-offs (Muresan et al., 2013) of this type of project are critical to the sustainability of a waste-to-energy system. The total capital cost was $1.5349 million while the total revenue from the system was $7.1587 million for the entire project life of 10 years (360000 Kg of MSW) with an annual average of $0.7159 million.

The quantitative economic evaluation measurements were NR = $0.20 million, ROI = 27.88 %, PBP = 2.3yrs, NPV = $1.1143 million and DCFROR = 24.80 % and 28.20 % respectively. All the economic measurements provided a positive evaluation of the project. It is also essential to conduct all these measures because they are complementary to one another with regard to an adequate economic analysis of the project.

The results of the economic evaluations revealed that an analysis of the economic benefits of this system would be viable if the operating MSW handling costs were further quantified into the costs analysis. The costs are high, but it would be viable if the government accepted responsibility for the MSW handling costs of the system. The system's final hypothetical profit was obtained by deducting the investment costs from the previously mentioned revenue. The summary of the research so far and recommendations for further research will be presented in chapter eight.

CHAPTER EIGHT

8 CONCLUSIONS AND RECOMMENDATIONS

8.1 Conclusions

The objective of this research was to investigate the feasibility of MSW-derived RDF gasification for use in a fuel cell-based CHP system. The investigation was pursued by identifying thermochemical methods and various physicochemical characterisation of pre-treated MSW, gasification simulation of RDF, quantification of the heavy metals concentrations in pre-treated MSW and the economic evaluation of the gasification system.

Gasification technology offers better gaseous products over other thermochemical conversions to produce syngas because MSW-derived RDF gasification technology demonstrates more efficient and cleaner products, specified oxidant flowrate, less volume but high density gaseous products and controlled of hazardous emission to the environment.

The gasification boosts hydrogen content of the products and reduces the carbon content of MSW to produce useful gases with a higher hydrogen-to-carbon (H/C) ratio. Carbon dioxide consumption during the boudouard reaction and CO_2-capturing opportunity show the viable potential of effective and sustainable MSWM, a better eco-friendly environment and generate socio-economic opportunities.

RDF pellets produced from the pre-treated MSW had packed bulk densities of 407.20 Kg/m^3- 515.00 Kg/m^3. The energy density increased from 4142.07 MJ/m^3 to 10735.8 MJ/m^3. The packed bulk densities were relatively good for thermochemical conversion.

The packed bulk density characteristics could serve as an indication of the potentials of RDF as an alternative source of solid fuel.

The HHV (18.17 - 28.91 MJ/Kg) obtained were better compared to the normal products of RDF from MSW or virgin biomass with a value of around 16 MJ/Kg - 18 MJ/Kg. The RDF pellets are a prospective alternative energy fuel and one of the prime substitutes to fossil fuels for cogeneration applications. The ultimate and proximate analyses demonstrated another opportunity for alternative solid fuel application. The data results of the ultimate analysis were good values while a low nitrogen composition, together with good HHV, were positive indicators of a good solid fuel. The molecular formulas derived from Ladies Smith drop-off site, Woodstock drop-off site and average molecular formula were $CH_{1.43}O_{1.02}$, $CH_{1.49}O_{1.19}$, and $CH_{1.50}O_{0.86}$ respectively. The molecular formula derived from the pre-treated MSW from Ladies Smith drop-off site was selected to be of better quality. The proximate analysis showed percentage compositions of MC (5 – 10 %), VM (10 – 75 %), FC (11- 30 %) and ash (4 – 21 %). The proximate analysis showed that combustible composition of range 68 % - 78 % and non-combustible of range 14% – 30 %. The proximate analysis was used to compare the combustible to non-combustible constituents of the solid fuel. The thermochemical degradation contribution of VM and FC was significant compared to MC and ash. The VM, FC and ash components showed similar patterns of combustion characteristics. The TGA analysis showed a degradation profile which was uniform for all the samples analysed. In theory, the temperature profiles for all the samples considered the net effect of the endothermic and exothermic reactions which matched the expected trend and they also predicted the expected temperature requirement for gasification. the ultimate analysis, proximate analysis, bulk density, and high heating values, the results were used in simulating gasification of the refuse-derived fuel (RDF) for onward application of hydrogen in fuel cell.

All the analyses provided a positive indication of using Cape Town's MSW for alternative solid fuel and possible exploitation for production of hydrogen that could be used as a feed to HTPEMFC.

The gasification process of RDF1, RDF2 and RDF3 were simulated via Aspen Model using a combination of various unit operation modules. The model developed enabled the prediction of the feasibility of RDFs gasification behaviour under various operating parameters in an air-blown downdraft gasifier. The effects of the ERs and the SFRs on gasification were relevant in the modelling. The simulation results obtained were for RDF1, RDF2 and RDF3, and they were 18.81 of H_2/CO, 18.12 of H_2/CO and 20.16 of H_2/CO molar ratios respectively. Apart from effects of gasifier parameters towards production of high molar ratios of H_2/CO, the 18.17 MJ/Kg - 28.91 MJ/Kg HHV data and ultimate analysis data contributed to ratios of H_2/CO obtained. The molar ratios of syngas were proportional to HHV and so were the ratios of H in ultimate analysis data of the RDFs. The RDF3 gasification Aspen model produced values for ER of 0.08 and SFR of 3.30. These values can satisfy the requirements of fuel cell application. The trend of results shows the complementary influence and dependence of ER values and SFR values on the desired product and co-products. For the integration of MSW gasification/HTPFEMFC, having seen the potentials of MSW to produce hydrogen, a separating unit may be required to ensure that pollutants are minimal when integrated into the fuel cell system.

The heavy metals quantification of pre-treated MSW showed that the concentrations of heavy metals obtained in all the pre-treated MSW samples of this study are less when compared to the unsorted MSW that had not been pre-treated. The heavy metals Pb, Zn and Hg) emissions were technically monitored because most emissions from simulated gasification processes are mainly heavy metals in non-oxidized form and their emission

into the atmosphere reduced. The gasification technology hence offers heavy metals emission mitigation to an uncontrolled emission from open-air incinerations.
However, before disposal or reuse of bottom ash residue, the residue will require further research for its potential environmental impact. This could be helpful for crucial considerations about policy and decision-making about the mobility of heavy metal in MSW thermochemical conversion technology from cradle-to-grave.

The economic evaluation result of the gasification system's total capital cost was $1.5349 million while the total revenue was $7.1587 million for the entire project life (10 yrs) with an annual average of $0.7159 million. The results of quantitative economic evaluation measurements were NR = $0.20 million, ROI = 27.88 %, PBP = 2.3yrs, NPV = $1.1143 million and DCFROR = 24.80 % and 28.20 % respectively. The system's final hypothetical profit was obtained by deducting the investment costs from the previously mentioned revenue. All the economic evaluation measurements are complementary to one another, thus ensuring the success of the project while not neglecting environmental cost considerations. Thus, a comprehensive judgment on the assessment of profitability should include evaluation measures.

The result provides a basis for the optimum performance of RDF gasification for the air-blown downdraft gasifier. The results of the economic evaluations revealed that an analysis of economic benefits, despite the high costs which could be viable if government accepted responsibility of conversion of MSW to RDF. This system would be feasible if the associated costs of conversion of MSW to RDF were further quantified in the cost analysis.

8.2 Recommendations

In this study, a techno-economic analysis of an MSW gasification system was simulated via Aspen Model to produce a high hydrogen yield in the syngas mixture. The quality of hydrogen produced by means of the Aspen Plus Model can still be improved upon by introducing the relevant parameters for a minimised CO concentration in the syngas mixture.

Another physicochemical characterisation should be considered for an RDF with a binder. This will harness a better quality of HHV or RDF generated without a binder, with a suitable binder from waste materials or resources.

RDF qualities need a further physicochemical characterisation by means of comprehensive thermal analyses. The choice of heat flow and temperature should be examined. The CO production from the Boudouard reaction is an important product of the last stage of TGA. The air-blown downdraft gasification should be investigated by experimentation.

All the balances in the gasification simulations were based on the Aspen Plus Model with an inbuilt thermodynamic equilibrium and kinetic limitations. In the course of further economic assessments, there is the possibility of further research into evaluating the current capital cost data based on Aspen's capital cost estimation to facilitate the importance of the low cost of MSW.

REFERENCES

ABDUL SAMAD, N. A. F., JAMIN, N. A. & SALEH, S. 2017. Torrefaction of Municipal Solid Waste in Malaysia. *Energy Procedia,* 138**,** 313-318.

ABU QDAIS, H. A. 2007. Techno-economic assessment of municipal solid waste management in Jordan. *Waste Management,* 27**,** 1666-1672.

ADAMS, P. W. R. & MCMANUS, M. C. 2014. Small-scale biomass gasification CHP utilisation in industry: Energy and environmental evaluation. *Sustainable Energy Technologies and Assessments,* 6**,** 129-140.

ADAPA, P., TABIL, L. & SCHOENAU, G. 2009. Compression Characteristics of Selected Ground Agricultural Biomass *Agricultural Engineering International,* XI**,** 1-19.

ADEFESO, I., RABIU, A. & IKHU-OMOREGBE, D. 2015. Refuse-derived Fuel Gasification for Hydrogen Production in High Temperature Proton Exchange Membrane Fuel Cell Base CHP System. *Waste and Biomass Valorization,* 6**,** 967-974.

AFRICA, S. S. 2012. Energy Account for South Africa: 2002-2009 Environmental Economic Accounts. Pretoria South Africa: Statistics South Africa

AHMED, I. & GUPTA, A. K. 2009a. Characteristics of cardboard and paper gasification with CO_2. *Applied Energy,* 86**,** 2626-2634.

AHMED, I. & GUPTA, A. K. 2009b. Syngas yield during pyrolysis and steam gasification of paper. *Applied Energy,* 86**,** 1813-1821.

AHMED, I. & GUPTA, A. K. 2011. Characteristic of hydrogen and syngas evolution from gasification and pyrolysis of rubber. *International Journal of Hydrogen Energy,* 36**,** 4340-4347.

AHMED, I. I. & GUPTA, A. K. 2009c. Hydrogen production from polystyrene pyrolysis and gasification: Characteristics and kinetics. *International Journal of Hydrogen Energy,* 34**,** 6253-6264.

AHMED, I. I., NIPATTUMMAKUL, N. & GUPTA, A. K. 2011. Characteristics of syngas from co-gasification of polyethylene and woodchips. *Applied Energy,* 88**,** 165-174.

ALAVI MOGHADAM, M. R., MOKHTARANI, N. & MOKHTARANI, B. 2009. Municipal solid waste management in Rasht City, Iran. *Waste Management,* 29**,** 485-489.

ALLEGRINI, E., MARESCA, A., OLSSON, M. E., HOLTZE, M. S., BOLDRIN, A. & ASTRUP, T. F. 2014. Quantification of the resource recovery potential of municipal solid waste incineration bottom ashes. *Waste Management,* 34**,** 1627-1636.

ALVAREZ, J., KUMAGAI, S., WU, C., YOSHIOKA, T., BILBAO, J., OLAZAR, M. & WILLIAMS, P. T. 2014. Hydrogen production from biomass and plastic mixtures by pyrolysis-gasification. *International Journal of Hydrogen Energy,* 39**,** 10883-10891.

ARAFAT, H. A. & JIJAKLI, K. 2013. Modeling and comparative assessment of municipal solid waste gasification for energy production. *Waste Management,* 33**,** 1704-1713.

ARENA, U. 2012. Process and technological aspects of municipal solid waste gasification. A review. *Waste Management,* 32**,** 625-639.

ARENA, U., ZACCARIELLO, L. & MASTELLONE, M. L. 2010. Fluidized bed gasification of waste-derived fuels. *Waste Management,* 30**,** 1212-1219.

ARTETXE, M., LOPEZ, G., AMUTIO, M., ELORDI, G., BILBAO, J. & OLAZAR, M. 2012. Light olefins from HDPE cracking in a two-step thermal and catalytic process. *Chemical Engineering Journal,* 207–208**,** 27-34.

ASSAMOI, B. & LAWRYSHYN, Y. 2012. The environmental comparison of landfilling vs. incineration of MSW accounting for waste diversion. *Waste Management,* 32**,** 1019-1030.

ASTM STANDARD & ASTM D 3172-73(84) 1989a. Standards Method of Proximate Analysis of Coal and Coke, in Gaseous Fuels; Coal and Coke Section 5 Volume 05 - 05;. *Annual book of ASTM standards.*

ASTM STANDARD & ASTM D 3173-87 1989d. Standards Method of Moisture of Coal and Coke, in Gaseous Fuels; Coal and Coke Section 5, Volume 05-05; Annual book of ASTM standards. *Annual book of ASTM.* US.

ASTM STANDARD & ASTM D 3174-89 1989c. Standards Method for Ash in the Analysis Sample of Coal and Coke, in Gaseous Fuels; Coal and Coke section 5 Volume 05 - 05; Annual book of ASTM standards. *Annual book of ASTM standards.* US.

ASTM STANDARD & ASTMD 3147-89 1989b. Standards Test method for Volatile Matter in the Analysis of Sample Coal ans Coke section 5 volume 05-05; Annual book of ASTM standards. *Annual book of ASTM standards.* US.

ATHANASSIOU, M. & ZABANIOTOU, A. 2008. Techno-economic assessment of recycling practices of municipal solid wastes in Cyprus. *Journal of Cleaner Production,* 16**,** 1474-1483.

BALAT, H. & KıRTAY, E. 2010. Hydrogen from biomass – Present scenario and future prospects. *International Journal of Hydrogen Energy,* 35**,** 7416-7426.

BALKHAIR, K. S. & ASHRAF, M. A. 2016. Field accumulation risks of heavy metals in soil and vegetable crop irrigated with sewage water in western region of Saudi Arabia. *Saudi Journal of Biological Sciences,* 23**,** S32-S44.

BARBIR, F. 2013. *PEM fuel cell: Theory and Practice,* USA, Academic Press Elsevier.

BARRETT, S. 2013a. HySA Infrastructure: producing and using hydrogen for energy in South Africa. *Fuel Cells Bulletin,* 2013**,** 12-17.

BARRETT, S. 2013b. HySA/Catalysis: Creating opportunities from South Africa's mineral wealth. *Fuel Cells Bulletin,* 2013**,** 12-15.

BARTELA, Ł., KOTOWICZ, J., REMIORZ, L., SKOREK-OSIKOWSKA, A. & DUBIEL, K. 2017. Assessment of the economic appropriateness of the use of Stirling engine as additional part of a cogeneration system based on biomass gasification. *Renewable Energy,* 112**,** 425-443.

BASU, P. 2010. *Biomass gasification and pyrolysis: Practical design and theory,,* US, ELSIVIER.

BASU, P. 2013. *Biomass Gasification, Pyrolysis and Torrefaction: Practical Design and Theory,* Burlington, MA 01803, USA, Elsevier Academic Press.

BELEVI, H. & MOENCH, H. 2000. Factors Determining the Element Behavior in Municipal Solid Waste Incinerators. 1. Field Studies. *Environmental Science & Technology,* 34**,** 2501-2506.

BELL, D. A., TOWLER, B. F. & FAN, M. 2011. *Coal Gasification and Its Applications,* Burlington, MA 01803, USA, Williams Andrew, Elsevier Academic Press.

BESSARABOV, D., VAN NIEKERK, F., VAN DER MERWE, F., VOSLOO, M., NORTH, B. & MATHE, M. 2012. Hydrogen Infrastructure within HySA National Program in South Africa: Road Map and Specific Needs. *Energy Procedia,* 29**,** 42-52.

BIANCHI, M., BRANCHINI, L., DE PASCALE, A. & PERETTO, A. 2014. Application of environmental performance assessment of CHP systems with local and global approaches. *Applied Energy,* 130**,** 774-782.

BING, X., BLOEMHOF, J. M., RAMOS, T. R. P., BARBOSA-POVOA, A. P., WONG, C. Y. & VAN DER VORST, J. G. A. J. 2016. Research challenges in municipal solid waste logistics management. *Waste Management,* 48**,** 584-592.

BOARD, P. S. & VIGNAROLI, L. 1976. Electrolytic tinplate for some Australian canned foods. *Food Technology in Australia,* 28**,** 486 - 487.

BRIDGWATER, A. V., ALCALA, A. & GYFTOPOULOU, M. E. 2011. 17 - Biomass-based small and micro combined heat and power (CHP) systems: application and status in the United Kingdom A2 - Beith, Robert. *Small and Micro Combined Heat and Power (CHP) Systems.* Woodhead Publishing.

BUJLO, P., PASUPATHI, S., ULLEBERG, Ø., SCHOLTA, J., NOMNQA, M. V., RABIU, A. & POLLET, B. G. 2013. Validation of an externally oil-cooled 1 kWel HT-PEMFC stack operating at various experimental conditions. *International Journal of Hydrogen Energy,* 38**,** 9847-9855.

BURNLEY, S., PHILLIPS, R., COLEMAN, T. & RAMPLING, T. 2011. Energy implications of the thermal recovery of biodegradable municipal waste materials in the United Kingdom. *Waste Management,* 31**,** 1949-1959.

CANNED FOOD INFORMATION SERVICE 1988. *Food Canning: An Introduction* Melbourne,Australia, Melbourne, Vic. : Canned Food Information Service, c1988.

CAO, L., YUAN, X., LI, H., LI, C., XIAO, Z., JIANG, L., HUANG, B., XIAO, Z., CHEN, X., WANG, H. & ZENG, G. 2015. Complementary effects of torrefaction and co-pelletization: Energy consumption and characteristics of pellets. *Bioresource Technology,* 185**,** 254-262.

CAO, Y., WANG, Y., RILEY, J. T. & PAN, W.-P. 2006. A novel biomass air gasification process for producing tar-free higher heating value fuel gas. *Fuel Processing Technology,* 87**,** 343-353.

CHACARTEGUI, R., CARVALHO, M., ABRAHÃO, R. & BECERRA, J. 2015. Analysis of a CHP plant in a municipal solid waste landfill in the South of Spain. *Applied Thermal Engineering,* 91**,** 706-717.

CHANDAN, A., HATTENBERGER, M., EL-KHAROUF, A., DU, S., DHIR, A., SELF, V., POLLET, B. G., INGRAM, A. & BUJALSKI, W. 2013. High temperature (HT) polymer electrolyte membrane fuel cells (PEMFC) – A review. *Journal of Power Sources,* 231**,** 264-278.

CHANG, F.-Y. & WEY, M.-Y. 2006. Comparison of the characteristics of bottom and fly ashes generated from various incineration processes. *Journal of Hazardous Materials,* 138**,** 594-603.

CHANNIWALA, S. A. & PARIKH, P. P. 2002. A unified correlation for estimating HHV of solid, liquid and gaseous fuels. *Fuel,* 81**,** 1051-1063.

CHAUDHARI, S. T., DALAI, A. K. & BAKHSHI, N. N. 2003. Production of Hydrogen and/or Syngas (H2 + CO) via Steam Gasification of Biomass-Derived Chars. *Energy & Fuels,* 17**,** 1062-1067.

CHEN, C., JIN, Y.-Q., YAN, J.-H. & CHI, Y. 2013. Simulation of municipal solid waste gasification in two different types of fixed bed reactors. *Fuel,* 103**,** 58-63.

CHEN, D., YIN, L., WANG, H. & HE, P. 2015a. Reprint of: Pyrolysis technologies for municipal solid waste: A review. *Waste Management,* 37**,** 116-136.

CHEN, S., MENG, A., LONG, Y., ZHOU, H., LI, Q. & ZHANG, Y. 2015b. TGA pyrolysis and gasification of combustible municipal solid waste. *Journal of the Energy Institute,* 88**,** 332-343.

CHENG, H. & HU, Y. 2010. Curbing dioxin emissions from municipal solid waste incineration in China: Re-thinking about management policies and practices. *Environmental Pollution,* 158**,** 2809-2814.

CHEREMISINOFF, N. P. & ROSENFELD, P. E. 2010. *Handbook of Pollution Prevention and Cleaner Production,* UK.

CHIFAMBA, P. 2007. Trace Metal Concentration of Water at a Solid Waste Disposal Site at Kariba Zimbabwe. *African Journal of Aquatic Science,* 32**,** 71 -78.

CHIMENOS, J. M., SEGARRA, M., FERNÁNDEZ, M. A. & ESPIELL, F. 1999. Characterization of the bottom ash in municipal solid waste incinerator. *Journal of Hazardous Materials,* 64**,** 211-222.

CORELLA, J. & SANZ, A. 2005. Modeling circulating fluidized bed biomass gasifiers. A pseudo-rigorous model for stationary state. *Fuel Processing Technology,* 86**,** 1021-1053.

COUTO, N. D., SILVA, V. B., MONTEIRO, E. & ROUBOA, A. 2015. Assessment of municipal solid wastes gasification in a semi-industrial gasifier using syngas quality indices. *Energy,* 93, Part 1**,** 864-873.

CROUCH, S. R., HOLLER, F. J. & SKOOG, D. A. 2007. *Principleof Instrumental Analysis,* US, Bellmonts.

CZAJCZYŃSKA, D., ANGUILANO, L., GHAZAL, H., KRZYŻYŃSKA, R., REYNOLDS, A. J., SPENCER, N. & JOUHARA, H. 2017. Potential of pyrolysis processes in the waste management sector. *Thermal Science and Engineering Progress,* 3**,** 171-197.

DAI, J., CUI, H. & GRACE, J. R. 2012. Biomass feeding for thermochemical reactors. *Progress in Energy and Combustion Science,* 38**,** 716-736.

DALAI, A. K., BATTA, N., ESWARAMOORTHI, I. & SCHOENAU, G. J. 2009. Gasification of refuse derived fuel in a fixed bed reactor for syngas production. *Waste Management,* 29**,** 252-258.

DE PAULI, A. R., ESPINOZA-QUIÑONES, F. R., TRIGUEROS, D. E. G., MÓDENES, A. N., DE SOUZA, A. R. C., BORBA, F. H. & KROUMOV, A. D. 2018. Integrated two-phase purification procedure for abatement of pollutants from sanitary landfill leachates. *Chemical Engineering Journal,* 334**,** 19-29.

DEMIRBAS, A. 2009. Global Renewable Energy Projections. *Energy Source,* 4**,** 212 - 224.

DEMIS, S., TAPALI, J. G. & PAPADAKIS, V. G. 2015. Plant Design and Economics of Rice Husk Ash Exploitation as a Pozzolanic Material. *Waste and Biomass Valorization***,** 1-11.

DEPARTMENT OF ENERGY SOUTH AFRICA 2011. Proposed Energy Mix Capacity Plan for Next Twenty Years - 2030. *Annual Report 2010/2011.*

DEPARTMENT OF ENVIRONMENTAL AFFAIRS 2012. National Waste Information Baseline Report. Pretoria, South Africa

DESWARTE, F. E. I., CLARK, J. H., WILSON, A. J., HARDY, J. J. E., MARRIOTT, R., CHAHAL, S. P., JACKSON, C., HESLOP, G., BIRKETT, M., BRUCE, T. J. & WHITELEY, G. 2007. Toward an integrated straw-based biorefinery. *Biofuels, Bioproducts and Biorefining,* 1**,** 245-254.

DIAZ, R. & WARITH, M. 2006. Life-cycle assessment of municipal solid wastes: Development of the WASTED model. *Waste Management,* 26**,** 886-901.

DORNBURG, V. & FAAIJ, A. P. C. 2001. Efficiency and economy of wood-fired biomass energy systems in relation to scale regarding heat and power generation using combustion and gasification technologies. *Biomass and Bioenergy,* 21**,** 91-108.

ENERGY, U. D. O. 2010. Worldwide Gasification Database US Department of Energy's National Energy Technology Laboratory. USA: US Department of Energy.

EUROPEAN COMMISSION 2010. Communication from the Commission to the Council and the European Parliament on Future Steps in Bio-waste Management in the European Union. *In:* COMMISSION, E. (ed.). COM(2010)235 Final, Brussels, Belgium.: European Commission.

EVANGELISTI, S., TAGLIAFERRI, C., CLIFT, R., LETTIERI, P., TAYLOR, R. & CHAPMAN, C. 2015. Life cycle assessment of conventional and two-stage advanced energy-from-waste technologies for municipal solid waste treatment. *Journal of Cleaner Production,* 100**,** 212-223.

FARHAD, S., HAMDULLAHPUR, F. & YOO, Y. 2010. Performance evaluation of different configurations of biogas-fuelled SOFC micro-CHP systems for residential applications. *International Journal of Hydrogen Energy,* 35**,** 3758-3768.

FARZANEH-KORD, V., KHOSHNEVIS, A. B., ARABKOOHSAR, A., DEYMI-DASHTEBAYAZ, M., AGHILI, M., KHATIB, M., KARGARAN, M. & FARZANEH-GORD, M. 2016. Defining a technical criterion for economic justification of employing CHP technology in city gate stations. *Energy,* 111**,** 389-401.

FATIH DEMIRBAS, M., BALAT, M. & BALAT, H. 2011. Biowastes-to-biofuels. *Energy Conversion and Management,* 52**,** 1815-1828.

FERNANDEZ-LOPEZ, M., PEDROCHE, J., VALVERDE, J. L. & SANCHEZ-SILVA, L. 2017. Simulation of the gasification of animal wastes in a dual gasifier using Aspen Plus®. *Energy Conversion and Management,* 140**,** 211-217.

FODOR, Z. & KLEMEŠ, J. J. 2012. Waste as alternative fuel – Minimising emissions and effluents by advanced design. *Process Safety and Environmental Protection,* 90, 263-284.

FORTEZA, R., FAR, M., SEGUí, C. & CERDÁ, V. 2004. Characterization of bottom ash in municipal solid waste incinerators for its use in road base. *Waste Management,* 24, 899-909.

FRIEDRICH, E. & TROIS, C. 2010. Greenhouse gases accounting and reporting for waste management – A South African perspective. *Waste Management,* 30, 2347-2353.

FRIEDRICH, E. & TROIS, C. 2013. GHG emission factors developed for the collection, transport and landfilling of municipal waste in South African municipalities. *Waste Management,* 33, 1013-1026.

FRIEDRICH, E. & TROIS, C. 2016. Current and future greenhouse gas (GHG) emissions from the management of municipal solid waste in the eThekwini Municipality – South Africa. *Journal of Cleaner Production,* 112, Part 5, 4071-4083.

FU, Z., ZHANG, S., LI, X., SHAO, J., WANG, K. & CHEN, H. 2015. MSW oxy-enriched incineration technology applied in China: Combustion temperature, flue gas loss and economic considerations. *Waste Management,* 38, 149-156.

GALVAGNO, S., CASCIARO, G., CASU, S., MARTINO, M., MINGAZZINI, C., RUSSO, A. & PORTOFINO, S. 2009. Steam gasification of tyre waste, poplar, and refuse-derived fuel: A comparative analysis. *Waste Management,* 29, 678-689.

GALVAGNO, S., CASU, S., CASCIARO, G., MARTINO, M., RUSSO, A. & PORTOFINO, S. 2006. Steam Gasification of Refuse-Derived Fuel (RDF): Influence of Process Temperature on Yield and Product Composition. *Energy & Fuels,* 20, 2284-2288.

GANDIGLIO, M., LANZINI, A., SANTARELLI, M. & LEONE, P. 2014. Design and optimization of a proton exchange membrane fuel cell CHP system for residential use. *Energy and Buildings,* 69, 381-393.

GHARFALKAR, M., COURT, R., CAMPBELL, C., ALI, Z. & HILLIER, G. 2015. Analysis of waste hierarchy in the European waste directive 2008/98/EC. *Waste Management,* 39**,** 305-313.

GODFREY, L. 2008. Facilitating the improved management of waste in South Africa through a national waste information system. *Waste Management,* 28**,** 1660-1671.

GRAVITIS, J. 2007. Zero techniques and systems – ZETS strength and weakness. *Journal of Cleaner Production,* 15**,** 1190-1197.

GREEN, D. W. & PERRY, R. H. 2008. *PERRY'S CHEMICAL ENGINEERS' HANDBOOK,* China, McGraw-Hill

HAIYING, Z., YOUCAI, Z. & JINGYU, Q. 2010. Characterization of heavy metals in fly ash from municipal solid waste incinerators in Shanghai. *Process Safety and Environmental Protection,* 88**,** 114-124.

HALDER, P. K., PAUL, N. & BEG, M. R. A. 2014. Assessment of biomass energy resources and related technologies practice in Bangladesh. *Renewable and Sustainable Energy Reviews,* 39**,** 444-460.

HAMAD, T. A., AGLL, A. A., HAMAD, Y. M., BAPAT, S., THOMAS, M., MARTIN, K. B. & SHEFFIELD, J. W. 2014. Study of a molten carbonate fuel cell combined heat, hydrogen and power system. *Energy,* 75**,** 579-588.

HASSELRIIS, F. & LICATA, A. 1996. Analysis of heavy metal emission data from municipal waste combustion. *Journal of Hazardous Materials,* 47**,** 77-102.

HAWKES, A., STAFFELL, I., BRETT, D. & BRANDON, N. 2009. Fuel cells for micro-combined heat and power generation. *Energy & Environmental Science,* 2**,** 729-744.

HAWKES, A. D., AGUIAR, P., HERNANDEZ-ARAMBURO, C. A., LEACH, M. A., BRANDON, N. P., GREEN, T. C. & ADJIMAN, C. S. 2006. Techno-economic modelling of a solid oxide fuel cell stack for micro combined heat and power. *Journal of Power Sources,* 156**,** 321-333.

HE, M., HU, Z., XIAO, B., LI, J., GUO, X., LUO, S., YANG, F., FENG, Y., YANG, G. & LIU, S. 2009a. Hydrogen-rich gas from catalytic steam gasification of municipal solid waste (MSW): Influence of catalyst and temperature on yield and product composition. *International Journal of Hydrogen Energy,* 34**,** 195-203.

HE, M., XIAO, B., HU, Z., LIU, S., GUO, X. & LUO, S. 2009b. Syngas production from catalytic gasification of waste polyethylene: Influence of temperature on gas yield and composition. *International Journal of Hydrogen Energy,* 34**,** 1342-1348.

HE, M., XIAO, B., LIU, S., GUO, X., LUO, S., XU, Z., FENG, Y. & HU, Z. 2009c. Hydrogen-rich gas from catalytic steam gasification of municipal solid waste (MSW): Influence of steam to MSW ratios and weight hourly space velocity on gas production and composition. *International Journal of Hydrogen Energy,* 34**,** 2174-2183.

HEDMAN, B., BURVALL, J., NILSSON, C. & MARKLUND, S. 2005. Emissions from small-scale energy production using co-combustion of biofuel and the dry fraction of household waste. *Waste Management,* 25**,** 311-321.

HINNELLS, M. 2008. Combined heat and power in industry and buildings. *Energy Policy,* 36**,** 4522-4526.

HOTTLE, T. A., BILEC, M. M., BROWN, N. R. & LANDIS, A. E. 2015. Toward zero waste: Composting and recycling for sustainable venue based events. *Waste Management,* 38**,** 86-94.

HUANG, Y., WANG, Y. D., REZVANI, S., MCILVEEN-WRIGHT, D. R., ANDERSON, M. & HEWITT, N. J. 2011. Biomass fuelled trigeneration system in selected buildings. *Energy Conversion and Management,* 52**,** 2448-2454.

HUI, Y., LI'AO, W., FENWEI, S. & GANG, H. 2006. Urban solid waste management in Chongqing: Challenges and opportunities. *Waste Management,* 26**,** 1052-1062.

HWANG, K.-L., CHOI, S.-M., KIM, M.-K., HEO, J.-B. & ZOH, K.-D. 2017. Emission of greenhouse gases from waste incineration in Korea. *Journal of Environmental Management,* 196**,** 710-718.

IKHU-OMOREGBE, D. & MAHOMED, S. 2012. Assessment of Calorific Value of Municipal Solid Wastes from City of Cape Town's Waste Disposal Facilities. *In:* NZIHOU, A. & CASTRO, F. (eds.) *Engineering for Waste and Biomass Valorisation* Porto, Portugal: Mines d' Albi.

IMAM, A., MOHAMMED, B., WILSON, D. C. & CHEESEMAN, C. R. 2008. Solid waste management in Abuja, Nigeria. *Waste Management,* 28**,** 468-472.

IOANNIDOU, A., MANENTI, S., LUIGI, G. & GROPPI, F. 2012. Fukushima fallout at Milano, Italy. *Journal of Environmental Radioactivity,* 114**,** 119-125.

IROBA, K. L., BAIK, O.-D. & TABIL, L. G. 2017. Torrefaction of biomass from municipal solid waste fractions II: Grindability characteristics, higher heating value, pelletability and moisture adsorption. *Biomass and Bioenergy,* 106**,** 8-20.

JANAJREH, I. & AL SHRAH, M. 2013. Numerical and experimental investigation of downdraft gasification of wood chips. *Energy Conversion and Management,* 65**,** 783-792.

JENKINS, B. M., BAXTER, L. L., MILES JR, T. R. & MILES, T. R. 1998. Combustion properties of biomass. *Fuel Processing Technology,* 54**,** 17-46.

JEONG, H. J., HWANG, I. S., PARK, S. S. & HWANG, J. 2017. Investigation on co-gasification of coal and biomass in Shell gasifier by using a validated gasification model. *Fuel,* 196**,** 371-377.

JIANG, L.-B., YUAN, X.-Z., LI, H., CHEN, X.-H., XIAO, Z.-H., LIANG, J., LENG, L.-J., GUO, Z. & ZENG, G.-M. 2016. Co-pelletization of sewage sludge and biomass: Thermogravimetric analysis and ash deposits. *Fuel Processing Technology,* 145**,** 109-115.

JIANG, L., LIANG, J., YUAN, X., LI, H., LI, C., XIAO, Z., HUANG, H., WANG, H. & ZENG, G. 2014. Co-pelletization of sewage sludge and biomass: The density and hardness of pellet. *Bioresource Technology,* 166**,** 435-443.

JIMENEZ, M. A. & KANE, E. H. 1974. Compatibility of Aluminum for Food Packaging. *Chemistry of Food Packaging.* AMERICAN CHEMICAL SOCIETY.

JUNG, C. H., MATSUTO, T., TANAKA, N. & OKADA, T. 2004. Metal distribution in incineration residues of municipal solid waste (MSW) in Japan. *Waste Management,* 24**,** 381-391.

KANEMATSU, Y., OOSAWA, K., OKUBO, T. & KIKUCHI, Y. 2017. Designing the scale of a woody biomass CHP considering local forestry reformation: A case study of Tanegashima, Japan. *Applied Energy,* 198**,** 160-172.

KANNAN, P., AL SHOAIBI, A. & SRINIVASAKANNAN, C. 2013a. Energy recovery from co-gasification of waste polyethylene and polyethylene terephthalate blends. *Computers & Fluids,* 88**,** 38-42.

KANNAN, P., AL SHOAIBI, A. & SRINIVASAKANNAN, C. 2013b. Energy recovery from co-gasification of waste polyethylene and polyethylene terephthalate blends. *Computers & Fluids,* 88**,** 38-42.

KARAKOULIDIS, K., MAVRIDIS, K., BANDEKAS, D. V., ADONIADIS, P., POTOLIAS, C. & VORDOS, N. 2011. Techno-economic analysis of a stand-alone hybrid photovoltaic-diesel–battery-fuel cell power system. *Renewable Energy,* 36**,** 2238-2244.

KELLY, E. P. 1996. *Quality Control Methods Ensure High-Quality Plastics for Recyling Resouce Recyling* US.

KHOO, H. H., LIM, T. Z. & TAN, R. B. H. 2010. Food waste conversion options in Singapore: Environmental impacts based on an LCA perspective. *Science of The Total Environment,* 408**,** 1367-1373.

KıRTAY, E. 2011. Recent advances in production of hydrogen from biomass. *Energy Conversion and Management,* 52**,** 1778-1789.

KLIMANTOS, P., KOUKOUZAS, N., KATSIADAKIS, A. & KAKARAS, E. 2009. Air-blown biomass gasification combined cycles (BGCC): System analysis and economic assessment. *Energy,* 34**,** 708-714.

KOCER, A., YAKA, I. F. & GUNGOR, A. 2017. Evaluation of greenhouse residues gasification performance in hydrogen production. *International Journal of Hydrogen Energy,* 42**,** 23244-23249.

KOPPEJAN, J. & VAN LOO, S. 2008. *Handbook of Biomass Combustion and Co-firing,* UK and USA Earthscan in the UK and USA

KORSGAARD, A. R., NIELSEN, M. P. & KÆR, S. K. 2008a. Part one: A novel model of HTPEM-based micro-combined heat and power fuel cell system. *International Journal of Hydrogen Energy,* 33**,** 1909-1920.

KORSGAARD, A. R., NIELSEN, M. P. & KÆR, S. K. 2008b. Part two: Control of a novel HTPEM-based micro combined heat and power fuel cell system. *International Journal of Hydrogen Energy,* 33**,** 1921-1931.

KORSGAARD, A. R., REFSHAUGE, R., NIELSEN, M. P., BANG, M. & KÆR, S. K. 2006. Experimental characterization and modeling of commercial polybenzimidazole-based MEA performance. *Journal of Power Sources,* 162**,** 239-245.

KORTOV, V. & USTYANTSEV, Y. 2013. Chernobyl accident: Causes, consequences and problems of radiation measurements. *Radiation Measurements,* 55**,** 12-16.

KOSSEVA, M. R. 2011. 6.44 - Management and Processing of Food Wastes. *In:* MOO-YOUNG, M. (ed.) *Comprehensive Biotechnology (Second Edition).* Burlington: Academic Press.

KOTZ, J. C., TREICHE, L. P. M. & TOWNSEND, J. R. 2010. *Chemisrtry and Chemical Reactivity,* 10 Davis Drive

Belmont, CA 94002-3098

USA, Mary Finch.

KUMAR, S., KWON, H.-T., CHOI, K.-H., HYUN CHO, J., LIM, W. & MOON, I. 2011. Current status and future projections of LNG demand and supplies: A global prospective. *Energy Policy,* 39**,** 4097-4104.

KWAK, T.-H., MAKEN, S., LEE, S., PARK, J.-W., MIN, B.-R. & YOO, Y. D. 2006. Environmental aspects of gasification of Korean municipal solid waste in a pilot plant. *Fuel,* 85**,** 2012-2017.

LEGGETT, L. M. W. & BALL, D. A. 2012. The implication for climate change and peak fossil fuel of the continuation of the current trend in wind and solar energy production. *Energy Policy,* 41**,** 610-617.

LI, C. & SUZUKI, K. 2009. Tar property, analysis, reforming mechanism and model for biomass gasification—An overview. *Renewable and Sustainable Energy Reviews,* 13**,** 594-604.

LI, H., JIANG, L.-B., LI, C.-Z., LIANG, J., YUAN, X.-Z., XIAO, Z.-H., XIAO, Z.-H. & WANG, H. 2015. Co-pelletization of sewage sludge and biomass: The energy input and properties of pellets. *Fuel Processing Technology,* 132**,** 55-61.

LI, H., LIU, X., LEGROS, R., BI, X. T., JIM LIM, C. & SOKHANSANJ, S. 2012a. Pelletization of torrefied sawdust and properties of torrefied pellets. *Applied Energy,* 93**,** 680-685.

LI, H., QIAN, X., HU, W., WANG, Y. & GAO, H. 2013. Chemical speciation and human health risk of trace metals in urban street dusts from a metropolitan city, Nanjing, SE China. *Science of The Total Environment,* 456–457**,** 212-221.

LI, Q., JENSEN, J. O., SAVINELL, R. F. & BJERRUM, N. J. 2009. High temperature proton exchange membranes based on polybenzimidazoles for fuel cells. *Progress in Polymer Science,* 34**,** 449-477.

LI, Y.-C., LIU, Y.-F., CHU, C.-Y., CHANG, P.-L., HSU, C.-W., LIN, P.-J. & WU, S.-Y. 2012b. Techno-economic evaluation of biohydrogen production from wastewater and agricultural waste. *International Journal of Hydrogen Energy,* 37**,** 15704-15710.

LIANG, L., SUN, R., FEI, J., WU, S., LIU, X., DAI, K. & YAO, N. 2008. Experimental study on effects of moisture content on combustion characteristics of simulated municipal solid wastes in a fixed bed. *Bioresource Technology,* 99, 7238-7246.

LINO, F. A. M. & ISMAIL, K. A. R. 2017. Incineration and recycling for MSW treatment: Case study of Campinas, Brazil. *Sustainable Cities and Society,* 35, 752-757.

LIU, A., REN, F., LIN, W. Y. & WANG, J.-Y. 2015. A review of municipal solid waste environmental standards with a focus on incinerator residues. *International Journal of Sustainable Built Environment,* 4, 165-188.

LIU, H., KONG, S., LIU, Y. & ZENG, H. 2012. Pollution Control Technologies of Dioxins in Municipal Solid Waste Incinerator. *Procedia Environmental Sciences,* 16, 661-668.

LIU, J., NIU, D. & SONG, X. 2013a. The Energy Supply and Demand Pattern of China: A Review of Evolution and Sustainable Development. *Renewable and Sustainable Energy Reviews,* 25, 220 - 228.

LIU, W.-W., HU, C.-W., YANG, Y., TONG, D.-M., ZHU, L.-F., ZHANG, R.-N. & ZHAO, B.-H. 2013b. Study on the effect of metal types in (Me)-Al-MCM-41 on the mesoporous structure and catalytic behavior during the vapor-catalyzed co-pyrolysis of pubescens and LDPE. *Applied Catalysis B: Environmental,* 129, 202-213.

LIU, Z., QUEK, A. & BALASUBRAMANIAN, R. 2014. Preparation and characterization of fuel pellets from woody biomass, agro-residues and their corresponding hydrochars. *Applied Energy,* 113, 1315-1322.

LONG, H., LI, X., WANG, H. & JIA, J. 2013. Biomass resources and their bioenergy potential estimation: A review. *Renewable and Sustainable Energy Reviews,* 26, 344-352.

LOPES, E. J., OKAMURA, L. A. & YAMAMOTO, C. I. 2015. FORMATION OF DIOXINS AND FURANS DURING MUNICIPAL SOLID WASTE GASIFICATION. *Brazilian Journal of Chemical Engineering,* 32, 87-97.

LOPEZ, G., ARTETXE, M., AMUTIO, M., ALVAREZ, J., BILBAO, J. & OLAZAR, M. 2018. Recent advances in the gasification of waste plastics. A critical overview. *Renewable and Sustainable Energy Reviews,* 82, Part 1**,** 576-596.

LOPPINET-SERANI, A., AYMONIER, C. & CANSELL, F. 2008. Current and Foreseeable Applications of Supercritical Water for Energy and the Environment. *ChemSusChem,* 1**,** 486-503.

LU, J.-W., ZHANG, S., HAI, J. & LEI, M. 2017. Status and perspectives of municipal solid waste incineration in China: A comparison with developed regions. *Waste Management.*

MAKARENKO, N. & BUDAK, O. 2017. Waste management in Ukraine: Municipal solid waste landfills and their impact on rural areas. *Annals of Agrarian Science,* 15**,** 80-87.

MAMLOUK, M. & SCOTT, K. 2011a. Analysis of high temperature polymer electrolyte membrane fuel cell electrodes using electrochemical impedance spectroscopy. *Electrochimica Acta,* 56**,** 5493-5512.

MAMLOUK, M. & SCOTT, K. 2011b. Phosphoric acid-doped electrodes for a PBI polymer membrane fuel cell. *International Journal of Energy Research,* 35**,** 507-519.

MANGIZVO, R. V. 2008. Management practices at the Mucheke municipal solid waste disposal site in Masvingo City, in

Zimbabwe. *Journal of Sustainable Development in Africa,* 10**,** 147-164

MASTELLONE, M. L., ZACCARIELLO, L. & ARENA, U. 2010. Co-gasification of coal, plastic waste and wood in a bubbling fluidized bed reactor. *Fuel,* 89**,** 2991-3000.

MATSUO, Y., YANAGISAWA, A. & YAMASHITA, Y. 2013. A global energy outlook to 2035 with strategic considerations for Asia and Middle East energy supply and demand interdependencies. *Energy Strategy Reviews,* 2**,** 79-91.

MCILVEEN-WRIGHT, D. R., HUANG, Y., REZVANI, S., REDPATH, D., ANDERSON, M., DAVE, A. & HEWITT, N. J. 2013. A technical and economic analysis of three large scale biomass combustion plants in the UK. *Applied Energy,* 112**,** 396-404.

MCILVEEN-WRIGHT, D. R., MOGLIE, M., REZVANI, S., HUANG, Y., ANDERSON, M., REDPATH, D., DAVE, A. & HEWITT, N. J. 2011. A techno-economic analysis of biomass gasifiers integrated with high and intermediate temperature solid oxide fuel cells. *International Journal of Energy Research,* 35**,** 1037-1047.

MCKAY, G. 2002. Dioxin characterisation, formation and minimisation during municipal solid waste (MSW) incineration: review. *Chemical Engineering Journal,* 86**,** 343-368.

MCMAHON, D. 2015. Viessmann installs first fuel cell CHP system in UK home, ahead of 2016 market rollout. *Fuel Cells Bulletin,* 2015**,** 12-14.

MELIKOGLU, M. 2013a. Vision 2023: Assessing the feasibility of electricity and biogas production from municipal solid waste in Turkey. *Renewable and Sustainable Energy Reviews,* 19**,** 52-63.

MELIKOGLU, M. 2013b. Vision 2023: Feasibility analysis of Turkey's renewable energy projection. *Renewable Energy,* 50**,** 570-575.

METIN, E., ERÖZTÜRK, A. & NEYIM, C. 2003. Solid waste management practices and review of recovery and recycling operations in Turkey. *Waste Management,* 23**,** 425-432.

METTANANT, V., BASU, P. & BUTLER, J. 2009a. Agglomeration of biomass fired fluidized bed gasifier and combustor. *The Canadian Journal of Chemical Engineering,* 87**,** 656-684.

METTANANT, V., BASU, P. & LEON, M. A. 2009b. Gasification of Rice Husk in Supercritical Water. *World Conference on Chemical Engineering.* Montreal, .

MEWR (MINISTRY OF THE ENVIRONMENT AND WATER RESOURCES) 2012. Singapore Green Plan 2012, 2008. Singapore: MEWR (Ministry of the Environment and Water Resources).

MIKALSEN, R., WANG, Y. D. & ROSKILLY, A. P. 2009. A comparison of Miller and Otto cycle natural gas engines for small scale CHP applications. *Applied Energy,* 86**,** 922-927.

MILNE, T. 2002. *Pyrolysis:The Thermal Behaviour of Biomass Below 600 ^{0}C,* UK, Biomass Energy Foundation Press.

MOGHADAM, R. A., YUSUP, S., UEMURA, Y., CHIN, B. L. F., LAM, H. L. & AL SHOAIBI, A. 2014. Syngas production from palm kernel shell and polyethylene waste blend in fluidized bed catalytic steam co-gasification process. *Energy,* 75**,** 40-44.

MOHAN, D., PITTMAN, C. U. & STEELE, P. H. 2006. Pyrolysis of Wood/Biomass for Bio-oil: A Critical Review. *Energy & Fuels,* 20**,** 848-889.

MONGIBELLO, L., BIANCO, N., CALIANO, M. & GRADITI, G. 2016. Comparison between two different operation strategies for a heat-driven residential natural gas-fired CHP system: Heat dumping vs. load partialization. *Applied Energy,* 184**,** 55-67.

MONICA, E. K. 2009. *Pulp and Paper Chemistry and Technology Volume 4 Paper Products Physics and Technology* KG, 10785 Berlin., Walter de Gruyter GmbH & Co. KG, 10785 Berlin.

MONTUORI, L., ALCÁZAR-ORTEGA, M., ÁLVAREZ-BEL, C. & DOMIJAN, A. 2014. Integration of renewable energy in microgrids coordinated with demand response resources: Economic evaluation of a biomass gasification plant by Homer Simulator. *Applied Energy,* 132**,** 15-22.

MONTUORI, L., VARGAS-SALGADO, C. & ALCÁZAR-ORTEGA, M. 2015. Impact of the throat sizing on the operating parameters in an experimental fixed bed gasifier: Analysis, evaluation and testing. *Renewable Energy,* 83**,** 615-625.

MORIARTY, P. & HONNERY, D. 2012. What is the global potential for renewable energy? *Renewable and Sustainable Energy Reviews,* 16**,** 244-252.

MOSER, H. 2010. *High Temperature Proton Exchange Membrane Fuel Cell:The Impact of Fuel Contanminant and Temperature on Fuel Cell Performance* USA, VDM Verlag Dr. Muller Aktiengesellschaft & Co.

MURESAN, M., CORMOS, C.-C. & AGACHI, P.-S. 2013. Techno-economical assessment of coal and biomass gasification-based hydrogen production supply chain system. *Chemical Engineering Research and Design,* 91**,** 1527-1541.

NAHMAN, A. 2011. Pricing landfill externalities: Emissions and disamenity costs in Cape Town, South Africa. *Waste Management,* 31**,** 2046-2056.

NAJAFI, B., HAGHIGHAT MAMAGHANI, A., RINALDI, F. & CASALEGNO, A. 2015. Long-term performance analysis of an HT-PEM fuel cell based micro-CHP system: Operational strategies. *Applied Energy,* 147**,** 582-592.

NAROBE, M., GOLOB, J., KLINAR, D., FRANCETIČ, V. & LIKOZAR, B. 2014. Co-gasification of biomass and plastics: Pyrolysis kinetics studies, experiments on 100 kW dual fluidized bed pilot plant and development of thermodynamic equilibrium model and balances. *Bioresource Technology,* 162**,** 21-29.

NAZARI, M. E. & ARDEHALI, M. M. 2017. Profit-based unit commitment of integrated CHP-thermal-heat only units in energy and spinning reserve markets with considerations for environmental CO2 emission cost and valve-point effects. *Energy,* 133**,** 621-635.

NEA (NATIONAL ENVIRONMENTAL AGENCY) 2009. Solid Waste Management. NEA (National Environmental Agency). .

NG, W. P. Q., LAM, H. L., VARBANOV, P. S. & KLEMEŠ, J. J. 2014. Waste-to-Energy (WTE) network synthesis for Municipal Solid Waste (MSW). *Energy Conversion and Management,* 85**,** 866-874.

NI, M., LEUNG, D. Y. C., LEUNG, M. K. H. & SUMATHY, K. 2006. An overview of hydrogen production from biomass. *Fuel Processing Technology,* 87**,** 461-472.

NORBU, T., VISVANATHAN, C. & BASNAYAKE, B. 2005. Pretreatment of municipal solid waste prior to landfilling. *Waste Management,* 25**,** 997-1003.

NOVATLANTIS 2005. Smarter Living - Generating a New Understanding for Natural Resources as the Key to Sustainable Development. *The 2000-Watt Society, Dübendorf, Switzerland.* The 2000-Watt Society, Dübendorf, Switzerland.: Dübendorf, Switzerland.

NOWAK, B., ASCHENBRENNER, P. & WINTER, F. 2013. Heavy metal removal from sewage sludge ash and municipal solid waste fly ash — A comparison. *Fuel Processing Technology,* 105**,** 195-201.

NZIHOU, A. & STANMORE, B. 2013. The fate of heavy metals during combustion and gasification of contaminated biomass—A brief review. *Journal of Hazardous Materials,* 256**,** 56-66.

OKONKWO, J. O. & MOTHIBA, M. 2005. Physico-chemical characteristics and pollution levels of heavy metals in the rivers in Thohoyandou, South Africa. *Journal of Hydrology,* 308**,** 122-127.

ORLANDO, J. A. 1996. Cogeneration Design Guide. USA: ASHRAE Inc. : USA: ASHRAE Inc. .

OTHMAN, S. N., ZAINON NOOR, Z., ABBA, A. H., YUSUF, R. O. & ABU HASSAN, M. A. 2013. Review on life cycle assessment of integrated solid waste management in some Asian countries. *Journal of Cleaner Production,* 41**,** 251-262.

OUADI, M., BRAMMER, J. G., KAY, M. & HORNUNG, A. 2013. Fixed bed downdraft gasification of paper industry wastes. *Applied Energy,* 103**,** 692-699.

PAN, C., HE, R., LI, Q., JENSEN, J. O., BJERRUM, N. J., HJULMAND, H. A. & JENSEN, A. B. 2005. Integration of high temperature PEM fuel cells with a methanol reformer. *Journal of Power Sources,* 145**,** 392-398.

PANTALEO, A. M., CAMPOREALE, S. & FORTUNATO, B. 2015. Small scale biomass CHP: Techno-economic performance of steam vs gas turbines with bottoming ORC. *Energy Procedia,* 82**,** 825-832.

PARIKH, J., CHANNIWALA, S. A. & GHOSAL, G. K. 2005. A correlation for calculating HHV from proximate analysis of solid fuels. *Fuel,* 84**,** 487-494.

PARK, J. H., PARK, H.-W., CHOI, S. & PARK, D.-W. 2016. Effects of blend ratio between high density polyethylene and biomass on co-gasification behavior in a two-stage gasification system. *International Journal of Hydrogen Energy,* 41**,** 16813-16822.

PATUZZI, F., PRANDO, D., VAKALIS, S., RIZZO, A. M., CHIARAMONTI, D., TIRLER, W., MIMMO, T., GASPARELLA, A. & BARATIERI, M. 2016. Small-scale biomass gasification CHP systems: Comparative performance assessment and monitoring experiences in South Tyrol (Italy). *Energy,* 112**,** 285-293.

PAZÓ, J. A., GRANADA, E., SAAVEDRA, A., EGUÍA, P. & COLLAZO, J. 2010. Biomass Thermogravimetric Analysis: Uncertainty Determination Methodology and Sampling Maps Generation. *Journal of International Molecular Sciences,* 11**,** 2701-2714.

PEIGHAMBARDOUST, S. J., ROWSHANZAMIR, S. & AMJADI, M. 2010. Review of the proton exchange membranes for fuel cell applications. *International Journal of Hydrogen Energy,* 35**,** 9349-9384.

PELLEGRINO, S., LANZINI, A. & LEONE, P. 2015. Techno-economic and policy requirements for the market-entry of the fuel cell micro-CHP system in the residential sector. *Applied Energy,* 143**,** 370-382.

PETERS, M. S., TIMMERHAUS, K. D. & WEST, R. E. 2013. *Plant Design and Economics for Chemical Engineers,* India, McGraw-Hill Chemical Engineers.

PINTO, F., FRANCO, C., ANDRÉ, R. N., MIRANDA, M., GULYURTLU, I. & CABRITA, I. 2002. Co-gasification study of biomass mixed with plastic wastes. *Fuel,* 81**,** 291-297.

PLIS, P. & WILK, R. K. 2011. Theoretical and experimental investigation of biomass gasification process in a fixed bed gasifier. *Energy,* 36**,** 3838-3845.

POLLET, B. G. 2013. Mission and objectives of the Hydrogen South Africa (HySA) Systems Competence Centre. *Fuel Cells Bulletin,* 2013**,** 10-17.

POLLET, B. G., PASUPATHI, S., SWART, G., MOUTON, K., LOTOTSKYY, M., WILLIAMS, M., BUJLO, P., JI, S., BLADERGROEN, B. J. & LINKOV, V. 2014. Hydrogen South Africa (HySA) Systems Competence Centre: Mission, objectives, technological achievements and breakthroughs. *International Journal of Hydrogen Energy,* 39**,** 3577-3596.

POUDEL, J., OHM, T.-I. & OH, S. C. 2015. A study on torrefaction of food waste. *Fuel,* 140**,** 275-281.

PUIG-ARNAVAT, M., SHANG, L., SÁROSSY, Z., AHRENFELDT, J. & HENRIKSEN, U. B. 2016. From a single pellet press to a bench scale pellet mill — Pelletizing six different biomass feedstocks. *Fuel Processing Technology,* 142**,** 27-33.

QUINA, M. J., BORDADO, J. C. & QUINTA-FERREIRA, R. M. 2008. Treatment and use of air pollution control residues from MSW incineration: An overview. *Waste Management,* 28**,** 2097-2121.

RAMOS, A., MONTEIRO, E., SILVA, V. & ROUBOA, A. 2018. Co-gasification and recent developments on waste-to-energy conversion: A review. *Renewable and Sustainable Energy Reviews,* 81**,** 380-398.

RAO, C. V., PARRONDO, J., GHATTY, S. L. & RAMBABU, B. 2010. High temperature polymer electrolyte membrane fuel cell performance of PtxCoy/C cathodes. *Journal of Power Sources,* 195**,** 3425-3430.

REN, H. & GAO, W. 2010. Economic and environmental evaluation of micro CHP systems with different operating modes for residential buildings in Japan. *Energy and Buildings,* 42**,** 853-861.

RIGHI, S., OLIVIERO, L., PEDRINI, M., BUSCAROLI, A. & DELLA CASA, C. 2013. Life Cycle Assessment of management systems for sewage sludge and food waste: centralized and decentralized approaches. *Journal of Cleaner Production,* 44**,** 8-17.

ROVAS, D. & ZABANIOTOU, A. 2015. Exergy analysis of a small gasification-ICE integrated system for CHP production fueled with Mediterranean agro-food processing wastes: The SMARt-CHP. *Renewable Energy,* 83**,** 510-517.

RUOPPOLO, G., AMMENDOLA, P., CHIRONE, R. & MICCIO, F. 2012. H2-rich syngas production by fluidized bed gasification of biomass and plastic fuel. *Waste Management,* 32**,** 724-732.

RYU, C., FINNEY, K., SHARIFI, V. N. & SWITHENBANK, J. 2008. Pelletised fuel production from coal tailings and spent mushroom compost — Part I: Identification of pelletisation parameters. *Fuel Processing Technology,* 89**,** 269-275.

SAHIN, H. T. & ARSLAN, M. B. 2008. A Study on Physical and Chemical Properties of Cellulose Paper Immersed in Various Solvent Mixtures. *International Journal of Molecular Sciences.,* 9**,** 78 - 88.

SALOMÓN, M., SAVOLA, T., MARTIN, A., FOGELHOLM, C.-J. & FRANSSON, T. 2011. Small-scale biomass CHP plants in Sweden and Finland. *Renewable and Sustainable Energy Reviews,* 15**,** 4451-4465.

SAXENA, R. C., SEAL, D., KUMAR, S. & GOYAL, H. B. 2008. Thermo-chemical routes for hydrogen rich gas from biomass: A review. *Renewable and Sustainable Energy Reviews,* 12**,** 1909-1927.

SCARLAT, N., MOTOLA, V., DALLEMAND, J. F., MONFORTI-FERRARIO, F. & MOFOR, L. 2015. Evaluation of energy potential of Municipal Solid Waste from African urban areas. *Renewable and Sustainable Energy Reviews,* 50**,** 1269-1286.

SCHEFFLAN, R. 2011. *Teach yourself the Basics of Aspen Plus,* USA, Hoboken, New Jersey, MA 07030, USA: AIChe and Wiley & Sons Inc. .

SECANELL, M., WISHART, J. & DOBSON, P. 2011. Computational design and optimization of fuel cells and fuel cell systems: A review. *Journal of Power Sources,* 196**,** 3690-3704.

SEKITO, T., DOTE, Y., ONOUE, K., SAKANAKURA, H. & NAKAMURA, K. 2014. Characteristics of element distributions in an MSW ash melting treatment system. *Waste Management,* 34**,** 1637-1643.

SEN, R. & BHATTACHARYYA, S. C. 2014. Off-grid electricity generation with renewable energy technologies in India: An application of HOMER. *Renewable Energy,* 62**,** 388-398.

SHAMARDINA, O., CHERTOVICH, A., KULIKOVSKY, A. A. & KHOKHLOV, A. R. 2010. A simple model of a high temperature PEM fuel cell. *International Journal of Hydrogen Energy,* 35**,** 9954-9962.

SHARAF, O. Z. & ORHAN, M. F. 2014. An overview of fuel cell technology: Fundamentals and applications. *Renewable and Sustainable Energy Reviews,* 32**,** 810-853.

SHARHOLY, M., AHMAD, K., MAHMOOD, G. & TRIVEDI, R. C. 2008. Municipal solid waste management in Indian cities – A review. *Waste Management,* 28**,** 459-467.

SHARIFI, Z. & RENELLA, G. 2015. Assessment of a particle size fractionation as a technology for reducing heavy metal, salinity and impurities from compost produced by municipal solid waste. *Waste Management,* 38**,** 95-101.

SHI, H., MAHINPEY, N., AQSHA, A. & SILBERMANN, R. 2016. Characterization, thermochemical conversion studies, and heating value modeling of municipal solid waste. *Waste Management,* 48**,** 34-47.

SIKARWAR, V. S. & ZHAO, M. 2017. Biomass Gasification A2 - Abraham, Martin A. *Encyclopedia of Sustainable Technologies.* Oxford: Elsevier.

SINGH, D. J. & KALAMDHAD, A. 2011. *Effects of Heavy Metals on Soil, Plants, Human Health and Aquatic Life.*

SINGH, R. P., TYAGI, V. V., ALLEN, T., IBRAHIM, M. H. & KOTHARI, R. 2011. An overview for exploring the possibilities of energy generation from municipal solid waste (MSW) in Indian scenario. *Renewable and Sustainable Energy Reviews,* 15**,** 4797-4808.

SINNOTT, R. & TOWLER, G. 2012. *Chemical Enginnering Design,* USA, Butterworth-Heinemann Elsevier.

SIRITHEERASAS, P., WAIYANATE, P., SEKIGUCHI, H. & KODAMA, S. 2017. Torrefaction of Municipal Solid Waste (MSW) Pellets using Microwave Irradiation with the Assistance of the Char of Agricultural Residues. *Energy Procedia,* 138**,** 668-673.

SKOULOU, V., KOUFODIMOS, G., SAMARAS, Z. & ZABANIOTOU, A. 2008a. Low Temperature Gasification of Olive Kernel in a 5-KW Fluidized Bed Reactor for H2-rich Production Gas. *International Journal of Hydrogen Energy,* 33**,** 6515 - 6524.

SKOULOU, V., KOUFODIMOS, G., SAMARAS, Z. & ZABANIOTOU, A. 2008b. Low temperature gasification of olive kernels in a 5-kW fluidized bed reactor for H2-rich producer gas. *International Journal of Hydrogen Energy,* 33**,** 6515-6524.

SKOULOU, V., ZABANIOTOU, A., STAVROPOULOS, G. & SAKELAROPOULOS, G. 2008c. Syngas production from olive tree cuttings and olive kernels in a downdraft fixed-bed gasifier. *International Journal of Hydrogen Energy,* 33**,** 1185-1194.

SMITH, R. 2005. *Chemical Process Design and Integration. ,* UK, John Wiley & Sons Ltd.

SMITH, S. R. 2009. A critical review of the bioavailability and impacts of heavy metals in municipal solid waste composts compared to sewage sludge. *Environment International,* 35**,** 142-156.

SOLTANI, A., SADIQ, R. & HEWAGE, K. Selecting sustainable waste-to-energy technologies for municipal solid waste treatment: a game theory approach for group decision-making. *Journal of Cleaner Production.*

SOLTANI, A., SADIQ, R. & HEWAGE, K. 2016. Selecting sustainable waste-to-energy technologies for municipal solid waste treatment: a game theory approach for group decision-making. *Journal of Cleaner Production,* 113**,** 388-399.

SOMORIN, T. O., ADESOLA, S. & KOLAWOLE, A. 2017. State-level assessment of the waste-to-energy potential (via incineration) of municipal solid wastes in Nigeria. *Journal of Cleaner Production,* 164**,** 804-815.

SONG, G.-J., KIM, K.-H., SEO, Y.-C. & KIM, S.-C. 2004. Characteristics of ashes from different locations at the MSW incinerator equipped with various air pollution control devices. *Waste Management,* 24**,** 99-106.

SONG, J., SUN, Y. & JIN, L. 2017. PESTEL analysis of the development of the waste-to-energy incineration industry in China. *Renewable and Sustainable Energy Reviews,* 80**,** 276-289.

SONG, Q., WANG, Z. & LI, J. 2013. Environmental performance of municipal solid waste strategies based on LCA method: a case study of Macau. *Journal of Cleaner Production,* 57**,** 92-100.

SOTUDEH-GHAREBAAGH, R., LEGROS, R., CHAOUKI, J. & PARIS, J. 1998. Simulation of circulating fluidized bed reactors using ASPEN PLUS. *Fuel,* 77**,** 327-337.

STAFFELL, I. 2015a. Zero carbon infinite COP heat from fuel cell CHP. *Applied Energy,* 147**,** 373-385.

STAFFELL, I. 2015b. Zero carbon infinite COP heat from fuel cell CHP. *Applied Energy,* 147**,** 373-385.

STAFFELL, I. & GREEN, R. 2013. The cost of domestic fuel cell micro-CHP systems. *International Journal of Hydrogen Energy,* 38**,** 1088-1102.

STELTE, W., CLEMONS, C., HOLM, J. K., SANADI, A. R., AHRENFELDT, J., SHANG, L. & HENRIKSEN, U. B. 2011a. Pelletizing properties of torrefied spruce. *Biomass and Bioenergy,* 35**,** 4690-4698.

STELTE, W., HOLM, J. K., SANADI, A. R., BARSBERG, S., AHRENFELDT, J. & HENRIKSEN, U. B. 2011b. Fuel pellets from biomass: The importance of the pelletizing pressure and its dependency on the processing conditions. *Fuel,* 90, 3285-3290.

STELTE, W., SANADI, A. R., SHANG, L., HOLM, J. K., AHRENFELDT, J. & HENRIKSEN, U. B. 2012. *RECENT DEVELOPMENTS IN BIOMASS PELLETIZATION – A REVIEW.*

SUHA YAZICI, M. 2010. Hydrogen and fuel cell activities at UNIDO-ICHET. *International Journal of Hydrogen Energy,* 35, 2754-2761.

TAN, R. B. H. & KHOO, H. H. 2006. Impact Assessment of Waste Management Options in Singapore. *Journal of Air Waste Management Association,* 56, 244 - 254.

TANG, P., FLOREA, M. V. A., SPIESZ, P. & BROUWERS, H. J. H. 2015. Characteristics and application potential of municipal solid waste incineration (MSWI) bottom ashes from two waste-to-energy plants. *Construction and Building Materials,* 83, 77-94.

TEYMOURIHAMZEHKOLAEI, F. & SATTARI, S. 2011. Technical and economic feasibility study of using Micro CHP in the different climate zones of Iran. *Energy,* 36, 4790-4798.

THAKARE, S. & NANDI, S. 2016. Study on Potential of Gasification Technology for Municipal Solid Waste (MSW) in Pune City. *Energy Procedia,* 90, 509-517.

TIAN, H., GAO, J., HAO, J., LU, L., ZHU, C. & QIU, P. 2013. Atmospheric pollution problems and control proposals associated with solid waste management in China: A review. *Journal of Hazardous Materials,* 252–253, 142-154.

TINAUT, F. V., MELGAR, A., PÉREZ, J. F. & HORRILLO, A. 2008. Effect of biomass particle size and air superficial velocity on the gasification process in a downdraft fixed bed gasifier. An experimental and modelling study. *Fuel Processing Technology,* 89, 1076-1089.

TORCHIO, M. F. 2015. Comparison of district heating CHP and distributed generation CHP with energy, environmental and economic criteria for Northern Italy. *Energy Conversion and Management,* 92**,** 114-128.

TÓTH, G., HERMANN, T., DA SILVA, M. R. & MONTANARELLA, L. 2016. Heavy metals in agricultural soils of the European Union with implications for food safety. *Environment International,* 88**,** 299-309.

TOWLER, G. & SINNOTT, R. 2013. *Chemical Engineering Design: Principles, Practice and Economics of Plant and Process Design,* United States of America, Butterworth-Heinemann is an imprint of Elsevier, 225 Wyman Street, Waltham, MA 02451, USA.

TOZLU, A., ÖZAHI, E. & ABUŞOĞLU, A. 2016. Waste to energy technologies for municipal solid waste management in Gaziantep. *Renewable and Sustainable Energy Reviews,* 54**,** 809-815.

TROSCHINETZ, A. M. & MIHELCIC, J. R. 2009. Sustainable recycling of municipal solid waste in developing countries. *Waste Management,* 29**,** 915-923.

TSAI, W.-T. & KUO, K.-C. 2010. An analysis of power generation from municipal solid waste (MSW) incineration plants in Taiwan. *Energy,* 35**,** 4824-4830.

UD DIN, Z. & ZAINAL, Z. A. 2016. Biomass integrated gasification–SOFC systems: Technology overview. *Renewable and Sustainable Energy Reviews,* 53**,** 1356-1376.

USEPA 1993. Clean Water Act., Section Volume 58 1993: USEPA (US Environmetal Protection Agency) 1993.

USEPA 2002. Solid Waste Management and Greenhouse Gases. A Life-cycle Assessment of Emissions and Sinks. *A Life-cycle Assessment of Emissions and Sinks.* USEPA (Environmental Protection Agency).

USEPA 2015. Advancing Sustainable Materials Management: Facts and Figures 2013. Assessing Trend in Materials Generation, Recycling and Disposal in the United States. US: USEPA (Environmetal Protection Agency) 2015.

VODYANITSKII, Y. N. 2016. Standards for the contents of heavy metals in soils of some states. *Annals of Agrarian Science,* 14**,** 257-263.

VOSSBERG, C., MASON-JONES, K. & COHEN, B. 2014. An energetic life cycle assessment of C&D waste and container glass recycling in Cape Town, South Africa. *Resources, Conservation and Recycling,* 88**,** 39-49.

VYAS, D. K. & SINGH, R. N. 2007. Feasibility study of Jatropha seed husk as an open core gasifier feedstock. *Renewable Energy,* 32**,** 512-517.

WANG, H., XU, J., YU, H., LIU, X., YIN, W., LIU, Y., LIU, Z. & ZHANG, T. 2015. Study of the application and methods for the comprehensive treatment of municipal solid waste in northeastern China. *Renewable and Sustainable Energy Reviews,* 52**,** 1881-1889.

WANG, J.-J., XU, Z.-L., JIN, H.-G., SHI, G.-H., FU, C. & YANG, K. 2014a. Design optimization and analysis of a biomass gasification based BCHP system: A case study in Harbin, China. *Renewable Energy,* 71**,** 572-583.

WANG, L., SKJEVRAK, G., HUSTAD, J. E. & SKREIBERG, Ø. 2014b. Investigation of Biomass Ash Sintering Characteristics and the Effect of Additives. *Energy & Fuels,* 28**,** 208-218.

WANG, L. K. & PEREIRA, N. C. 1980. *Solid waste processing and resource recovery*, Humana Press.

WANG, Y., CHEN, K. S., MISHLER, J., CHO, S. C. & ADROHER, X. C. 2011. A review of polymer electrolyte membrane fuel cells: Technology, applications, and needs on fundamental research. *Applied Energy,* 88**,** 981-1007.

WANG, Z. & GENG, L. 2015. Carbon emissions calculation from municipal solid waste and the influencing factors analysis in China. *Journal of Cleaner Production,* 104**,** 177-184.

WILLIAMS, B. C. & MCMULLAN, J. T. 1996. Techno-economic analysis of fuel conversion and power generation systems — the development of a portable chemical process simulator with capital cost and economic performance analysis capabilities. *International Journal of Energy Research,* 20**,** 125-142.

WILLIAMS, I. D. 2015. Forty years of the waste hierarchy. *Waste Management,* 40**,** 1-2.

WISSING, F., WIRTZ, S. & SCHERER, V. 2017. Simulating municipal solid waste incineration with a DEM/CFD method – Influences of waste properties, grate and furnace design. *Fuel,* 206**,** 638-656.

WOOD, S. R. & ROWLEY, P. N. 2011. A techno-economic analysis of small-scale, biomass-fuelled combined heat and power for community housing. *Biomass and Bioenergy,* 35**,** 3849-3858.

WRIGHT, M. M. & BROWN, R. C. 2007. Comparative economics of biorefineries based on the biochemical and thermochemical platforms. *Biofuels, Bioproducts and Biorefining,* 1**,** 49-56.

WU, C. & WILLIAMS, P. T. 2010a. Pyrolysis–gasification of plastics, mixed plastics and real-world plastic waste with and without Ni–Mg–Al catalyst. *Fuel,* 89**,** 3022-3032.

WU, C. & WILLIAMS, P. T. 2010b. Pyrolysis–gasification of post-consumer municipal solid plastic waste for hydrogen production. *International Journal of Hydrogen Energy,* 35**,** 949-957.

WU, D., XU, T., WU, L. & WU, Y. 2009. Hybrid acid–base polymer membranes prepared for application in fuel cells. *Journal of Power Sources,* 186**,** 286-292.

WU, M.-H., LIN, C.-L. & ZENG, W.-Y. 2014. Effect of waste incineration and gasification processes on heavy metal distribution. *Fuel Processing Technology,* 125**,** 67-72.

WU, Z., MENG, H., LUO, Z., CHEN, L., ZHAO, J. & WANG, S. 2017. Performance evaluation on co-gasification of bituminous coal and wheat straw in entrained flow gasification system. *International Journal of Hydrogen Energy,* 42**,** 18884-18893.

WUANA, R. A. & OKIEIMEN, F. E. 2011. Heavy Metals in Contaminated Soils: A Review of Sources, Chemistry, Risks and Best Available Strategies for Remediation. *ISRN Ecology,* 2011**,** 20.

XIAOLI, C., SHIMAOKA, T., XIANYAN, C., QIANG, G. & YOUCAI, Z. 2007. Characteristics and mobility of heavy metals in an MSW landfill: Implications in risk assessment and reclamation. *Journal of Hazardous Materials,* 144**,** 485-491.

XU, P., JIN, Y. & CHENG, Y. 2017. Thermodynamic Analysis of the Gasification of Municipal Solid Waste. *Engineering,* 3**,** 416-422.

YAN, F., ZHANG, L., HU, Z., CHENG, G., JIANG, C., ZHANG, Y., XU, T., HE, P., LUO, S. & XIAO, B. 2010. Hydrogen-rich gas production by steam gasification of char derived from cyanobacterial blooms (CDCB) in a fixed-bed reactor: Influence of particle size and residence time on gas yield and syngas composition. *International Journal of Hydrogen Energy,* 35**,** 10212-10217.

YAO, J., LI, W.-B., KONG, Q.-N., WU, Y.-Y., HE, R. & SHEN, D.-S. 2010. Content, mobility and transfer behavior of heavy metals in MSWI bottom ash in Zhejiang province, China. *Fuel,* 89**,** 616-622.

YAZICI, M. S. 2011. UNIDO-ICHET support to hydrogen and fuel cell technologies in Turkey. *International Journal of Hydrogen Energy,* 36**,** 11239-11245.

YOUCAI, Z. & ZIYANG, L. 2017. Chapter One - General Structure of Sanitary Landfill. *Pollution Control and Resource Recovery.* Butterworth-Heinemann.

YUNUS, M. K., AHMAD, M. M., INAYAT, A. & YUSUP, S. Simulating of Enhanced Biomass Gasification for Hydrogen Production Using iCON. World Academy od Science Engineering and Technology, 2010 2010 US. 661- 667.

ZHANG, D. Q., TAN, S. K. & GERSBERG, R. M. 2010. Municipal solid waste management in China: Status, problems and challenges. *Journal of Environmental Management,* 91**,** 1623-1633.

ZHANG, Q., DOR, L., FENIGSHTEIN, D., YANG, W. & BLASIAK, W. 2012. Gasification of municipal solid waste in the Plasma Gasification Melting process. *Applied Energy,* 90**,** 106-112.

ZHAO, Y., XING, W., LU, W., ZHANG, X. & CHRISTENSEN, T. H. 2012. Environmental impact assessment of the incineration of municipal solid waste with auxiliary coal in China. *Waste Management,* 32, 1989-1998.

ZHENG, X., CHEN, C., YING, Z. & WANG, B. 2016. Experimental study on gasification performance of bamboo and PE from municipal solid waste in a bench-scale fixed bed reactor. *Energy Conversion and Management,* 117, 393-399.

ZHOU, H., MENG, A., LONG, Y., LI, Q. & ZHANG, Y. 2014a. An overview of characteristics of municipal solid waste fuel in China: Physical, chemical composition and heating value. *Renewable and Sustainable Energy Reviews,* 36, 107-122.

ZHOU, H., MENG, A., LONG, Y., LI, Q. & ZHANG, Y. 2014b. An overview of characteristics of municipal solid waste fuel in China: Physical, chemical composition and heating value. *Renewable and Sustainable Energy Reviews,* 36, 107-122.

ZOULIAS, E. I. & LYMBEROPOULOS, N. 2007. Techno-economic analysis of the integration of hydrogen energy technologies in renewable energy-based stand-alone power systems. *Renewable Energy,* 32, 680-696.

APPENDIX A

Solid Waste Disposal Facility and Map sites around Cape Town

Solid Waste Disposal Facility	Location (S' E')	Distance from CPUT Cape Town	Vehicles /day	Tonnes/day
Ladies Miles (DO)	-34.030072, 18445121	17 km	230 - 750	150 – 500
Belhar (DO)		35km	10 - 49	±50
Killarney (DO)	-33.829811, 18.526669	19.2 km	±200	±220
Welgelengen (DO)	-33.8735374, 18.5696545	17.3km	100 - 200	200 - 400
Delft (DO)	-33.978125, 18.642142	27.1 km	15 - 30	20 – 40
De Grendel (DO)	-33.8939147,18.5767901	17.8 km	14 - 83	±80
Woodstock (DO)	-33.9263086, 18.4332658	2.9 km	130 - 150	±242
Tygerdal (DO)	-33.9390663, 18.4528555	13.1 km	±100	±100
Kraaifontein (IWM)	-33.9163982, 18.4461799	33.9 km	±200	±800
Athlone (TS)	-33.949205, 18.516379	11.6 km	30 - 100	±1980

Solid Waste Disposal Facility	Location	Distance from CPUT Cape Town	Size (Hectare)	Tonnes/day	Age
Bellville South	33.9356509, 18.6552615	25.7 km	73		
Coastal Park	-34.0170711, 18.3298305	28.9 km	68	1000 - 2500	34
Vissershok	-33.773931, 18.545786	25.4 km	150		

Map of Solid Waste Disposal Facility around Cape Town

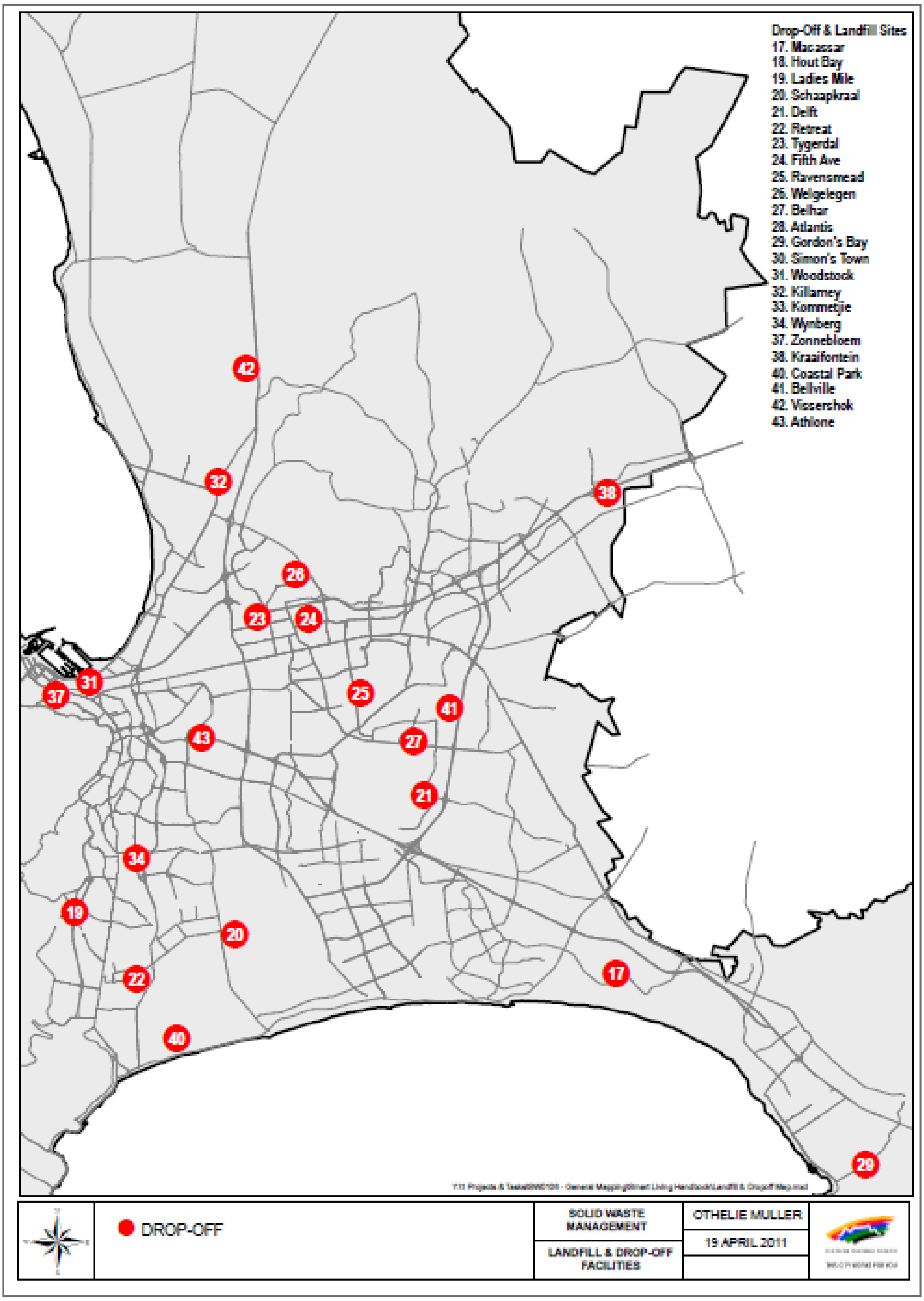

APPENDIX B

Raw Data of Thermo-Gravimetric Analysis of Pre-treated MSW

Time (min)	Temp (°C)	Weight (mg)	Heat Flow (mW)	Temp Diff (°C)	Temp Diffe (μV)	Sample Purge Flow (mL/min)	Deriv. Weight (%/°C)
0.0032	21.32765	19.64663	-8.2996	2.530684	15.39913	49.98402	0.102305
1.000167	23.44006	19.59132	-10.8257	2.34079	14.36092	50.00262	0.084599
2.000166	35.5052	19.49383	-16.3133	1.876732	12.0319	49.99199	0.031558
3.000166	66.5791	19.14795	-33.473	0.516311	3.665355	49.98762	0.10458
4.000167	85.9939	18.51184	-42.5602	-0.47707	-3.57653	49.99422	0.220662
5.004334	92.98813	18.16098	-32.1554	0.194368	1.483813	50.01217	0.285395
5.991832	93.54369	18.03154	-19.9769	1.15113	8.801218	50.00116	0.258175
6.004334	93.54745	18.03052	-19.8558	1.160693	8.874436	49.9834	0.258172
7.004334	95.25728	17.97016	-12.6938	1.714971	13.1636	50.00313	0.180503
8.004334	98.1266	17.93094	-8.99433	1.992857	15.40233	50.00943	0.099271
9.004334	100.375	17.90246	-7.00685	2.14242	16.64384	49.98744	0.056466
10.00433	102.3185	17.88132	-5.91134	2.223225	17.34404	49.99691	0.060085
15.0085	106.8601	17.82738	-4.04551	2.359074	18.58625	49.99608	0.104335
20.00434	107.3616	17.80802	-3.69044	2.387213	18.82882	49.98833	0.106536
25.00434	107.4058	17.79665	-3.58765	2.395842	18.89864	50.00612	0.106045
30.0085	107.4052	17.78862	-3.52248	2.401439	18.94276	50.00166	0.106045
35.00017	107.4173	17.78244	-3.45768	2.406953	18.98667	49.99343	0.106042
40.00433	107.4165	17.77784	-3.39416	2.412411	19.02968	49.98516	0.106042
45.0085	138.0984	17.75572	-3.57527	2.241748	18.76308	50.00261	0.006411
50.00016	147.2244	17.71859	-2.5908	2.287344	19.45242	50.00007	0.023803
55.00434	147.3078	17.70881	-2.37374	2.308286	19.63358	50.0059	0.023611
60.0085	187.6345	17.67658	-2.18711	2.097566	18.92661	49.99958	0.007876
65.00018	237.5972	17.45184	-1.17245	1.867695	17.85611	49.99947	0.05141
70.00434	287.4297	16.21756	0.236215	1.628658	16.28401	49.98734	0.199886
95.00018	499.5295	11.36132	-14.2668	-0.31582	-3.56522	50.0125	0.322913
100.0043	499.7329	11.31396	-13.5894	-0.28327	-3.19813	49.97219	0.320505
105.0085	499.743	11.28965	-13.3936	-0.27371	-3.09019	50.00176	0.320491
110.0002	499.7394	11.27388	-13.3655	-0.27232	-3.07444	50.00166	0.320496
115.0043	499.7284	11.26289	-13.4395	-0.27592	-3.11507	49.9982	0.320512
120.0085	499.7221	11.2546	-13.5533	-0.28147	-3.1778	50.00855	0.320521
125.0002	499.7134	11.24803	-13.693	-0.28828	-3.25469	50.01406	0.320534
130.0043	499.7045	11.2426	-13.8391	-0.29542	-3.33524	49.98384	0.320547
135.0044	499.6981	11.23816	-13.9776	-0.30218	-3.41156	50.00614	0.320556

140.0002	499.6947	11.23451	-14.0983	-0.30808	-3.47819	49.99511	0.320561
145.0044	499.6847	11.23118	-14.2225	-0.31414	-3.54654	49.98598	0.320575
150.0044	499.6812	11.22804	-14.3266	-0.31922	-3.60388	50.00008	0.320579
155.0085	572.6246	11.1985	-4.51372	-0.08137	-0.9475	50.00926	0.005398
160.0044	598.7613	11.08545	-25.4272	-1.03512	-12.1833	50.00134	0.803853
195.0044	598.3316	8.310712	-40.4636	-1.66802	-19.6292	49.98408	-0.24144
200.0085	598.3274	8.272175	-40.4836	-1.66886	-19.6391	49.99854	-0.24146
205.0002	598.33	8.24115	-40.5109	-1.67001	-19.6526	50.0021	-0.24145
210.0044	672.1429	8.174138	-19.9181	-0.88792	-10.7815	50.00396	0.008148
215.0085	697.3559	8.036811	-61.6993	-2.42114	-29.7181	49.99988	0.178312
220.5002	697.6243	8.026721	-60.6411	-2.38239	-29.2456	49.99881	0.185879
220.5127	697.6256	8.026699	-60.6399	-2.38234	-29.2451	49.97885	0.185884
220.5252	697.6228	8.026669	-60.6386	-2.3823	-29.2446	50.00971	0.185873
220.5377	697.6225	8.026635	-60.6377	-2.38227	-29.2442	49.97864	0.185872
220.546	697.6266	8.026598	-60.6367	-2.38222	-29.2436	50.01696	0.185888
220.5585	697.6218	8.026596	-60.6351	-2.38217	-29.2431	50.00266	0.185869
220.571	697.6228	8.02658	-60.6344	-2.38215	-29.2427	49.98891	0.185873
220.5835	697.6243	8.02658	-60.6331	-2.3821	-29.2421	49.9999	0.185879
220.596	697.6251	8.026602	-60.6316	-2.38204	-29.2414	50.00266	0.185882
220.9418	697.627	8.026455	-60.5862	-2.38039	-29.2212	49.98516	0.18589
220.9543	697.6256	8.02646	-60.5842	-2.38032	-29.2204	50.0112	0.185884

Raw Data of Thermo-gravimetric Analysis of Pre-treated MSW Cont'd

Time (min)	Temp (°C)	Weight (mg)	Heat Flow (mW)	Temp Diffe (°C)	Temp Diff (µV)	Sample Pur Flow (mL/min)	Deriv. Weight (%/°C)
0.0032	21.32765	19.64663	-8.2996	2.530684	15.39913	49.98402	0.102305
0.916833	23.22696	19.59634	-10.6416	2.35531	14.43734	50.00674	0.085983
0.975167	23.37585	19.59284	-10.7723	2.345007	14.3831	49.99536	0.085861
0.987667	23.40752	19.59208	-10.799	2.342898	14.372	49.98712	0.084624
1.000167	23.44006	19.59132	-10.8257	2.34079	14.36092	50.00262	0.084599
1.012667	23.46638	19.59057	-10.8526	2.338668	14.34974	50.00203	0.084579
1.021	23.49164	19.59002	-10.8704	2.337265	14.34235	50.00379	0.084559
2.371	46.31116	19.41637	-21.7364	1.462333	9.735509	50.00364	0.04392
3.350166	75.43662	18.92064	-39.0236	-7.99E-03	-0.05861	49.99911	0.161499
6.737666	94.58445	17.98322	-14.1674	1.602784	12.28292	49.9949	0.208512
8.937668	100.244	17.90415	-7.10543	2.134997	16.58134	49.99884	0.057044
11.93767	106.2128	17.85244	-4.822	2.295852	18.06142	50.00219	0.100285
13.37934	106.595	17.83823	-4.27484	2.340626	18.43154	49.99994	0.103526

13.39184	106.5935	17.83811	-4.27178	2.340897	18.43357	50.004	0.103526
18.7335	107.3108	17.81189	-3.74028	2.383174	18.7947	49.99636	0.106078
18.746	107.3114	17.81188	-3.7399	2.383203	18.79496	50.01396	0.106078
18.75434	107.308	17.81187	-3.73953	2.383241	18.79529	49.99676	0.106079
18.76684	107.3116	17.81183	-3.73862	2.38331	18.79586	50.00278	0.106078
18.77934	107.3127	17.81178	-3.73783	2.383373	18.79639	49.98519	0.106077
18.79183	107.312	17.81176	-3.73751	2.3834	18.79664	50.00744	0.106078
20.046	107.3703	17.80796	-3.68955	2.387264	18.82931	49.98534	0.106534
20.0585	107.3687	17.80792	-3.68895	2.387318	18.82975	49.99856	0.106534
61.43768	202.1056	17.64787	-1.93387	2.032965	18.68466	49.99002	0.013103
61.45016	202.2323	17.64756	-1.93092	2.032464	18.68283	50.00437	0.013162
69.99184	287.304	16.2225	0.235764	1.629498	16.29079	49.99871	0.199743
70.00434	287.4297	16.21756	0.236215	1.628658	16.28401	49.98734	0.199886
70.22516	289.626	16.13036	0.253139	1.61444	16.17002	49.98285	0.202188
80.86266	395.176	12.51341	-1.87624	0.799662	8.57941	50.00416	0.070902
80.871	395.2587	12.51226	-1.88013	0.798967	8.572351	49.99267	0.070862
87.57516	461.7354	11.75476	-5.95168	0.244911	2.716985	50.0047	0.046274
87.58768	461.8574	11.75362	-5.95854	0.244023	2.707295	49.99162	0.04622
87.60016	461.9824	11.75251	-5.96621	0.243096	2.697163	50.00376	0.046164
87.61266	462.108	11.75141	-5.97378	0.242174	2.68709	49.99897	0.046108
87.62101	462.1904	11.75068	-5.97882	0.241558	2.680358	49.99536	0.046058
90.93768	495.1194	11.4862	-8.04479	0.006708	0.07556	49.9996	0.213552
90.95016	495.2415	11.48538	-8.05258	0.00587	0.066128	50.00054	0.216434
90.96268	495.3667	11.48454	-8.0604	0.005033	0.056696	50.00266	0.219398
99.99184	499.7325	11.31404	-13.5902	-0.28331	-3.19858	50.01092	0.320506
100.0043	499.7329	11.31396	-13.5894	-0.28327	-3.19813	49.97219	0.320505
108.9418	499.7386	11.27659	-13.3622	-0.27216	-3.07263	50.0008	0.320497
120.971	499.7188	11.2534	-13.5791	-0.28272	-3.19193	50.00837	0.320526
120.9835	499.7209	11.25336	-13.5794	-0.28274	-3.19209	49.99256	0.320523
120.996	499.723	11.25333	-13.5805	-0.28279	-3.19269	50.01742	0.32052
121.0085	499.7203	11.25334	-13.5814	-0.28284	-3.19324	49.99026	0.320524
130.2835	499.7058	11.24228	-13.846	-0.29576	-3.33906	50.00675	0.320545
140.571	499.6889	11.23404	-14.1136	-0.30882	-3.48655	50.01588	0.320569
146.6794	499.684	11.23014	-14.2587	-0.31591	-3.56657	49.98957	0.320575
150.1127	499.679	11.22787	-14.3282	-0.3193	-3.60479	50.00817	0.320582
150.121	499.679	11.22784	-14.3288	-0.31933	-3.60512	50.00209	0.320582
158.0835	598.1149	11.11635	-26.8058	-1.09234	-12.8534	49.98698	0.667247
181.0544	598.3741	8.473249	-39.7666	-1.63867	-19.2841	50.00144	-0.24192
181.0627	598.3726	8.473093	-39.7673	-1.6387	-19.2845	50.00376	-0.24193
181.0752	598.3729	8.472922	-39.7693	-1.63878	-19.2855	49.9996	-0.24193
181.0876	598.3748	8.472708	-39.7711	-1.63886	-19.2863	49.99908	-0.24192

181.1002	598.3715	8.472532	-39.7734	-1.63896	-19.2875	49.9968	-0.24193
181.1127	598.3726	8.472397	-39.7758	-1.63906	-19.2887	49.9979	-0.24193
181.121	598.3719	8.472282	-39.7773	-1.63912	-19.2894	50.01016	-0.24193
181.1335	598.3716	8.472082	-39.7795	-1.63921	-19.2906	50.00015	-0.24193
181.146	598.3719	8.471913	-39.782	-1.63931	-19.2917	49.99728	-0.24193
181.1585	598.3717	8.471724	-39.7839	-1.6394	-19.2927	50.00078	-0.24193
181.171	598.3725	8.471561	-39.7859	-1.63948	-19.2937	49.99563	-0.24193
181.1794	598.3699	8.471432	-39.7876	-1.63955	-19.2946	49.9971	-0.24194
181.1918	598.3708	8.471245	-39.789	-1.63961	-19.2952	50.00365	-0.24193
181.2044	598.3722	8.471048	-39.7899	-1.63965	-19.2957	49.98448	-0.24193
181.2168	598.3707	8.470895	-39.7919	-1.63973	-19.2966	50.00828	-0.24193
181.2294	598.3718	8.470745	-39.7939	-1.63982	-19.2976	49.97698	-0.24193
181.2377	598.3734	8.470674	-39.7952	-1.63987	-19.2982	50.00297	-0.24192
181.2502	598.37	8.470503	-39.7966	-1.63993	-19.299	49.99965	-0.24194
181.2627	598.3699	8.470348	-39.798	-1.63999	-19.2997	50.02402	-0.24194
181.2752	598.3712	8.470163	-39.8003	-1.64008	-19.3008	49.99847	-0.24193
181.2877	598.3697	8.469976	-39.8022	-1.64017	-19.3017	49.97222	-0.24194
181.296	598.3717	8.46987	-39.8031	-1.6402	-19.3022	50.00656	-0.24193
181.3085	598.3709	8.469718	-39.8047	-1.64027	-19.303	50.00568	-0.24193
181.321	598.3702	8.469535	-39.8073	-1.64038	-19.3043	50.00494	-0.24193
181.3335	598.3706	8.469363	-39.8092	-1.64046	-19.3052	50.00039	-0.24193
181.346	598.3711	8.469178	-39.8103	-1.64051	-19.3058	50.0003	-0.24193
181.3544	598.372	8.469056	-39.8111	-1.64054	-19.3061	50.0037	-0.24193
181.3668	598.3703	8.468894	-39.8122	-1.64059	-19.3067	49.99253	-0.24193
181.3794	598.3714	8.46872	-39.8138	-1.64065	-19.3075	49.99602	-0.24193
181.3918	598.3692	8.468524	-39.8162	-1.64076	-19.3087	50.00531	-0.24194
181.4043	598.3712	8.468334	-39.8175	-1.64081	-19.3093	50.0007	-0.24193
181.4127	598.3687	8.468204	-39.8188	-1.64087	-19.31	49.98704	-0.24194
181.4252	598.368	8.468012	-39.8212	-1.64097	-19.3112	50.003	-0.24194
181.4377	598.369	8.467845	-39.8236	-1.64107	-19.3123	50.02716	-0.24194
181.4502	598.3706	8.467663	-39.8255	-1.64114	-19.3133	49.99598	-0.24193
181.4626	598.367	8.467469	-39.8269	-1.64121	-19.314	49.99562	-0.24195
181.471	598.3688	8.467378	-39.8269	-1.64121	-19.314	49.99616	-0.24194
181.4835	598.3691	8.467179	-39.8283	-1.64127	-19.3147	49.99903	-0.24194
181.496	598.3687	8.467024	-39.8296	-1.64132	-19.3153	49.99064	-0.24194
181.5044	598.3713	8.466925	-39.831	-1.64137	-19.3159	50.00528	-0.24193
181.5168	598.3698	8.466736	-39.8323	-1.64143	-19.3166	50.00484	-0.24194
181.5293	598.3711	8.466561	-39.8339	-1.6415	-19.3174	49.975	-0.24193
181.5418	598.368	8.466382	-39.8358	-1.64158	-19.3184	50.0004	-0.24194
181.5544	598.3736	8.4662	-39.8387	-1.6417	-19.3197	50.01978	-0.24192
181.5627	598.3708	8.466079	-39.839	-1.64172	-19.32	49.98578	-0.24193

181.5752	598.3707	8.465908	-39.8406	-1.64178	-19.3208	50.00546	-0.24193
181.5876	598.372	8.465699	-39.8421	-1.64184	-19.3215	49.9982	-0.24193
181.6002	598.3716	8.46553	-39.8435	-1.6419	-19.3222	50.00226	-0.24193
181.6127	598.3709	8.465339	-39.8453	-1.64198	-19.3231	49.99742	-0.24193
181.621	598.37	8.465231	-39.8465	-1.64203	-19.3237	50.00732	-0.24194
181.6335	598.3705	8.46505	-39.8481	-1.6421	-19.3245	49.9906	-0.24193
181.646	598.3716	8.464891	-39.8504	-1.64219	-19.3256	50.00734	-0.24193
181.6585	598.3711	8.464695	-39.8523	-1.64227	-19.3266	50.0032	-0.24193
181.671	598.3682	8.464531	-39.8543	-1.64237	-19.3276	50.00519	-0.24194
181.6794	598.369	8.464405	-39.8562	-1.64244	-19.3286	49.98533	-0.24194
181.6918	598.3695	8.464228	-39.8589	-1.64256	-19.3299	50.00317	-0.24194
181.7044	598.3711	8.464044	-39.8607	-1.64263	-19.3307	50.00639	-0.24193
181.7168	598.3717	8.463876	-39.8619	-1.64268	-19.3313	49.99934	-0.24193
181.7294	598.3717	8.463712	-39.863	-1.64272	-19.3318	49.99874	-0.24193
181.7377	598.3722	8.463609	-39.8641	-1.64277	-19.3324	50.00088	-0.24193
181.7502	598.3715	8.463432	-39.8658	-1.64284	-19.3332	49.9916	-0.24193
181.7627	598.3695	8.463289	-39.8669	-1.64289	-19.3338	50.01812	-0.24194
181.7752	598.3687	8.463126	-39.8683	-1.64296	-19.3346	49.99917	-0.24194
181.7877	598.3688	8.462962	-39.8707	-1.64305	-19.3357	49.98642	-0.24194
181.796	598.3684	8.462834	-39.8727	-1.64314	-19.3367	50.00141	-0.24194
181.8085	598.3687	8.462631	-39.8751	-1.64324	-19.3379	50.0173	-0.24194
181.821	598.3705	8.462442	-39.8778	-1.64335	-19.3392	49.96372	-0.24193
181.8335	598.3678	8.462272	-39.8797	-1.64343	-19.3401	50.00058	-0.24194
181.846	598.3666	8.462066	-39.8818	-1.64352	-19.3412	50.01254	-0.24195
181.8544	598.3679	8.461936	-39.8829	-1.64357	-19.3417	50.00504	-0.24194
181.8668	598.3688	8.461762	-39.8843	-1.64362	-19.3424	49.99116	-0.24194
181.8794	598.369	8.461559	-39.8859	-1.64369	-19.3432	50.0155	-0.24194
181.8918	598.3678	8.461394	-39.8887	-1.64381	-19.3446	49.99968	-0.24194
181.9043	598.3672	8.461197	-39.8908	-1.6439	-19.3456	50.00116	-0.24194
181.9127	598.37	8.461085	-39.8923	-1.64396	-19.3463	49.99911	-0.24194
181.9252	598.3692	8.460924	-39.8947	-1.64406	-19.3476	49.99239	-0.24194
181.9377	598.3703	8.460764	-39.8969	-1.64415	-19.3486	50.01103	-0.24193
181.9502	598.3682	8.460595	-39.8987	-1.64423	-19.3496	50.00141	-0.24194
181.9626	598.3672	8.460468	-39.9005	-1.64431	-19.3505	49.98839	-0.24194
183.2877	598.358	8.442344	-40.0423	-1.65027	-19.4205	50.01109	-0.24197
183.3002	598.357	8.442142	-40.0429	-1.6503	-19.4209	49.99619	-0.24198
183.3127	598.3572	8.441972	-40.0436	-1.65033	-19.4212	49.98548	-0.24198
183.321	598.3575	8.441856	-40.0446	-1.65037	-19.4217	49.99862	-0.24198
183.3335	598.3567	8.441681	-40.0465	-1.65045	-19.4227	50.0039	-0.24198
183.346	598.3567	8.441524	-40.0475	-1.65049	-19.4232	50.00824	-0.24198
183.3585	598.3576	8.441355	-40.0489	-1.65055	-19.4239	49.9905	-0.24198

183.371	598.357	8.441181	-40.0502	-1.65061	-19.4245	50.0177	-0.24198
183.3794	598.3601	8.441098	-40.0507	-1.65062	-19.4247	49.99684	-0.24197
183.4252	598.3563	8.440538	-40.0557	-1.65084	-19.4273	49.99526	-0.24198
183.4377	598.36	8.440368	-40.057	-1.65089	-19.4278	49.9923	-0.24197
183.4502	598.3576	8.440172	-40.0575	-1.65091	-19.4281	50.002	-0.24198
183.4626	598.3569	8.439981	-40.059	-1.65098	-19.4289	50.00422	-0.24198
183.471	598.3554	8.439844	-40.0597	-1.65101	-19.4293	50.0029	-0.24198
183.4835	598.357	8.439644	-40.0613	-1.65107	-19.43	50.00581	-0.24198
184.146	598.3522	8.430875	-40.1228	-1.65367	-19.4605	49.98514	-0.24199
185.896	598.3479	8.408409	-40.2601	-1.65945	-19.5285	50.00309	-0.24201
186.0335	598.3412	8.406684	-40.2669	-1.65973	-19.5318	49.99342	-0.24203
186.046	598.3434	8.406522	-40.2678	-1.65977	-19.5322	50.01258	-0.24202
220.8044	697.6272	8.026581	-60.6039	-2.38104	-29.2291	49.9982	0.18589
220.8168	697.6286	8.026574	-60.6027	-2.38099	-29.2285	50.00788	0.185896
220.896	697.6255	8.026492	-60.5915	-2.38059	-29.2237	49.98696	0.185884
220.9085	697.6278	8.02647	-60.5901	-2.38054	-29.223	50.00746	0.185893
220.921	697.6275	8.026474	-60.5881	-2.38046	-29.2221	50.01116	0.185892
220.9294	697.627	8.026458	-60.5876	-2.38044	-29.2219	50.00314	0.18589
220.9418	697.627	8.026455	-60.5862	-2.38039	-29.2212	49.98516	0.18589
220.9543	697.6256	8.02646	-60.5842	-2.38032	-29.2204	50.0112	0.185884

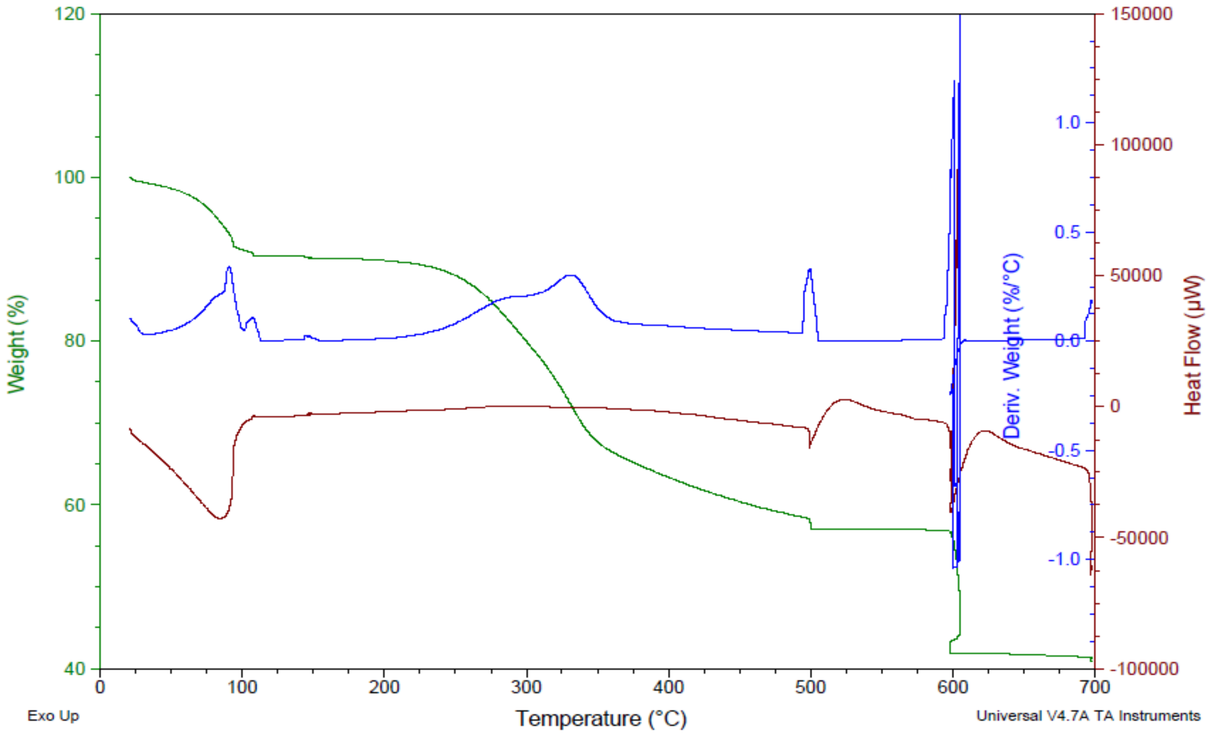

The TGA of TWS Showing Pre-treated MSW Degradation vs Temperature

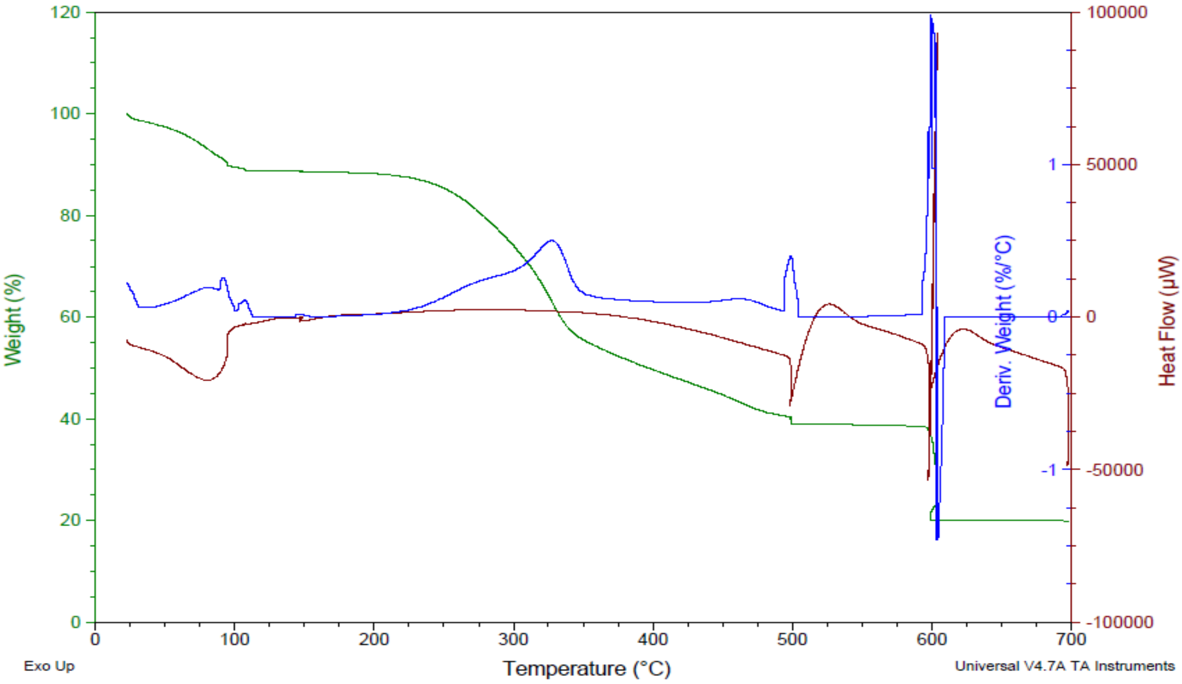

The TGA of TKL Showing Pre-treated MSW Degradation vs Temperature

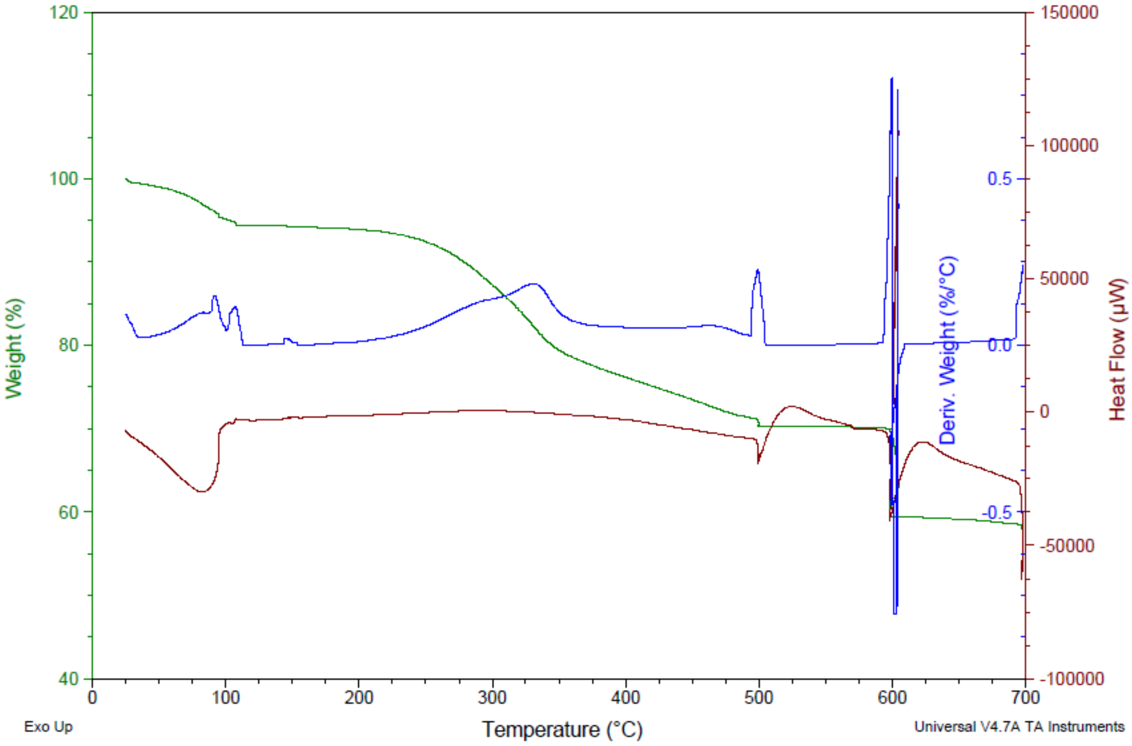

The TGA of TCL Showing Pre-treated MSW Degradation vs Temperature

Procedure and Equipment calibration of Thermo-Gravimetric Analysis of Pre-treated MSW

```
VERSION       2.0
Version       2.0
Language      English
Run     1
Run Serial    2497
Instrument    SDT Q600 V20.9 Build 20
Module        DSC-TGA Standard
Inst Serial   0600-0804
Operator      Neal
File    \\Q600\ta\UKZN Q600 Data\Q600
Data\Chemistry\Ismail\March2015\PTCI.001
Sample        Plant TCI
Size    22.3310       mg
X comment     Pan: Alumina
X comment     Gas1: Nitrogen 50.0 ml/min
X comment     Gas2: Nitrogen 0.0 ml/min
Text
Exotherm      Up
K cell  0.965000
Ins tCal Date Weight: 2014-11-27 Time: 08:42:57 Temp Range 32.81 to 1389.18 °C
Inst Cal File Weight: \\Q600\ta\UKZN Q600 Data\Q600
Data\Calibration\Calibration Nov2014\TGA empty beams.001
Inst Cal Date Heat Flow: 2015-01-13 Time: 11:00:47 Temp Range 50.05 to 1287.37 °C
Inst Cal File Heat Flow: \\Q600\ta\UKZN Q600 Data\Q600 Data\Calibration\DSC
calibration 12jan15\DSC empty pans2 nitrogen.001
Inst Cal Date DTA Baseline: 2015-01-13 Time: 13:55:03 Temp Range 500.12 to 1400.07 °C
Inst Cal File DTA Baseline: C:\TA\Data\SDT\0600-0804\3337\Beamwo.002
Temp Cal      3       pts     157.59 156.60,421.50 419.53,664.61 660.33
Controls      Gas 1  Event OFF  Sampling 0.5 sec/pt
Auto Analysis Off
Macro File
N sig   8
Sig1    Time (min)
Sig2    Temperature (°C)
Sig3    Weight (mg)
Sig4    Heat Flow (mW)
Sig5    Temperature Difference (°C)
Sig6    Temperature Difference (μV)
Sig7    Sample Purge Flow (mL/min)
```

```
Sig8   Deriv. Weight ( %/°C)
Date   2015-04-22
Time   14:10:18
Org Method   1: Select gas 1
Org Method   2: Data storage On
Org Method   3: Mass flow 50.00 mL/min
Org Method   4: Isothermal for 1.00 min
Org Method   5: Ramp 30.00 °C/min to 70.00 °C
Org Method   6: Ramp 15.00 °C/min to 90.00 °C
Org Method   7: Ramp 2.00 °C/min to 105.00 °C
Org Method   8: Isothermal for 30.00 min
Org Method   9: Ramp 10.00 °C/min to 145.00 °C
Org Method   10: Isothermal for 10.00 min
Org Method   11: Ramp 10.00 °C/min to 500.00 °C
Org Method   12: Isothermal for 60.00 min
Org Method   13: Ramp 20.00 °C/min to 600.00 °C
Org Method   14: Isothermal for 10.00 min
Org Method   15: Select gas 2
Org Method   16: Mass flow 50.00 mL/min
Org Method   17: Isothermal for 40.00 min
Org Method   18: Ramp 20.00 °C/min to 700.00 °C
Org Method   19: Isothermal for 10.00 min
```

APPENDIX C

Raw Data of Proximate and Ultimate Analysis of Pre-treated MSW

Samples Names↓	Sample	C	H	N	S	O	Date
and Elemental% →	Weight (mg)						
UA	2.225	16.712	1.943	0.661	2.521	78.163	90215
UA	2.132	19.592	2.421	0.892	2.567	74.528	90215
UA	2.216	17.012	1.81	0.536	2.529	78.113	240215
UB	1.946	29.404	3.835	1.046	3.123	62.592	121914
UB	1.808	29.211	3.831	0.908	3.37	62.68	90215
UCI	1.866	34.979	4.603		2.934	57.484	90215
UCI	1.799	29.441	3.483	0.875	3.151	63.05	240215
UCI	2.088	32.692	3.854	0.935	2.718	59.801	240215
UCII	1.808	35.265	4.504		3.057	57.174	90215
UCII	2.028	33.378	4.137	1.166	2.839	58.48	240215
UCII	1.801	38.081	4.75	1.075	3.171	52.923	240215
UCP	2.201	22.316	2.624		2.469	72.591	90215
UCP	2.191	20.285	2.361		2.489	74.865	90215
UCP	2.069	21.65	2.459	0.902	2.707	72.282	240215
UCP	1.928	21.288	2.366	0.824	2.887	72.635	240215
UKF	1.942	23.912	2.751		2.831	70.506	90215
UKF	1.992	22.977	2.627		2.719	71.677	90215
UKF	2.024	22.734	2.44	0.797	2.772	71.257	240215
UKF	1.763	23.111	2.475	0.928	3.112	70.374	240215
ULM	2.012	39.283	4.817	0.959	2.719	52.222	240215
ULM	2.06	38.385	4.486	0.752	2.694	53.683	240215
UR	1.889	34.08	4.396	1.194	2.851	57.479	90215
URL	2.076	30.869	3.918		2.613	62.6	90215
URL	1.863	32.049	4.048		2.908	60.995	90215

URL	2.073	30.606	3.838	1.409	2.741	61.406	240215
UT	1.954	36.877	4.872	0.991	2.786	54.474	90215
UT	2.086	35.476	4.634	0.997	2.592	56.301	90215
UT	1.858	36.584	4.599	1.058	3.001	54.758	240215
UW	1.853	15.131	2.093	0.526	3.55	78.7	90215
UWS	2.128	33.827	4.144	1.009	2.565	58.455	90215
UWS	1.802	33.891	4.239	1.183	3.04	57.647	90215
UXDO	2.199	35.125	4.23		2.488	58.157	90215
UXDO	1.924	31.685	3.923		2.837	61.555	90215
UXDO	1.987	34.419	4.115	1.235	2.782	57.449	240215

C	H	N	S	O
0.371842	0.043232	0.014707	0.056092	1.739127
0.417701	0.051616	0.019017	0.054728	1.588937
0.376986	0.04011	0.011878	0.056043	1.730984
0.572202	0.074629	0.020355	0.060774	1.21804
0.528135	0.069264	0.016417	0.06093	1.133254
0.652708	0.085892	0	0.054748	1.072651
0.529644	0.062659	0.015741	0.056686	1.13427
0.682609	0.080472	0.019523	0.056752	1.248645
0.637591	0.081432	0	0.055271	1.033706
0.676906	0.083898	0.023646	0.057575	1.185974
0.685839	0.085548	0.019361	0.05711	0.953143
0.491175	0.057754	0	0.054343	1.597728
0.444444	0.05173	0	0.054534	1.640292
0.447939	0.050877	0.018662	0.056008	1.495515
0.410433	0.045616	0.015887	0.055661	1.400403
0.464371	0.053424	0	0.054978	1.369227
0.457702	0.05233	0	0.054162	1.427806
0.460136	0.049386	0.016131	0.056105	1.442242
0.407447	0.043634	0.016361	0.054865	1.240694

0.790374	0.096918	0.019295	0.054706	1.050707
0.790731	0.092412	0.015491	0.055496	1.10587
0.699294	0.088697	0.023534	0.054016	1.202459
0.643771	0.08304	0.022555	0.053855	1.085778
0.64084	0.081338	0	0.054246	1.299576
0.597073	0.075414	0	0.054176	1.136337
0.634462	0.079562	0.029209	0.056821	1.272946
0.720577	0.095199	0.019364	0.054438	1.064422
0.740029	0.096665	0.020797	0.054069	1.174439
0.679731	0.085449	0.019658	0.055759	1.017404
0.302214	0.042476	0.009117	0.067049	1.523143
0.280377	0.038783	0.009747	0.065782	1.458311
0.719839	0.088184	0.021472	0.054583	1.243922
0.610716	0.076387	0.021318	0.054781	1.038799
0.772399	0.093018	0	0.054711	1.278872
0.609619	0.075479	0	0.054584	1.184318
0.683906	0.081765	0.024539	0.055278	1.141512

APPENDIX D

Raw Gross Calorific Measurement of Pre-treated MSW from MSWDF in Cape Town

Gross Calorific Measurement of MSW					
Sample ID	Sample Mass (g)	CV(MJ/kg)	Ave CV	Samples Completed	Sites Completed
Kraaifontein 01	0.501	23.3700	22.1043	53	12
Kraaifontein 02	0.2495	21.2720	1.114107		
Kraaifontein 03	0.2509	21.671			
Athlone 01	0.2494	21.266	20.7623		
Athlone 02	0.2508	15.4310	5.098194		
Athlone 03	0.2498	25.5900			
Woodstock 01	0.2494	14.487	14.8453		
Woodstock 02	0.2492	13.849	1.215772		
Woodstock 03	0.2512	16.200			
Tygerdal 01	0.2508	27.503	22.7723		
Tygerdal 02	0.249	20.103	4.108141		
Tygerdal 03	0.25	20.711			
Belhar 01	0.251	16.404	16.5047		
Belhar 02	0.2505	18.601	2.047857		
Belhar 03	0.2501	14.509			
Killarney 01	0.2513	17.435	20.8463		
Killarney 02	0.2512	28.648	6.77415		
Killarney 03	0.2492	16.456			
X.DO 01	0.2496	14.823	15.6870		
X.DO 02	0.2492	15.8	0.813408		
X.DO 03	0.2493	16.438			
Welengen 01	0.2501	17.121	16.7213		
Welengen 02	0.25	12.468	4.068251		
Welengen 03	0.2504	20.575			
Retreat 01	0.2499	17.711	18.1693		
Retreat 02	0.2502	18.951	0.6803		

Retreat 03	0.2498	17.846			
Coastal Park 01	0.2489	14.114	15.9697		
Coastal Park 02	0.2497	14.462	2.917925		
Coastal Park 03	0.2499	19.333			
Ladies miles 01	0.2498	21.881	24.6553		
Ladies miles 02	0.2506	28.907	3.738724		
Ladies miles 03	0.2497	23.178			
Composite 01	0.2502	19.257	20.1691		
Composite 02	0.2493	13.512	2.98154		
Composite 03	0.2507	20.201			
Composite 04	0.2502	17.553			
Composite 05	0.2508	19.738			
Composite 06	0.2495	19.03			
Composite 07	0.2497	18.488			
Composite 08	0.2501	16.3			
Composite 09	0.2495	21.554			
Composite 10	0.25	23.445			
Composite 11	0.2495	21.129			
Composite 12	0.2504	20.171			
Composite 13	0.2502	19.846			
Composite 14	0.2501	17.859			
Composite 15	0.2514	23.941			
Composite 16	0.2501	24.137			
Composite 17	0.2496	19.648	Median	19.257	
Composite 18	0.2497	25.872	STDVA	3.905568	
Composite 19	0.251	18.119	Ave CV	19.44332	
Composite 20	0.2504	23.582	Min CV	12.4680	

APPENDIX E

Al	102.2	**HM CI**	**HM KF**	**HM CD**	**HM XDO**	**HM R**	**HM LM**	**HM WS**	**HM A**
Ti	107.4	6804.54	5893.80	13508.10	3101.70	1488.93	5077.84	5376.15	593.44
V	98.7	73.64	71.56	89.98	111.11	59.54	89.07	149.65	82.39
Cr	99.4	5.46	10.67	5.70	8.20	2.68	4.81	10.23	8.29
Mn	100.0	187.89	312.63	178.74	137.44	148.73	206.30	219.32	268.91
Fe	98.0	81.46	131.12	99.24	112.96	62.29	130.02	148.41	95.69
Co	100.0	4664.17	10230.42	6143.52	5094.27	5565.97	9519.54	6414.23	788.01
Ni	97.9	29.25	27.17	25.32	20.12	23.05	26.86	28.05	26.96
Cu	99.5	74.27	122.51	72.34	53.98	62.74	86.56	83.15	107.37
Zn	98.2	43.57	83.91	51.26	16.47	18.56	134.40	42.24	62.46
As	103.5	163.56	105.59	147.23	100.66	213.16	181.32	117.18	218.27
Se	93.7	6.37	11.10	2.68	3.24	3.25	3.10	15.24	14.08
Mo	100.2	0.49	0.88	0.82	1.08	0.33	0.98	1.80	0.87
Cd	96.3	4.16	6.28	4.96	2.78	2.85	3.92	4.05	5.47
Sb	96.6	0.77	14.57	0.30	0.16	0.32	0.24	0.18	0.57
Ba	101.3	1.46	1.62	0.79	0.34	1.21	2.99	1.53	2.42

Hg	105.3	60.84	50.40	48.74	37.97	123.44	40.83	103.58	88.84
Pb	97.5	0.21	0.10	0.18	0.10	0.14	0.65	0.13	0.09
Al	102.2	36.98	11.36	23.47	14.34	44.71	16.53	40.80	88.91

		Values in mg/kg					
	Control Standard						
	Recovery (%)	**HM KL**	**HM CII**	**HM B**	**HM B dupl**	**HM T**	**HM W**
Al	102.2	4026.48	7478.29	7141.92	6306.41	8213.83	3196.17
Ti	107.4	71.03	138.37	100.01	101.43	97.80	81.34
V*	98.7	5.86	7.59	7.10	6.81	6.69	5.92
Cr*	99.4	224.63	138.83	66.44	72.08	122.06	191.99
Mn	100.0	123.16	145.56	58.90	57.96	199.10	91.67
Fe	98.0	4550.90	5879.66	3007.12	2931.62	5862.44	3924.50
Co*	100.0	26.35	27.99	6.12	6.21	10.82	16.89
Ni*	97.9	92.95	53.65	27.20	27.03	50.78	78.46
Cu*	99.5	30.88	37.76	33.27	25.83	62.58	15.81
Zn*	98.2	173.84	181.56	130.73	127.14	316.14	67.76
As**	103.5	7.51	7.13	2.68	2.49	4.68	2.23
Se*	93.7	0.78	1.04	0.83	0.73	0.55	1.09
Mo	100.2	8.85	3.73	3.23	3.42	3.60	3.78
Cd*	96.3	0.65	0.79	0.14	0.13	0.54	0.13
Sb*	96.6	1.01	2.24	1.42	2.11	0.96	0.18
Ba**	101.3	39.59	77.41	71.49	159.85	69.15	40.48
Hg**	105.3	0.09	0.20	0.08	0.09	0.16	0.04
Pb**	97.5	9.49	30.22	27.16	50.01	27.98	9.41

	HM CI	**HM KF**	**HM CD**	**HM XDO**	**HM R**	**HM LM**	**HM WS**	**HM A**
	6804.54	5893.80	13508.10	3101.70	1488.93	5077.84	5376.15	593.44
	73.64	71.56	89.98	111.11	59.54	89.07	149.65	82.39
	5.46	10.67	5.70	8.20	2.68	4.81	10.23	8.29
	187.89	312.63	178.74	137.44	148.73	206.30	219.32	268.91
	81.46	131.12	99.24	112.96	62.29	130.02	148.41	95.69
	4664.17	10230.42	6143.52	5094.27	5565.97	9519.54	6414.23	788.01
	29.25	27.17	25.32	20.12	23.05	26.86	28.05	26.96
	74.27	122.51	72.34	53.98	62.74	86.56	83.15	107.37
	43.57	83.91	51.26	16.47	18.56	134.40	42.24	62.46
	163.56	105.59	147.23	100.66	213.16	181.32	117.18	218.27
	6.37	11.10	2.68	3.24	3.25	3.10	15.24	14.08
	0.49	0.88	0.82	1.08	0.33	0.98	1.80	0.87
	4.16	6.28	4.96	2.78	2.85	3.92	4.05	5.47
	0.77	14.57	0.30	0.16	0.32	0.24	0.18	0.57
	1.46	1.62	0.79	0.34	1.21	2.99	1.53	2.42
	60.84	50.40	48.74	37.97	123.44	40.83	103.58	88.84
	0.21	0.10	0.18	0.10	0.14	0.65	0.13	0.09
	36.98	11.36	23.47	14.34	44.71	16.53	40.80	88.91

APPENDIX F

Mass and Energy Balance Parameters in Gasification

Major, Minor and other Chemical Reactions in Gasification

$$C + O_2 \rightarrow CO_2 \qquad -393.98 \quad KJ/Mol \qquad (1)$$

$$2H_2 + O_2 \rightarrow 2H_2O \qquad -484.23\, KJ/Mol \qquad (2)$$

$$2CH_4 + O_2 \rightarrow 2CO + 4H_2 \qquad -71.44\, KJ/Mol \qquad (3)$$

$$C + 2H_2 \leftrightarrow CH_4 \qquad -74.94\, KJ/Mol \qquad (4)$$

$$CH_4 + H_2O \rightarrow CO + 3H_2 \qquad +206.61\, KJ/Mol \qquad (5)$$

$$CO + 0.5O_2 \rightarrow CO_2 \qquad -288.48\; KJ/Mol \qquad (6)$$

$$C + 0.5O_2 \rightarrow CO \qquad -111 \quad KJ/Mol \qquad (7)$$

$$C + H_2O \leftrightarrow CO + H_2 \qquad +131\, KJ/Mol \qquad (8)$$

$$C + CO_2 \leftrightarrow 2CO \qquad +172 \;\; KJ/Mol \qquad (9)$$

$$CO + H_2O \leftrightarrow CO_2 + H_2 \qquad -41\, KJ/Mol \qquad (10)$$

$$H_2O_{(l)} \rightarrow H_2O_{(g)} \qquad +44\, KJ/Mol \qquad (11)$$

$$C_mH_nO_{q_{(s)}} \rightarrow C_mH_{n-2q_{(s)}} + qH_2O_{(g)} \qquad (12)$$

$$C_mH_nO_{q_{(s)}} \rightarrow C_{m-q/2}H_{n_{(s)}} + q/2C0_{2(g)} \qquad (13)$$

$$C_nH_m + xH_2\mathrm{O} \rightarrow yCO + zH_2 + C_pH_q \qquad (14)$$

$$C_p^{\circ} = a1 + a2C + a3H + a4O + a5N + a6S + a8Cl + a9I + a10Br + a11Si \qquad (15)$$

$$C_{pS} = \sum_{i=1}^{n} N_i \, \Delta_{Ei} \quad (16)$$

Where:

C_{pS} = solid heat capacity at 298.15 K, J/mol K

n = number of different atomic elements in the compound

N_i = number of atomic elements i in the compound

D_{Ei} = numeric value of the contribution of atomic element I found in Table 2-393

$$C_{pL} = \sum_{i=1}^{n} N_i \, \Delta_{Cpi} + 18.83m \quad (17)$$

Where:

C_{pL} = liquid heat capacity at 293.15 K, J/mol K.

n = number of different atomic groups in the compound

N_i = number of atomic groups i in the compound

D_{cpi} = numeric value of the contribution of atomic element I found in Table 2-394. The original units of cal/mol K have been converted to J/mol K by the conversion 1 cal/mol K = 4.184 J/mol K

m = number of carbon groups requiring an additional contribution, which are those that are joined by a single bond to a carbon group, which in turn is connected to a third carbon group by a double or triple bond. If a carbon group meets this criterion in more than one way, m should be increased by one for each of the ways.

$$ACp_aT_0 + FCp_fT_0 + WH_0 + F * HHV + Q_{ext} = T_g\left(C_{CO}V_{CO} + C_{CO_2}V_{CO_2} + C_{CH_4}V_{CH_4} + C_{H_2}V_{H_2} + C_{O_2}V_{O_2} + C_{N_2}V_{N_2}\right) + WH_g\left(1 - X_g\right) + P_cq_c \quad Q_{(gasification+loss+products)} \quad (18)$$

$$\Delta H^{\circ}{}_{298} = \sum H^{\circ}{}_{f,product} - \sum H^{\circ}{}_{f,reactant} \qquad (19)$$

$$\boldsymbol{\Delta H^{\circ}{}_{r(1100)} = \Delta H^{\circ}{}_{298} + \sum\left(\int_{298}^{1100}(C_{p,CH_4} + C_{p,CO_2})dT\right)_{products} - \sum\left(\int_{298}^{1100}(C_{p,H_2O})dT\right)_{reactants}} \qquad (20)$$

Atomic Element Contributions to Estimate Solid Heat Capacity 298.15 K Table 2-393 (Perry and Green, 2008)

Atomic Element	Δ_E	Atomic Element	Δ_E	Atomic Element	Δ_E
C	10.89	Ba	32.37	Mo	29.44
H	7.56	Be	12.47	Na	26.19
O	13.26	Ca	28.25	Ni	25.46
N	18.74	Co	25.71	Pb	31.60
S	12.36	Cu	26.92	Si	17.00
F	26.16	Fe	29.08	Sr	28.41
Cl	24.69	Hg	27.87	Ti	27.24
Br	25.36	K	28.78	V	29.36
I	25.29	Li	23.25	W	30.87
Al	18.07	Mg	22.69	Zr	26.82
B	10.10	Mn	28.06	All other	26.63

Specific Heat Capacity of Some Compounds

Hydrogen

$$\mathrm{Cp_{H_2}} = 27.71 + 0.0034\mathrm{T} = \left[27.71\mathrm{T} + \frac{0.034\mathrm{T}^2}{2}\right]_{\mathrm{T}_1}^{\mathrm{T}_2} \qquad (21)$$

Carbon monoxide

$$\mathrm{Cp_{CO}} = 27.62 + 0.005\mathrm{T} = \left[27.62\mathrm{T} + \frac{0.005\mathrm{T}^2}{2}\right]_{\mathrm{T_1}}^{\mathrm{T_2}} \tag{22}$$

Carbon dioxide

$$\mathrm{Cp_{CO_2}} = 48.28 + 0.0114\mathrm{T} - \frac{818363}{\mathrm{T}^2} = \left[48.28\mathrm{T} + \frac{0.0114\mathrm{T}^2}{2} - \frac{818363}{\mathrm{T}}\right]_{\mathrm{T_1}}^{\mathrm{T_2}} \tag{23}$$

Water

$$\mathrm{Cp_{H_2O}} = 34.4 + 0.000628\mathrm{T} + 0.0000052\mathrm{T}^2 = \left[34.4\mathrm{T} + \frac{0.000628\mathrm{T}^2}{2} + \frac{0.0000052\mathrm{T}^3}{3}\right]_{\mathrm{T_1}}^{\mathrm{T_2}} \tag{24}$$

Methane

$$\mathrm{Cp_{CH_4}} = 22.35 + 0.048\mathrm{T} = \left[22.35\mathrm{T} + \frac{0.048\mathrm{T}^2}{2}\right]_{\mathrm{T_1}}^{\mathrm{T_2}} \tag{25}$$

Oxygen

$$\mathrm{Cp_{O_2}} = 34.62 + 0.00108\mathrm{T} - \frac{785712}{\mathrm{T}^2} = \left[34.62\mathrm{T} + \frac{0.00108\mathrm{T}^2}{2} - \frac{785712}{\mathrm{T}}\right]_{\mathrm{T_1}}^{\mathrm{T_2}} \tag{26}$$

Naphthalene

$$\mathrm{Cp_{Naphthalene}} = 29800 + 527.5\mathrm{T} = \left[29800\mathrm{T} + \frac{527.5\mathrm{T}^2}{2}\right]_{\mathrm{T_1}}^{\mathrm{T_2}} \tag{27}$$

Toluene

$$\mathrm{Cp_{Toluene}} = 0.584 + 2.863\left[\frac{1.4406/\mathrm{T}}{\mathrm{Sinh}\,\frac{1.4406}{\mathrm{T}}}\right]^2 + 1.1898\left[\frac{650.43/\mathrm{T}}{\mathrm{Cosh}\ 650.43/\mathrm{T}}\right]_{\mathrm{T_1}}^{\mathrm{T_2}} \tag{28}$$

Enthalpy or Heat Reactions of Some Thermochemical Conversions

Drying (Dehydration and Decarboxylation)

$C_m H_n O_q + H_2O \rightarrow C_m H_{n-2q} + H_2O$ $\Delta°H_{r,380} = +21.4900$ KJ/Mol (29)

$C_m H_n O_q \rightarrow C_{m-\frac{q}{2}} H_n + \left(\frac{q}{2}\right) CO_2$ (Negligible) (30)

Thermal Decomposition

$C + 0.5O_2 \rightarrow CO$ $\Delta°H_{r,773} = -103.6412$KJ/Mol (31)

$C + H_2O \leftrightarrow CO + H_2$ $\Delta°H_{r,773} = 150.2474$KJ/Mol (32)

$C H_{1.14} + 0.5O_2 \rightarrow CO + 0.57H_2$ $\Delta°H_{r,773} = -189.1009$ KJ/Mol (33)

$C H_{0.8} + 0.5O_2 \rightarrow CO + 0.4H_2$ $\Delta°H_{r,773} = -254.1860$ KJ/Mol (34)

Char Combustion and Reforming

$C + O_2 \rightarrow CO_2$ $\Delta°H_{r,1123} = -376.2210$ KJ/Mol (35)

$2CO + O_2 \rightarrow 2CO_2$ $\Delta°H_{r,1123} = -554.6342$ KJ/Mol (36)

$C + CO_2 \rightarrow 2CO$ $\Delta°H_{r,1123} = +178.4130$ KJ/Mol (37)

$C + H_2O \leftrightarrow CO + H_2$ $\Delta°H_{r,1123} = +212.6505$ KJ/Mol (38)

$CH_4 + H_2O \leftrightarrow CO + H_2$ $\Delta°H_{r,1123} = +326.4565$ KJ/Mol (39)

$C_{0.54}H_{0.54} + 0.27O_2 \rightarrow 0.54CO + 0.27H_2$ $\Delta°H_{r,1123} = -25.6824$ KJ/Mol (40)

Gasification and Char Gasification

$$CH_{0.2}\,O_{0.13} + \ 0.87H_2O \ \rightarrow \ CO + 0.97H_2 \qquad \Delta°H_{r,1123} \ = +166.5928\ \text{KJ/Mol} \qquad (41)$$

$$C_{0.54}H_{0.54} + \ 0.27O_2 \ \rightarrow \ 0.54CO + 0.27H_2 \qquad \Delta°H_{r,1123} \ = -25.6824\ \text{KJ/Mol} \qquad (42)$$

Water-gas Shift Reaction (WGS)

$$CO + \ H_2O \ \leftrightarrow \ CO_2 + \ H_2 \qquad \Delta°H_{r,628} \ = +10.4000\ \text{KJ/Mol} \qquad (43)$$

Chemical Reactions

Chemical Reactions	**No**	$\in \Delta°\mathbf{H}_{\mathbf{r},}$
Exothermic Reactions	Six	-1503.4834 KJ/Mol
Endothermic Reactions	Seven	+1066.2502 KJ/Mol
Total or Net Energy of Reactions	Eleven	-437.2332

Material Balance

One mole of MSW is 29.75 kg/mol ~ 2.50 Kmol of MSW

10 Kg of MSW represents 0.334 Kmole

Bulk Density 367 Kg/m^3

HHV = 24.6553 MJ/Kg

Basis of the reactions 5 Kg/Hr

MSW Proximate Analysis

FC = 11.12 %

VM = 74.17 %

MC = 10.70 %

ASH = 4.00 %

MSW Ultimate Analysis

C = 30.40 %

H = 3.830 %

O = 52.82 %

S = 2.87 %

N = 0.98 %

MSW molecular formula = $CH_{1.43}O_{1.03}$

Overall Balance

$$M_{msw+ash} + M_{afr} + M_{sfr} = M_{gp} + M_{ash} + M_{tar} + M_{stem}$$

Components Balances

Carbon Balance

C in MSW = C in CO + C in CO_2 + C in Ashe

0.3040/12 = (0.30 + 0.20 0.001)

Water/Steam Balance

Water + Water in MSW (0.09) = Water + Water$_{(WGS)}$ +

18 x f + 0.09/18 = 18 x q 18 x0.15x

Nitrogen for Air Balance

0.0098/28 + 0.7677X + 0 = 0.72 x Y

Hydrogen Balance

H in MSW + H in H_2O = H in syngas + H in Tar + H in Char

0.0383/1 + 0.11/1 = 0.66/1 +

Efficiency of Gasification

$$\zeta = \frac{Q_g M_g}{LHV_f M_f}$$

ζ = Efficiency, $Q_g =$ LHV of product gas, $M_g =$ Mass of product gas, $LHV_f =$ LHV of solid fuel, M_f = Mass of solid fuel.

$Q_g =$ LHV of product gas CO (10.112MJ/Kg) H(120.971MJ/Kg)

M_g= Mass of product gas 1.112 Kg/Hr 1.112 Kg/Hr 1.288 Kg/Hr

LHV_f = LHV of solid fuel (19.88, 20.85, 24.66 MJ/Kg)

M_f = Mass of solid fuel. (5kg) (10 Kg)

	RDF1	RDF2	RDF3
Q_g CO (MJ/Kg)	10.112	10.112	10.112
Q_g H (MJ/Kg)	120.971	120.971	120.971
M_g (Kg)	0.52	1.112	1.288
LHV_f (MJ/Kg)	19.88	20.85	24.66
M_f (Kg)	5	10	10
η = Efficiency	68.57 %	69.91 %	68.46 %

From the above values, the cold gas efficiency is approximately **69 %** with consideration on quality of hydrogen/CO molar concentration of gaseous products.

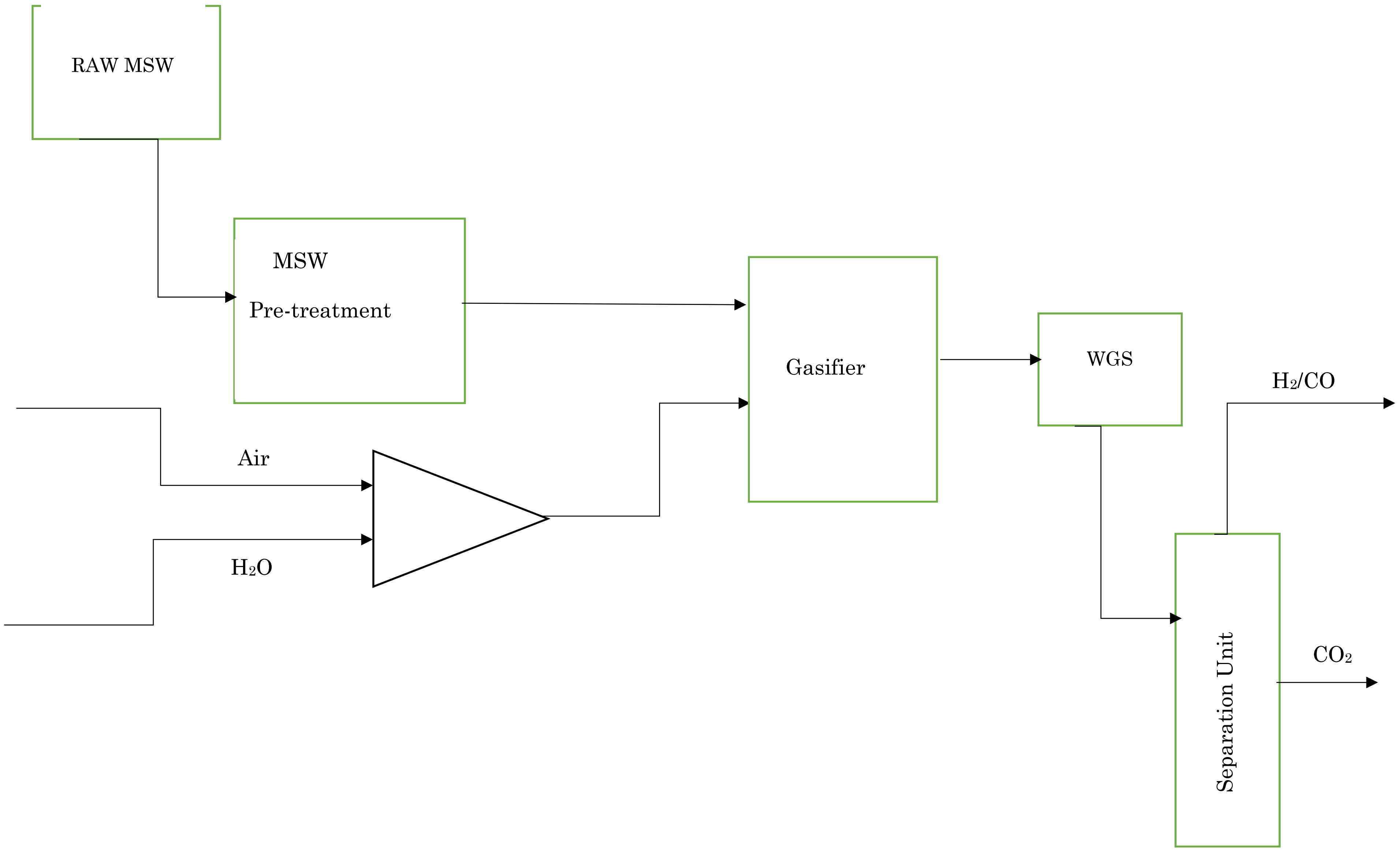

The Block Diagram of Gasification System with a Separation Unit to Purify Hydrogen

APPENDIX G

Input Summary

```
Input Summary created by Aspen Plus Rel. 24.0 at 02:46:23 Fri Oct 28, 2016
Directory          C:\Users\Adefeso\Desktop\2016                    Filename
C:\Users\Adefeso\AppData\Local\Temp\~apb6d5.txt
DYNAMICS
   DYNAMICS RESULTS=ON
IN-UNITS MET VOLUME-FLOW='cum/hr' ENTHALPY-FLO='MMkcal/hr'  &
      HEAT-TRANS-C='kcal/hr-sqm-K' PRESSURE=bar TEMPERATURE=C  &
      VOLUME=cum DELTA-T=C HEAD=meter MOLE-DENSITY='kmol/cum'  &
      MASS-DENSITY='kg/cum' MOLE-ENTHALP='kcal/mol'  &
      MASS-ENTHALP='kcal/kg' HEAT=MMkcal MOLE-CONC='mol/l'  &
      PDROP=bar
DEF-STREAMS MCINCPSD ALL
DIAGNOSTICS
   TERMINAL SIM-LEVEL=4 CONV-LEVEL=4 COST-LEVEL=4 PROP-LEVEL=4  &
      ECON-LEVEL=4 STREAM-LEVEL=4 SYS-LEVEL=4
SIM-OPTIONS
   IN-UNITS ENG
   SIM-OPTIONS OLD-DATABANK=YES
   DESCRIPTION "
   RDF1 represents RDF produce from KL raw MSW.'Aspen Plus
   Modeling Processes with Solids
    DATABANKS PURE22  / AQUEOUS  / SOLIDS  / INORGANIC  /  &
```

```
    NOASPENPCD
PROP-SOURCES PURE22  / AQUEOUS  / SOLIDS  / INORGANIC
COMPONENTS
  H2O H2O /
  N2 N2 /
  O2 O2 /
  RDF1 /
  TOLUE-01 C7H8 /
  NAPHT-01 C10H8 /
  H2 H2 /
  C C /
  CO CO /
  CO2 CO2 /
  ASH
FLOWSHEET
  BLOCK DRY-REAC IN=WET-RDF1 NITROGEN OUT=IN-DRIER
  BLOCK DRY-FLSH IN=IN-DRIER OUT=EXHAUST DRY-RDF1
  BLOCK DECOMP IN=DRY-RDF1 OUT=INBURNER Q-DECOMP
  BLOCK BURN IN=INBURNER AIR WATER Q-DECOMP OUT=PRODUCTS
  BLOCK SEPARATE IN=PRODUCTS OUT=GASES SOLIDS
  BLOCK WGS1 IN=GASES OUT=HH2
  BLOCK WGS2 IN=HH2 OUT=H2-SYNG
PROPERTIES IDEAL
NC-COMPS RDF1 PROXANAL ULTANAL SULFANAL
NC-PROPS RDF1 ENTHALPY HCOALGEN 6 / DENSITY DCOALIGT
```

```
NC-COMPS ASH PROXANAL ULTANAL SULFANAL
NC-PROPS ASH ENTHALPY HCOALGEN / DENSITY DCOALIGT
PROP-DATA HEAT
   IN-UNITS ENG MASS-ENTHALP='MJ/kg'
   PROP-LIST HCOMB
   PVAL RDF1 19.88
PROP-SET ALL-SUBS
   IN-UNITS ENG
   PROPNAME-LIS VOLFLMX MASSVFRA MASSSFRA RHOMX MASSFLOW TEMP
&
      PRES UNITS='lb/cuft' SUBSTREAM=ALL
;  "Entire Stream Flows, Density, Phase Frac, T, P"
   STREAM AIR
   IN-UNITS ENG
   SUBSTREAM MIXED TEMP=77. PRES=14.7 MASS-FLOW=7.5 <kg/hr>
   MOLE-FRAC N2 0.79 / O2 0.21
STREAM NITROGEN
   IN-UNITS ENG
   SUBSTREAM MIXED TEMP=270.0 PRES=14.7 MASS-FLOW=50. <kg/hr>
   MOLE-FRAC N2 0.999 / O2 0.001
STREAM WATER
   SUBSTREAM MIXED TEMP=110. PRES=1. MASS-FLOW=5.9
   MOLE-FRAC H2O 1.
STREAM WET-RDF1
   IN-UNITS ENG
```

```
    SUBSTREAM NCPSD TEMP=77.0 PRES=14.7 MASS-FLOW=10. <kg/hr>
    MASS-FLOW RDF1 5. <kg/hr>
    COMP-ATTR RDF1 PROXANAL ( 0. 6.8 79.7 13.5 )
    COMP-ATTR RDF1 ULTANAL ( 13.5 48.8 7.8 0.7 0. 0. 29.2  )
    COMP-ATTR RDF1 SULFANAL ( 0. 0. 0. )
    SUBS-ATTR PSD ( 0 0 0 0 0 0 0.1 0.2 0.3 0.4 )
DEF-STREAMS HEAT Q-DECOMP
BLOCK DRY-FLSH FLASH2
    IN-UNITS ENG
    PARAM PRES=14.7 DUTY=0.0
BLOCK DRY-REAC RSTOIC
    IN-UNITS ENG
    PARAM PRES=14.7 DUTY=0.0
    STOIC 1 NCPSD RDF1 -1 / MIXED H2O 0.0555084
    CONV 1 NCPSD RDF1 0.2
    COMP-ATTR NCPSD RDF1 PROXANAL ( 1.0 )
BLOCK WGS1 RSTOIC
    PARAM TEMP=530. PRES=1. NPHASE=1 PHASE=V SERIES=YES
    STOIC 1 MIXED H2O -1. / CO -1. / H2 1. / CO2 1.
    STOIC 2 MIXED H2 -1. / CO2 -1. / H2O 1. / CO 1.
    CONV 1 MIXED CO 1.
    CONV 2 MIXED CO2 0.5
    BLOCK-OPTION FREE-WATER=NO
BLOCK WGS2 RSTOIC
    PARAM TEMP=230. PRES=1. NPHASE=1 PHASE=V
```

```
    STOIC 1 MIXED H2O -1. / CO -1. / H2 1. / CO2 1.
    STOIC 2 MIXED H2 -1. / CO2 -1. / H2O 1. / CO 1.
    CONV 1 MIXED CO 1.
    CONV 2 MIXED CO2 0.2
    BLOCK-OPTION FREE-WATER=NO
BLOCK DECOMP RYIELD
    IN-UNITS ENG
    PARAM TEMP=1562. PRES=14.7
    MASS-YIELD MIXED H2O 0.2 / NCPSD ASH 0.2 / CIPSD C  &
        0.1 / MIXED H2 0.1 / N2 0.1 / TOLUE-01 0.1 /  &
        NAPHT-01 0.1 / O2 0.1
    COMP-ATTR NCPSD ASH PROXANAL ( 0 0 0 100 )
    COMP-ATTR NCPSD ASH ULTANAL ( 100 0 0 0 0 0 0 )
    COMP-ATTR NCPSD ASH SULFANAL ( 0 0 0 )
    SUBS-ATTR 1 CIPSD PSD ( 0 0 0 0 0 0 0.1 0.2 0.3  &
        0.4 )
    SUBS-ATTR 2 NCPSD PSD ( 0 0 0 0 0 0 0.1 0.2 0.3  &
        0.4 )
BLOCK BURN RGIBBS
    IN-UNITS ENG
    PARAM PRES=14.7
BLOCK SEPARATE SSPLIT
    IN-UNITS ENG
    FRAC MIXED GASES 1.0
    FRAC CIPSD GASES 0.0
```

```
   FRAC NCPSD GASES 0.0
EO-CONV-OPTI
CALCULATOR COMBUST
   IN-UNITS ENG
   VECTOR-DEF ULT COMP-ATTR STREAM=DRY-RDF1 SUBSTREAM=NCPSD  &
      COMPONENT=RDF1 ATTRIBUTE=ULTANAL
   DEFINE WATER COMP-ATTR-VAR STREAM=DRY-RDF1 SUBSTREAM=NCPSD  &
      COMPONENT=RDF1 ATTRIBUTE=PROXANAL ELEMENT=1
   DEFINE H2O BLOCK-VAR BLOCK=DECOMP VARIABLE=YIELD  &
      SENTENCE=MASS-YIELD ID1=MIXED ID2=H2O
   DEFINE ASH BLOCK-VAR BLOCK=DECOMP VARIABLE=YIELD  &
      SENTENCE=MASS-YIELD ID1=NCPSD ID2=ASH
   DEFINE CARB BLOCK-VAR BLOCK=DECOMP VARIABLE=YIELD  &
      SENTENCE=MASS-YIELD ID1=CIPSD ID2=C
   DEFINE H2 BLOCK-VAR BLOCK=DECOMP VARIABLE=YIELD  &
      SENTENCE=MASS-YIELD ID1=MIXED ID2=H2
   DEFINE N2 BLOCK-VAR BLOCK=DECOMP VARIABLE=YIELD  &
      SENTENCE=MASS-YIELD ID1=MIXED ID2=N2
   DEFINE O2 BLOCK-VAR BLOCK=DECOMP VARIABLE=YIELD  &
      SENTENCE=MASS-YIELD ID1=MIXED ID2=O2
C     FACT IS THE FACTOR TO CONVERT THE ULTIMATE ANALYSIS TO
C     A WET BASIS.
F     FACT = (100 - WATER) / 100
F     H2O  = WATER / 100
F     ASH  = ULT(1) / 100 * FACT
```

```
F    CARB = ULT(2) / 100 * FACT
F    H2   = ULT(3) / 100 * FACT
F    N2   = ULT(4) / 100 * FACT
F    CL2  = ULT(5) / 100 * FACT
F    SULF = ULT(6) / 100 * FACT
F    O2   = ULT(7) / 100 * FACT
    EXECUTE BEFORE BLOCK DECOMP
CALCULATOR WATER
    IN-UNITS ENG
    DEFINE H2OIN COMP-ATTR-VAR STREAM=WET-RDF1 SUBSTREAM=NCPSD  &
        COMPONENT=RDF1 ATTRIBUTE=PROXANAL ELEMENT=1
    DEFINE CONV BLOCK-VAR BLOCK=DRY-REAC VARIABLE=CONV  &
        SENTENCE=CONV ID1=1
    DEFINE H2ODRY BLOCK-VAR BLOCK=DRY-REAC VARIABLE=VALUE  &
        SENTENCE=COMP-ATTR ID1=1 ELEMENT=1
F    H2ODRY = 10.0
F    CONV = (H2OIN - H2ODRY) / (100 - H2ODRY)
    EXECUTE BEFORE BLOCK DRY-REAC
STREAM-REPOR MOLEFLOW MASSFLOW PROPERTIES=ALL-SUBS
PROPERTY-REP PCES
```

Gasification Simulation Raw Results

RDF1

RDF1 1.004/1.0991

SFR = 2.1

AFR	H2	CO	CO2	H2O	H2/CO
7.5	0.138	0.103	1.456	4.458	1.339806
10	0.266	0.25	3.536	3.317	1.064
15	0.588	0.535	7.561	1.149	1.099065
17.5	0.533	0.806	8.576	0.928	0.66129
20	0.46	0.606	8.576	1.584	0.759076
22.5	0.386	0.606	8.576	2.239	0.636964
25	0.313	0.606	8.576	2.895	0.516502
27.5	0.239	0.606	8.576	3.551	0.394389
30	0.104	0.603	8.509	4.221	0.172471

RDF1 1.0637/0.9557

SFR = 3.1

AFR	H2	CO	CO2	H2O	H2/CO
7.5	0.136	0.102	1.44	5.473	1.333333
10	0.267	0.251	3.55	4.305	1.063745
15	0.518	0.542	7.66	2.064	0.95572
17.5	0.533	0.606	8.576	1.928	0.879538
20	0.46	0.606	8.576	2.584	0.759076
22.5	0.386	0.606	8.576	3.239	0.636964
25	0.313	0.606	8.576	3.895	0.516502
27.5	0.239	0.606	8.576	4.551	0.394389
30	0.08	0.63	8.509	4.221	0.126984

RDF1 1.064/0.9596

SFR = 3.8

AFR	H2	CO	CO2	H2O	H2/CO
7.5	0.135	0.101	1.425	6.186	1.336634
10	0.267	0.251	3.548	5.006	1.063745
15	0.523	0.545	7.714	2.718	0.959633
17.5	0.533	0.606	8.576	2.628	0.879538
20	0.46	0.606	8.576	3.284	0.759076
22.5	0.46	0.606	8.576	3.284	0.759076
25	0.46	0.606	8.576	3.284	0.759076

27.5	0.239	0.606	8.576	5.251	0.394389
30	0.164	0.63	8.539	5.921	0.260317

RDF1 1.027/0.9598

SFR = 4.2

AFR	H2	CO	CO2	H2O	H2/CO
7.5	0.134	0.1	1.415	6.594	1.34
10	0.266	0.259	3.544	5.41	1.027027
15	0.525	0.547	7.739	3.096	0.959781
17.5	0.533	0.606	8.576	3.028	0.879538
20	0.46	0.606	8.576	4.339	0.759076
22.5	0.386	0.606	8.576	5.61	0.636964
27.5	0.239	0.606	8.576	6	0.394389
30	0.164	0.63	8.539	6.321	0.260317

RDF1 1.064/0.96

SFR = 4.8

AFR	H2	CO	CO2	H2O	H2/CO
7.5	0.133	0.099	1.401	7.206	1.343434
10	0.266	0.25	3.534	6.018	1.064
15	0.528	0.55	7.771	3.668	0.96
17.5	0.533	0.606	8.576	3.628	0.879538
20	0.46	0.606	8.576	4.284	0.759076
22.5	0.386	0.606	8.576	4.939	0.636964
27.5	0.239	0.606	8.576	6.251	0.394389
30	0.101	0.63	8.539	6.921	0.160317
32.5	0.0706	0.834	8.219	7.708	0.084652

RDF1 1.0643/0.9619

SFR = 5.2

AFR	H2	CO	CO2	H2O	H2/CO
7.5	0.132	0.098	1.391	8.33	1.346939
10	0.265	0.249	3.526	7.14	1.064257
15	0.53	0.551	7.788	4.734	0.961887
17.5	0.533	0.606	8.576	4.728	0.879538
20	0.46	0.606	8.576	5.384	0.759076
22.5	0.386	0.606	8.576	6.039	0.636964
27.5	0.239	0.606	8.576	7.351	0.394389
30	0.164	0.63	8.539	8.539	0.260317

32.5	0.076	0.834	8.219	8.808	0.091127

RDF1 1.0605/0.9638

SFR = 5.9

AFR	H2	CO	CO2	H2O	H2/CO
7.5	0.13	0.097	1.373	8.33	1.340206
10	0.263	0.248	3.509	7.14	1.060484
15	0.532	0.552	7.81	4.734	0.963768
17.5	0.533	0.606	8.576	4.728	0.879538
20	0.46	0.606	8.576	5.384	0.759076
22.5	0.386	0.606	8.576	6.039	0.636964
27.5	0.239	0.606	8.576	7.351	0.394389
30	0.164	0.63	8.539	8.021	0.260317
32.5	0.076	0.834	8.219	8.808	0.091127

RDF1 1.0607/1.000

SFR = 6.3

AFR	H2	CO	CO2	H2O	H2/CO
7.5	0.129	0.096	1.363	8.739	1.34375
10	0.262	0.247	3.497	7.55	1.060729
15	0.533	0.533	7.82	5.126	1
17.5	0.533	0.606	8.576	5.128	0.879538
20	0.46	0.606	8.576	5.784	0.759076
22.5	0.386	0.606	8.576	6.439	0.636964
27.5	0.239	0.606	8.576	7.751	0.394389
30	0.164	0.63	8.539	8.421	0.260317
32	0.074	0.834	8.219	9.208	0.088729

RDF1 1.0569/0.9639

SFR = 6.9

AFR	H2	CO	CO2	H2O	H2/CO
7.5	0.127	0.095	1.348	9.352	1.336842
10	0.262	0.246	3.479	8.166	1.065041
15	0.534	0.554	7.829	5.718	0.963899
17.5	0.533	0.606	8.576	5.728	0.879538
20	0.406	0.606	8.576	6.384	0.669967

22.5	0.386	0.606	8.576	7.039	0.636964
27.5	0.239	0.606	8.576	8.351	0.394389
30	0.164	0.63	8.559	9.021	0.260317
32	0.076	0.834	8.219	9.808	0.091127

RDF1 1.0607/1.000

SFR = 7.3

AFR	H2	CO	CO2	H2O	H2/CO
7.5	0.127	0.095	1.338	9.76	1.336842
10	0.259	0.245	3.466	8.577	1.057143
15	0.534	0.554	7.833	6.115	0.963899
17.5	0.533	0.606	8.576	6.128	0.879538
20	0.46	0.606	8.576	6.784	0.759076
22.5	0.386	0.606	8.576	7.439	0.636964
27.5	0.239	0.606	8.576	8.751	0.394389
30	0.164	0.63	8.539	9.421	0.260317
32	0.076	0.834	8.219	10.208	0.091127

RDF1 1.0527/0.9639

SFR = 8.5

AFR	H2	CO	CO2	H2O	H2/CO
7.5	0.124	0.093	1.309	10.985	1.333333
10	0.255	0.242	3.425	9.813	1.053719
15	0.534	0.554	7.831	7.316	0.963899
17.5	0.533	0.606	8.576	7.328	0.879538
20	0.46	0.606	8.576	7.984	0.759076
22.5	0.386	0.606	8.576	8.639	0.636964
27.5	0.239	0.606	8.576	9.951	0.394389
30	0.164	0.63	8.539	10.621	0.260317
32	0.076	0.834	8.219	11.408	0.091127

RDF 2 KL

RDF2 0.87

SFR = 2.1

AFR	H2	CO	CO2	H2O	H2/CO
5	0.765	4.455	7.66	0	0.171717
7.5	0.765	3.465	9.244	0	0.220779

10	0.765	2.453	10.805	0	0.311863
14.5	0.765	0.877	13.281	0.205	0.872292
15	0.742	0.933	13.193	0.806	0.795284
17.5	0.675	0.933	13.193	1.337	0.723473
21	0.592	0.933	13.193	1.337	0.634512
22	0.572	0.933	13.193	1.738	0.613076
23	0.549	0.933	13.193	1.3378	0.588424

RDF2 1

SFR = 3.1

AFR	H2	CO	CO2	H2O	H2/CO
5	0.877	2.897	10.108	0	0.302727
7.5	0.877	1.883	11.701	0	0.465746
10	0.877	2.453	13.281	0	0.357521
15	0.732	0.817	13.193	1.29	0.895961
17.5	0.666	0.933	13.193	1.88	0.713826
20	0.664	0.933	13.193	2.437	0.711683
23	0.535	0.933	13.193	3.058	0.573419

RDF2 1.11

SFR = 3.8

AFR	H2	CO	CO2	H2O	H2/CO
5	0.955	1.807	10.82	0	0.5285
7.5	0.95	0.854	13.317	0.04	1.112412
10	0.872	0.933	13.193	0.742	0.93462
15	0.73	0.933	13.193	2.014	0.782422
17.5	0.662	0.933	13.193	2.62	0.709539
20	0.598	0.933	13.193	3.194	0.640943
23	0.526	0.933	13.193	3.836	0.563773

RDF2 1.03

SFR = 4.2

AFR	H2	CO	CO2	H2O	H2/CO
5	1	1.185	12.787	0	0.843882
7.5	0.946	0.916	13.219	0.481	1.032751
10	0.872	0.933	13.199	1.144	0.93462
15	0.729	0.933	13.199	2.424	0.78135
17.5	0.66	0.933	13.199	3.038	0.707395

20	0.594	0.933	13.199	3.623	0.636656
23	0.521	0.933	13.199	4.277	0.558414
25	0.476	0.933	13.199	4.682	0.510182

RDF2 1.21

SFR = 4.8

AFR	H2	CO	CO2	H2O	H2/CO
3.5	1.067	0.863	13.303	0	1.236385
4	1.052	0.867	13.297	0.134	1.213379
5	1.02	0.908	13.233	0.422	1.123348
7.5	0.945	0.933	13.193	1.093	1.012862
10	0.872	0.933	13.193	1.746	0.93462
15	0.727	0.933	13.193	3.635	0.779207
17.5	0.657	0.933	13.193	3.66	0.70418
20	0.59	0.933	13.193	4.259	0.632369
23	0.515	0.933	13.193	4.93	0.551983

RDF2 1.31

SFR = 5.2

AFR	H2	CO	CO2	H2O	H2/CO
1.5	1.112	1.26	12.675	0	0.88254
2	1.112	0.852	13.32	0	1.305164
2.5	1.096	0.868	13.295	0.141	1.262673
3	1.08	0.933	13.263	0.286	1.157556
4.5	1.033	0.933	13.193	0.707	1.107181
5	1.018	0.933	13.193	0.029	1.091104
7.5	0.945	0.933	13.193	1.493	1.012862
10	0.871	0.933	13.193	2.147	0.933548

RDF3 0.79

SFR = 2.1

AFR	H2	CO	CO2	H2O	H2/CO
5	0.752	7.922	2.843	0	0.094926
7.5	0.752	6.908	4.436	0	0.108859
10	0.752	5.902	6.017	0	0.127414
15	0.752	3.943	9.094	0	0.190718
17.5	0.752	3.011	10.559	0	0.249751
20	0.752	2.122	11.559	0	0.354383

23	0.752	1.116	13.536	0	0.673835
23.5	0.752	0.955	13.789	0	0.787435

RDF3 0.9

SFR = 3.1

AFR	H2	CO	CO2	H2O	H2/CO
5	0.864	6.368	5.285	0	0.135678
7.5	0.864	5.352	6.881	0	0.161435
10	0.864	4.341	8.469	0	0.199032
15	0.864	2.357	11.587	0	0.366568
17.5	0.864	1.4	13.09	0	0.617143
20	0.832	0.925	13.836	0.286	0.899459
23	0.753	0.973	13.761	0.989	0.773895
25	0.706	0.973	13.761	1.412	0.725591

RDF3 0.95

SFR = 3.8

AFR	H2	CO	CO2	H2O	H2/CO
5	0.942	5.279	6.996	0	0.178443
7.5	0.942	4.262	8.594	0	0.221023
10	0.942	3.249	10.1186	0	0.289935
15	0.942	1.25	13.326	0	0.7536
17.5	0.894	0.945	13.705	0.429	0.946032
20	0.825	0.975	13.761	1.051	0.846154
23	0.748	0.975	13.761	2.175	0.767179
25	0.699	0.975	13.761	2.175	0.716923

RDF3 1.0604

SFR = 4.2

AFR	H2	CO	CO2	H2O	H2/CO
5	0.987	4.657	7.974	0	0.211939
7.5	0.987	3.639	9.572	0	0.271228
10	0.987	2.625	11.166	0	0.376
15	0.966	0.911	13.858	0.188	1.060373
17.5	0.891	0.973	13.761	0.857	0.915725
20	0.823	0.973	13.761	1.467	0.845838
23	0.745	0.973	13.761	2.167	0.765673
25	0.695	0.973	13.761	2.629	0.714286

RDF3 0.9877

SFR = 4.8

AFR	H2	CO	CO2	H2O	H2/CO
5	1.054	3.723	9.44	0	0.283105
7.5	1.054	2.705	11.039	0	0.389649
10	1.054	1.69	12.635	0	0.623669
15	0.961	0.973	13.761	0.835	0.987667
17.5	0.89	0.973	13.761	1.407	0.914697
20	0.82	0.973	13.761	2.089	0.842754
23	0.741	0.973	13.761	2.805	0.761562
25	0.69	0.973	13.761	3.255	0.709147

RDF3 1.1065

SFR = 5.2

AFR	H2	CO	CO2	H2O	H2/CO
5	1.099	3.101	10.417	0	0.354402
7.5	1.099	2.083	12.017	0	0.527604
10	1.099	1.066	13.614	0	1.030957
12	1.049	0.948	13.761	1.238	1.10654
15	0.96	0.973	13.761	1.872	0.986639
17.5	0.889	0.973	13.761	1.872	0.913669
20	0.819	0.973	13.761	2.502	0.841727
23	0.738	0.973	13.761	3.253	0.758479
25	0.687	0.973	13.761	3.682	0.706064

RDF3 1.1357

SFR = 5.9

AFR	H2	CO	CO2	H2O	H2/CO
5	1.177	2.013	12.128	0	0.584699
7.5	1.177	0.944	13.728	0	1.246822
10	1.105	1.066	13.761	0.641	1.036585
15	0.96	0.948	13.761	1.943	1.012658
17.5	0.888	0.973	13.761	2.587	0.912641
20	0.817	0.973	13.761	3.219	0.839671
23	0.735	0.973	13.761	3.955	0.755396

RDF3 1.3068

SFR = 6.3

AFR	H2	CO	CO2	H2O	H2/CO
5	1.222	1.391	13.105	0	0.878505
6	1.222	0.983	13.745	0	1.243133
7	1.197	0.916	13.851	0.219	1.306769
7.5	1.181	0.936	13.819	0.363	1.261752
10	1.105	0.973	13.761	1.041	1.135663
15	0.959	0.973	13.761	2.345	0.985612
17.5	0.887	0.973	13.761	2.991	0.911614
20	0.816	0.973	13.761	3.627	0.838643
23	0.733	0.973	13.761	4.127	0.75334
25	0.69	0.973	13.761	4.846	0.709147

RDF3 1.4521

SFR = 6.9

AFR	H2	CO	CO2	H2O	H2/CO
4	1.288	0.887	13.897	0.014	1.452086
5	1.255	0.927	13.833	0.302	1.35383
7.5	1.174	0.973	13.761	0.987	1.206578
10	1.105	0.973	13.761	1.642	1.135663
15	0.959	0.973	13.761	2.948	0.985612
17.5	0.887	0.973	13.761	3.596	0.911614
20	0.815	0.973	13.761	4.237	0.837616
23	0.731	0.973	13.761	4.989	0.751285

RDF3 1.4482

SFR = 7.3

AFR	H2	CO	CO2	H2O	H2/CO
2	1.334	1.059	13.686	0	1.259679
3	1.315	0.908	13.863	0.165	1.448238
3.5	1.299	0.928	13.831	0.309	1.399784
4	1.283	0.949	13.799	0.309	1.351949
4.5	1.267	0.969	13.767	0.598	1.307534
5	1.252	0.973	13.761	0.752	1.286742
7.5	1.179	0.973	13.761	1.387	1.211716
10	1.105	0.973	13.761	2.042	1.135663

13	0.959	0.973	13.761	3.349	0.985612
17.5	0.886	0.973	13.761	3.999	0.910586
20	0.816	0.973	13.761	4.142	0.838643
23	0.73	0.973	13.761	5.399	0.750257

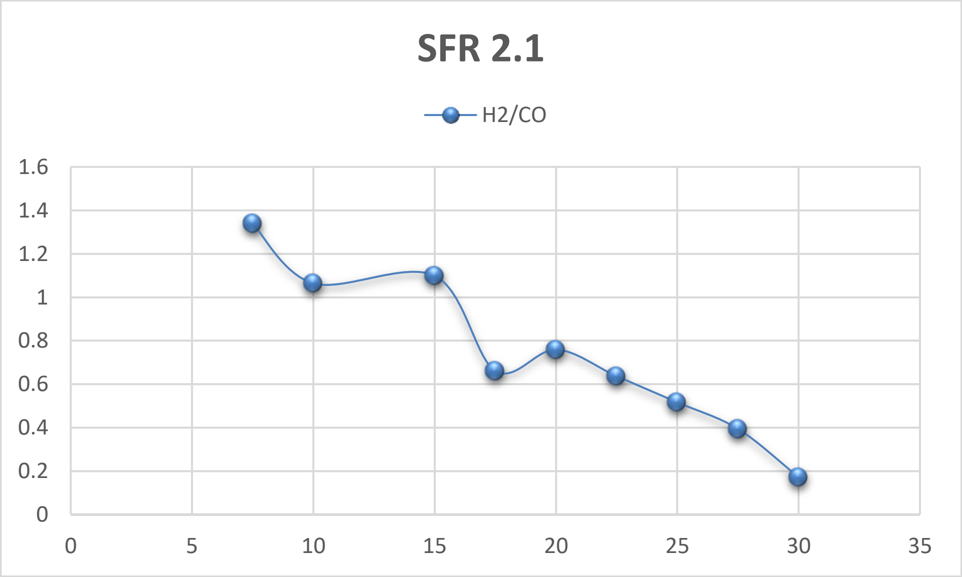

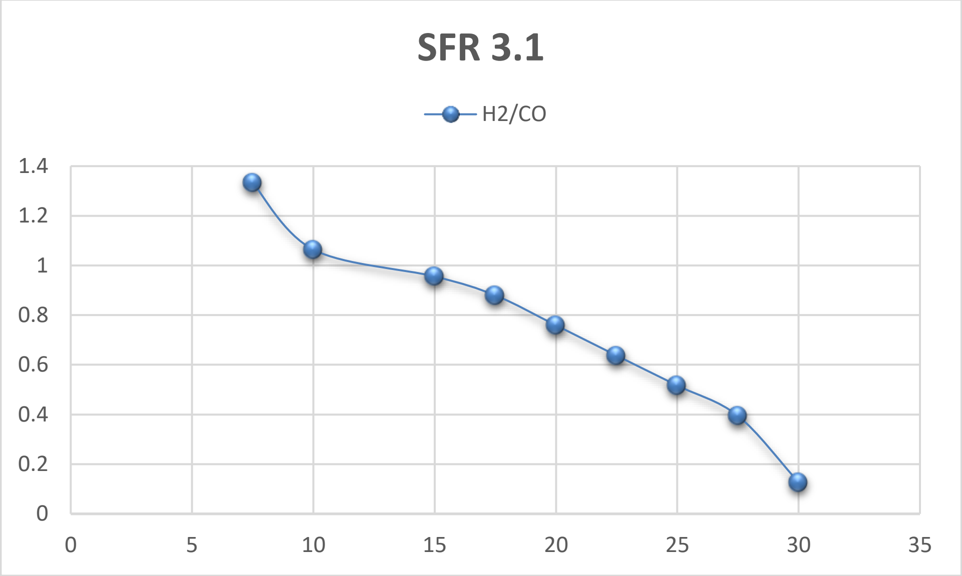
SFR 3.1
H2/CO
1.4
1.2
1
0.8
0.6
0.4
0.2
0
0
5
10
15
20
25
30
35

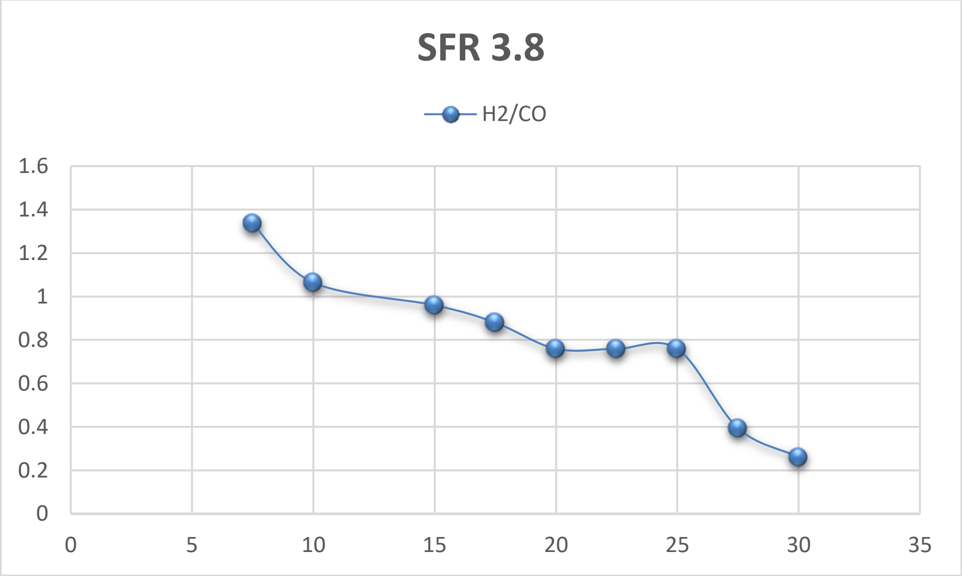
SFR 3.8
H2/CO
1.6
1.4
1.2
1
0.8
0.6
0.4
0.2
0
0
5
10
15
20
25
30
35

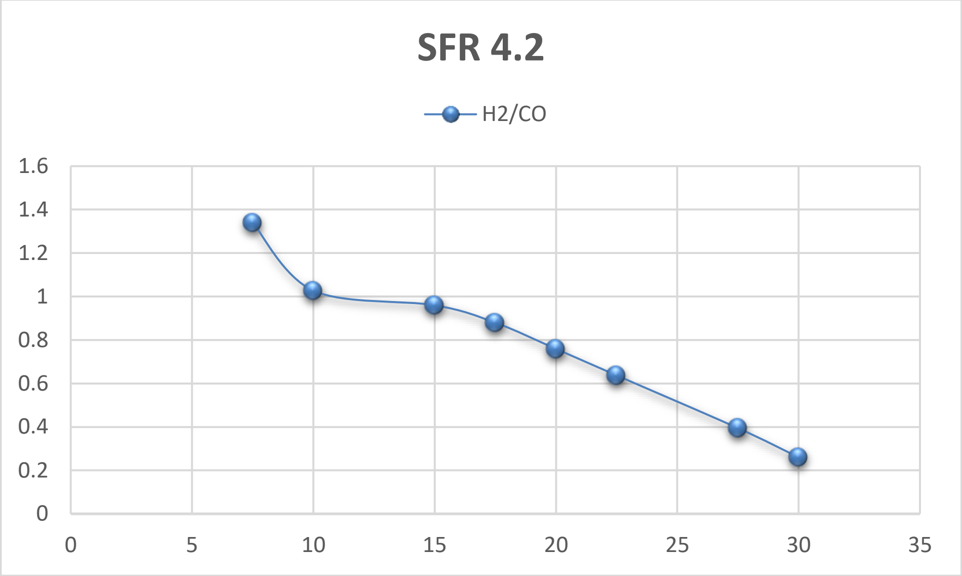
SFR 4.2
H2/CO
1.6
1.4
1.2
1
0.8
0.6
0.4
0.2
0
0
5
10
15
20
25
30
35

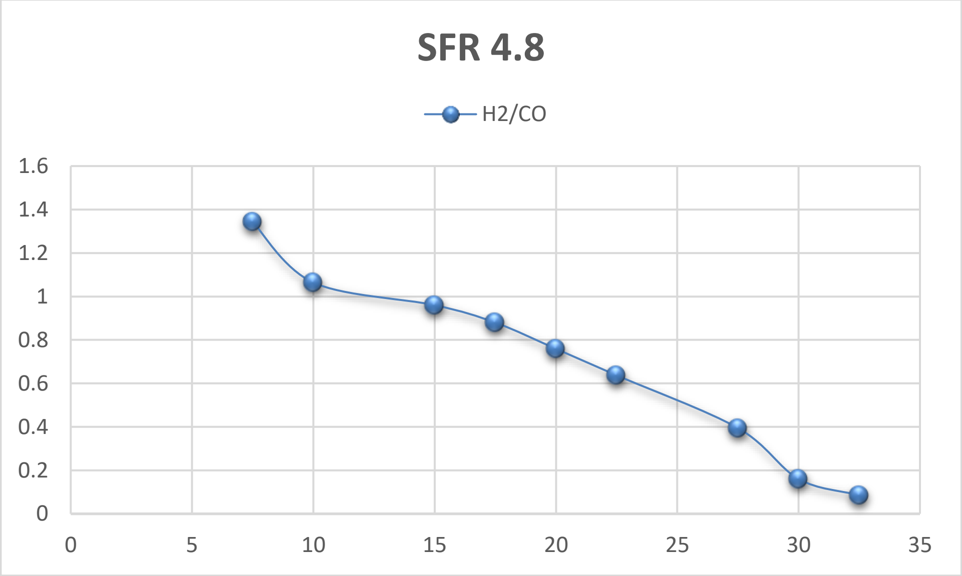
SFR 4.8
H2/CO
1.6
1.4
1.2
1
0.8
0.6
0.4
0.2
0
0
5
10
15
20
25
30
35

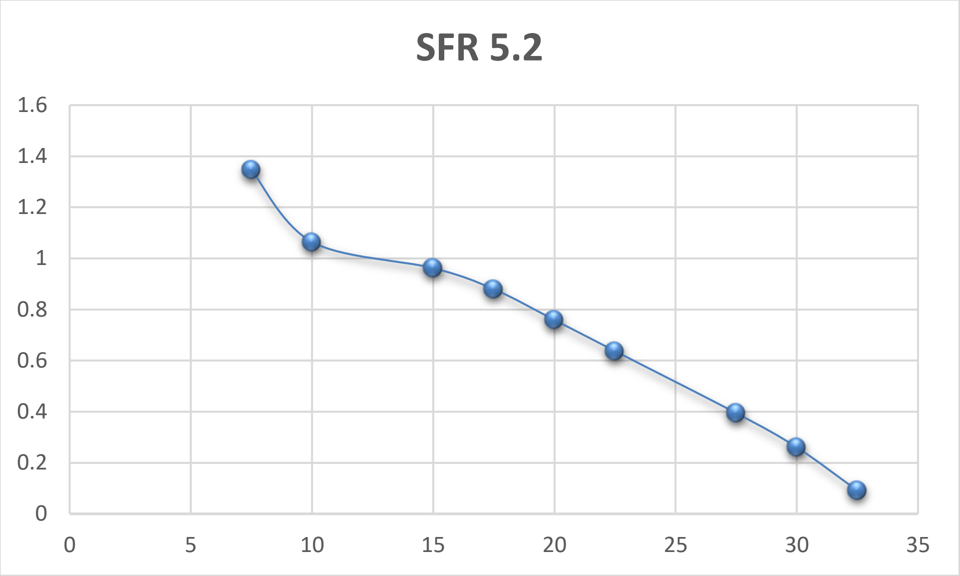
SFR 5.2
1.6
1.4
1.2
1
0.8
0.6
0.4
0.2
0
0
5
10
15
20
25
30
35

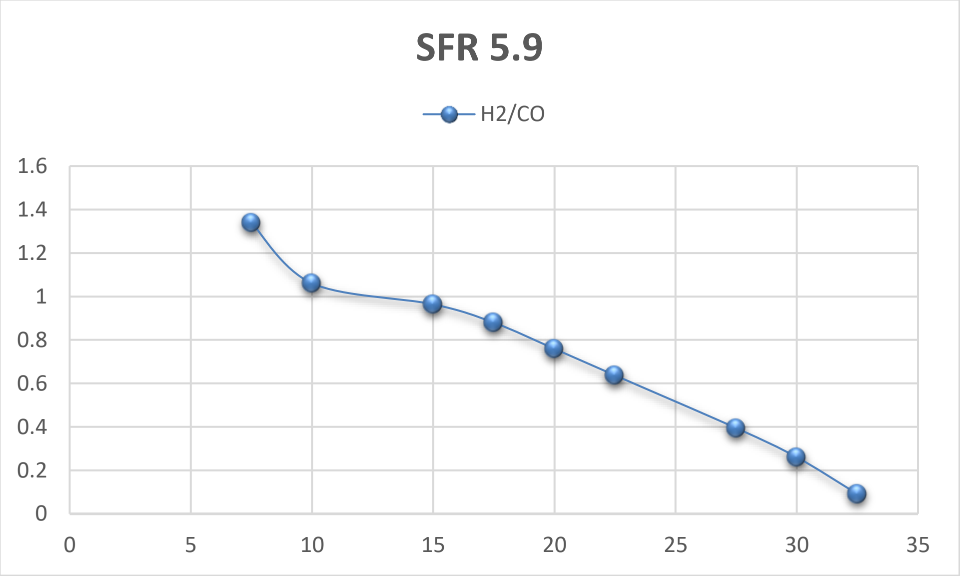
SFR 5.9
H2/CO
1.6
1.4
1.2
1
0.8
0.6
0.4
0.2
0
0
5
10
15
20
25
30
35

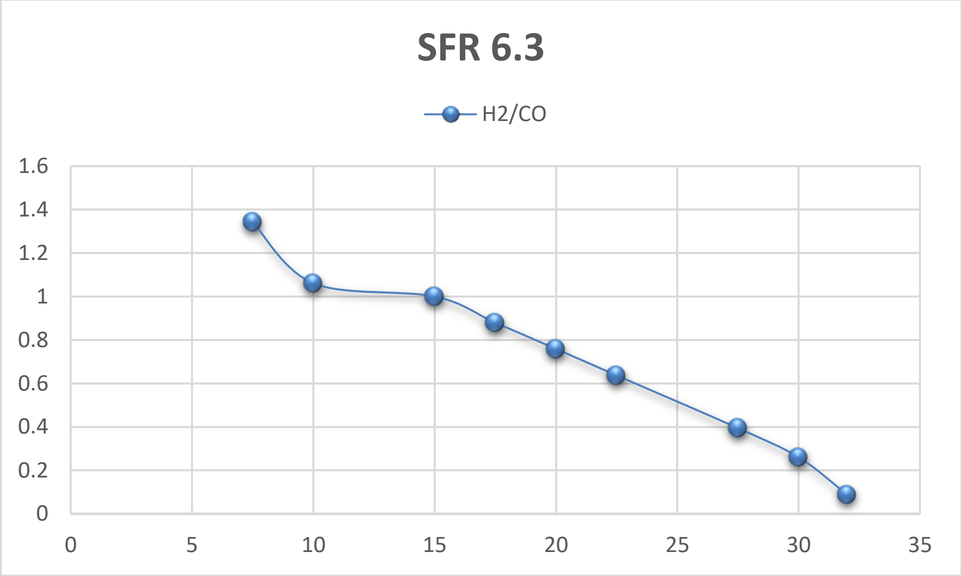
SFR 6.3
H2/CO
1.6
1.4
1.2
1
0.8
0.6
0.4
0.2
0
0
5
10
15
20
25
30
35

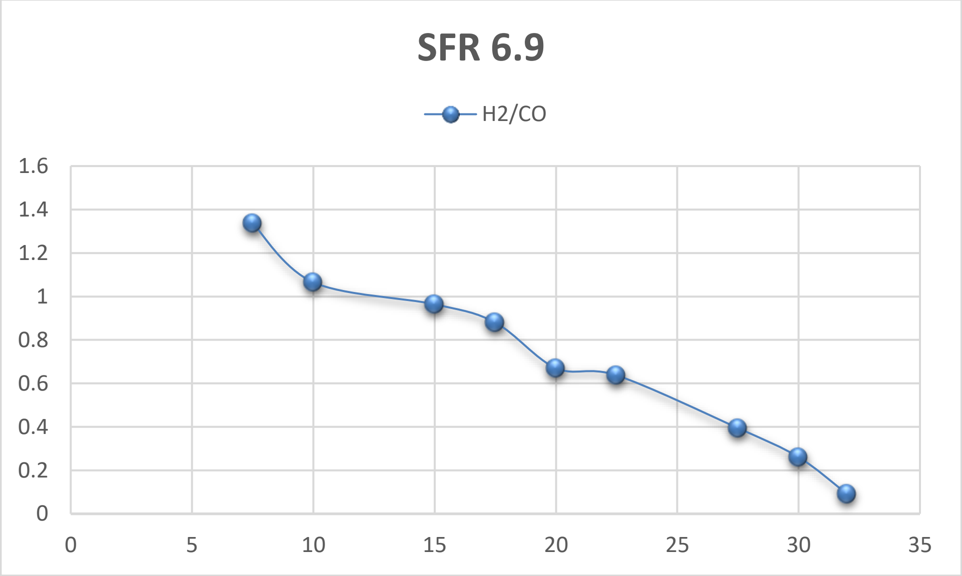
SFR 6.9
H2/CO
1.6
1.4
1.2
1
0.8
0.6
0.4
0.2
0
0
5
10
15
20
25
30
35

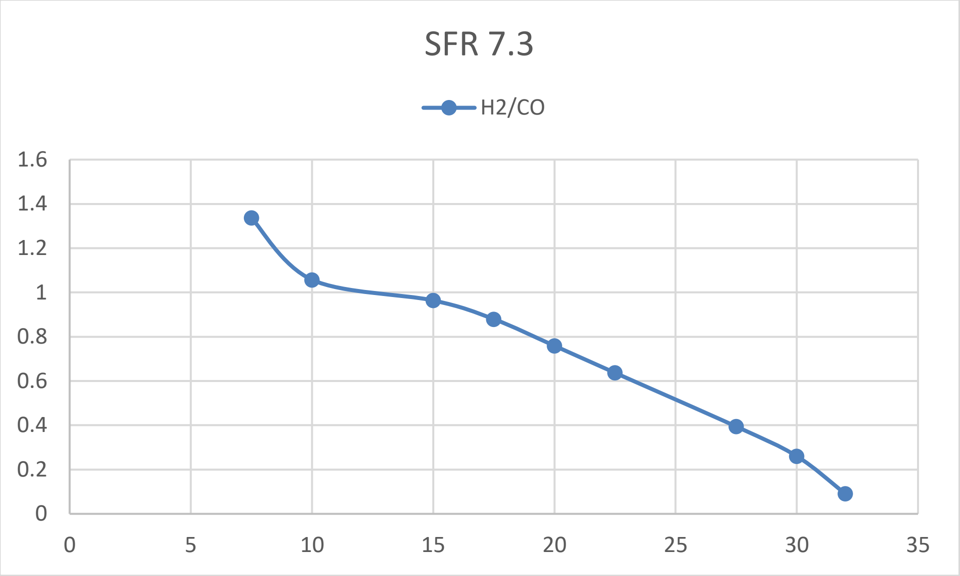
SFR 7.3
H2/CO
1.6
1.4
1.2
1
0.8
0.6
0.4
0.2
0
0
5
10
15
20
25
30
35

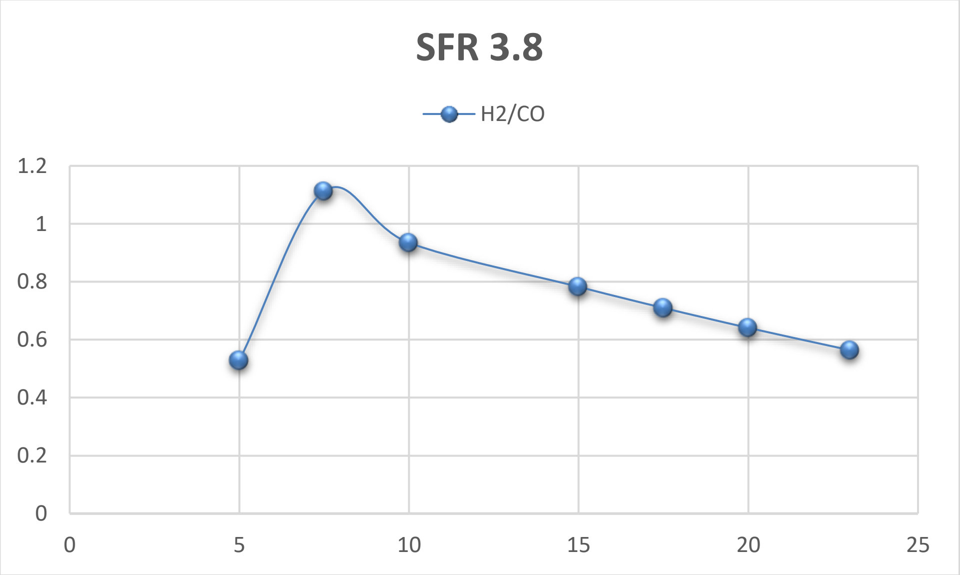
SFR 3.8
H2/CO
1.2
1
0.8
0.6
0.4
0.2
0
0
5
10
15
20
25

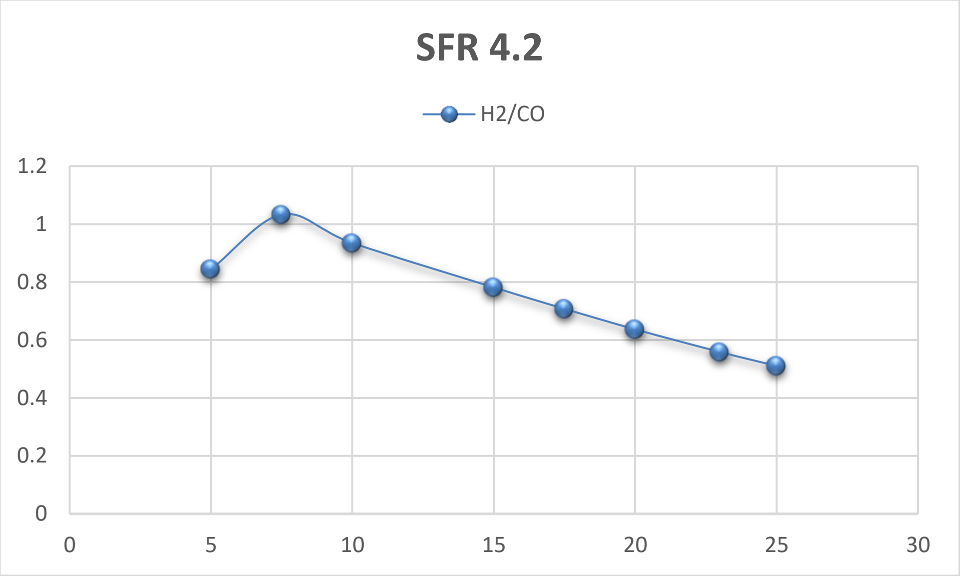
SFR 4.2
H2/CO
1.2
1
0.8
0.6
0.4
0.2
0
0
5
10
15
20
25
30

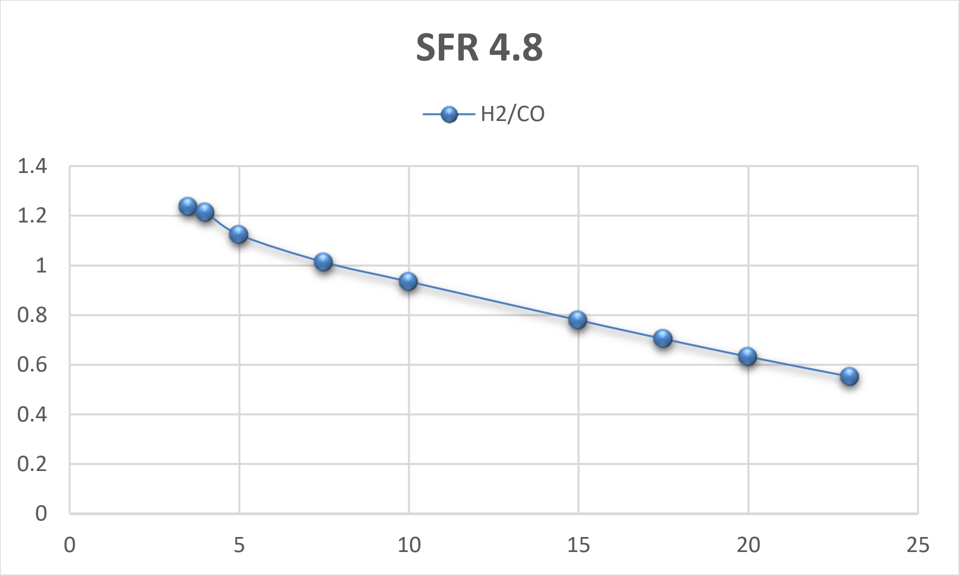
SFR 4.8
H2/CO
1.4
1.2
1
0.8
0.6
0.4
0.2
0
0
5
10
15
20
25

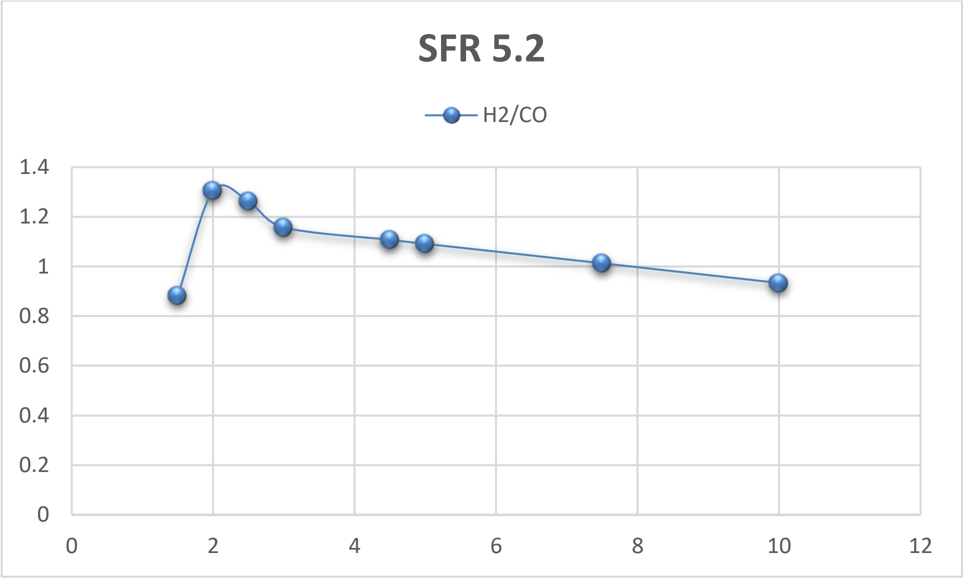
SFR 5.2
H2/CO
1.4
1.2
1
0.8
0.6
0.4
0.2
0
0
2
4
6
8
10
12

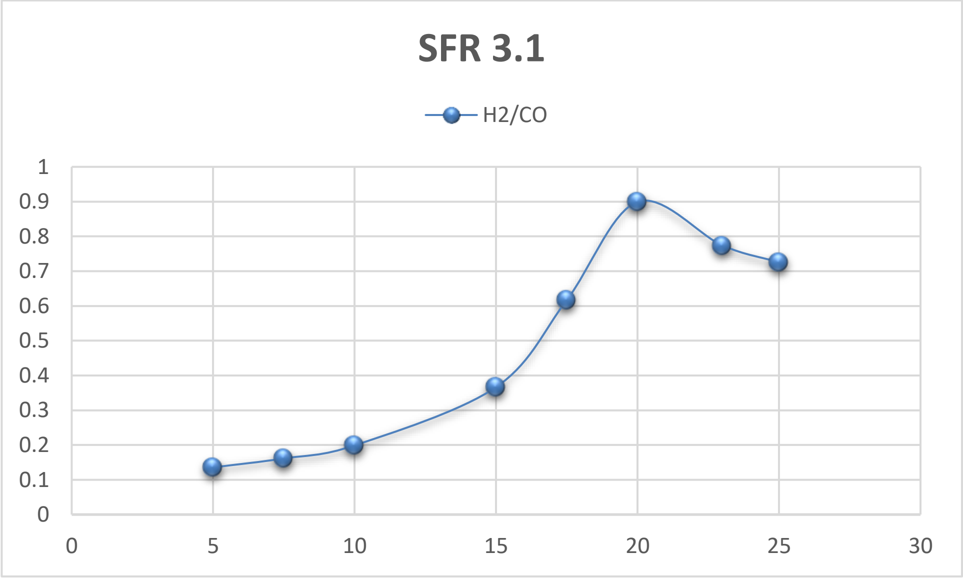
SFR 3.1
H2/CO
1
0.9
0.8
0.7
0.6
0.5
0.4
0.3
0.2
0.1
0
0
5
10
15
20
25
30

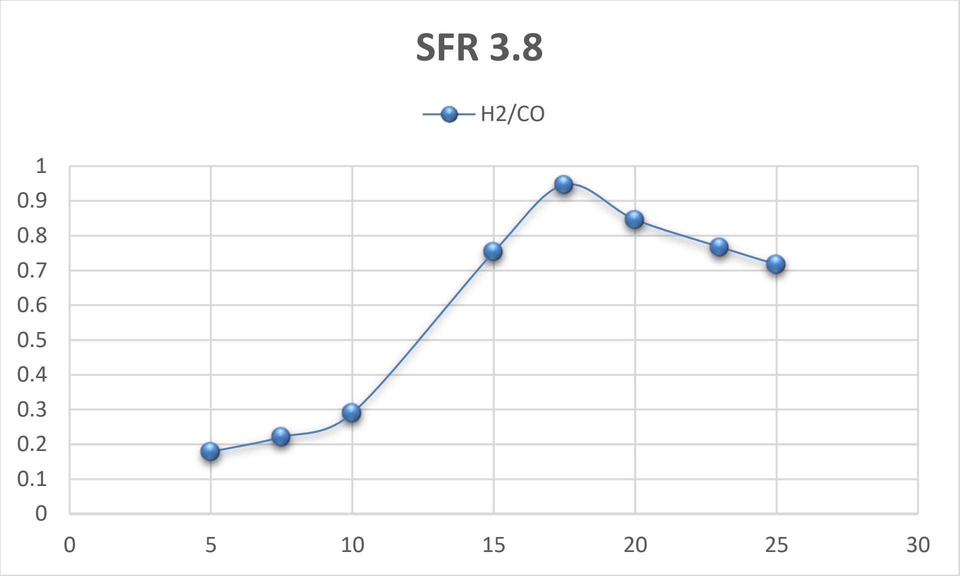
SFR 3.8
H2/CO
1
0.9
0.8
0.7
0.6
0.5
0.4
0.3
0.2
0.1
0
0
5
10
15
20
25
30

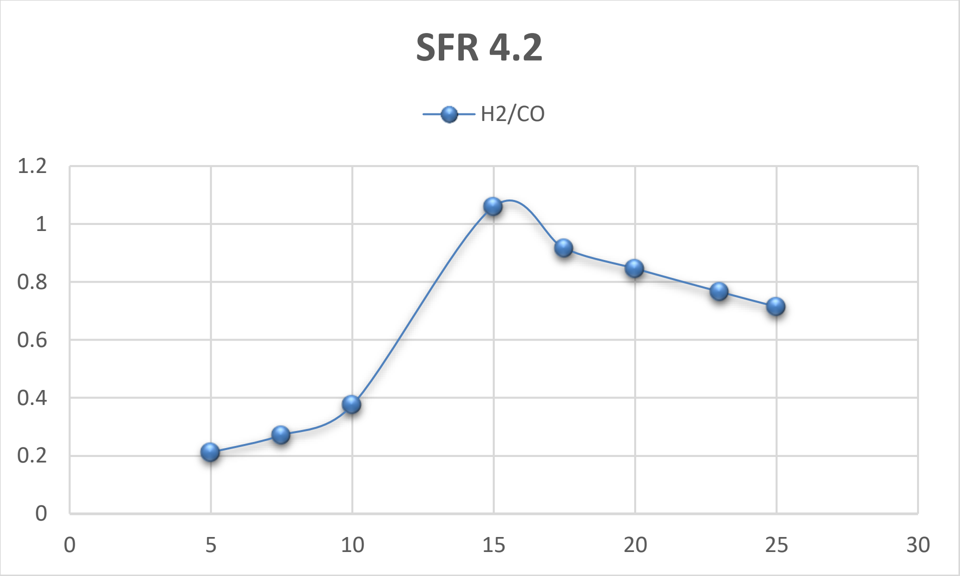
SFR 4.2
H2/CO
1.2
1
0.8
0.6
0.4
0.2
0
0
5
10
15
20
25
30

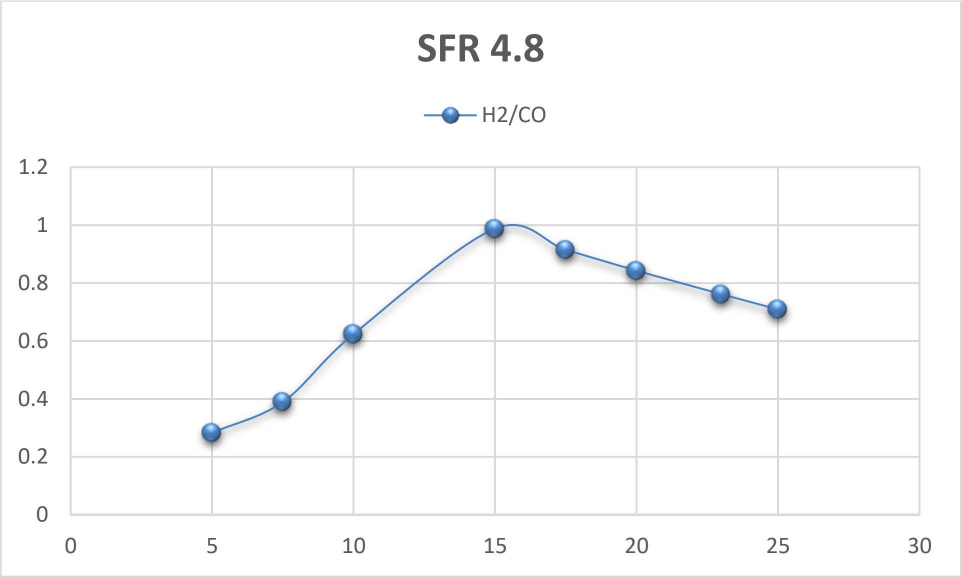
SFR 4.8
H2/CO
1.2
1
0.8
0.6
0.4
0.2
0
0
5
10
15
20
25
30

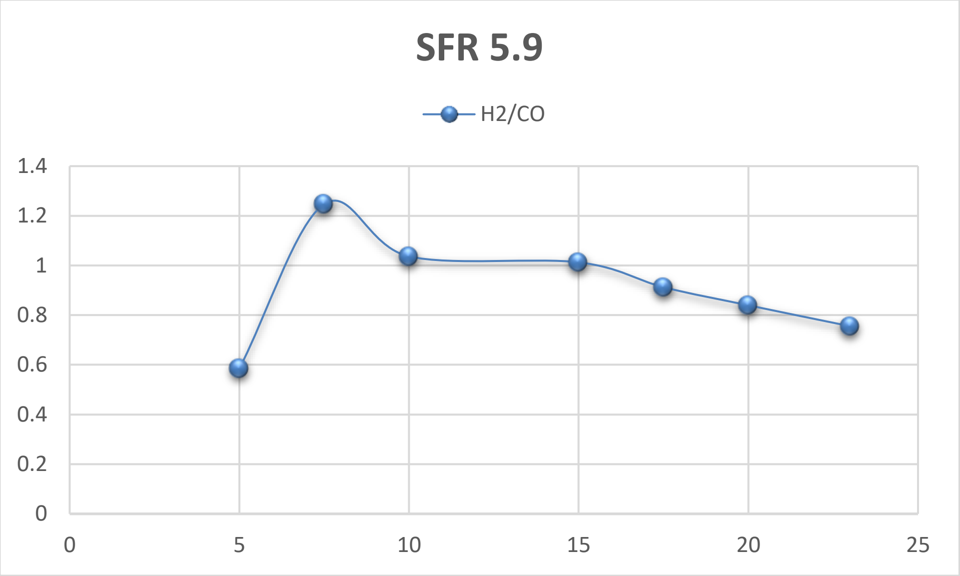
SFR 5.9
H2/CO
1.4
1.2
1
0.8
0.6
0.4
0.2
0
0
5
10
15
20
25

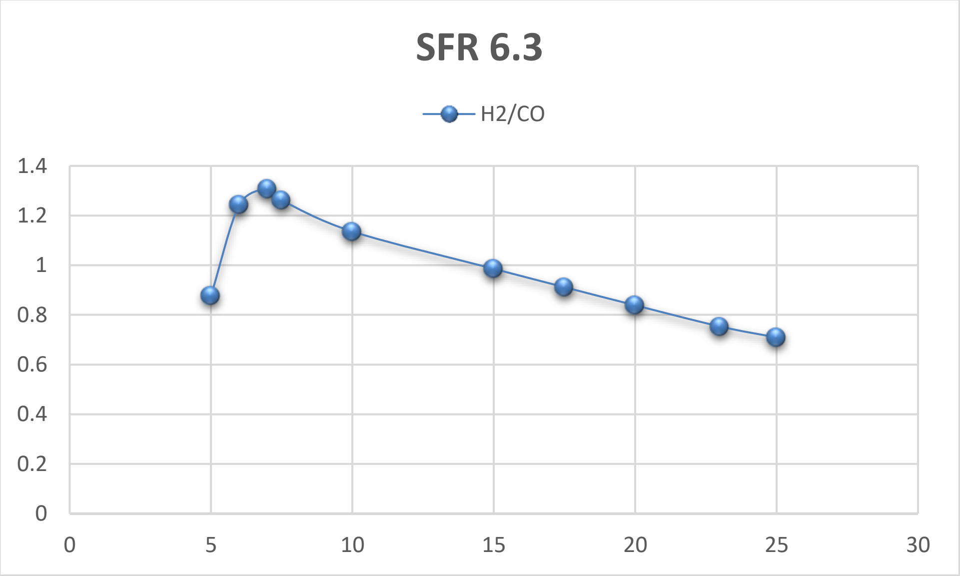
SFR 6.3
H2/CO
1.4
1.2
1
0.8
0.6
0.4
0.2
0
0
5
10
15
20
25
30

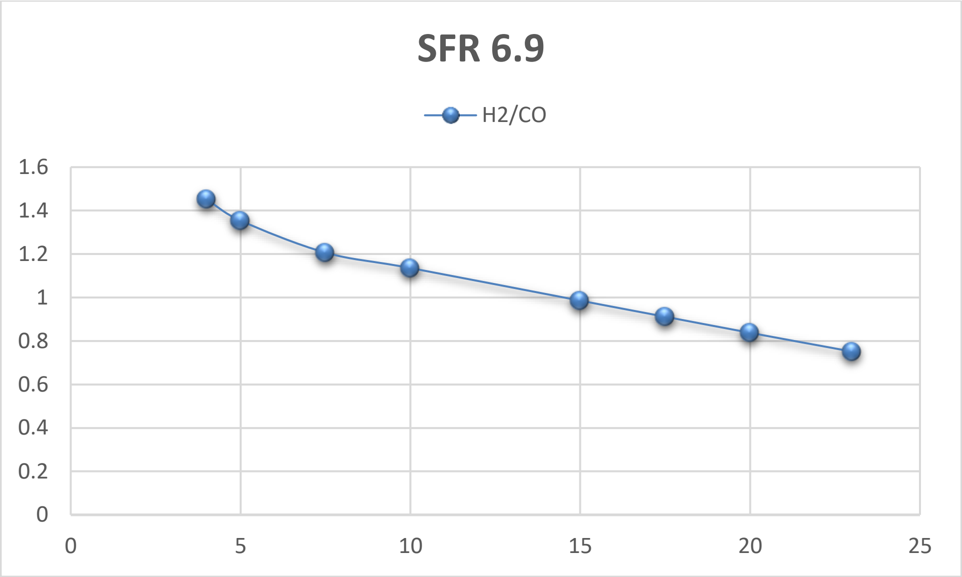
SFR 6.9
H2/CO
1.6
1.4
1.2
1
0.8
0.6
0.4
0.2
0
0
5
10
15
20
25

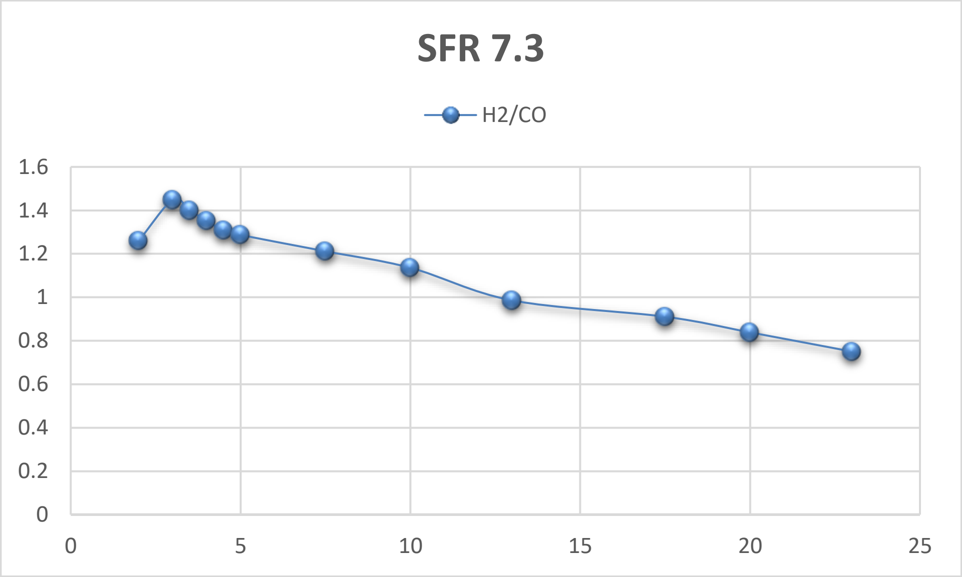
SFR 7.3
H2/CO
1.6
1.4
1.2
1
0.8
0.6
0.4
0.2
0
0
5
10
15
20
25